GEOLOGICA ULTRAIECTINA

Mededelingen van de
Faculteit Aardwetenschappen
Universiteit Utrecht

No. 162

The Alpine evolution of Thessaly (NW Greece) and late Tertiary Aegean kinematics

C. Rachel Walcott

GEOLOGICA ULTRAIECTINA

Mededelingen van de
Faculteit Aardwetenschappen
Universiteit Utrecht

No. 162

The Alpine Evolution of Thessaly (NW Greece) and late Tertiary Aegean kinematics

C. Rachel Walcott

Members of the dissertation committee:

Prof. J.-P. Burg	Department of Earth Sciences, Eidgenossische Technische Hogschule, Switzerland
Prof. J.E. Meulenkamp	Department of Stratigraphy, Utrecht University The Netherlands
Prof. A.H. Robertson	Department of Geology and Geophysics University of Edinburgh, Scotland
Prof. M.J.R. Wortel	Department of Geophysics Utrecht University, The Netherlands

The research for this thesis was carried out at:
Department of Structural Geology, Vening Meinesz Research School of Geodynamics. Utrecht University, Budapestlaan 4, PO Box, 80.021, 3508 TA, Utrecht, The Netherlands

ISBN 90-5744-020-2

The Alpine evolution of Thessaly (NW Greece) and Late Tertiary Aegean kinematics

De Alpiene evolutie van Thessalië (NW Griekenland) en de Laat Tertiaire Egeïsche kinematiek

(met een samenvatting in het Nederlands)

Proefschrift

ter verkijging van de graad van doctor aan de Universiteit Utrecht
op gezag van de Rector Magnificus, Prof. Dr. H.O. Voorma
ingevolge het besluit van het College van Decanen
in het openbaar te verdedigen op
dinsdag 18 mei 1998
des ochtends om 10.30 uur

door

Clare Rachel Walcott

geboren op 23 april 1966 te Londen (Engeland)

Promotor: Prof. S.H. White

CONTENTS

Chapter 4: Structural Evolution of the Thessaly

Chapter 5: Constraints on Aegean Kinematics

Chapter 6: Discussion and Conclusions

Summary

The Aegean region is one of the most studied regions currently undergoing post-orogenic extension. Numerous kinematic and dynamic models have been proposed to account for its active tectonics. Most recent studies have demonstrated that, since the onset of extension in the early Miocene, there has been a major reorganisation of the regional kinematics in the last 5 Ma. Hence, the mechanisms and models which account for active deformation may not necessarily be extrapolated backwards in time.

To date little is known about either the Tertiary kinematic evolution of the Aegean or the exact kinematic configuration before and after the post 5 Ma reorganisation. This thesis reconstructs the Alpine kinematic evolution of the NW Aegean and then uses this information to place constraints on possible models for the Alpine tectonic development of the Aegean area.

Initially, this thesis concentrates on the structural and metamorphic evolution of the Thessaly region of northern Greece which is situated near the northwest margin of the area of Aegean extension. A field study was carried out to determine lithological subdivisions, and their kinematic and metamorphic history in the Thessaly region. The size of the area selected lies between the scale of previous local studies and regional studies of Aegean tectonics. The location of the studied area, which lies between the well-studied areas of the Cycladic islands and Mt Olympos, means that the data presented and models formulated in the course of this study provide a crucial geographical and structural link in an Aegean-wide synthesis. Most importantly, it also provides a comprehensive set of kinematic constraints on regional dynamic models for the tectonic evolution of the Aegean area.

Thessaly: Lithologies and metamorphic evolution

One of the main barriers to correlating metamorphic, kinematic and structural results from previous local studies has been their use of inconsistent and/or undefined criteria to describe different tectonostratigraphic units or kinematic indicators. Hence, a new rigorous and objective system for discriminating between different lithologies and their recorded metamorphic, structural and kinematic environments has been developed. This system led to the lithological and metamorphic subdivisions outlined below.

The basement of the Thessaly region comprises a complexly deformed assemblage of Hercynian quartzofeldspathic gneiss and schist, mid-Mesozoic ultramafic ophiolite fragments, late Paleozoic to Mesozoic marble and early Paleogene flysch, as well as mafic and calcareous schists of unknown age.

Three major metamorphic events are recorded. The first two events (M1 and M2) occurred in the early Cretaceous period and late Cretaceous to Eocene period, respectively. At high structural levels, these two events involved greenschist facies metamorphism (M1.gns, M2.gns). However, at lower structural levels conditions evolved from higher grade epidote-albite amphibolite (M1.amph) through to epidote blueschist facies (M2.bls). The third metamorphic event is largely confined to east Thessaly and involved greenschist facies conditions.

The basement comprises two major metamorphic units or complexes in the east and west

respectively. The West Thessaly Complex preserves greenschist facies metamorphic events (M1.gns and M2.gns) whereas the East Thessaly Complex records a more involved metamorphic history. In the East Thessaly Complex, an initial phase of amphibolite facies metamorphism (M1.amph) has been overprinted by blueschist facies assemblages (M2.bls) and then again by greenschist facies (M3.gns) assemblages. Two further subdivisions of the East Thessaly Complex are recognised: an upper East Thessaly Complex which preserves pre late Cretaceous metamorphic events (e.g. M1.amph), and the lower East Thessaly Complex which records largely late Cretaceous and younger metamorphic events (e.g. M2.bls and M3.gns).

The relationships between the metamorphic, structural and lithological units presented in this thesis are complex and illustrate that any assumption that the boundaries of the different units necessarily coincide with each other is incorrect.

Thessaly: Kinematic evolution

The West Thessaly Complex records largely early Cretaceous ductile deformation whereas the East Thessaly Complex records entirely late Cretaceous and younger deformation. Details of these events are as follows:

1. Early Cretaceous, top-to-the-SSE thrusting (D1) is preserved only in the West Thessaly Complex but likely to have been an Aegean wide event, related to the onset of ophiolite obduction.
2. Early Cretaceous, E-W extension (D2) is preserved along the boundary between the West and East Thessaly Complex. The boundary may be a local feature related to ductile rotation in the Tertiary.
3. Late Cretaceous to Eocene, top-to-the-SW thrusting (D3) and erosion causing exhumation of blueschists occurred in the East Thessaly Complex and of the eastern portion of the West Thessaly Complex.
4. Oligocene to Pliocene, layer-parallel extension is observed across east Thessaly (D4) with top-to-the-N sense of shear and associated greenschist facies metamorphism. This event also involved widespread development of a fibrous calcite fabric which is interpreted to be formed under regionally low differential stress during exhumation of the basement.
5. A reorganisation of Aegean kinematics in the Pliocene (see below) is recorded across Thessaly by recent NNE-SSW extension along ~E-W trending normal faults (D6).

Regional Kinematics of the Aegean area

Kinematic indicators (ductile and semi-ductile stretching lineations, semi-brittle and brittle slickenlines) from across Thessaly were combined and correlated with similar data from published studies spanning the entire Aegean region. These were supplemented with new kinematic data from the Peloponnesos, Antiparos and Kea, areas which were poorly covered in the regional database and which prove to provide important kinematic constraints in a regional context.

The regional distribution of the orientation of stretching lineations is shown to be spatially consistent with paleomagnetic declinations. Together these record lithospheric-scale block rotation of the western Aegean since the early to mid Miocene. The combined regional kinematic and paleomagnetic data define the margins of a portion of the Aegean which has

undergone 30 degrees rotation during the late Neogene. Thessaly forms a central portion of this region which is termed the West Aegean Block. The block is bounded by the Scutari-Pec Line to the northwest, by the subduction zone to the west and by the Mid-Cycladic Lineament to the southeast. The border to the east is gradational and located in the northern Rhodope/ northern Aegean Sea region.

The kinematic evolution of the Aegean during the Tertiary

The Tertiary kinematic evolution of the Aegean has not been dominated by any single event but involved three stages:

1. Initial uniform NNE (~023 degrees) directed extension across the whole region.
2. Between the Oligocene and the late Miocene, the crust subdivided into two parts. The western part formed the West Aegean Block which rotated ~30 degrees clockwise. The eastern part, termed the east Aegean region, contemporaneously rotated ~19 degrees anticlockwise, although in a less coherent manner than the West Aegean Block.
3. After the latest Miocene, E-W trending faults developed across the west Aegean and the West Aegean Block subdivided into two portions. The southeastern portion (NW Cycladic area) coupled with the SE Cycladic area to form the Central Aegean Block which began to translate SW. The remained northern-northwestern portion of the West Aegean Block, which includes the Thessaly region, continued to rotate a further ~10-15 degrees clockwise.

Rotation of the West Aegean Block was aided by thermal weakening of the crust along its northeastern and southern margins, indicated by the distribution and timing of volcanism and igneous intrusions.

The outward bending of the Aegean Arc during the Miocene to Pliocene regional extension of the Aegean hinterland has not occurred by radial outward flow of the crust or by the rotation of a single block but by the partitioning and repartitioning of strain into a series of large (100 km) blocks, each of which comprised a complex amalgamation of smaller (10 km) crustal scale blocks.

It is suggested that the regional sharply defined Mid-Cycladic Lineament may have represented a zone of localised shear strain in the upper mantle induced by roll back and detachment of the subducted Mediterranean oceanic slab.

Chapter 1: Introduction

1.1 Preamble

Crustal deformation

Oceanic crust, unlike continental crust, tends to comprise coherent units many times wider than they are thick. As a consequence, the kinematics around their margins can be used to define the kinematics of the plate itself.

Continental deformation on the other hand, is much more enigmatic. Extensional and compressional deformation in the continental crust is usually distributed over wide areas on fault-bounded segments (thrust slices, half grabens). As a consequence, kinematics of the deforming region can not be constrained by data from along their margins alone.

Models that describe the kinematics of continental crust range from those that model deformation as an interaction of discrete microplates, or as widely distributed strain in response to ductile flow at depth. In all cases, it is agreed that any dynamic explanation of the observed kinematics must include the interaction of boundary forces and internal body forces.

Direct measurements of magnitude of stress in the crust are rare. Most 'stress measurements' are in fact derived from strain indicators (e.g. from plate motions, observed seismicity, or brittle and ductile strain directions). Thus, in the absence of direct stress data, the degree to which different dynamic models explain observed kinematics forms one of the few testable criteria with which the applicability of models can be discriminated. Since internal body forces often play important roles in dynamic models, kinematic constraints must be distributed within and on the boundaries of the deforming volume.

One process in which internal body forces play a significant role is post-orogenic extension. Throughout the world it is observed that mountain belts all ultimately collapse. In most current models it is assumed that this occurs because the extra mass of the thickened lithosphere of the mountain belt itself can not be supported by the surrounding crust and mantle. However, different models assume different processes by which the post-orogenic extensional strain is accommodated (for instance, the micro-plate versus continuum dichotomy introduced above). Thus, detailed kinematic data can be used to discriminate between dynamic models since different processes would usually cause differing distributions of strain across the volume.

Many previous studies on post-orogenic extension have focused on providing data which are used to construct and constrain models of the thermal and metamorphic evolution of the lithosphere. Few studies have concentrated on the link between the dynamic models and the resulting kinematics of crustal deformation which might be observed in any particular area.

Aegean post-orogenic extension

A classic location for studying post-orogenic extensional collapse is the Aegean region. This region comprises principally Greece, western Turkey and the Aegean Sea. Post-orogenic extension of the Aegean is thought to involve SSW directed extrusion of the crust from a once broadly east-west trending orogen (Le Pichon and Angelier 1979; Le Pichon et al. 1995). At the same time the western and southeastern Aegean margins rotated outward in diverging

directions (clockwise and anticlockwise respectively, Kissel et al. 1986, 1987; Kissel and Laj 1988; Morris and Anderson 1996).

Models proposed to account for the accommodation of the post-orogenic extensional strain in the region range from radial viscous spreading models to block rotation models (see section 2.5.3). Surface kinematics should help to discriminate between these models, but the kinematics of regional extension are not well understood.

1.2 Aims of this thesis

The aim of this thesis is to provide ductile, semi-ductile and brittle kinematic constraints across the whole Aegean region. To achieve this it was first necessary to carry out a detailed field- and laboratory-based lithological, structural and metamorphic study of the Thessaly region, north-central Greece. This region lies at the northwest margin of the focus of post-orogenic extension and its rocks record deformation during all stages of the Alpine Orogeny.

The kinematic data from Thessaly crucially link similar data from previous studies in the northern and southern Aegean. This allowed a meaningful compilation and correlation of Aegean-wide kinematics to be carried out and the formulation of a dynamic model to account for the kinematic evolution.

Questions addressed:

1. What was the kinematic and metamorphic evolution of the Thessaly region?
2. How does the evolution of Thessaly relate to that of the rest of the Aegean?
3. What is the relationship between active Aegean kinematics and kinematics of earlier deformation?
4. What constraints does the kinematic evolution of the Aegean basement impose on models of late-orogenic extension?

1.3 Organisation of this thesis

This thesis is organised into 6 chapters. The first chapter gives the outline of this thesis, and the second chapter concerns the evolution of the Aegean region. Chapters 3 and 4 present results of the detailed study of the Thessaly region, Chapter 5 extends this study to consider the Aegean-wide kinematic evolution, and finally Chapter 6 discusses the geological implications arising from this study. The chapters are outlined below.

Chapter 2 presents a review of the principle geological observations on the evolution of the Aegean. The review begins by presenting the Aegean in the context of its neighbouring areas, then discusses the evolution of the Aegean region in more detail and ends with a discussion of published dynamic and kinematic models propsed to account for late Tertiary evolution of the Aegean.

Chapter 3 presents a detailed lithological and metamorphic review of the Thessaly region, and a compilation of previous results from the Thessaly region. To accomplish this it was necessary to provide a rigorous and objective chronological and metamorphic framework since none has been used in the previous literature. Such a framework is a key necessity for correlating results of local field studies across large areas.

In Chapter 4, the meso- and microstructural evolution of the Thessaly region is presented. The region records a complex kinematic evolution. The earliest (lower Cretaceous) and latest

(Pliocene) stages of the Alpine evolution involve fundamental changes in kinematics.

In Chapter 5, stretching lineations developed during exhumation of the basement are analysed and correlated across the Aegean. In conjunction with paleomagnetic data, the lineations allow the kinematic evolution of the post-orogenic extension of the Aegean to be deduced.

Finally, in Chapter 6 the regional significance of the early stages of the Alpine evolution preserved in the Thessaly region and the possible mechanisms involved during post-orogenic extension are discussed in a regional context, and in terms of dynamic models presented in Chapter 2. The chapter concludes with a recommendation for future studies.

Chapters 3, 4, and 5 are written as self standing entities, to be published as individual papers and as such involve a detailed discussion at the end of each chapter. As a result it is inevitable that some repetition may incure. Chapter 6 provides a more general discussion about the regional significance of the findings of this thesis.

Chapter 2: Introduction to Aegean geology

2.1 Introduction

The Aegean region lies within the Alpine-Himalayan orogenic belt and as a result has experienced many of the major tectonic events observed in other parts of this zone of convergence. These include opening and closure of the Tethyan oceans, the onset of the Alpine-Himalayan Orogeny and the late-orogenic extensional collapse of segments along the orogenic belt. Other important tectonic events, such as the collision and suturing of the Apulian microplate in the early Tertiary and westward expulsion of the Turkey microplate in the late Tertiary, however, render the tectonics of the Aegean unique.

As the Aegean is one of the most accessible segments of the Alpine-Himalayan belt which is currently undergoing post-orogenic extension, the region has been the focus of much study. Many of the models presented to account for the region's tectonic evolution relate specifically to the unique conditions describe above. For this reason, the geological evolution of the region is discussed prior to a summary of dynamic and kinematic models that have been proposed to account for the late Tertiary extension and tectonics of the Aegean.

This chapter is divided into 3 parts. In the first part, a brief summary of review volumes and of key papers on Aegean geology is presented (Section 2.2). In the second part, aspects of the geological evolution of the Aegean relevant to this thesis are discussed. This discussion is separated into two sections. In the first section (Section 2.3), the evolution of the Aegean is placed in its regional (mediterranean) context. This section is important for the discussion in the final chapter (Chapter 6, Section 6.3). In the second section (Section 2.4), the structural, lithological, thermal and kinematic evolution of the Aegean region is summarised in more detail. This latter section provides an introduction to Chapters 2, 4, and 5 and helps provide the basis for the final part of this chapter (Section 2.5) which summarises tectonic models for the late Alpine tectonic evolution of the Aegean.

2.2 Previous reviews of Aegean geology

Due to intense study of the Aegean over the last 30 years, a plethora of information is published in the German, Dutch, French, Greek, Turkish and English literature. Despite this vast amount of work, remarkably few review volumes or papers have been published. As a result there is much debate and confusion concerning almost all aspects of the regional history. Many of these aspects are highlighted in the following two sections and in Chapters 3 and 4. Aspects of the regional evolution which have been addressed and reviewed are summarised below.

Some of the most general review or overview volumes on Aegean geology were published in the 1970's. Smith and Moores (1974) summarised the major structures, composition and timing of important events related to the Alpine Orogeny in the western Aegean. Early geological, geophysical and geochronological data are summarised in a series of review papers in Closs et al. (1978). Although no single volume or paper spanning such a range of subjects has been published since, several volumes have focused on various aspects of Aegean geology.

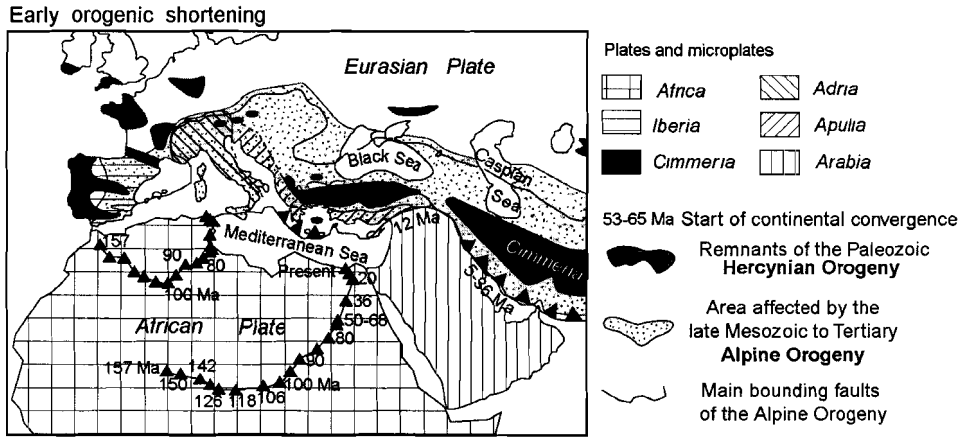

Figure 2.01

Map of the Alpine orogenic belt of the Mediterranean region showing some of the micro-continents (Apulia, Adria, Cimmeria and Arabia) that have been shed from Gondwana and have since sutured along the southern margin of Eurasia. The Alpine orogenic belt has formed subparallel to Hercynian orogenic belt. Also shown are the rotation paths of two points in Africa (shown as black triangles) through the Mesozoic from the data presented in Müller and Roest (1992). Map adapted from Dewey (1988) with additional data from Makris (1984), Mountrakis (1986) and Sengör et al. (1984b).

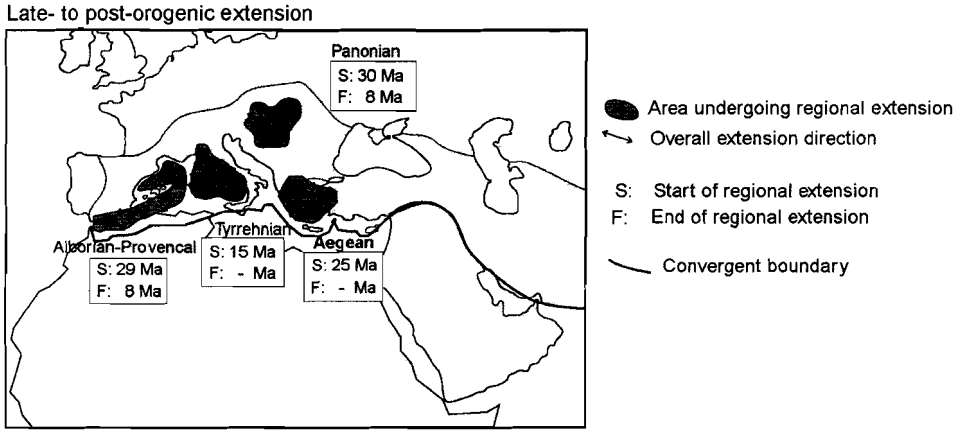

Figure 2.02

Map of areas within the Alpine orogenic belt which have undergone or are currently undergoing post- to syn-orogenic regional extension. Note that most areas of post-orogenic extension in the Mediterranean started to extend in the Oligocene to early Miocene (Lister et al. 1984; Lonergan and White 1997). The Aegean region is one of the few regions which is actively extending. Map adapted from Dewey (1988).

For example, the Paleozoic to early Tertiary evolution of the eastern Mediterranean was addressed in detail by Robertson and Dixon (1984).

Detailed descriptions of the region's lithologies (primarily cover sediments) are presented in the theses of French doctorate students (Brunn 1956; Aubouin 1959, 1962; Dercourt 1964;

Godfriaux 1968; Mercier 1973) whereas the subdivisions of west Aegean basement lithologies is discussed in Dürr et al. (1978) and in the volume of Jacobshagen (1986).

Okay (1989), summarises the Aegean blueschist facies metamorphism but few other papers discuss the evolution of metamorphism in the Aegean region. Rather, such discussion have tended to focus on smaller regions within the Aegean such as the Cyclades, Crete and the Peloponnesos (e.g., Okrusch and Bröcker 1990; Seidel et al. 1982), western Turkey (Okay 1989), Mt. Olympos area (Schermer et al. 1990). To date relatively little is known about the temporal evolution of the northern and eastern Aegean. The evolution of Tertiary volcanism across the Aegean however has been summarised in Fytikas et al. (1984) and again in Pe-Piper and Piper (1989).

Little work has been carried out on the kinematics of the early to mid-Alpine evolution of the Aegean. Regional Tertiary paleomagnetic data are summarised in the papers of Kissel and Laj (1988) and Marton (1993), and more recently were the focus of a volume edited by Morris and Tarling (1996). The results of these studies have been compared to kinematic indicators preserved in the basement by Jolivet et al. (1994a) and Gautier and Brun (1994). The kinematics of active deformation is relatively well understood. In the 1979's and 1980's data on active kinematic data were largely based on seismological studies (McKenzie 1972, 1978a; Le Pichon and Angelier 1979, 1981; Jackson and McKenzie 1988a, 1988b; Taymaz et al. 1991). However recent studies of active kinematics are largely based on displacements calculated by satellite geodetic techniques (see Le Pichon et al. 1995). Many of these papers are reviewed in Jackson (1994).

As this thesis is primarily concerned with the kinematic evolution of (western) Aegean basement rocks, this chapter concentrates in particular on some of the relevant aspects of the regional geological evolution (chiefly criteria used to subdivide the basement, the boundary conditions used in dynamic models and current kinematic data) which have received less attention in the publications described above.

2.3 The Aegean in its wider context: The Mediterranean

In this section, the evolution of the Aegean is discussed in a regional, Mediterranean-scale, context. The purpose of this discussion is two-fold. One purpose is to introduce a framework for the discussion of more specific aspects of the Aegean evolution which are presented in the next section (Section 2.4). A second purpose is to highlight features which may be common to other regions which have experienced a similar tectonic evolution to the Aegean (e.g. the Pannonian and Alboran basins, see below), and thus help to differentiate local and regional effects when trying to determine mechanisms involved in the Aegean tectonics.

The Alpine orogenic belt of the Mediterranean, lies subparallel to the Paleozoic Hercynian (or Variscan) orogenic belt (Figure 2.01). Hercynian metasediments, metavolcanics and intrusives now forms a significant portion of the basement of the Mediterranean. The collapse of the Hercynian Orogeny in the early to late Jurassic culminated in the development of the broadly E-W trending Tethys ocean. The presence a of major Paleozoic to Mesozoic Tethys ocean is inferred from ophiolitic fragments preserved within the Alpine-Himalayan belt, large volumes of passive margin sediments (which now form the bulk of the Mediterranean region) on the Hercynian basement and paleomagnetic declination data.

The southern margin of the Tethys ocean, Gondwanaland, is now represented by the African continent whereas the northern margin, Laurasia, is represented by the Eurasian continent (see Figure 2.01). The relative motion of these two continents reflects major changes in the tectonics of the Mediterranean and hence are discussed below. It should be noted that throughout the Mesozoic to the Tertiary, Eurasia has remained more or less stationary relative to the world hot-spot framework (Meijer 1995), thus only the motion of Africa is discussed.

Although there is a general consensus that the Tethys ocean consisted of a complex array of continental fragments and marginal seas, two major Tethyan oceans or oceanic systems have been proposed (see Robertson and Dixon 1984). These comprise a northern, late Paleozoic to early Mesozoic 'Paleotethys' separated by the Cimmerian continent (see Figure 2.01) from a southern, late Triassic-early Jurassic 'Neotethys'. Originally, the Paleotethys was thought to terminate west of the Black Sea (Figure 2.01; Sengör et al. 1984b), however, a Paleotethyan accretionary prism sequence has been identified recently which is located well to the south, in northwestern Turkey (Pickett and Robertson 1997). Thus, although there are two dominant paleo-oceanic systems recognised, the Aegean region appears to be dominated by the southern Neotethyan oceans (this is discussed in more detail in Section 2.4.3.2). This observation has important implications for Chapter 3 as relic ultramafics are used in this Chapter as marker horizons.

Reconstruction of plate movements using magnetic anomalies (see Figure 2.01 and Müller and Roest, 1992) show that the opening of the Neotethyan ocean complex was associated with left-lateral transtension between Africa and Eurasia continents. This transtensional displacement ceased in the early Cretaceous (~126 Ma) when Africa changed course by ~30° and started to translate eastwards, subparallel to the Eurasian margin (Figure 2.01). During this time the continental fragment of Apulia was shed from the northern margin of the African continent creating the Mediterranean sea in its wake. Magnetic anomalies suggest that the convergence of the two continents did not start to occur until ~100 Ma, in the early Cretaceous, when the African Plate changed course again by almost 45° anticlockwise and started to converge obliquely with Eurasian Plate (Figure 2.01). The convergence between the two plates first resulted in the collision of Apulia against the southern Eurasian margin in the mid-Cretaceous, and then the indentation of the Adria microplate in the latest Cretaceous (Le Pichon et al. 1988). Magnetic anomalies also show that relative convergence between the African and Eurasian Plates was at its most rapid between 110 and 60 Ma (Figure 2.01).

Traces of deformed basement related to a late Jurassic orogeny along the length of the Alpine-Himalayan orogenic belt have been interpreted as evidence for closure of the Paleotethys by suturing of the Cimmerian continent to the Eurasian continent (Mountrakis 1986; Sengör et al. 1984b). This orogeny is thought to have affected the basement in central and northern Greece. The closure of the Neotethys in the late Mesozoic/early Paleogene was marked by development of the Alpine-Himalayan Orogeny (Figure 2.01).

In the late Eocene-early Paleocene (70-50 Ma) the African Plate was almost stationary and as a result convergence ceased (Figure 2.01). Between 50 and 20 Ma, the convergence rate between Africa and Eurasia resumed its pre-mid-Cretaceous pace. This rate of convergence decreased by 50% approximately 20 Ma ago as the convergence direction between Africa and Eurasia became oblique (trending at 350°) to the broadly E-W trend of the Alpine orogenic belt (Figure 2.01). The effects of this change in convergence rate on regional tectonics is discussed in Chapter 6.

The change in convergence direction between the two plates in the early Miocene occurred

as many sites along the Alpine orogenic belt began to undergo late-orogenic extension (Figure 2.02). Despite many problems estimating the exact timing of the onset of extension, the period of regional extension typically lasted 20-25 Ma, as evidenced by the Pannonian and Alboran-Provençal regions which have ceased to extend (Figure 2.02). Thus, the Aegean region is unusual in that it is still undergoing active extension although extension there started over 25 Ma ago (Figure 2.02).

Most areas subject to post-orogenic extension are semi-circular in shape (Figure 2.02), with a diameter of ~ 600 km. The direction of maximum extension varies from extensional zone to extensional zone but always occurs either parallel or at right angles to the convergent plate boundaries (Figure 2.02).

About 10-15 Ma ago, collision between Eurasia and Arabia closed the Mediterranean Sea to the east (Dewey et al. 1986). This event has been related to onset of westward movement of Turkey (see Section 2.4.3.5).

2.4 The Aegean

This section concentrates on the lithologies and tectonic evolution of the Aegean region, but focuses in particular on the western Aegean which is the subject of Chapters 3 and 4. In this section, a general introduction to the regional distribution of lithologies across the Aegean is followed by a summary and a discussion of published lithological classifications. The first two sections are of particular importance to the discussion on criteria used to make lithotectonic subdivisions discussed in Chapter 3. The third section presents a detailed chronological review of Aegean tectonics.

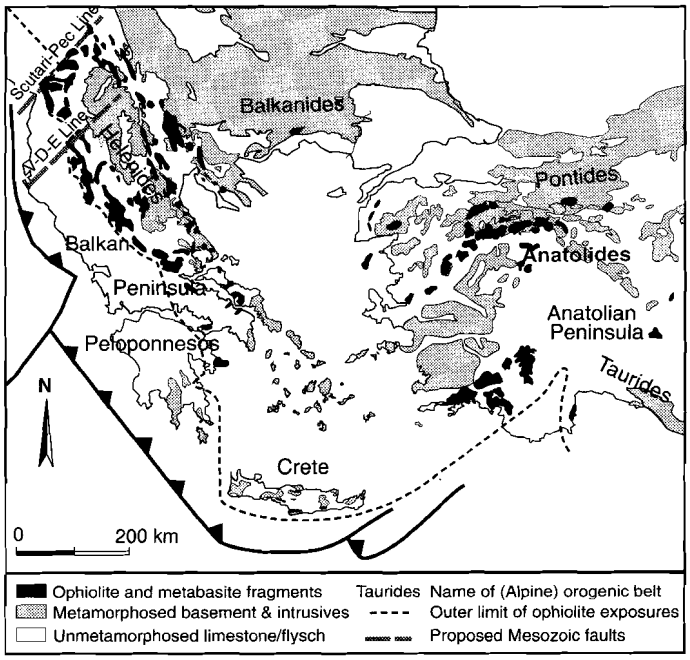

Figure 2.03
Map showing the distribution of ophiolite, metabasite units and metamorphosed basement in the Aegean. Note that ophiolites are mostly concentrated in two bands, although small areas are found scattered behind the ophiolite thrust front shown as a dashed line (Papanikolaou 1984). Other data from Spray et al. (1984) and Okay (1989). V-D-E Line = Vlore-Diber-Elborsan Line. See text for discussion.

2.4.1 Regional distribution of lithologies in the Aegean

To a first approximation, the lithologies of the Aegean can be divided into two major zones: (1) an inner basement 'core' that is largely composed of highly deformed, pre- and syn-Alpine metavolcanics, metasediments, limestones and intrusives that are unconformably covered by unconsolidated Neogene sediments and; (2) an outer margin, that is dominantly composed of weakly- to unmetamorphosed sheets of limestone and flysch (Figure 2.03). Note, however, that some basement also crops out on Crete and the Peloponnesos areas which form part of the 'rim' (Figure 2.03). The semi-arcuate shape of the outer margin (Figure 2.03) reflects a change in the orientation of faults and major lithological contacts from NW-SE on the Balkan Peninsula to E-W direction in western Anatolia.

A more detailed examination of the boundary between the inner core and outer rim reveals that the boundary is marked by a 50-400 km zone of scattered ophiolite, ultramafic and mafic blocks (Figure 2.03). Although the scattered blocks are found across much of the Aegean, inland of the dashed front shown in Figure 2.03, the ophiolitic blocks are mostly concentrated along two narrower (~80 km wide) bands. One ophiolite band lies within the basement 'core', thus subdividing the basement into two parts. The other ophiolite band lies along the outer edge of the basement core and marks the contact between the core and the outer margin (Figure 2.03). The ophiolite is thought to represent obducted Tethys ocean floor obducted during the early stages of the Alpine Orogeny (see Section 2.4.3.2).

2.4.2 Tectonostratigraphy of the Aegean

Several orogenic belts are recognised within the Aegean region. The trend of the orogenic belts is broadly parallel to that of the present subduction margin (see Figure 2.03). In the western Aegean, NW-SE trending mountains of the Balkan Peninsula and of the Peloponnesos are commonly referred to as the Hellenides. Geographically, the Hellenides pass into the Dinarides northwest of the Scutari-Peç Line. The Dinarides trend slightly more towards the WNW-ESE. In the eastern Aegean, mountain ranges trend broadly E-W, and form three orogenic belts. From north to south these are the Pontides, the Anatolides, and the Taurides. In the northern Aegean, a WNW-ESE trending belt is called the Balkanides.

2.4.2.1 Hellenides and Balkanides (Western and Northern Aegean)

Detailed sedimentological and structural studies between the 1940's to early 1970's led to the subdivision of the Hellenides and southern Dinarides into a series of elongate, NW-SE trending zones which lie parallel to the main structural fabric (Renz 1940; Brunn 1956; Aubouin 1959, Aubouin and Dercourt 1962; Godfriaux 1963; Mercier 1973). Some workers based the subdivisions on structural evolution (e.g. Brunn 1956), whereas other workers based the subdivision primarily on lithological and paleogeographical criteria (e.g. Aubuoin 1959). A summary of the criteria used to subdivide the lithologies and their compositions are outlined in more detail below.

Brunn (1956) divided the western Aegean into 3 major regions based on their structural evolution: (1), the external Dinarides (now called the External Hellenides), (2) the Internal Dinarides (now called the Internal Hellenides), and (3) the Rhodopian massif. The External Dinarides were interpreted to have undergone a single post-middle Cretaceous (Dinaric) orogeny whereas the Internal Dinarides contain evidence for both a Dinaric and an early

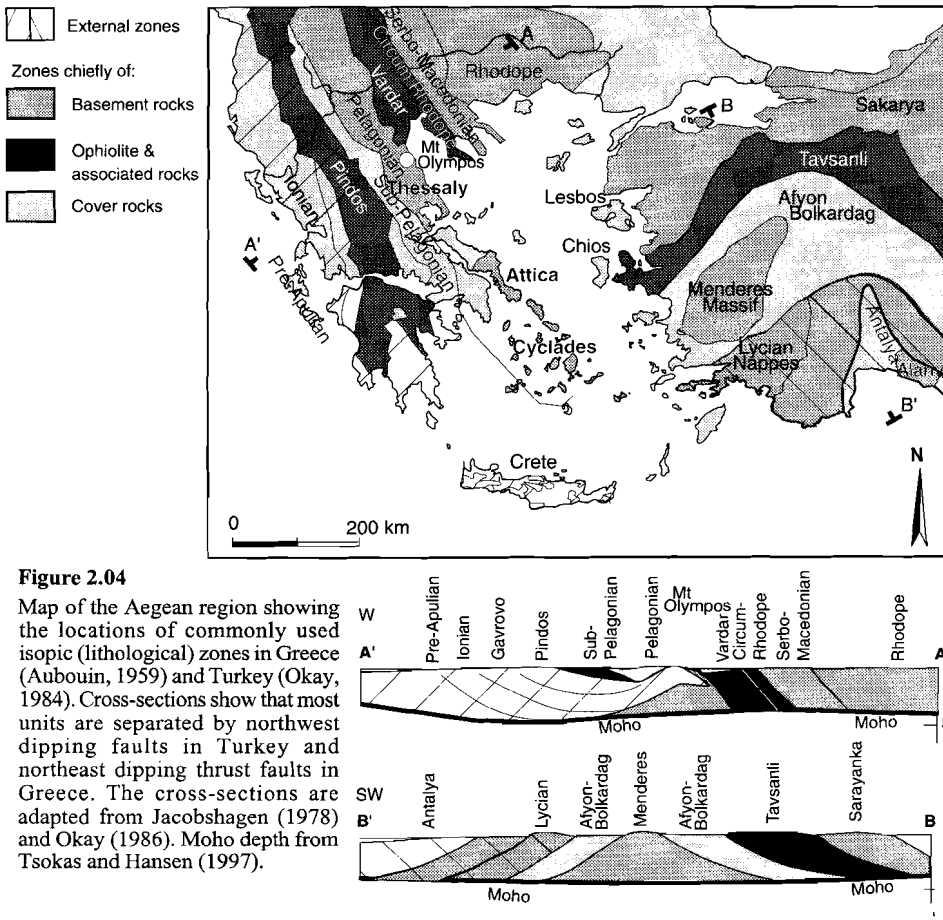

Figure 2.04
Map of the Aegean region showing the locations of commonly used isopic (lithological) zones in Greece (Aubouin, 1959) and Turkey (Okay, 1984). Cross-sections show that most units are separated by northwest dipping faults in Turkey and northeast dipping thrust faults in Greece. The cross-sections are adapted from Jacobshagen (1978) and Okay (1986). Moho depth from Tsokas and Hansen (1997).

(Hercynian and Cimmerian) orogeny. The Rhodopian massif, on the other hand, was thought to be part of a separate Carpathian-Balkan or Alpine Orogeny of late Cretaceous age and was argely unaffected by Aegean tectonics.

Within the three major tectonic regions of Brunn (1956), Aubouin (1959) recognised 12 smaller 'tectonic-isopic zones', i.e., zones of similar lithological and structural style (summarised in Figure 2.04). These 'isopic' zones, were defined in terms of a geosynclinal model and thus had specific paleogeographic interpretations (Figure 2.05). For example, the neritic and pelagic limestones of the External Hellinides (Figure 2.05) are interpreted as alternating, individual carbonate platforms (Pre-Apulian, Parnassos, Gavrovo Zones) and basins (Ionian and Pindos Zones) respectively. The Internal Hellenides comprised the Sub-Pelagonian, Pelagonian, Vardar, Serbo-Macedonian and Rhodope Zones, although, at that time, the latter two zones were not recognised by Aubouin (1959). The Pelagonian, Serbo-Macedonian and Rhodopian Zones are thought to represent a Hercynian continental basement and cover sequence, whereas the Sub-Pelagonian and Vardar Zones represent oceanic basins.

Mercier (1973), who emphasised a structural basis for the subdivision of units, later moved the boundary of the Internal Hellinides further east between the newly recognised Serbo-

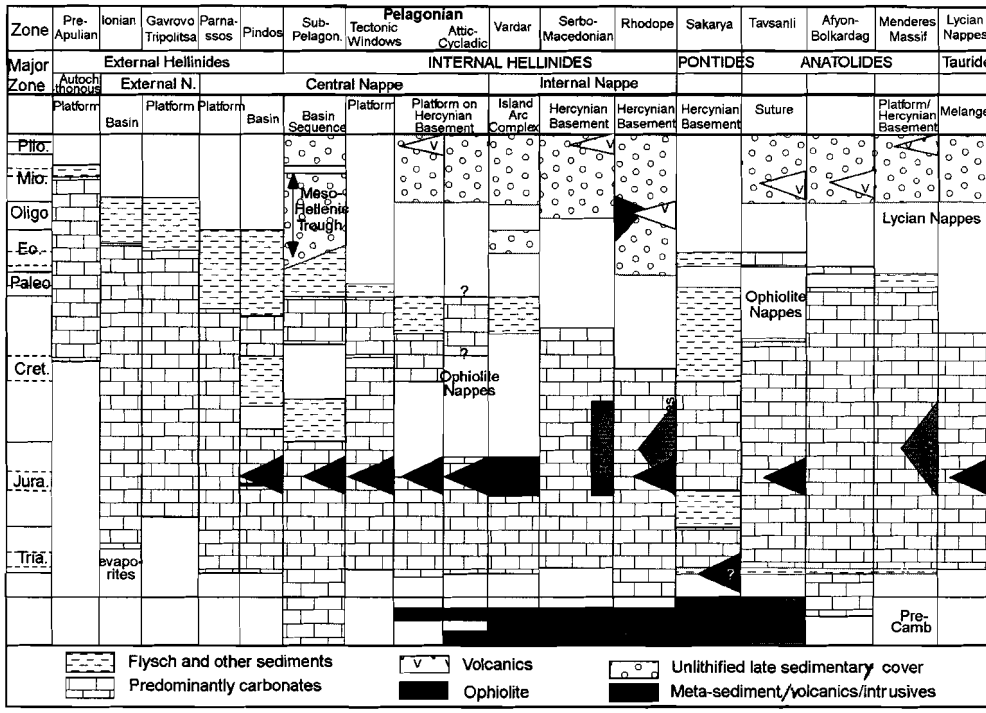

Figure 2.05: A table showing the typical lithological composition of Aubouin's (1959) isopic zones. See figure 2.04 for location of these units. Below the names of the individual zones are the names of groups of zones as proposed by; (1) by Aubouin (1959) in the western Aegean and Okay (1984) in the eastern Aegean, and by (2) Jacobshagen (1978). The lithological columns in the External Hellenides group, broadly represent stratigraphic sections. However, the columns in the Internal Hellenides, Pontides, and Anatolides are only estimates of the stratigraphic sections, severe tectonism in these regions has obscured many stratigraphical relationships. The widespread deposition of flysch across all external units in the mid- to late-Tertiary is thought to signal the end of passive margin sedimentation (represented by the thick sequences of carbonates). Unconformities above the flysch units in the early to middle Miocene provides a minimum time limit for the westward thrusting along faults bounding the zones (Figure 2.03). See text for discussion of the debates about the stratigraphy of some of these sections. Data from Godfriaux (1968), Dürr et al (1978), Jacobshagen et al. (1978), Roester (1978), Nance (1981), Okay (1984), Sengör et al (1984a) and Vergély and Mercier (1990).

Macedonian Zone and the redefined Rhodope Zone. He interpreted the Rhodope Zone as a relatively tectonically stable 'Zwischengebirge' between the Alpine belts of the Hellenides and Dinarides. Other workers have subdivided the Serbo-Macedonian unit into two, calling the contact zone between the Vardar and Serbo-Macedonian Zones, the Circum-Rhodope Zone (e.g. Jacobshagen et al. 1978). This latter zone is thought to represent a Paleotethys suture zone (as opposed to the Neotethyan suture zone represented by the Vardar Zone).

The modern boundaries between the isopic zones in the Aegean are generally NW-SE trending, NE dipping faults (Smith and Moores 1974). The contacts between the isopic zones of the External Hellenide zones are typically, medium to low-angle, reverse faults which sole into northeast dipping, ductile detachments (e.g. Hatzfeld et al. 1995), whereas the Internal

Hellenides are often bounded by normal faults which cross-cut the early thrust faults (e.g. the eastern margin of the Pelagonian Zone). Thus, the borders of the isopic zones are largely defined by Tertiary tectonic features and therefore may influence the interpretation of paleogeography.

As more information has become available, the variety of criteria used to define an 'isopic' zone has increased. Combined with the implication that there is a distinct paleogeographic setting for each isopic zone, this has lead to much confusion in defining the zones precisely. Thus although the 'isopic' zones are useful in a broad geographic sense, the use of variable criteria in combination with the long and complex evolution of the each isopic zone means that, in detail, these definitions are difficult to use.

Several suggestions have been proposed to resolve these problems. Some workers favour the use of the term 'isopic' for only specific time periods. For example, as the non-metamorphosed zones within the External Hellinides (as defined by Aubouin 1959) have similar late Tertiary histories, Underhill (1989) suggested that Aubouin's definition of isopic zones may only be applied usefully to describe the early Tertiary evolution. Similarly, Celet and Ferrière (1978) have noted that the structural history (in the case of the Pelagonian Zone) was regionally consistent only prior to the late Jurassic and hence proposed a revised definition the zone.

With the advent of plate tectonics, other workers have attempted to redefine the units into important tectonic or nappe slices. Such subdivisions have been undertaken by Jacobshagen et al. (1978) and later by Papanikolaou (1984). Jacobshagen et al. (1978) reinterpreted the lithologies of the west Aegean in terms of 6 major tectonic sheets (or 'Decken') lying between relatively undeformed foreland (pre-Apulian Zone) and hinterland (the Rhodope) zones. Another reinterpretation of the west Aegean basement has been presented by Papanikolaou (1984), who subdivided the basement into a complex array of smaller units. Although, these workers applied criteria more applicable for highly deformed basement, the definitions are loosely defined and synchronously use a range of lithological, metamorphic and structural criteria. Consequently, in many cases, the units are difficult to distinguish from one another. Problems with the criteria used by Jacobshagen and Papanikolaou and other workers in the Pelagonian Zone are discussed and addressed in Chapter 3.

Despite the complications outlined above, most of the literature still uses the isopic subdivisions of Aubouin (1959). One exception is the term 'Phyllitic Nappe' to refer to basement units of Crete and the Peloponnesos (see Figure 2.03) derived from Jacobshagen et al. (1978). In this thesis, Aubouin's (1959) isopic zones are used in a geographical sense only - no paleogeographic, tectonic or metamorphic interpretations are implied (see Figure 2.04). Where possible, simply the region is referred to. For example, the Pelagonian Zone (sensu Aubouin 1959), comprises of basement from three areas (Figure 3.01a), the Macedonian and Thessaly and Attic-Cycladic regions. The first half of this thesis focuses on the evolution of the Thessaly region in particular. It will be shown that the structural evolution of this region differs in many respects from the evolution of the Macedonian Massif and the Attic-Cycladic regions in Chapter 5.

2.4.2.2 Pontides, Anatolides and Taurides (Eastern Aegean)

Lithologies of western Anatolia are subdivided into a series of broadly E-W trending tectonostratigraphic zones (rather than isopic zones), which from north to south are: the Sakarya, Tavsanli and Afyon-Bolkardag Zones, the Menderes Massif unit and the Lycian

Nappes (Figure 2.04; Okay 1986). The Sakarya Zone consists of Paleozoic gneisses and schists which are topped by Mesozoic limestones and sediments and intruded by Cretaceous diorites and granodiorites. The sequence of a basement with a metamorphosed 'cover' is repeated further to the south but are interpreted as two separate zones, the basement zone is represented by the Menderes Massif whereas the cover is another zone (Afyon-Bolkardag Zone). The Tavsanli Zone represents a melange of mid-Mesozoic ophiolites, blueschist-facies metasediments and metavolcanics, and limestone. On the southern side of the Afyon-Bolkardag Zone are the Lycian Nappes. These nappes form a fold and thrust belt of Mesozoic sedimentary and volcanic lithologies which incorporate a peridotite-rich nappe (Okay 1986). All tectonostratigraphic zones north of the Lycian Nappes are unconformably covered by unconsolidated Tertiary sediments (Figure 2.05). The external zones of the Anatolian Peninsula includes the platform carbonates of the Alanya and Afyon-Bolkardag Zones. The Antalya Zone between these two is interpreted as a continental margin situated on the southern margin of a basin (Okay 1986).

2.4.2.3 Correlation of units between the western and eastern Aegean

The arcuate shape of the Aegean region has led many workers to try to correlate tectonostratigraphic and isopic zones between the western and eastern Aegean. However, differences in the metamorphic history and lithological compositions between these zones have presented many problems.

In the northern Aegean, it has been proposed that the NW-SE trending Vardar and Circum-Rhodope Zones are westward extensions of the Sakarya Zone and thus form an outer envelope of the Rhodope and Circum-Rhodope Zones (Papanikolaou 1984, Jacobshagen 1986, Koukouvelas and Doutsos 1990: see also Figure 2.04). In contrast, Okay (1989) suggested that the Rhodope/Serbo-Macedonian Zones are the western continuations of the Sakarya Zone. In this case the Serbo-Macedonian Zone is interpreted to include the Circum-Rhodope Zone. Okay (1989) also linked the northern Cycladic islands of Lesbos and Chios (Figure 2.04) to the Sakarya Zone whereas other workers have suggested that these islands are more likely to be part of the Vardar Zone (Papanikolaou 1984), or the Pelagonian Zone (Jacobshagen 1986).

Another correlation is between the basement of the Menderes Massif and the Attic-Cycladic region (e.g. Brunn 1956; Jacobshagen 1986; Papanikolaou 1984). Although, Bonneau and Kiesnast (1982) suggest that the cover of the Menderes Massif (the Afyon-Bolkardag Zone) is more similar to the basement units of the External Hellenides (i.e. the Pindos Zone, or Phyllitic nappe of Jacobshagen et al. 1978) rather than the Internal Hellenides. The Lycian Nappes of Turkey have been correlated with the Pelagonian/Sub-Pelagonian Zone (Jacobshagen et al. 1978) and with the Ionian Zone (Dürr et al. 1978).

Thus, despite the amount of work carried out in the Aegean there is very little consensus about how the eastern and western Aegean are linked. In Chapter 3 (Section 3.7.4), the results of study into the criteria used to define units in metamorphosed basement provide an insight into the causes for such difficulties.

2.4.3 Tectonic Evolution of the Aegean

There follows a chronological description of Aegean lithologies, metamorphism and tectonics. Although Aegean tectonics is dominated by the Alpine Orogeny and its subsequent

collapse, the lithologies which are affected by Alpine deformation are mainly derived from early Hercynian and Tethyan events, and thus these events are outlined below.

2.4.3.1 Paleozoic: The Hercynian Orogeny

Relics of the Hercynian Orogeny largely consist of granites, gneisses and the (as yet undated) metasediments they intrude, and are present in most basement zones of the Aegean (Figure 2.05). In the Thessaly region these lithologies form important marker horizons with which to understand the tectonic evolution of the region (Chapter 3). Little is known about the metamorphic conditions and tectonics of Hercynian deformation in the Aegean, although some workers have suggested that conditions may have reached upper greenschist to upper amphibolite facies (Dürr et al. 1978; Schermer et al. 1990).

2.4.3.2 Early to mid Mesozoic: Opening of the Tethys Ocean

Lithologies derived from the opening of the Tethyan ocean(s) include ophiolites and thick carbonate sequences. The composition, age and distribution of these lithologies across the Aegean is discussed below.

Tethyan oceans and ophiolite sequences

Remnants of the Tethyan oceans are predominantly concentrated along two bands, ~ 200 km apart, that run down the centre of both the Balkan and Anatolian Peninsulas (Figure 2.03). In the western Aegean, the ophiolite belts correspond to the Vardar and Sub-Pelagonian Zones respectively (also called the 'inner' and 'outer' ophiolite belts, Smith and Spray 1984), flanking the Thessaly region (Figure 2.04). In the eastern Aegean ophiolites are concentrated in the Tavsanli Zone and Lycian Nappes, and thus flank the Menderes Massif.

Although there is a difference in composition between the outer ophiolite belt in the western Aegean (which is dominantly composed of lherzolites, ferrogabbros, and olivine theoliites) and the inner belt (which is dominantly composed of dunites and olivine gabbros), geochronological studies reveal that the ages of both belts are very similar (160-180 Ma: Spray et al. 1984) and are therefore likely to form part of the same oceanic complex. The two major northern ophiolite bands in western Anatolia, are also interpreted as part of the same oceanic complex (Okay 1986).

Debate about the number and locations of Neotethyan oceans in the eastern Mediterranean has been discussed in detail by Robertson and Dixon (1984) and the reader is referred to this paper for further information. However, as the Thessaly region which lies within the Pelagonian Zone is flanked on all sides by ophiolite, this region has been an important focus for studies concerning the number and locations of oceans in this region (see Figure 2.06). Variation in the metamorphic evolution, associated kinematic structures and structural levels have led to a variety of interpretations of the source of ultramafic and basic blocks within Thessalian basement. These include the presence of a small 'Ambelakia' ocean (Figure 2.06a: Doutsos et al. 1993), incorporation of the part of the Vardar ocean (Figures 2.06 b, c, and d: Nance 1981; Schermer et al. 1990) or Pindos ocean (Barton 1975) (see Table 2.1).

It is not a primary object of this study to contribute further to the debate on the kinematics of ophiolite obduction, however, the number and locations of basins has important implications for the lithological study of Chapter 3 and the kinematic study of Chapter 4. Figure 2.06 demonstrates that while many workers agree that Vardar ophiolites are semi-autochthonous

	Outer Ophiolite Belt		Vardar Zone Inner Ophiolite Belt		Pelagonian Zone continental affiliation	Reference
One Ocean	no ocean		Vardar (Neotethys)	←	Apulian Plate	Aubouin (1970), Schermer et al. (1993), Papanikolaou (1984)
	no ocean		Vardar	(1) ← (2) ←		Jacobshagen et al. (1978)
	Othris	→	—			Barton (1990)
	Paleotethys	→	no ocean			Dercourt et al. (1990)
Two Oceans	Pindos	→	Vardar			Smith et al. (1975), Jones and Robertson (1991)
	Pindos (Neotethys)		Vardar (Paleotethys)		Cimmerian Plate/s	Mountrakis (1986)
	Pindos	← →	Vardar	←		Vergely & Mercier (1990)
	Pindos	→ (1)	Ambelakia	→ (2)	Pelagonian	Doutsos et al. (1993)

Figure 2.06: A figure demonstrating that the range in interpretations of the kinematics involved in ocean closure in the Alpine Orogeny is largely a function of the number and locations of oceans flanking the Thessaly region which is represented here by Pelagonian Zone (shown in a grey shade). Oceanic material is shown in black.

(e.g. Figure 2.06 b, c, and d), there is much debate regarding the derivation of ophiolites west of the Thessaly region (represented by gray shading in Figure 2.06). Some workers have interpreted the Pindos as a basin developed on thinned continental crust (Aubouin et al. 1970), while others have suggested that the basin became thin enough to be floored by ophiolite (Smith et al. 1975; Robertson et al. 1991).

Limestone sequences

Most of the external Aegean units (e.g. the External Hellinides, and Alanya and Antalya Zones) and much of the internal Aegean (e.g., the Pelagonian Zone) are composed of passive margin sequences (primarily carbonates, with minor cherts and radiolarites) which were deposited on the rifted Hercynian basement during the opening of the Tethyan oceans (Figure 2.05).

The stratigraphy of the external Aegean units represents the southerly flanks of the Apulian microplate. The Apulian microplate was bound to the north by the Neotethyan ocean(s) (see Table 2.1) and to the south by the Mediterranean Sea.

The thick sequences of early to mid Mesozoic limestones grade upward into a late Mesozoic flysch (Figure 2.05) which signalled the end of passive margin sedimentation and the onset of closure of the Tethys (Figure 2.05). Such a sequence of limestone and flysch forms the Mt. Olympos marble which lies in northern Thessaly within Pelagonian Zone and is of importance in the structural study of Thessaly (Chapter 4).

Mesozoic transform faults

Ophiolite bands are sharply offset along the Scutari-Peç Line in the northwestern Aegean (Figure 2.03). Approximately 60 km to the southeast of the Scutari-Peç Line, there is another northeast trending lineament, the Vlore-Diber-Elbasan Line (V-D-E Line in Figure 2.03). Both lineaments are thought to represent Mesozoic transform faults within Neotethyan oceans. These faults are amongst the few faults in the region which trend at a high angle to the subduction zone boundary. A similarly orientated structure involved in later Tertiary tectonics occurs in the central Cyclades area and is discussed in Chapter 5.

2.4.3.3 Mid-Mesozoic to early Tertiary: Closure of the Neotethyan oceans

Closure of the Neotethyan oceans is estimated to have started in the late Jurassic (Robertson and Dixon 1984). Evidence for this is largely based on the similarity in the ages (150-170 Ma) of granitic intrusives near the inner ophiolite band of northern Greece and the amphibolite sole (~150-178 Ma) of ophiolites (Spray et al. 1984). As the ages of limestone between the pillow laves associated with ophiolite is approximately the same, the ophiolites are thought to have started to obduct shortly after they were extruded (Spray et al. 1984). However, in most regions, e.g. the Thessaly region, there is a gap between the estimate of ophiolite obduction (>150 Ma) and the onset of tectonism estimated from the age of metamorphic fabrics (<135 Ma). This observation has led some workers to propose a two stage obduction process, termed the 'Eohellenic' and 'Mesohellenic' tectonic events respectively (Jacobshagen 1986). The 30 Ma period between these two Hellenic phases have been variously interpreted as a period of tectonic quiescence (Jacobshagen 1986), or as a period of rifting which resulted in formation of a small 'Ambelakia' marginal basin (Doutsos et al. 1993). Unfortunately, much of the evidence of these early tectonic events has been obscured by later tectonism and most workers in the region have not adopted this terminology.

Both Jacobshagen et al. (1978) and Doutsos et al. (1993) have suggested that thrusting during the early Alpine Orogeny (Eohellenic tectonic event) occurred in a NE-SW direction. The interpreted sense of thrusting however, differs between these two groups of workers. Yet other workers (Kilias et al. 1991) have suggested that the early Alpine deformation involved top-to-the-S directed thrusting in the present geographic reference frame (see Section 3.3.3.1 for a detailed discussion). To date the kinematics of the early stages of the Alpine Orogeny have received minimal attention. Structures related to this period, preserved in the Thessaly region, are examined in Chapter 4.

2.4.3.4 Peak of the Alpine Orogeny

Introduction

The Alpine Orogeny is the result of the closure of the Neotethyan oceans and continent-continent collision of Apulian and Adriatic microplates with Eurasia. Evidence for this orogeny includes widespread preservation of high-pressure metamorphism, late-orogenic intrusions, intense ductile deformation (chiefly folding) of the metamorphic basement, and the onset of flysch and molasse deposition over the passive margin sequences. Alpine structures are of vital importance in the study of the regional kinematic evolution (the subject of Chapter 5), thus the areas affected by metamorphic events related to the Alpine Orogeny are discussed below.

Metamorphic Events related to the Alpine Orogeny

Regional metamorphic events related to the Alpine Orogeny are summarised in Figure 2.07. An important point to note is that high-pressure metamorphism in the west of the region (Thessaly and Attic-Cycladic regions) during the Alpine Orogeny occurred contemporaneously with high-temperature metamorphism in the east and north of the region (Rhodope, NW Turkey and Menderes Massif). The significance of the thermal variations in terms of the regional kinematic evolution is discussed in Chapter 5 (Section 5.4.7).

In the eastern Aegean, blueschist facies metamorphism is primarily confined to a single band within the Tavsanli Zone of northern Anatolia (Figure 2.04: Okay 1989). In the western

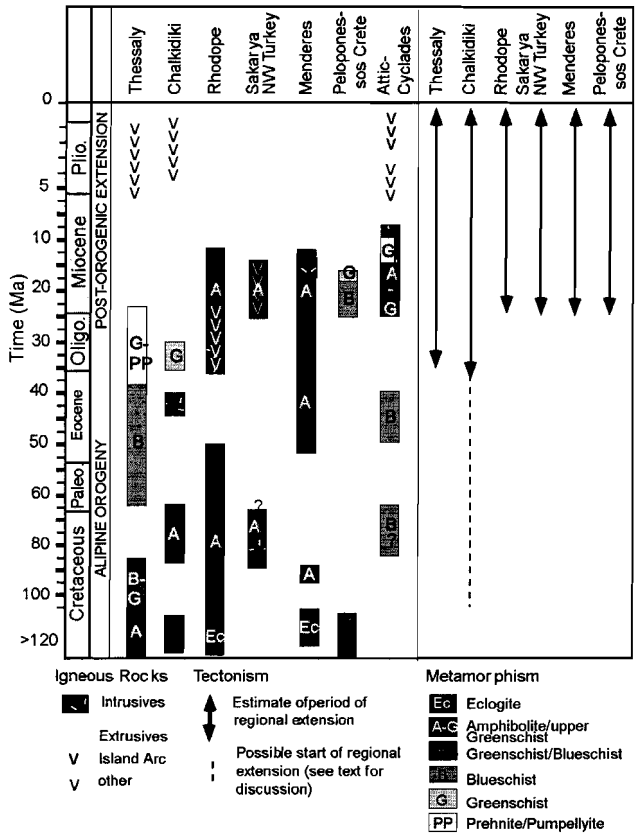

Figure 2.07

Integration of metamorphic histories of the various isopic zones in the Aegean with published estimates of the onset of regional extension (right hand column). Metamorphism during the peak of the Alpine Orogeny involved blueschist facies metamorphism in the western Aegean contemporaneous with higher temperature greenschist/amphibolite facies metamorphism of more western and northern regions. Note that the Thessaly region was not subject to volcanism until the Pliocene, and that it never experienced the thermal metamorphism experience in the Rhodope, Attic-Cycladic, and Menderes Massif regions. Data compiled from Seidel et al. (1982) Fystikas et al. (1984), Andriessen et al. (1987), Seyitoglu et al. (1992), Schermer (1993), Dinter and Royden (1993), Fassoulas et al. (1994) Pe-Piper and Piper (1989), Gautier (1995) Dinter et al. (1995), Hetzel et al. (1995, 1996).

Aegean, two bands of blueschist facies metamorphism are identified. The blueschist of the Thessaly and Attic-Cycladic regions are collectively referred to as the 'internal blueschist unit' or 'Cycladic blueschist belt' (Blake et al. 1981), whereas the blueschists which form the basement units of Peloponnesos and Crete (Figure 2.03) are referred to as the 'external blueschist unit' (Theye and Seidel 1991) or 'external metamorphic belt' (Papanikolaou and Skarpelis 1986). Blueschist metamorphism in the inner belts is Cretaceous in age in Anatolia (~88 Ma), and Cretaceous to Eocene in age in the Thessaly region (100-38 Ma: Schermer et al. 1990). The age of blueschist facies metamorphism appears to be younger in the Attic-Cycladic region (85-35 Ma ; Bröcker et al. 1993) and younger still in the external metamorphic belt (~20 Ma: Seidel et al. 1982). Thus, blueschists form three zones which trend subparallel to the present subduction zone and which decrease in age southwards but are all related to Alpine tectonism.

Structures and Kinematics related to regional shortening

Blueschist facies structures in the internal blueschist belt have often been used to determine the kinematics of the peak of Alpine metamorphism (e.g. Blake et al. 1981; Schermer 1993). The Thessaly region in northern Greece has been particularly important in such studies, as this region is less affected by a late Tertiary metamorphic overprint than the Cycladic region (Figure 2.07).

Stretching lineations and sheath fold axes typically trend NE-SW in the western Aegean and this observation has led many workers to suggest that the dominant trend of tectonic transport was in a NE-SW direction (e.g. Doutsos et al. 1993; Schermer 1993). As explained more fully in Chapter 4 (Section 4.2), there is little agreement on the sense of tectonic transport during the peak Alpine Orogeny (late Cretaceous to Oligocene), which varies between dominantly NE-directed (see also Figure 2.06: Barton 1975) dominantly SW direction (Figure 2.06b, c and d), synchronous divergent directions, and an initially SW followed by NE orientation (Figure 2.06a). The kinematics of the early Alpine Orogeny is closely linked to the interpreted position of Neotethyan oceans which were present or developed during the early stages of the Alpine Orogeny relative to the Pelagonian Zone (e.g. Figure 2.08 and Table 2.1).

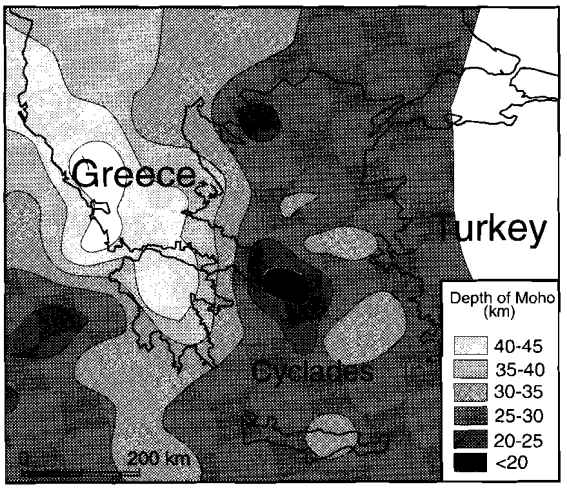

Figure 2.08

Map of the depth to the Moho determined by Tsokas and Hansen (1997). The thinnest section of the Aegean, corresponds to the location of the northwestern Cycladic islands. In the northwest Cyclades the Moho is ~15 km shallower than the Moho on the southeastern side of the Cyclades. The significance of this observation is discussed in more detail in Chapter 5.

An alternative interpretation of the early Alpine tectonics has been proposed by Blake et al. (1981). They noted that while stretching and mineral lineations are orientated NE-SW in the western Aegean, stretching lineations in the SE Aegean are consistently orientated N-S. They discussed the possibility of divergent rotation of the Aegean, however, they interpreted the orientations of stretching lineations to be the result of two separate subduction events (Blake et al. 1981). The first event was thought to involve NW-directed subduction under the western Aegean, forming NE-SW trending stretching lineations, whereas the second event was interpreted to involve east-directed subduction.

Thrusting during the Alpine Orogeny is thought to have imposed a strong structural fabric across the western Aegean which is now preserved as southwestward verging sheets (Burg et al. 1996; Dinter and Royden 1993; Jolivet et al. 1994a). Above one of the largest thrusts, the Pindos Thrust, is the Meso-Hellenic Trough (Figure 2.05). This 7 km deep, NE-SW trending trough lies due west of Thessaly, and records almost continual sedimentary infill from the mid-Eocene through to middle-Miocene (Figure 2.05). The trough is thought to have developed as a piggy-back basin, (Wilson 1993). This basin together with the late Cretaceous flysch of Pindos and Paleocene to Eocene flysch of the Ionian Zones, contains detrital glaucophane (Faupl et al. 1996) presumable derived from Alpine blueschists in the Thessaly region, of the Pelagonian Zone. These detrital glaucophanes thus provide constraints on the timing of blueschist exhumation.

Other basins developed in the Eocene are best preserved in the northern Aegean and tend to be small and E-W trending. The orientations of these basins change during the course of the post-orogenic extension (see Section 2.4.3.6).

Many workers have interpreted deformation during blueschist facies conditions as a result of regional shortening (Avigad 1991; Schermer et al. 1990; Schermer 1993). However, Gautier and coworkers noted that blueschist facies structures are apparently continuous with later extensional fabrics (see Section 2.4.3.5) and thus suggested that the last stages of blueschist metamorphism may have occurred during an extensional regime (Gautier et al. 1993; Gautier and Brun 1993, 1994).

2.4.3.5 Early-Late Tertiary: Late-orogenic extension

Approximately 25 Ma ago, as Apulia ceased suturing to Eurasia (Dewey and Sengör 1979), the Aegean started to undergo regional extension. Evidence of a regional extensional period is preserved as ductile shear zones progressively overprinted by increasingly brittle faults which demonstrate normal offset, as widespread development of grabens and half-grabens, as anomalously thinned crust (Figure 2.08) associated with high heat flow, and finally as widespread active normal faulting. The orientation of the boundaries of this extending zone (particularly the subduction boundaries) play an important role in providing boundary conditions for geodynamic and kinematic models discussed in Section 2.5. Uncertainties in the timing and position of the boundaries, as well as the thermal evolution of the extension, are discussed. Other important structural features to have developed during the late Tertiary are the North Anatolian Fault, the subduction zone and the Mediterranean Rise (as accretionary prism situated on the Africa plate). Each of these features are discussed in turn below.

The timing of the onset of extension

The first studies of extension in the Aegean region were based on active kinematic studies. McKenzie (1972) extrapolated active strain rates and calculated that regional extension had started in the late Pliocene to late Miocene. Lister et al. (1984), however, identified core complex style deformation in the central Cyclades and from the age of the ductile fabric suggested extension started 10 to 20 Ma earlier, in the early Miocene. Since Lister et al.'s observations, core complex style deformation has been observed in many other regions, e.g. Rhodope (Dinter and Royden 1993) most of which shows a Miocene age of extension. This suggests that much of the Aegean basement (other than some of the blueschists described above) was involved in extensional tectonics and exhumed semi-contemporaneously during the mid-late Miocene. This observation has important implications in Chapter 5. In this chapter, Tertiary ductile kinematic indicators developed in the basement are assumed to have behaved as passive markers above the brittle-ductile transition.

An Oligocene to mid-Miocene estimate for the onset of regional extension, is supported by the start of widespread basin development. Many of these basins form half grabens (Caputo 1990; Cohen et al. 1995; ten Veen and Meijer 1998). In the western Aegean, e.g. the Thessaly region, these basins typically trend NW-SE, parallel to the trend of the orogenic fabric, e.g. thrusts faults such as the Pindos Thrust which marks the western boundary of the Pindos Zone (Figure 2.09a). The Oligocene to mid-Miocene period is also marked by the onset of volcanism, discussed in the section on the thermal evolution of the Aegean below.

Development of the subduction zone

The current southern and western boundaries of the deforming Aegean region are formed by the subduction of the African Plate below Eurasia (Figure 2.09b). This subduction zone is thought have initiated in response to continued convergence of Africa towards Eurasia after Apulia became sutured to Eurasia.

In the literature, there are two positions that the subduction zone may be located (Figure 2.09b). This discrepancy is due to the presence of two major thrust zones, spaced 50-100 km apart (Figure 2.09). The southern thrust occurs where the African Plate starts to descend below a ~200 km wide wedge of accreted sediments. This wedge is termed the Mediterranean Rise and is composed of sediments resting on the African Plate which have been thrust back southwestward over the plate. The northern thrust zone occurs just south of Crete and marks the position where the Eurasian Plate overrides the African Plate. The latter zone is marked by a trench (called the Hellenic Trench). The contact between the sediments of the Mediterranean Rise and the thrust units above the Hellenic Trench is well defined southwest of the Peloponnesos and Crete. However, elsewhere it is very poorly defined. For example, the plate boundary in NW Greece is interpreted as a continental fault (e.g. Dinter and Royden 1993; Reilinger et al. 1997) or an offshore fault (e.g. Le Pichon et al. 1995). The confusion arises in part, as this boundary delineates continental-continent collision rather than ocean-continent collision. The Mediterranean Rise is mentioned here as recent studies suggest that the central part of this 'rise' collided with the African Plate 3-6 Ma ago and resulted in substantial impact on Aegean tectonics causing a rearrangement of the surface kinematics of the Aegean (Le Pichon et al. 1995) hence is important in the discussion of Chapter 5 and 6.

Estimates for the timing of the onset of subduction vary from 5 to 50 Ma ago depending on the data used to estimate the onset. As island arc volcanism in the Aegean only started 2-4 Ma ago (black dots in Figure 2.10) some authors have favoured a late Miocene/Pliocene age for the start of subduction (McKenzie 1978a; Taymaz et al. 1990). On the basis of the oldest rocks of island arc affinity, Le Pichon and Angelier (1979) calculated an age of 13 Ma. Seismic tomography, on the other hand, has shown that the current slab may extend to >800 km depth and assuming between 200 and 400 km of stretching in the upper crust and a subducting rate of 15 km/Ma, a much longer period of subduction (26-40 Ma) was estimated by Meulenkamp et al. (1988) and Spakman et al. (1988).

Development of the North Anatolian Fault

The North Anatolian Fault (NAF) is one of the most prominent features of the Aegean and now forms the abrupt boundary between the actively deforming portions of the Aegean and relatively stable Eurasia (Figure 2.09b and 2.11). The NAF is a major right-lateral, convex-northwards, strike-slip fault which runs from the central Zagros mountains in eastern Anatolia, across the northern Anatolian Peninsula where it bifurcates into two major strands into the north Aegean Sea (Figure 2.11). These strands have an important role in the broken-slat model proposed by Taymaz et al. (1991) discussed in Section 2.5.3.

The location of the North Anatolian Fault coincides with location of the Neotethys and Paleotethys suture zones (see Figure 3 in Mountrakis 1986). McKenzie (1978a) demonstrated the regional importance of this fault by noting that movement along the NAF (36 mm/year; Jackson 1994) entirely accounts for the westward translation of central Anatolia (31 mm/ yr). This rate is intermediate between the rate of Arabia-Eurasia convergence at its eastern termination (22 mm/yr: Reilinger et al. 1997) and Africa-Aegean convergence near its western

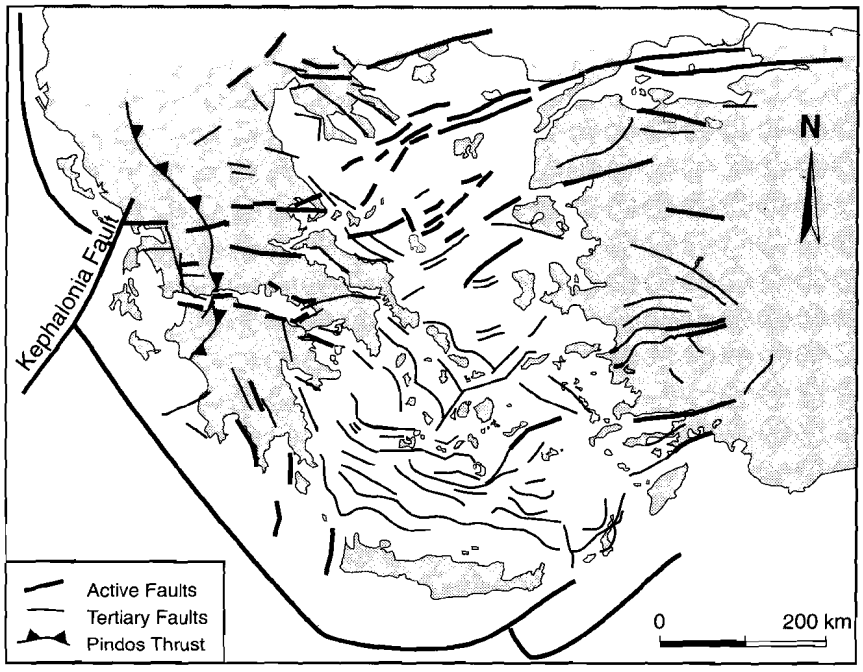

Figure 2.09a

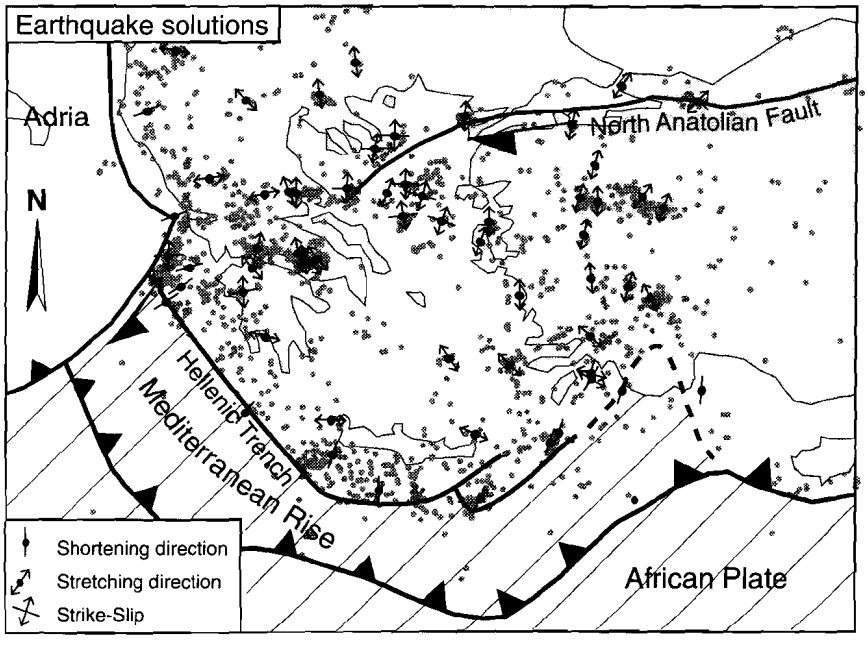

Figure 2.09b

Figure 2.09a and b: Maps of active and inactive Neogene faults (Figure 2.09a) and earthquake solutions (Figure 2.09b) determined in the Aegean region. Striped area in Figure 2.09b represents the African Plate. The boundary between the African Plate and the Eurasian Plate is marked by the Hellenic Trench. Right-lateral, strike-slip displacement occupies a wedge shape zone at the western end of the North Anatolian Fault (Figure 2.09b). Apart from a narrow rim of subduction zone-normal shortening, the rest of the region is undergoing regional north-south extension. Most active faults trend broadly E-W on both sides of the Aegean. Note the lack of active faulting in the central Cycladic region compared to the surrounding regions. Data from Gautier (1995), Meijer (1995), and Armijo et al. (1996).

termination (~40 mm/yr: Le Pichon et al. 1995).

Although, the North Anatolian Fault is clearly an important structure and has ruptured over almost its entire length during the last century (Ketin 1966), there is little earlier historical evidence for tectonic activity concentrating along the fault break itself (McKenzie 1978a). Only 25 km of post-early Pliocene offset is recorded (Barka and Hancock 1984; Barka and Kadinsky-Cade 1988), i.e., half of what might be expected at the current rates. While extensional basins situated along the fault started to fill in the Oligocene, current data suggests there was little significant movement along the fault until the late Seravallian-Tortonian (6-12 Ma: Seyitoglu et al. 1992). Hence, the North Anatolian Fault is interpreted to have initiated in eastern Turkey ~10 Ma ago and migrated westwards by linking extensional basins until it reached the north Aegean sea ~5 Ma ago (Armijo et al. 1996).

Thermal evolution during late orogenic extension

A thermal pulse associated with the start of regional extension resulted in widespread moderate to high temperature metamorphism and volcanism in the northern and eastern margins of the Aegean (Figure 2.07 and 2.10). This metamorphic event has overprinted much of the early Tertiary blueschist facies metamorphism in the central Cyclades discussed in Section 2.4.3.4.

Late Tertiary metamorphism locally reached amphibolite facies (Figure 2.07) However, large areas such as northern Greece (e.g. the Thessaly region) remained only weakly affected by this event (Figure 2.07). In the northwestern Turkey, Rhodope, and Menderes Massif much geochronological work needs to be done to constrain this event better (Figure 2.07 and references therein). However, the timing of the event is well constrained in the Cyclades region in the central Aegean where it spanned the Oligocene to early Miocene period. The metamorphism culminated in a series of mid-Miocene (9-15 Ma) felsic to intermediate intrusions (Altherr et al. 1982, 1979; Andriessen et al. 1979, 1987; Bröcker et al. 1993; Dinter et al. 1995; Kreuzner et al. 1978; Schliestedt et al. 1987; Wijbrans and McDougall 1986,1988).

The Oligocene was also marked by the start of volcanism in the Rhodope region of the northeast Aegean (Fytikas et al. 1984). Until the late Miocene, volcanism primarily affected the northern and eastern Aegean (Figure 2.10 and references therein). The next phase of volcanism started in the latest Miocene and was the first event to affect the Pelagonian Zone in the western Aegean (Figure 2.10). This was followed by development of an island arc in the Pliocene (~3 Ma: Fytikas et al. 1984).

Volcanism in the Aegean is both alkali and calc-alkali and varies from basaltic to rhyolitic composition (Figure 2.10: Fytikas et al. 1984). Alkali magmas form a volumetrically minor percentage of the total regional volcanism, hence most volcanism appears to be directly related to subduction (Pe-Piper and Piper 1989). Although volcanism is spatially associated with areas of high seismicity (compare Figures 2.09 and 2.10), the composition of volcanism appears

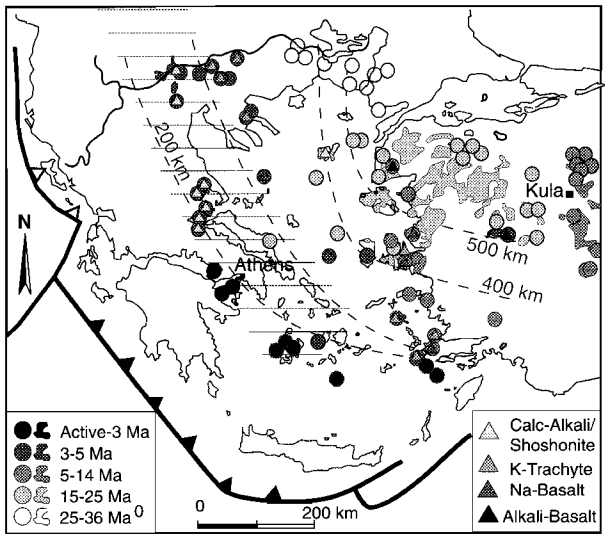

Figure 2.10
Map depicting the distribution, composition and age of volcanic rocks in the Aegean region. Volcanism is oldest in the northern Aegean and becomes progressively younger towards the east and south. The volcanic arc is less than 3 Ma old. Also shown are the estimated depths of the subducting plate (dashed line). The cross-hatched area represents the location where the subducting slab is thought to be detached. Data from Pe-Piper and Piper (1989, 1991) Seyitoglu et al (1997), and Spakman et al. (1988).

to be more closely associated with the depth of the subducting slab (as determined from seismic tomography, Figure 2.10) than to areas which have undergone the most crustal extension (Pe-Piper and Piper 1989). Nevertheless, a sudden change from calc-alkali to alkali volcanism ~15 Ma ago in Kula, western Anatolia, is thought to reflect a decreasing amount of crustal contamination due to thinning of the crust by regional extension (Seyitoglu et al. 1992). The outward (towards the subduction zone) decrease in age of volcanism described in the previous paragraph applies only to calc-alkali volcanism.

The causes of the mid-Tertiary regional thermal high have been interpreted variously as the result of crustal thinning (Lister et al. 1984; Faure et al. 1988, 1991; Lee and Lister 1992), the formation of back-arc basins related to the subduction of the African Plate under the Apulian microplate (Dürr et al. 1978; Papanikolaou and Zambetakis-Lekkas 1980; Blake et al. 1981; Altherr et al. 1982; Wijbrans and McDougall 1988), a jump in the subduction zone (Boccaletti et al. 1974; Fytikas et al. 1984) or of the injection of mantle into the base of the crust (McKenzie 1978a).

In Chapter 5 of this thesis the spatial and temporal evolution of regional volcanism is linked to the kinematic evolution of the Aegean.

The kinematics of late-Tertiary deformation

Paleomagnetic data provide an external reference frame with which to examine structural evolution. This is key to arguments presented in Chapter 5 and hence is discussed in more detail there. In this section, only data relevant to the discussion of models presented in the next section are summarised.

Paleomagnetic studies show that there are two zones of opposing rotation since the Eocene (Speranza et al. 1995) or mid-Miocene (Kissel and Laj 1988; Morris and Anderson 1996). Western Greece is thought to have undergone approximately 45° clockwise rotation whereas the eastern Aegean exhibits a less consistent pattern. The eastern Aegean is interpreted to have undergone between 25° and 33° anticlockwise rotation (Kissel and Laj 1988; Morris

and Anderson 1996). Rotation of western Anatolia is thought to have accelerated in the last 5 Ma to 5°/Ma (Kissel and Laj 1988). Taymaz et al. (1991) suggest that the eastern Aegean is currently undergoing 7°/Ma rotation. For many years, the boundary between these two zones of rotation has been interpreted as a gradual feature. However, Morris and Anderson (1996) recently suggested that the boundary was marked by a sub-marine fault (see Section 5.4 for detailed discussion).

The slickenlines developed on fault surfaces of known displacement age have been used to determine paleostress orientations. This is based on the assumption that if the crust is cross-cut by faults of all orientations then the resulting displacements represent the regional stress field. Using this method, Mercier et al. (1989) carried out a detailed study of faults and their slickenlines in northern Greece. From these data, they determined three events. First, WNW-ESE extension in the late Miocene, second NE-SW extension between the Pliocene to early Pleistocene, and finally N-S extension from the Pleistocene to present. Similar patterns have been observed in the Thessaly region (Caputo and Pavlides 1993), and are discussed in Chapter 4.

In the Pliocene, new faults with an approximately E-W orientation began to cross-cut the older NW-SE trending basins. The significance of this cross-cutting event as an important kinematic event has not received much attention in the literature, and is addressed in Chapters 5 and 6.

2.4.3.6 Active kinematics

Kinematic models of active extension are largely based on satellite geodesy and earthquake solutions (Figures 2.09 and 2.11). Many were reviewed in Jackson (1994). Other data sources spanning longer time periods include displacement data obtained from faults of, wherever possible, known age (e.g. Mercier et al. 1989). The SW Aegean is moving in a 236° direction at the rate of ~30 mm/yr (Figure 2.11 and references therein) and the northward velocity of

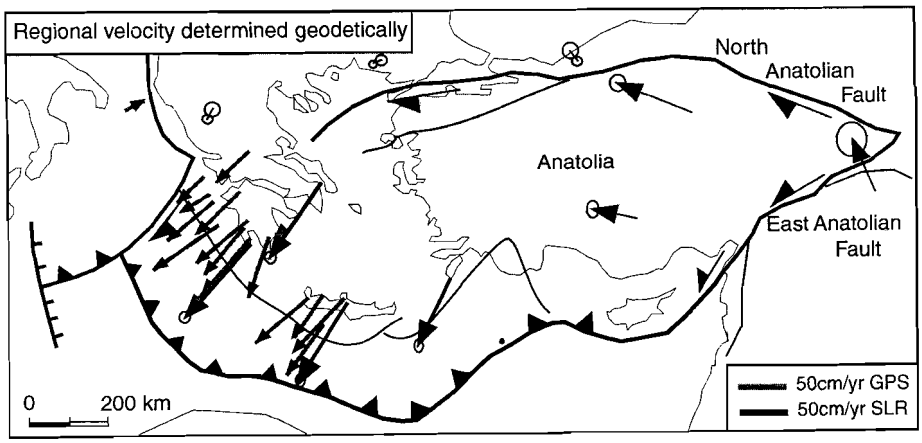

Figure 2.11: Satellite Laser Ranging and Global Positioning Satellite displacement data (relative to Eurasia) show that there is little displacement immediately north of the North Anatolian Fault. In eastern Anatolia the crust is translating towards the westnorthwest whereas in the Aegean the crust is translating fairly uniformly towards the southwest. Data from Le Pichon et al. (1995).

the African Plate is 10 mm/yr. Hence there is an overall convergence rate of 40 mm/yr at the Mediterranean trench. Despite intense seismic activity (Figure 2.09b), the northern Aegean is undergoing much less translation relative to Europe. The area undergoing the fastest extension is on the western Peloponnesos (0-5 mm/yr, Figure 7 in Le Pichon et al. 1995).

Seismicity in the Aegean is widely distributed. In general, earthquake solutions indicate that there is compressive stress along the perimeter of the Aegean with some degree of tension in a direction parallel to the margin (Figure 2.09b). Earthquake solutions from the central Aegean show dominantly normal senses of slip, whereas earthquakes with right-lateral, strike-slip displacements are localised around the North Anatolian Fault. Note however, that seismic activity appears to have ceased in the central southern Aegean (Jackson 1994). The lack of seismicity in this region indicates the possibility that the region may behave as a relatively rigid plate; this will be explored in the discussion of regional tectonics addressed in Chapter 5.

2.4.3.7 Summary in relation to later chapters

The summary of the geological evolution of the Aegean outlined throughout Section 2.4.3 provides background information on the following:

- recent Alpine to post-Alpine thermal and kinematic evolution necessary for the discussion of kinematic and dynamic models in Section 2.5,
- the spatial and temporal distribution of Mesozoic and Paleozoic lithologies which form the basis for the lithological study of eastern Thessaly presented in Chapter 3,
- an Aegean-wide context for the structural study of eastern Thessaly presented in Chapter 4,
- the lithological and metamorphic basement evolution across the Aegean which is important for both the study of Alpine kinematics of Aegean basement presented in Chapter 5, and for the discussion of the relationships between kinematic and thermal evolution of the Aegean discussed in Chapter 5.

2.5 Models of Aegean Tertiary tectonics

2.5.1 Introduction

The Aegean region was one of the first areas in which active regional post-orogenic extension was recognised. Together with studies of the Tibetan region, and the Basin and Range province of North America, the Aegean has played an important role as a testing ground for models proposed to account for such extensional kinematics. While many workers have discussed aspects of regional tectonics, this section concentrates primarily on work which aims to explain the regional-scale kinematics or dynamics. To date, the most reliable regional kinematic data are active displacements determined from earthquake source solutions, and more recently, Satellite Laser Ranging (SLR) and Global Positioning System (GPS) geodesy. Accordingly, most detailed kinematic and dynamic models are primarily concerned with active post-orogenic deformation. The theories proposed are separated into two groups, dynamic and kinematic models. Although in some cases kinematic models have been linked to a dynamic interpretation, few dynamic models predict the observed evolution of surface kinematics.

2.5.2 Dynamic Models

In this section, the dynamic models which may explain the Tertiary tectonics and in particular the extension of the Aegean are reviewed. All models involve a balance of the forces which act within and across the margins of the Aegean boundaries. The Aegean boundaries are defined to be the subduction zone in the west and south Aegean and south of Turkey (see Section 2.4.3.5), and diffuse boundaries in western Anatolia, northern and northwestern Greece. However, as the North and East Anatolian Faults effectively appear to transfer motion from eastern Anatolia westwards (Figure 2.11), the dynamics of the whole of the Anatolian region are important in some of the models discussed below. Forces which are derived from processes inside the boundaries are discussed first, followed by a discussion of forces which act across the boundaries. Various authors balance these forces to account for the observed extension in different ways and these variations are examined in the final section.

2.5.2.1 Forces involved in dynamic models

(1) Within the Aegean boundaries

Forces that are derived internal to the boundaries comprise those that act within the crust or lithosphere, and that act at the base of the crust or lithosphere. Forces within the crust/ lithosphere are largely due to the gravitational potential energy gradient between either an orogen (high gravitational potential) and neighbouring regions (lower gravitational potential) or between density inhomogeneities within the orogen. In the absence of resistive forces, material tends to flows from areas of high gravitational potential to areas of low gravitational potential. Forces at the base of the crust may be induced by the flow of the upper mantle which causes a shear force at the base of the crust/mantle interface (Karig 1974).

(2) Across Aegean boundaries

Forces at the margins of the Aegean include those due to interaction between the overriding Aegean crust and the (old) subducting Mediterranean slab and those derived from continent-continent interactions. The high density of the subducting slab relative to the surrounding mantle causes the subduction zone hinge to retreat (southward in this case) which in turn reduces the frictional force on the margin of the overriding plate (Wortel 1980). This frictional force varies with changes in the rate of subduction, the angle of subduction, and the mechanism of accretion (e.g. frontal versus underplating) (Platt 1986).

Forces which act across continent-continent boundaries include a compressive force across eastern Anatolia, due to the northwards movement of the Arabian Plate which forces the area between the eastward converging North and East Anatolian Faults westwards (Figure 2.11), much like a pip squeezed between two fingers (Dewey and Sengör 1979). An alternative explanation for the westward displacement of estern Anatolia is that the gravitational potential of the Zagros Mountains of eastern Anatolia and Georgia creates a negative gravitational potential gradient to the west. This causes an east-west compressional stress which pushes Turkey westwards (McKenzie 1972). Finally, a compressional force in the north and northwest of Greece caused by the presence of Adriatic microcontinent which is thought to resist northwards or westwards motion of the Aegean (Taymaz et al. 1991).

Model	Key observations addressed	
Models based on forces at the base of the continental crust		
A: Back-Arc extension Retreating subduction zone due to: (1) Secondary convection	(1) Maximum extension often is located behind island arcs where heat flow is the highest	
Models based on gravitational potential		
B: Orogenic Collapse Potential energy of orogen drives extension due to catastrophic removal of the base of the crust by: (1) Convection (2) Eclogitisation	(1) Oceans often develop parallel to the trend of old orogenic belts and visa versa. (2) Orogenic belts are relatively weak (3) Exposure of deep basement with relatively little erosion (4) HP followed by HT metamorphism	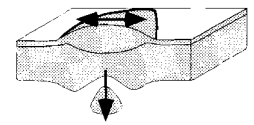
Models based on differential boundary forces		
C: Expulsion of Turkey (1) Squeezing Turkey westwards due to the collision of Arabia with Eurasia (2) By the potential gradient of the Caucasus Mountians relative to the Mediterranean	(1) Movement of the NAF is similar in magnitude to westward movement of Turkey (2) Some paleomagnetic rotations in Turkey are anticlockwise (3) A calculated potential gradient between the Caucuses and the Mediterranean	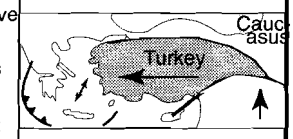
Models based on forces within the slab		
D: Subduction Pull Retreating subduction zone due to: A potential gradient which causes the flow of material over a free boundary	(1) The subduction zone is retreating southwards relative to Eurasia (2) A calculated potential gradient between the overriding plate and the Mediterranean	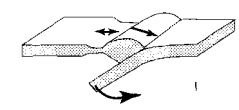
E: Slab Detachment Tear in the slab increases and concentrates pull on the downgoing slab	(1) Tomographic images suggest the slab is detached at 270 km depth under western Greece but is continuous under Crete	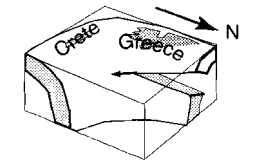
Models based on a combination of internal and external forces		
F: Accretionary Wedge Extension occurs when there is a decrease in basal friction relatative to the potential energy of an accretionary prism.	(1) The presence of blueschists in many accretionary prisms. (2) blueschist in the footwalls of normal faults	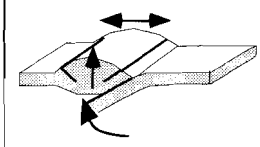

Figure 2.12a

Dynamic (Figure 2.12a) and kinematic (Figure 2.12b on page 43) models for late to post orogenic extension of the Aegean region with the key observations upon which a particular model is based. See text for discussion. Published in Dewey et al. (1988), Dewey et al. (1993), Le Pichon & Angelier (1979), McKenzie (1978a), Platt (1986), Platt and Vissers, 1989, and Spakman et al. (1988).

2.5.2.2 Models of extension

(1) Models based on forces at the base of the continental crust *(Model A in Figure 2.12a)*

Back-arc extension or secondary convection has been proposed to explain the presence of basins behind island arcs such as in the Japanese Sea (Karig 1974). Although back-arc extension was originally defined as extension that occurs behind an island arc in a direction at right angles to the line marked by volcanoes, it has often been used to refer to any extension above a subducting margin in an intra-oceanic setting. Back-arc extension is thought to be the result of convection currents situated between the overriding plate and the subducting slab which diverge at the base of the overriding plate exerting an extensional shear force (Figure 2.12a). Though much of the thinned region within the Aegean occurs behind the island arc, the thinnest area is in the northwest Cyclades (Figure 2.08) where the subducting slab is less than 200 km below the surface. This suggests that there may not be enough space for significant convection currents to occur.

(2) Models based on delamination of the crustal root *(Model B in Figure 2.12a)*

Regional extension due to gravitational potential energy gradient was first suggested by Molnar and co-workers to explain active normal faulting observed at high structural levels in Tibet (Molnar and Tapponier 1975) and the Andes (Dalmayrac and Molnar 1981). In the Aegean, McKenzie (1978a) suggested that although regional tectonics is largely controlled by external forces, extension within the Aegean is the result of a detachment of part of the lithosphere which causes the crust to sink and extend outwards (Figure 2.12a).

Dewey (1988) expounded these theories by suggesting that orogens are anomalously weak due to the presence of numerous shear zones (e.g. thrusts), and become weaker with time due to reequilibration of the geothermal gradient. Furthermore, he suggested that the 'collapse' of orogens is one part of an 'orogenic cycle' and one of the main reasons why orogens and oceans tend to be located in the same regions (see Wilson 1966). In Dewey's model, regions above 3000 m extend due to their inherent gravitational potential energy, regions undergoing extension at lower elevations require some sort of catastrophic removal of the crustal root of the orogen, e.g. by convective removal. Alternatively, Platt and Vissers (1989) suggested that an increase in density of the crustal root through eclogitisation could cause the root to 'drop' off.

By removing a portion of the crust instantaneously, the influx of mantle results in an increase in the integrated density of the orogen, causing the crust to sink and extend outwards under gravitational forces. However, to thin the crust sufficiently to form a new oceanic rift, other external plate boundary forces are required (see below).

Note that none of the above models predict surface kinematics in detail. Support for these orogenic collapse models, in particular, is based primarily on the observation that extension tends to occur near the (presumed) centre of the ex-orogen and that a thermal pulse is often associated with, or shortly post-dates, the onset of regional extension. However, it is often difficult to determine whether the thermal pulse is the cause or effect of extension (see McKenzie 1978b). Orogenic collapse also aims to explain the observation that, in many orogens deep crustal lithologies are exposed without evidence of massive erosion. Their exhumation is thought to occur through exposure of the rocks in the footwalls of normal faults (Platt 1986). Note, however, that the latter mechanism need not be confined to gravitational collapse models alone.

(3) Models based on differential boundary forces *(Model C in Figure 2.12a)*

In other models driven by a gravitational potential gradient, extension is caused by the flow of crust over the subducting Mediterranean oceanic floor (Figure 2.12a). Subduction of the Mediterranean is thought to have initiated about 10-12 Ma ago. Hence, this margin may offer less resistance than the other margins surrounding the Aegean which are undergoing continent-continent collision at their boundaries. In these models, the crust in the overlying plate in these models flows south faster than material is input from westward translating Anatolian margin and therefore resulting in extension (Le Pichon and Angelier 1979; Dewey and Sengör 1979).

(4) Models based on forces within the slab *(Model D and E in Figure 2.12a)*

Retreat of the subducting slab due to its own weight is called 'slab roll-back' (relative to an external reference frame) and can be either the cause or consequence of extension (Figure 2.12a). One specific example of such a process is 'slab detachment' (Figure 2.12a). This theory developed from the results of seismic tomography which appeared to show that while the downgoing slab could be imaged to >700 km depth under Crete, a 150 km long segment between 100 and 250 kms depth, below western Greece may be missing (Spakman et al. 1988). The missing section of slab was interpreted as a tear or break in the slab (Wortel and Spakman 1992). Since the magnitude of slab pull is in part, due to the length of the subducted portion of the slab, it was proposed that the magnitude of the resistance between the subducting and overriding plates would be least near the nose of the tear where the lower portion of the slab is still joined to the upper portion. The weight of the detached portion of the slab would cause the tear in the slab to propagate (under its own gravitational forces) and cause localised slab retreat and in turn cause variations in the internal stress in the overriding Aegean plate.

(5) Models based on a combination of internal and boundary forces *(Model F in Figure 2.12a)*

In the deforming wedge model of Platt (1986), the tectonics of the wedge are controlled by ratio of two major forces. These are: 1) the outward and downward force induced by the gravitational potential of the accretionary wedge; and 2) the resistive force due to the interaction of the subduction zone with the overriding margin (Figure 2.12a). Extension within the overriding plate in this model may be caused by a decrease in the rate of subduction or the slope of the subducting plate, and a 'weakening' of the rheology in the overriding plate.

2.5.3 Kinematic Models

One of the most fundamental differences between the various kinematic models of the Aegean, is how strain is distributed across the deforming region. There are two end-member possibilities: one is that strain is greatest along discrete horizons bounding areas in which little deformation occurs (plate-like models), the other is that strain is distributed evenly across the whole deforming area (distributed-strain models). Although the latter theory has recently been used to describe the kinematics of regions such as the Himalayas (England and Houseman 1988), a mechanism between the two end-members is probably the most realistic in the Aegean (e.g. Armijo et al. 1996). Indeed most of the models described below lie between

Figure 2.12b

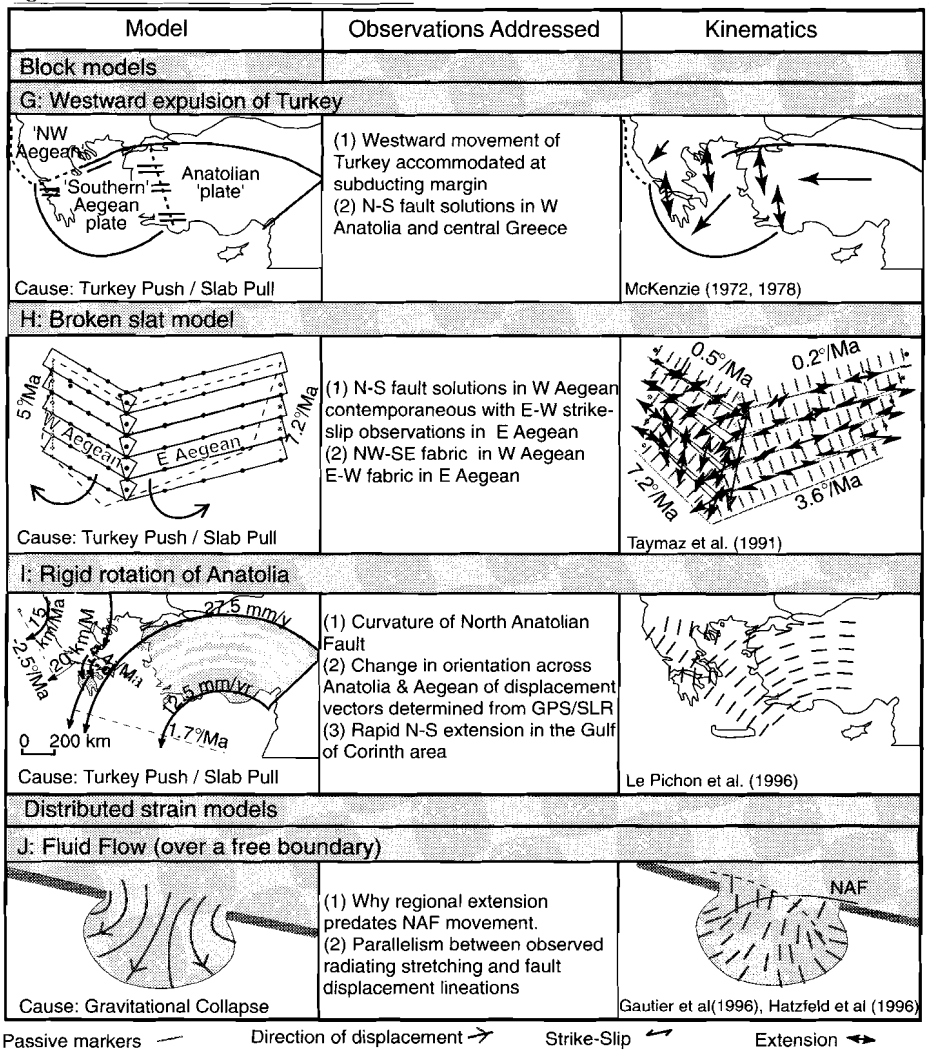

the two end-members. Note that the categories of models below are not necessarily those used by the authors themselves. In what follows, models are described in order of the number of discrete plates incorporated in the model.

2.5.3.1 Block models

Three-plate model: *(Model G in Figure 2.12b)*

In this model, McKenzie (1972, 1978a) used earthquake solutions to suggest that the Aegean region could be subdivided into 3 domains. The western Aegean comprises two domains: a northwestern and a 'southern' Aegean microplate, whereas the eastern Aegean comprises a

single Anatolian microplate (Figure 2.12b). The region between the Anatolian microplate and the two western Aegean plates was modeled as a wide zone of north-south extension (i.e. E-W grabens) whereas, the region between the northwest and southern Aegean plates was modeled as a zone of distributed right-lateral slip and north-south displacement (McKenzie 1978a). Only the central portion of the southern Aegean microplate region is characterised by a lack of seismicity.

Two-plate uniaxially-rigid model: *Broken slat model (Model H in Figure 2.12b)*

A two-part, uniaxially rigid block model, again based on earthquake solutions (as well as the dominant regional faulting fabric), is commonly known as the broken slat model (Taymaz et al. 1991). This model has recently gained much support in the literature from paleomagnetics (Figure 2.08; Atzemoglu et al. 1994; Kondopoulou et al. 1996; Morris and Anderson 1996), although the model was originally intended to explain active kinematics. The crust is modelled as a series of slats (representing elongate half-grabens), which are fixed by a pin (or hinge) onto a 'plate' at each end. The plates represent the Eurasian Plate and Anatolian microplate respectively. Each slat is broken in half in the middle and rejoined by a hinge (Figure 2.12b). The left side of the uppermost slat is fixed, representing the relatively stable Eurasian Plate. When the end of one group of slats are pushed towards the other group of slats (representing the westward motion of Turkey), the broken slats kink about their hinges, resulting in outward bending of the slat sets and extension near the hinges (Figure 2.12b). This extension represents the N-S extension that is currently observed in the northern Aegean sea (Taymaz et al. 1991).

The strength of this model is that it explains a possible relationship between many seemingly disparate features, in particular how the E-W slats representing Turkey can undergo right-lateral, simple shear whereas the NW-SE trending slats of Greece simultaneously rotate and undergo dominantly N-S extension. However, recent studies have shown that these features may indeed be disparate. The most recent active faults and basins developed in the west Aegean have an E-W orientation and not NW-SE as required in the model (Figure 2.09a). Hence, for active deformation, which is what the model was originally designed for, this model is not valid. Nevertheless, the model may still be useful to describe older deformation. A second problem is that the model is a simplified tectonic mechanism and hence requires some modification before it can be applied to describe region kinematics accurately.

Single plate model: *Rigid Anatolia model (Model I in Figure 2.12b)*

In the single rigid block model of Le Pichon et al. (1995), the south Aegean is rigidly coupled to a westward moving Anatolia and together they rotate anticlockwise into the Mediterranean basin. The northern margin of the Aegean/Anatolian block with Eurasia is modelled as a wedge-shaped zone. This zone is narrowest in the NE Aegean (where it is bounded by the right-lateral North Anatolian Fault) and widens westwards into a zone of dominantly N-S displacement. Thus, although the model requires a rigid plate, surface kinematics do not show a sharp boundary between zones. The model aims to describe the seemingly gradual rotation of displacement vectors in Anatolia (Figure 2.12b), the semi-arcuate shape of the North Anatolian Fault, and the recent anticlockwise opening of the western margin of the gulf of Corinth. This model is again based on active kinematic data (satellite geodetic measurements) and hence is an active/instantaneous model. Le Pichon et al. (1995) noted that the kinematics of the region probably underwent a major change in the late Miocene/ early Pliocene. Note that the model does not account for any north-south extension observed

across western Anatolia (Figure 2.10).

2.5.3.2 Distributed-strain models (Models J in Figure 2.12b)

Anatolia-dominated models

Jolivet et al. (1994a) compared data for active displacements with stretching lineations preserved in the exhumed basement and suggested that parallelism between the directions of active displacement and stretching lineations in the northeastern Aegean (Rhodope region) supported anticlockwise rotation of this area during regional extension. The northeast Aegean was therefore interpreted to have been linked to Anatolia during this period. Thus, this model has some features in common with the 'single-plate model' of Le Pichon et al. (1995) above. Recent paleomagnetic results, however, show that the northern Aegean basement has rotated in the opposite sense (see Chapter 5); thus this area appears to be more closely linked with the western Aegean (Atzemoglu et al. 1994).

Gravitational collapse-type models

Gautier (1995) suggested that stretching lineations in the central Cyclades form a radiating pattern which is roughly normal to the subduction zone, and that the lineations were formed by the outward spread of a viscous fluid, which they modelled experimentally (Figure 2.12b, Gautier et al. 1996). One of the primary experimental observations they made was that during deformation (i.e. after the onset of extension), an E-W trending fracture zone developed in a similar position to that of the North Anatolian Fault.

The observation that the lineations formed a radial pattern was contested by Morris and Anderson (1996) on the basis of paleomagnetic data. They showed that magnetic lineations, which are subparallel to stretching lineations, from two islands (Mykonos and Naxos) in the northern Cyclades form two distinct data sets separated by a NE trending fault. Hence the long term evolution of deformation must constrain non-fluid like discontinuities, e.g. faults and shear zones.

2.6 Summary of contentious issues and their bearing on this thesis

1. In this chapter, it is shown that many of the major tectonic events observed in the Aegean are also recorded elsewhere in the Mediterranean region. These events have resulted in a strong (originally E-W trending) structural fabric in the region. They include:
   (a) the Hercynian Orogeny which is preserved across the region,
   (b) the opening of the Neotethyan ocean, the Paleotethys is not recorded in the western Aegean,
   (c) the suturing of Cimmerian (in the mid-Triassic), Pelagonian (mid-Jurassic) and Apulian (late Cretaceous-Miocene) continental fragments onto a broadly E-W trending Eurasian continental margin.
2. Despite intensive study in the Aegean region, Section 2.4.2 showed that there is little consensus on the definition of major lithotectonic units and how these units may be correlated across the region. Hence, in Chapter 3 previous work is coalesced with new data under a standardised system of description. Thus, clarifying and extending the current lithotectonic knowledge.
3. It is generally assumed that the kinematics of the early Alpine Orogeny are reflected in the kinematics of ophiolite and in the basement over which the ophiolite was obducted. Despite

intensive study, however, there is still little agreement over early tectonic evolution of the region as shown in Section 2.4.3.2. Furthermore, there are few studies of the effects of later deformation on the earlier structures. The structures related to the early Alpine evolution in the Thessaly region are discussed in Chapter 4 and in a regional context in Chapter 6.

4. The Pelagonian Zone forms a basement slice between two ophiolitic zones. There has been much debate about the number and obduction direction of oceans that these zones represent. All studies to date have focused on NE-SW transport direction. Little is known about how the timing and kinematics of deformation of the Olympos region are linked to other regions along the suture zone. These problems are the main focus of Chapter 4.
5. The Aegean is one of the few regions currently undergoing active post-orogenic extension and its active regional kinematics are relatively well understood (Section 2.4.3.6). However, studies of the Mediterranean Rise (i.e. the southern margin of the deforming zone), the North Anatolian Fault (the northern margin of the deforming zone), and paleomagnetism (internal deformation) suggest that there have been major changes in the regional kinematics since the late Miocene. Does this mean the Aegean was affected by two distinct kinematic mechanisms or can one mechanism account for both situations? This relationship between paleo-kinematics and active-kinematics has not previously been addressed in detail and is resolved in Chapter 5.

   As reviewed in Section 2.5, many dynamic and kinematic models have been proposed to account for late-orogenic extension in the Aegean. Also in Chapter 5, kinematic and thermal constraints from the rock record are used to discriminate between the dynamic and kinematic models.
6. Major changes in the convergence rate and directions between Africa and Eurasia occurred at 126 Ma (cessation of relative divergence), and 20 Ma (associated with a reduction in the rate of convergence). However, the relationship between these major events and the tectonics of the Aegean region is not clear. These problems are discussed in the light of the findings of this thesis in Chapter 6.

Chapter 3:
Lithological and metamorphic evolution of Thessaly

3.1 Introduction

The metamorphosed basement of the central Hellenides has played an important role in Aegean tectonics, both as a central part of the Tethyan suture zone (see Section 2.4.3.3) and as a locus of post-orogenic extension. Consequently this region, often referred to as the Pelagonian Zone (see below), has been the subject of intense geochronological, metamorphic and structural study. To date, most lithological and metamorphic studies in this region have concentrated on the Alpine and post-Alpine evolution of metamorphosed basement in relatively small areas within northern Thessaly (Mt. Olympos area) and the Cycladic islands (e.g. Avigad 1991; Schermer et al. 1990; Vandenberg and Lister 1996). Although these and other studies have highlighted numerous important metamorphic and structural relationships (see Sections 3.3.3 and 4.2), it is demonstrated in this chapter that a lack of a common framework in such a complex region has hindered detailed correlation between studies. The problems encountered when trying to correlate units between the studies have not been highlighted in the past because relatively few studies have tried to integrate lithological, metamorphic and structural data across the entire region.

The aim of this chapter is threefold. Firstly, the chapter aims to present an integrated lithological and metamorphic study of the Thessaly region (and thus help to link the results of the two well-studied areas described above). Secondly, to determine a temporal framework from metamorphic overprinting relationships for the structural data which will be discussed in the following chapter. Finally, as a consequence of the literature review, the third aim is to discuss how a sequence of metamorphic rocks such as the basement of Thessaly may be subdivided.

The chapter is introduced with a detailed review of published lithological and metamorphic studies in the Thessaly region. Thessaly occupies the central part of the Pelagonian Zone of Aubouin (1959, and Figure 2.04). Therefore, the literature review starts with a discussion of this large scale unit before progressing to more detailed subdivisions of lithologies. In both cases attention is focused on the criteria used to subdivide units. The rocks of Thessaly (eastern Thessaly in particular) are then carefully examined using three separate criteria: (1) lithological units are defined and the mappable lithological associations (on 10 km scale) are presented; (2) a regional chronological framework is determined by first examining the age of formation of the lithologies, and then for the changing metamorphic evolution of similar lithologies across the region and, (3) the orientation of the regional phyllitic, schistose, or gneissic foliation provides a regional framework with which to determine the lithological and metamorphic structure of the region. This chapter concludes that the basement of Thessaly comprises a variably metamorphosed, tectonic melange (termed the East Thessaly Complex) which forms a sheet between weakly metamorphosed quartzofeldspathic gneiss-rich horizons (termed the West Thessaly Complex). The age of the lithologies and metamorphism decreases towards the southeast of the region.

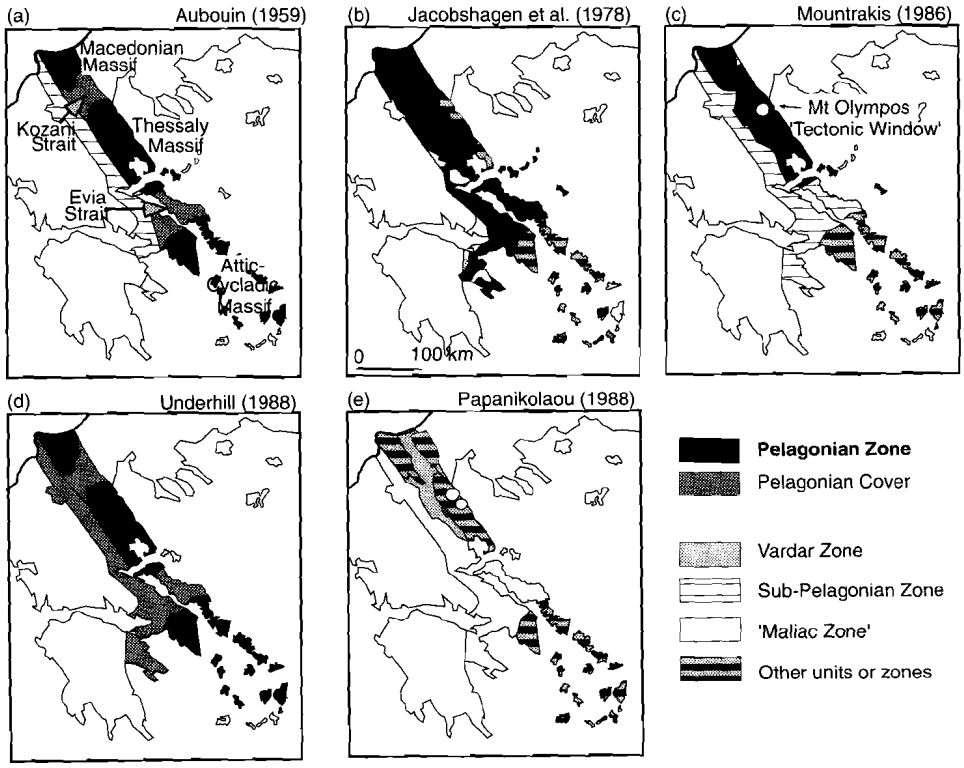

Figure 3.01: A selection of definitions of the Pelagonian Zone as recorded in the literature and discussed in the text. The interpretations vary from those who use the term 'Pelagonian' to apply to all basement between the Vardar and Pindos Zones (Figure 3.01d) to those who use the term Pelagonian to refer to a single nappe (Figure 3.01b). The Pelagonian Zone comprises three massifs which expose metamophosed basement. These are, from NW to SE, the Macedonian, the Thessalian and the Attic-Cycladic Massifs (see Figure 3.01a).

3.2 Definition of the Pelagonian zone

A quick perusal of the current literature reveals that there is a wide variety of interpretations of the geographical boundaries (and consequently the criteria) used to define the Pelagonian Zone (see Figure 3.01), hence the origin of the term is discussed in more detail.

The term 'Pelagonian Massif' was first used by Kossmat (1924) to describe the crystalline basement of the eastern Balkan Peninsula. Brunn (1956) later redefined the lithologies of the massif as part of an 'isopic-tectonic' zone based on 'similar looking' tectonic evolution in the rocks. Most workers, however, use the 'isopic' subdivisions of Aubouin's (1959) which were based largely on the presence on a similar stratigraphy. As the isopic units of Aubouin (1959) were interpreted to represent different parts of a geosyncline (i.e. the early stages of the Alpine Orogeny) each unit had well defined paleogeographic interpretation (see Figure 2.05). As a result, the Pelagonian Isopic Zone is primarily characterised by the stratigraphy of the Mesozoic platform cover rather than the tectonic evolution of its metamorphosed basement (for further discussion see Celet and Ferrière 1978).

Since the term 'isopic zone' was first proposed, much detailed lithological and structural work has been carried out in the region which has resulted in both large- and small-scale modifications to the margins of the Pelagonian Zone in Thessaly (Figure 3.01). Other workers have observed that the weakly metamorphosed ophiolite and flysch-rich lithologies of the southern Pelion Peninsula is lithologically similar to parts of the weakly metamorphosed Sub-Pelagonian Zone (Figure 3.01a). This has led some workers to group the two similar lithological/tectonostratigraphic units together, as either part of a single greater Pelagonian Zone (e.g. Figure 3.01d), as part of a new isopic zone, the Maliac Zone (Figure 3.01b: Celet and Ferrière 1978), or to group these lithologies as part of a separate Eohellenic tectonic nappe (Figure 3.01b: Jacobshagen et al. 1978). Many other workers limit the Pelagonian Zone to the mainland and interpret the basement to the south as part of a separate Attic-Cycladic Massif (Figure 3.01c).

Several workers, however, have recognised more fundamental problems with the use of the term isopic zone, noting that few of the isopic zones exhibit internally consistent structural, lithological, paleogeographic and metamorphic histories over such a long time span. One possible solution to this problem is to restrict the time range over which the term isopic zone (such as Pelagonian Zone) can be applied (Celet and Ferrière 1978; Underhill 1989). In the Thessaly region, Celet and Ferrière (1978) have suggested that the term 'Pelagonian Zone' should refer only to the Mesozoic cover lithologies: lithologies associated with younger events should be grouped as part of the Maliac Zone (described above). Rather confusingly, they suggested that the region should be called simply the 'Pelagonian' to distinguish it from the 'Pelagonian Zone'. Others have tried to redefine the large scale units on the basis of other, predominantly structural and metamorphic, criteria (Jacobshagen et al. 1978; Papanikolaou 1984). For example, Jacobshagen et al. (1978) suggested that the Pelagonian (Nappe) should refer only to basement that has not undergone extensive, high pressure metamorphism (Figure 3.01f). The latter unit is linked to the Attic-Cycladic basement which together form the 'Median Crystalline Belt'.

The limestone/flysch sequence of the Mt. Olympos 'tectonic window' has also commonly been interpreted as part of a separate zone, the Gavrovo-Tripolitsa Zone (Figure 2.04), based on similarities between the late Cretaceous fossil assemblages in conjunction with the weak degree metamorphism of the limestone (Godfriaux 1968). This observation has since been contested by Schmitt (1983) who documented a previously unreported hiatus of sedimentation between the late Jurassic and early Cretaceous in the Olympos limestone, thus setting the Olympos limestone apart from the continuous sedimentation observed to the west (Figure 2.05) and has been interpreted by Schermer (1993) to represent an allocthonous tectonic slice. However, most recent workers still view the limestone of Mt. Olympos as separate from the Pelagonian Zone (Figure 3.01c and 3.01e).

To summarize, the term Pelagonian was originally defined as a geographical term (Kossmat 1924). Since then, the term has been variously used to imply structural (e.g. Jacobshagen et al. 1978), lithological and paleogeographic conditions (Aubouin 1959) peculiar to this zone. Although problems with the indiscriminate use of the term (Pelagonian) 'isopic zone' were first highlighted 20 years ago (Celet and Ferrière 1978), no consistent alternative has been presented and most workers continue to use the first order subdivisions of Aubouin (1959). None of the more involved definitions are fully consistent for all geological observations. Therefore, in this text, the geographic term Thessalian basement is used in preference to central 'Pelagonian Zone'.

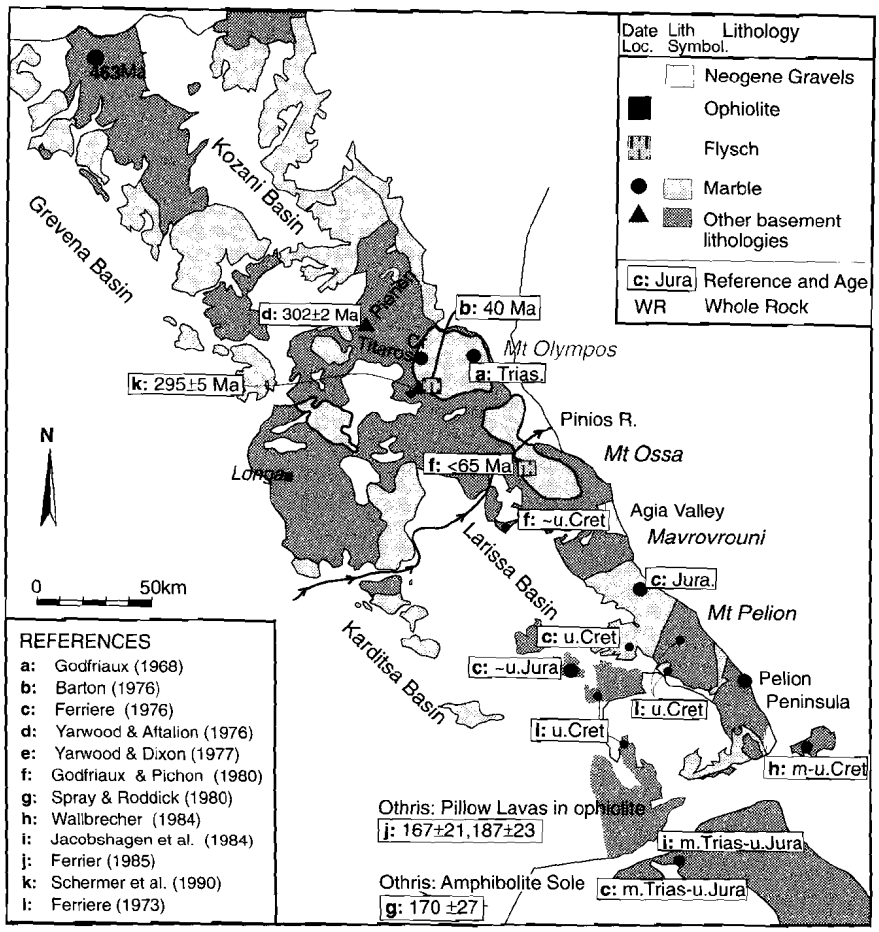

Figure 3.02
A map of basement in the Thessaly and Macedonia regions showing the crystallisation/deposition ages of igneous and sedimentary units respectively obtained from the published literature. See bottom left of figure for references.

3.3 Previous lithological and metamorphic studies in Thessaly

3.3.1 Introduction

Since the Mt. Olympos region was interpreted as a tectonic window approximately 30 years ago much attention has been focused on the evolution of northern Thessaly (Barton 1976; Godfriaux and Pichon 1980; Doutsos 1984; Kilias and Mountrakis 1989; Schermer et al. 1990; Sfeikos et al. 1991; Doutsos et al. 1993; Schermer 1993). With the exception of the southern half of the Pelion Peninsula (see Figure 3.01 for location), most of the region has been mapped between the 1950's and 1980's by the Greek institute of Geology, Mining and Engineering (IGME) on a 1:50,000 scale. The Pelion Peninsula, however, has been mapped by French and German geologists (see Ferrière 1976a, 1976b, 1982; Jacobshagen and

Wallbrecher 1984). The most regional descriptions of the metamorphic and lithological evolution of Thessaly, to date, are by Celet and Ferrière (1978) and Katsikatsos et al. (1982). This chapter builds upon these studies and incorporates the results of a detailed field examination and recently published work. Abbreviations of minerals are summarised in Appendix A and follow Kretz (1983) where possible.

3.3.2 Unmetamorphosed Cover Sediments

Although this chapter is primarily concerned with the lithologies within the metamorphosed basement in Thessaly, the unconsolidated sediment cover of the basement is introduced here as it is of importance in the following structural analysis.

Unconsolidated sediments in the Thessaly and Macedonia regions occur predominantly in four NW-SE trending major basin systems: the Grevena, Kozani, Karditsa and Larissa Basins (see Figure 3.02; Caputo and Pavlides 1993). Of the four basins, the Grevena Basin is the oldest and deepest. The mid/late Eocene basal sediments of the Grevena Basin contain detrital glaucophane (Faupl et al. 1996). A marine transgressive sequence occurs at the very base of the sequence and is overlain by an Eocene flysch. The youngest of the four basins is the Larissa Basin in the southeast which has Pliocene fluvial and lacustrine sediments deposited directly on the metamorphic basement. These sediments are in stratigraphic continuity with Quaternary fluvial sediments of the Karditsa Basin to the west (Caputo and Pavlides 1993). The Kozani Basin contains a 200-400 m succession of late Miocene to Pliocene freshwater limestones, marls and lignite (Calvo et al. 1995).

Smaller areas of Neogene sediments crop out in three areas along the east coast of Olympos-Pelion range (indicated by stripes in Figure 3.02). Sediments of the Agia Valley form a 20-400 m thick, intermixed gravel, lacustrine and sandy marl unit which is tilted to the southwest (see Chapter 4). As yet these gravels have not been dated although they are thought to be Neogene in age (Caputo 1990). The delta of the Pinios River northeast of Mt. Ossa however has been dated by Faugères (1977) and is Villefranchian (~1.8 Ma).

3.3.3 The Metamorphosed Basement

3.3.3.1 Distribution, age and metamorphic history of the basement lithologies

The metamorphosed basement of the Thessalian region is characterised by highly deformed and strongly foliated, 200-4000 m thick, alternating sheets of limestone, flysch, marble, meta-sediments, meta-volcanics and ortho- and para-gneisses of varying degrees of metamorphism (e.g., Schermer 1993). Together these units comprise a thickness estimated to be over 4 km in the Mt. Olympos region (Barton 1975). The gneisses are most common in the north and west of the region, whereas, metasediments/metavolcanics dominate the east and south. Marble on the other hand is distributed throughout and accounts for approximately 40% of the regions lithologies. The marble is composed primarily of calcite, although some areas (e.g. eastern Thessaly) also contain variable amounts of dolomite, graphite and, less commonly, bauxite. Blocks of mafic and ultramafic lithologies (predominantly serpentinite, peridotite and diorite) are most common towards the eastern and western margins of the Thessalian region although 1-10 m sized blocks of serpentinite are also found in the intervening regions. Scattered occurrences of ophiolitic conglomerate occur on the SW flanks of Mt. Ossa and on the summit of Mt. Pelion.

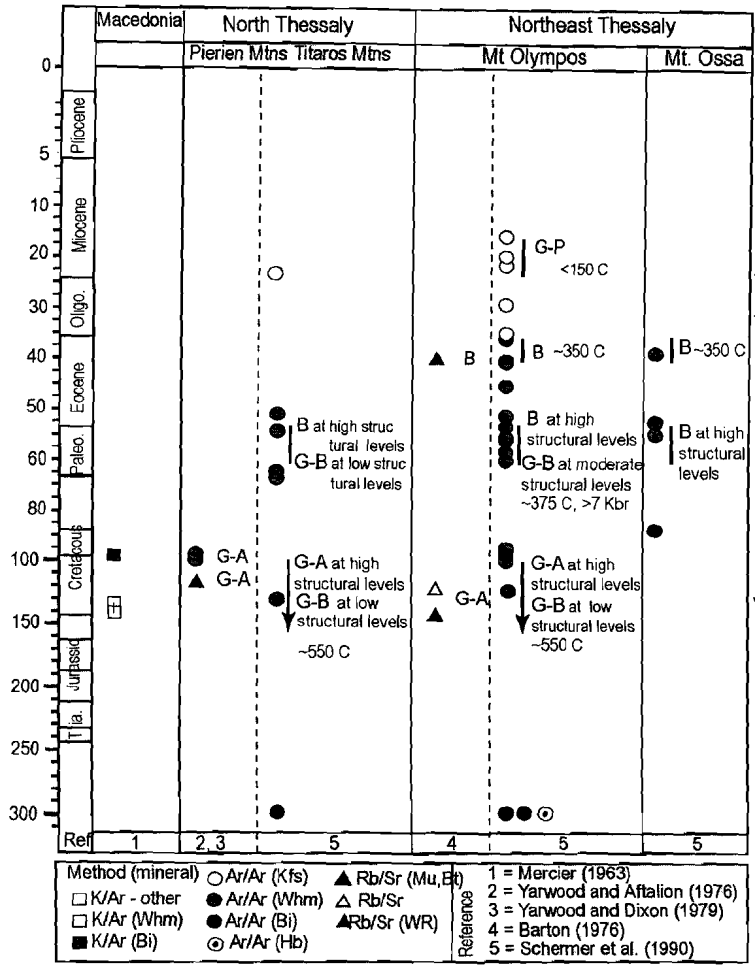

Figure 3.03
A summary of metamorphic cooling ages from the Macedonian and the Thessalian metamorphosed basement derived from the published literature.

Abbreviations of minerals are summarised in Appendix B. Other abbreviations are: A: Amphibolite facies, B: Blueschist facies, G: Greenschist facies, and P: Prehnite-Pumpellyite facies.

Geochronological determinations of the age of Thessaly basement are summarised in Figure 3.02. The following trends are apparent (for references see Figure 3.02 caption): the oldest dated lithologies are granites and granites-gneisses which are typically of Hercynian age (290 ± 10 Ma); lithologies of late Paleozoic to Mesozoic age include neritic limestones of Triassic to late Jurassic age although some limestone may be up to Permian in age (e.g. on Evia, Katsikatsos 1984a), and ophiolites of late Jurassic age (170 ± 30 Ma). The latter are typically associated with late Cretaceous limestones and flysch of Paleocene-Eocene age. The meta-sediments and meta-volcanics into which the Hercynian granites intruded have not yet been dated, and the original intrusive relationships have largely been obscured by later deformation. The bauxite and laterite horizons, which are thought to indicate periods of non-deposition, correspond to a mid-Jurassic level in limestones north of Volos (Katsikatsos 1984a, 1987) and early Cretaceous level on the southern Pelion Peninsula (Jacobshagen and Wallbrecher 1984).

Petrological studies of the region have been carried out by Katsikatsos et al. (1982),

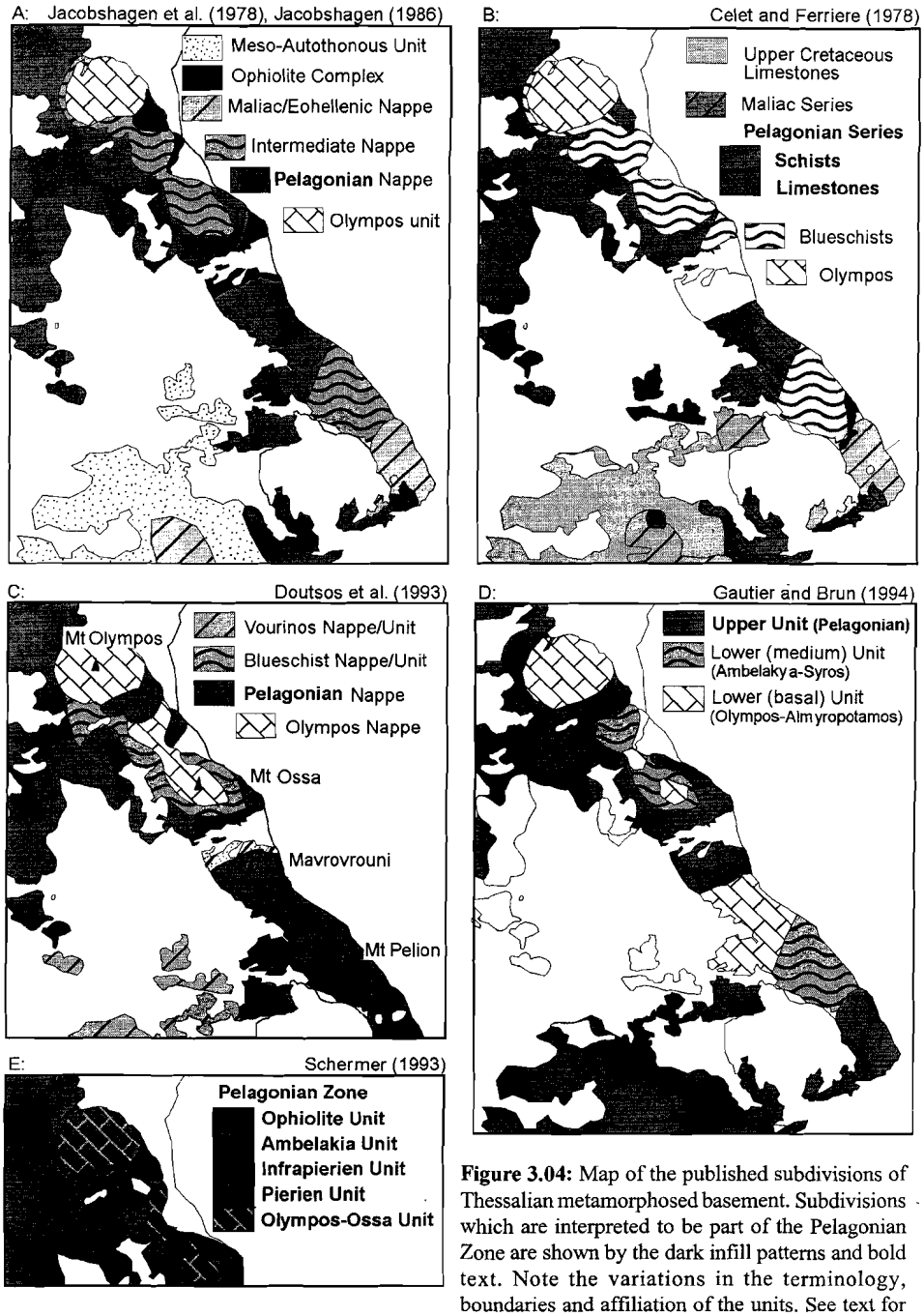

Figure 3.04: Map of the published subdivisions of Thessalian metamorphosed basement. Subdivisions which are interpreted to be part of the Pelagonian Zone are shown by the dark infill patterns and bold text. Note the variations in the terminology, boundaries and affiliation of the units. See text for discussion.

Jacobshagen and Wallbrecher (1984) and Mposkos (1987) with more detailed studies of the metamorphic evolution by Schermer et al. (1990) and Nance (1981). These studies, in particular the work of Schermer et al. (1990) on Mt. Olympos, demonstrated that the metamorphic basement of Thessaly preserves three distinct 'metamorphic events', the timing of which are shown Figure 3.03. The spatial relationships between these events, however, are complex. The oldest event identified in the region is estimated to have started in the early Cretaceous (<135 Ma) and is an amphibolite to upper greenschist facies event at high structural levels. This first event is marked as 'metamorphic event 1' in Figure 3.03. Metamorphic event 1 is interpreted to have been broadly synchronous with a blueschist-greenschist facies metamorphism that occurred lower in the metamorphic pile (Schermer 1993). This blueschist-greenschist facies event signalled the onset of the second, blueschist facies metamorphic event (shown as metamorphic event 2 in Figure 3.03) which continued until the Eocene and affected all structural levels presently exposed in the Olympos region. Finally, Schermer et al. (1990) observed that the blueschist event was followed , in the early Miocene, by a weak overprint of greenschist to pumpellyite grade metamorphism (metamorphic event 3) in the Olympos region.

This spatial and temporal evolution of the 'metamorphic events' is refined in Section 3.5 and a new one proposed.

Although much attention has focused on the best 'preserved' blueschist facies units which are exposed in Mt. Olympos, Mt. Ossa and the northern Pelion Peninsula (e.g., Doutsos et al. 1993; Jacobshagen 1986; Katsikatos et al. 1982), blueschist facies metamorphic units have also been observed in the southern Pelion Peninsula and many other regions across eastern Thessaly (see maps of IGME (Katsikatos et al. 1984a,b, 1985, 1986, 1987); Ferrière 1976a, 1976b; Jacobshagen and Wallbrecher 1984).

Although the Mt. Olympos tectonic window, was the first, largest, and least tectonically disturbed of the windows identified in the Aegean, other limestone units have been interpreted as tectonic windows. These include the limestones of Mt. Ossa (Godfriaux and Pichon 1980), of Kranea (Kilias et al. 1991; Sfeikos et al. 1991), of Rizomata (Kilias and Mountrakis 1985) and of Mavrovrouni-West Pelion (Gautier 1995). The limestones in most of these areas are also topped with flysch or silty limestone horizons. However, they exhibit more tectonic disturbance than is observed on Olympos (Godfriaux and Pichon 1980; Kilias 1991; Sfeikos et al. 1991). Other proposed tectonic windows 'expose' schists with high-pressure assemblages rather than low grade marble. These include the Verdikoussa Window (Doutsos 1984) and the High Pelion Window (Katsikatsos et al. 1976). Note that the latter 'window' has also been interpreted as a metamorphic core complex (Kilias et al. 1995).

In summary, the lithologies of Thessaly form two distinct sets separated by an unconformity, namely Miocene to Pliocene fluvial sediments which rest on complexly metamorphosed and deformed basement. The basement of Thessaly comprises Paleozoic granites and schist, topped by ophiolite, which thrust over Mesozoic marble, during a phase of Eocene, high pressure metamorphism. Underthrusting of cooler material has resulted in an inverted geothermal gradient (Schermer et al. 1990). The basement sequence underwent retrogressive, greenschist facies metamorphism in the Oligocene to Miocene. The spatial relationship of the metamorphic events across Thessaly, however, is poorly understood and is a primary focus of this chapter.

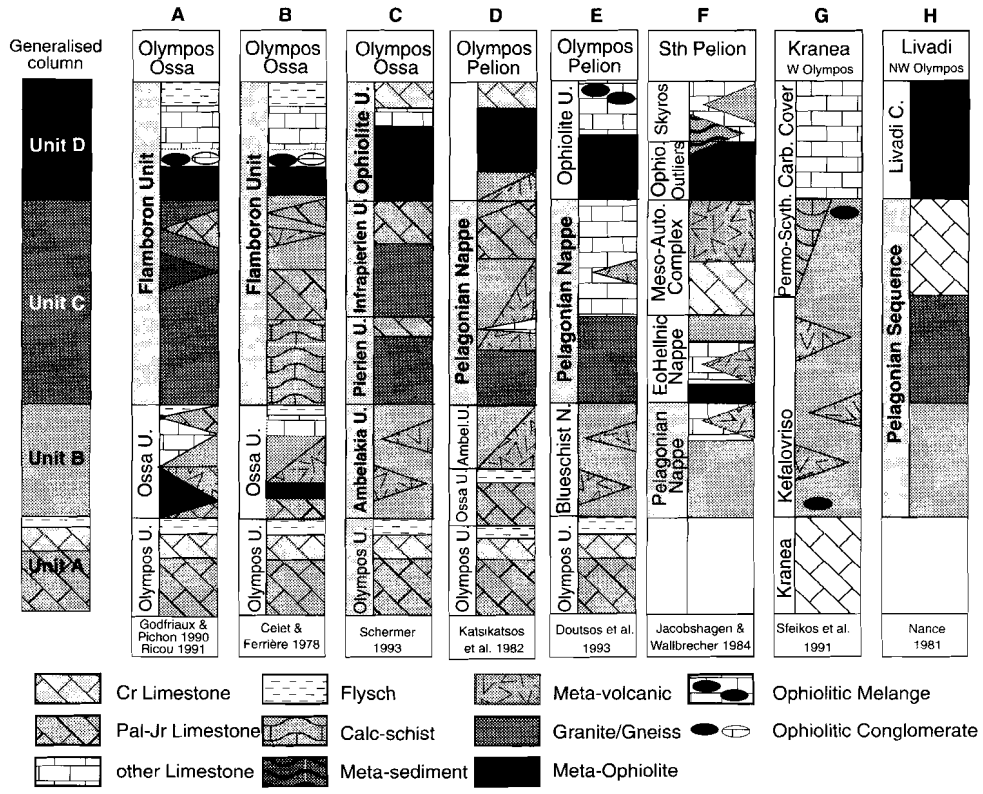

Figure 3.05: Lithotectonic sections from the published literature. The composition of sections have been simplified and the thickness of each section has been scaled to enable easier comparison between the different lithotectonic sections. Although there is a large variation in the composition of each unit even within the same region (compare columns A-E), there are also many similarities between the units which are summarised in the generalised column on the left. The units A-D in the generalised column are unofficial units used for discussion (see text).

3.3.3.2 Published lithological subdivisions

Most workers agree that the following very general lithological sequence may be observed in the Olympos-Ossa area (see Figures 3.04 and 3.05). The structural base of the sequence is occupied by low-grade marbles which are topped by greenschist-facies meta-flysch (phyllites). For convenience, this will informally be referred to as Unit A (Figure 3.05). Unit A is typically covered by a sequence of intercalated metasediments, metavolcanics, marbles and amphibolites, which contain particularly well preserved high-pressure minerals such as glaucophane and epidote or lawsonite (Unit B). Above Unit B, the lithologies become-richer in granite gneiss and quartzofeldspathic schist (Unit C). Finally, higher structural levels are occupied by ophiolite, limestone and meta-flysch (Unit D). There are, of course, variations on this scheme, e.g., in some areas ultramafic lithologies occur at low as well as at high levels (column A, B, F, and G, Figure 3.05). Despite local discrepancies, however, the generalized sequence of units A-D, provides a convenient basis for discussion of tectonostratigraphic units below.

Although there is general agreement about the broad lithological sequence described above, on closer inspection there is very little consensus on the nomenclature, composition, affiliation, stratigraphic significance and boundary of *any* of the units. Thus, correlation of the units is in practice difficult. Some of the disagreements in the affiliation and nomenclature are discussed below. In this discussion, the *Pelagonian Zone* is referred to as a 'zone' not as a unit, nappe or subcomplex as it may be referred to by the original workers (see Figure 3.04 for their terminology).

The limestone/flysch sequences of Mt. Olympos and Mt. Ossa have been variously interpreted as: (1) *separate units* at *different structural levels* (i.e, Ossa marble/flysch sequence above the Olympos marble/flysch sequence: Godfriaux and Pichon 1980; Schmitt 1983; Jacobshagen 1986) or (2) part of the *same unit* but which crop out at *different structural levels* (Figure 3 in Katsikatos et al. 1982) or (3) *separate units* which crop out *at a similar structural level* (Figure 1 in Doutsos et al. 1993; Gautier and Brun 1994). The Ossa marble has been interpreted as either part of the Pelagonian Zone (Schermer 1993) or as part of a separate zone (Doutsos et al. 1993; Gautier and Brun 1994; Jacobshagen 1986).

Unit B is a sequence of schists which exhibit well preserved blueschist facies minerals. This unit has been interpreted as part of the underlying Ossa flysch/limestone (Godfriaux and Pichon 1980); as a distinct unit separate from the Pelagonian Zone (Doutsos et al. 1993; Gautier and Brun 1994; Jacobshagen 1986) and as a distinct unit but part of the Pelagonian Zone (Schermer 1993). The greater part of Unit B has been variously referred to in the literature as the Ossa Unit/Nappe/Formation (Katsikatsos et al. 1982; Schmitt 1983; Schermer 1990), the Blueschist Unit (Doutsos et al. 1993) or the Intermediate Nappe (Jacobshagen et al. 1978).

Most workers agree that the granite-gneisses which characterise Unit C are an integral part of the 'Pelagonian Zone', although this unit is interpreted both as part of a wider Pelagonian Zone or as a subsection of Aubouin's (1959) Pelagonian Zone (discussed earlier in Section 3.3). Schermer et al. (1990) identified two sub-groups, the Infrapierien and Pierien units, on the basis of differences in metamorphic grade and structural evolution. Other workers have termed Unit C type lithologies as the Flamboron Unit (Godfriaux and Pichon 1980).

Finally, parts of the ultramafic-rich Unit D, have been interpreted as part of the Vardar Zone to the east (Vergély and Mercier 1990), or as part of the Pelagonian Zone (e.g. Doutsos et al. 1993). Yet other workers have suggested that parts of Unit D which exhibit relic blueschist facies metamorphism form *part* of an 'Eohellenic Nappe' within a Maliac Zone to the west, whereas other parts comprise an 'Ophiolite Complex' (Jacobshagen 1986). Conversely, Katsikatsos et al. (1982) include *all* of unit D in the 'Eohellenic Nappe'.

Discussion of previous work

Despite numerous studies in the northeastern Thessalian metamorphic basement, little consensus has been reached in the definition of units. As the lithological subdivisions are important to define the key building blocks with which to understand the lithological and tectonic evolution of a region, the next step is to determine why there is so little agreement and how to resolve the problem.

The simplest explanation is mistakes and errors in mapping. This is the case in some but not all instances. For example, the 'lower basal unit' of Gautier and Brun (1994) south of Mavrovrouni actually occurs at higher structural levels. Another possible cause is that the conflicting interpretations may be due to difficulty in defining boundaries of the units. For example, Units C and D both contain variable proportions of interlaminated marbles,

amphibolites, and felsic schists, thus the exact position of the borders depends on other criteria used to characterise each unit such as presence of glaucophane (cf. Figure 3.04 c and e). This highlights another possible cause of the confusion, resulting from the differences in the criteria used to define units.

Nance (1981) interpreted most structures in the Livadi region of northwest Olympos as sedimentary in origin and hence defined an essentially stratigraphic section (albeit of metamorphic units). Most other workers, however, have subdivided the lithological sequence into 'structural' or 'tectonic' units. Closer examination of the criteria used to define these units reveals that most units are not identified solely on the basis of structural criteria but by a range of factors, which vary not only between workers but also within each study. For example, some units are defined by the presence of high-pressure minerals (Blueschist Unit), while others are based on structural position (Intermediate Nappe), lithological assemblage (Ossa Unit), interpreted origin (Ophiolitic Nappe, Meso-Autochthonous Unit) and/or structural and metamorphic evolution (Pierien and Infraperien Units). In fact, in no instance are the

	Name	Mineral constituents	Other observations
1	Marble-Serpentinite meta conglomerate	Srp ± Asb, Cal, opaques, Spl, Ol	A rare lithology found only on Mt Pelion and Agia Valley. Clear primary conglomerate texture.
2	Serpentinites and Peridotites	Srp ± Asb, Cal, opaques, Spl, Ol	
3	Tremolite-Plagioclase amphibolite	Tr, Plg, Act, Px, Ser, Cal, opaques	This rock is often relatively coarse-grained (5mm), weak to unfoliated. Often only the relic crystal forms of pyroxene and plagioclase remain.
4	Marble *Varieties include:* Mica-rich marble Amphibole-rich marble	Cal ± Dol, Chl, Gr, Tr/Act, Whm Cal, Whm, Chl, opaques Tr/Act, Cal	Dolomite typically occurs as fine lenses whereas graphite is spread evenly throughout the rock.
5	Quartzofeldspathic gneiss and schist *Variation includes:* Quartzofeldspathic-mica schist	Qtz, Plg, K-spar, Whm, Bt, Ep, Gnt (Alm), Chl, Gln Qtz, Ab, Whm, Chl, Ep	In northwestern Thessaly the gneisses grade into (mica-rich) quartzofeldspathic schists along their margins, on a 1-10 m scale.
6	Albite-amphibolite gneiss and schists	Ab, Bar, Chl ± Tc, Gln, Bt, small amounts of Ep/Zo, interstitial Cal	Albite often forms porphyroblasts.
7	Pyroxene-epidote gneisses schists	Px (Aug) as relic grains, Ep, Qtz, Ab, Bar, Act, Chl)	Epidote often forms porphyroblasts.
8	Epidote-chlorite-albite schists Quartz-epidote schists	Ep, Ab, Chl, ± Gln, Phg, Lws, Qtz	Epidote often occurs as porphyroblasts.
9	Calc schist/phyllite	Cal, Whm, Ab, Chl ± Act, Fpsr	
10	Quartz schist/phyllite	Qtz, Chl, Whm, Ab, relic Kspr ± Cal	
11	Undifferentiated schists *Other varieties:* quartzites	Cal, Qtz, Whm, Ab, Ep, Zo, Chl ± Act, ± Kpsr Qt, Whm, Ep	

Table 3.1: Table of lithological units showing the main mineral constituents of the eastern Thessaly region. Abbrieviations of minerals summarised in Appendix A.

criteria clearly outlined in a given publication. The problem with this approach is that without a clearly defined, consistent system, the subdivision of the lithotectonic assemblage of rocks has become a largely subjective exercise and thus impractical for others to apply and build upon.

In summary, it is concluded that no one worker adequately defines the criteria used to determine regional units in the Pelagonian metamorphic basement. Therefore, a more objective system is required before the lithological or tectonic evolution can be determined. This system will be outlined in the next section.

3.4 The metamorphic basement of Thessaly: This study

3.4.1 Introduction

In regions of highly deformed, metamorphosed rock, the rock pile may be subdivided by using a variety of criteria (e.g. Yardley 1989). Although some workers advocate the use of clearly defined criteria to subdivide lithologies (e.g. Fry 1984) this is usually not done (as in the Thessaly region). To avoid the ambiguities induced by using multiple criteria, the basement of Thessaly is systematically examined in this section, e.g. lithologies are used to define *lithological* units, preserved metamorphic evolution is used to defined *metamorphic* units etc..

Firstly, lithologies are defined based simply on average grain size, e.g. phyllitic <1 mm, schistose, 1-5 mm, gneissic >~5 mm, (see Yardley 1989) and the major rock forming mineral constituents (Section 3.4.2). Imprecise, genetic interpretations such as the term 'metasediment' are avoided unless unequivocal primary structures are identified. The scale range over which these units are mappable is discussed. Then, the lithologies of Thessaly are examined using temporal criteria; that is, the age of formation of each lithology (Section 3.4.3) and the ages (and conditions) of major metamorphic events (Section 3.4.4). The metamorphic events are determined from a detailed petrographic study of overprinting relationships between key (index) minerals and mineral assemblages. Finally, all units are examined using the age of the regionally pervasive foliation as a regional framework.

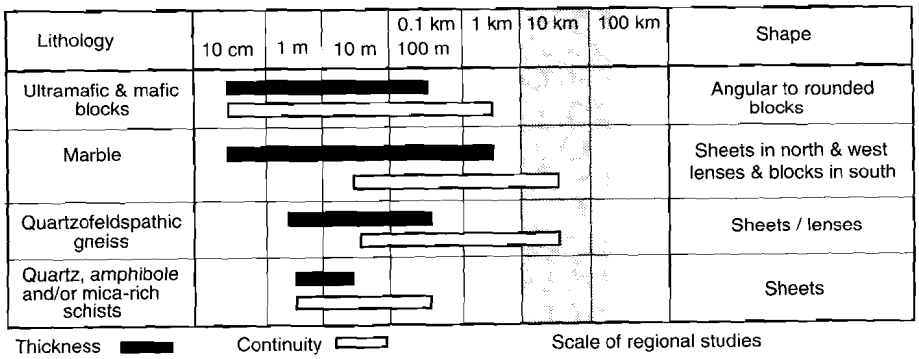

Figure 3.06: A summary of the estimates of the range of scales across which lithologies within the metamorphosed basement of Thessaly are mappable. The width of each lithology is taken normal to the pervasive foliation (phyllitic, schistose or gneissic foliation), whereas the length is taken parallel to the pervasive foliation.

3.4.2 Lithological subdivisions

3.4.2.1 Lithological units

The metamorphic rocks of the Thessaly region grade broadly from gneissic in the northwest of the region, through schistose in the centre to phyllitic in the south and east of the region.

Contrary to the observations of Nance (1981), the metamorphosed basement does not exhibit primary (e.g. sedimentary and intrusive) features. The only such structures that were identified were small exposures of marble and ultramafic conglomerates with a calcite matrix (1 in table 3.1). Other lithologies are defined on the basis of distinct, dominant mineral constituents.

Lithologies 8-11 in table 3.1 contain variable amounts of albite, epidote, calcite, chlorite, actinolite/tremolite and quartz, and as a result form less distinct units.

3.4.2.2 Scale range of lithological units

As subdivision of the rock pile is a direct function of the scale at which the units are defined, it is instructive to examine the range of sizes in which the lithological units described in table 3.1 occur. An indication of the range of thickness and continuity is depicted in Figure 3.06. The thickness and continuity is measured normal and parallel to the pervasive foliation (i.e. phyllitic, schistose or gneissic foliation) direction respectively. This range of scales is estimated from field observations made in this study.

Ultramafic and unfoliated to weakly foliated mafic lithologies (numbers 1 and 2 in the table above) tend to form rounded to angular blocks of 1 cm to 100's of meters in diameter. The most angular mafic and ultramafic blocks occur at high structural levels. Quartzofeldspathic gneiss units occur in large lensoidal sheets, as do other mica-, calcite- and quartz-rich lithologies such as quartzofeldspathic schist, albite gneiss, quartz phyllites, calc phyllites and epidote schists (Figure 3.06). Quartzofeldspathic gneisses have a thickness on the order of 1-100's m and continue along strike for 10 m to 10 kms. Individual quartz-, calcite- and mica-rich schistose units and albite-amphibole gneiss typically form thinner sheets (1-10's m thickness and 1-100's m continuity). These units are typically intercalated with sheets/lenses of marble. Marble units within schistose layers can be anywhere between 10 cm and 1 km in thickness, and a few centimeters to kilometers in length. The range of thickness and continuity of marble in the northern Pelion Peninsula is depicted in Figures 3.07a-d. In a schist-marble breccia of southern Pelion Peninsula, the schist tends to form angular blocks of 1-10 metres in diameter whereas the marble exhibits a more ductile rheology.

It should be noted that as most units have many minerals in common, the boundaries between units are not always sharply defined. In some cases, one unit may grade into another unit at outcrop scale. For example, ultramafic breccia graded into amphibole (tremolite-) and calcite-rich phyllite over a distance of 2-3 meters in the southern and eastern Pelion Peninsula. The area between consisted of an impure marble matrix with small lensoidal grains (1-5 cm in length) of chlorite and tremolite concentrations.

Thus, most lithologies are observed over a range of length scales. The schists of eastern and southeast Thessaly characteristically form thinner beds and is more complexly interlayered than the more gneissic lithologies of northern and western Thessaly.

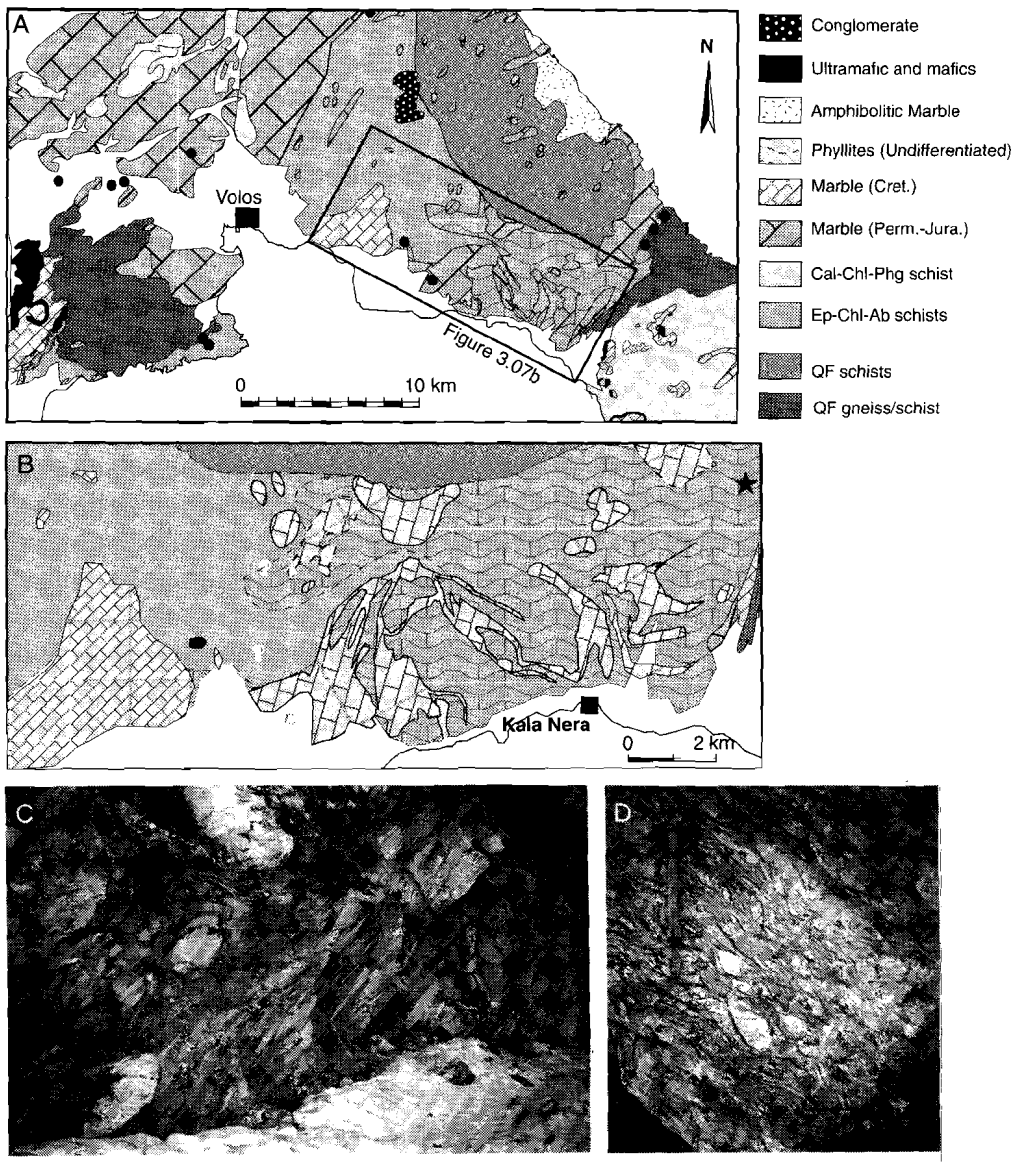

Figure 3.07: A set of two maps (Figure 3.07a, b) and two photos (Figure 3.07c, d) from the northern Pelion Peninsula demonstrating the range of scales across which lithologies, in particular marble, form discrete mappable units. The map is partially the result of this study and partially adapted from fourth year mapping reports by Ries (1993) and Verkuijl (1995). The hammer is 33 cm long.

3.4.2.3 Regionally mappable lithological associations

Most individual lithological units, discussed above, do not form mappable units on the 10-100 km scale, therefore for mapping purposes (primarily), the lithological units were assembled into mappable 'lithological associations'. These are summarised in Figure 3.08 (right hand side of figure).

Some lithological 'associations' consist of only 1-2 lithological units (for example, the Trikeri quartzofeldspathic gneiss). However, most lithological association comprises 1-3 dominant lithologies (shown as a bold line, Figure 3.08) and several other less voluminous lithologies (indicated by thinner lines, Figure 3.08). The 'dominant' lithological units within each association distinguishes the association from the neighbouring associations. For example, the West Pelion schists dominantly contains epidote-rich schists and marble whereas the East Pelion schists is dominated by quartzofeldspathic schists and minor marble, and quartz phyllite. Note that in all cases the lithological associations grade into each other.

Many lithological units occur in a large number of lithological associations as clearly demonstrated in Figure 3.08. Marble and serpentinites crop out within almost all schist- and phyllite-rich associations. Both units are also found intercalated with quartzofeldspathic gneisses in Mavrovrouni (lithological association, number 15 in Figure 3.08, 3.09a).

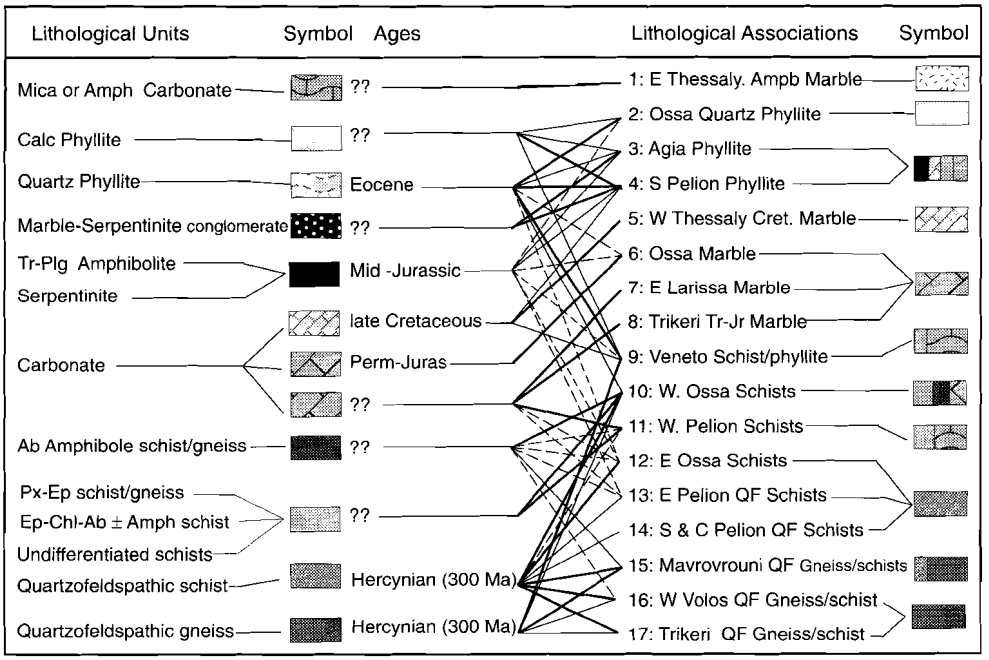

Figure 3.08: Summary of the relationships between lithological units, determined ages, and the constitution of regionally mappable units on a scale of 10-100 km in east Thessaly. The thickness of the lines between the 'ages' and the mappable 'lithological association' is proportional to the volume of the particular lithology within each lithological association; a thin dashed line = uncommon, a medium weight continuous line = relatively common, and a heavy continuous line = dominant lithology. This diagram shows that almost all units consist of a tectonic 'melange' comprising different percentages of different rock types which represent a variety of ages. The filled boxes provide the key for the lithological maps in Figures 3.09a and b.

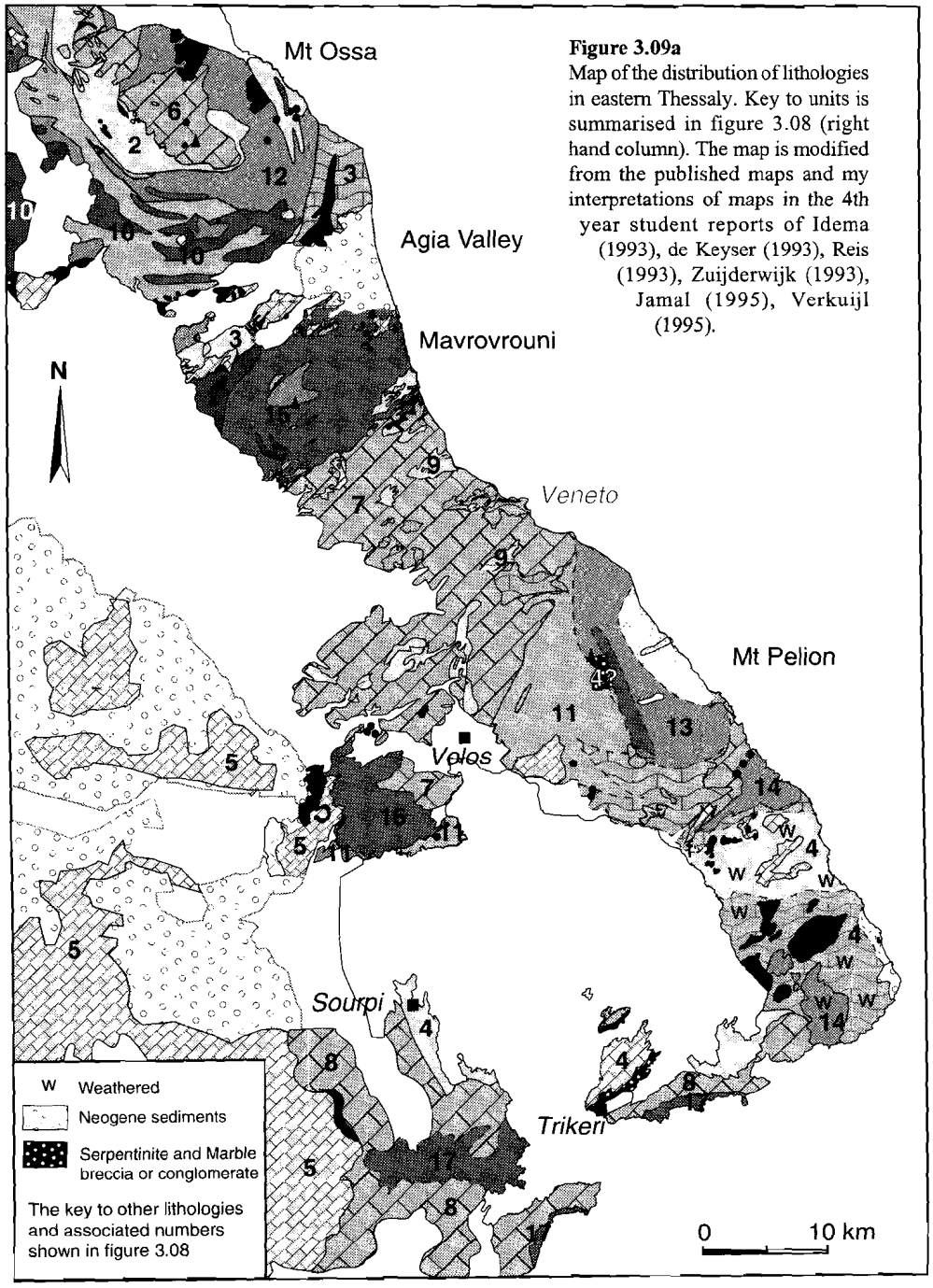

Figure 3.09a
Map of the distribution of lithologies in eastern Thessaly. Key to units is summarised in figure 3.08 (right hand column). The map is modified from the published maps and my interpretations of maps in the 4th year student reports of Idema (1993), de Keyser (1993), Reis (1993), Zuijderwijk (1993), Jamal (1995), Verkuijl (1995).

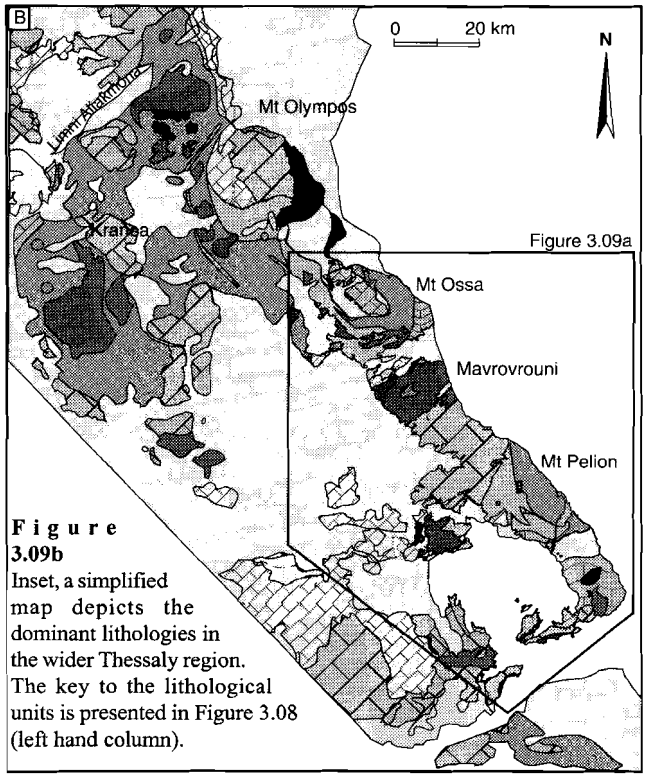

Figure 3.09b Inset, a simplified map depicts the dominant lithologies in the wider Thessaly region. The key to the lithological units is presented in Figure 3.08 (left hand column).

The distribution of these lithological associations (Figure 3.09a) essentially represents a modification of maps published by IGME (Geological Society of Greece), Ferrière (1976a, 1976b, 1977) and Jacobshagen and Wallbrecher (1984). The modifications are the result of my own study and of my own interpretations of the detailed field studies of regions (~5 by ~5 km) west of Mt. Ossa by fourth year students from the Department of Structural Geology in Utrecht University. Due to dense vegetation and reduced accessibility, the eastern margin of the studied area is less constrained than the west. A summary of the major results of this study in eastern Thessaly is presented below.

Mt. Ossa, in the northern part of the study area, comprises 4 major units. These are the Ossa marble, the Ossa quartz phyllite, the West Ossa schists and the East Ossa schists. The West Ossa schists consist of quartzofeldspathic gneisses/schists complexly interlayered with epidote-rich schists. The East Ossa schists are more quartzofeldspathic. Rocks on the eastern side also tend to be finer grained and more deeply weathered than the west. Note that ultramafic blocks of the Agia phyllite in the Agia Valley region are also interlayered with the schists and gneisses of Mavrovrouni and Ossa. Although albite-amphibole gneiss is a rare lithology in eastern Thessaly (compared to the region northwest of Olympos), it is present on the northern flanks of Mt. Ossa.

The composition of lithologies in Mavrovrouni and northern Pelion Peninsula regions are much more variable than has been documented previously. Most of Mavrovrouni consists of intercalated quartzofeldspathic and albite-amphibole schists/gneisses (collectively termed the Mavrovrouni quartzofeldspathic gneiss). No 'gneissic' core was observed in contrast to observations by other workers (Katsikatsos 1984b). The southern and northern margins of the Mavrovrouni quartzofeldspathic gneiss/schists contain numerous lenses and sheets of marble and serpentinites (Figure 3.09a). Marble is rarely observed in the centre of Mavrovrouni, but it commonly forms thin well distributed units near its southern margin (near the contact with the East Larissa marble).

The northern Pelion Peninsula consists of a range of lithological associations. In the

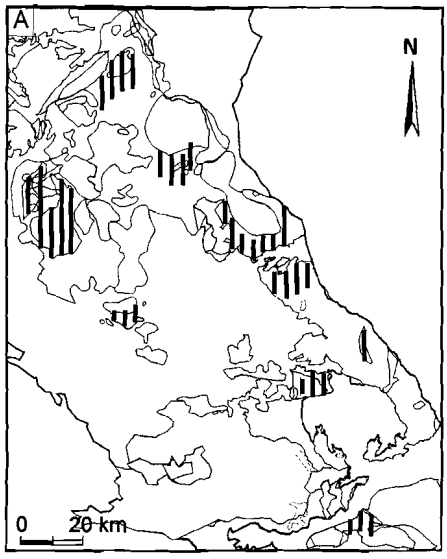

Primary biotite ± hornblende in QF schists/gneisses & mafic lithologies

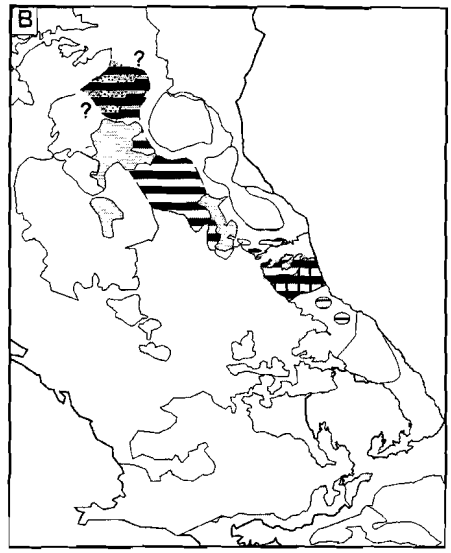

Widespread Barroisite in mafic lithologies
± Barroisite in mafic lithologies
Garnet ± biotite in QF gneisses
Widespread Biotite overprinting Barroisite

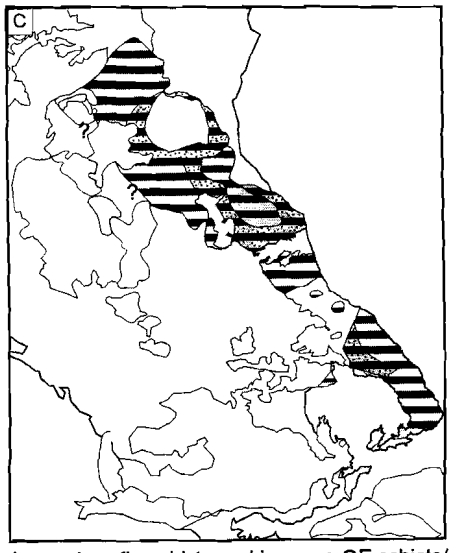

In most mafic schists and in some QF schists/ gneisses:

Widespread glaucophane + albite ± lawsonite epidote
Rare occurrences of glaucophane + albite ± lawsonite ± epidote

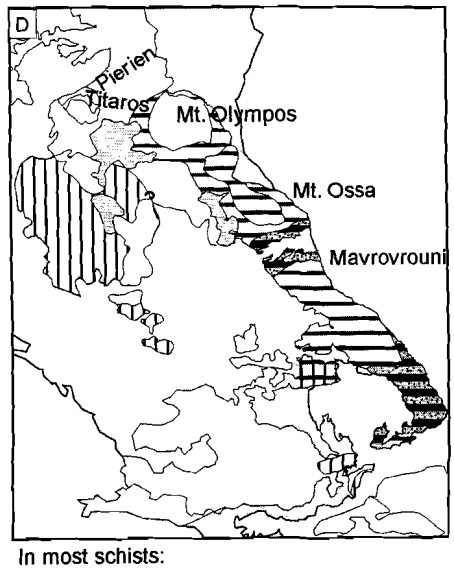

In most schists:

Widespread chlorite + white mica ± stilpnomelane ± pumpellyite
Occasional chlorite + white mica ± stilpnomelane ± pumpellyite
Phengitic white mica + chlorite

Figure 3.10: Simplified maps showing the distribution of the index minerals across Thessaly. Early biotite clasts (Figure 3.10a) is preserved in small amounts across the whole region. Mafic schists of northeastern Thessaly exhibit a well developed barroisite ± biotite overprint. Although the glaucophane-albite-epidote/ lawsonite assemblage occurs in many mafic to intermediate lithologies across much of east Thessaly, they are best developed in the West Pelion, East and West Ossa schists (Figure 2.09a for locations). An overprint of chlorite-white mica-stilpnomelane-pumpellyite mainly affected southeast Thessaly whereas lithologies in west Thessaly was only affected by chlorite-white mica overprint. The temporal relationship between these two metamorphic assemblages is unclear.

northeast, the rocks are fine-grained and predominantly quartzofeldspathic in composition (East Pelion schists). Near the summit of Mt. Pelion the quartzofeldspathic schists become coarser grained. To the west epidote-rich lithologies intercalated with thin blocks and lenses of marble dominate. The rocks become progressively more calcite-rich towards the south (Figure 3.07b).

The lithologies of the southern Pelion Peninsula are difficult to map due to their fine grain size and the degree of weathering. The quartzofeldspathic gneiss southwest of the Pelion Peninsula has been interpreted variously as metaconglomerate or metasediments (e.g. Jacobshagen and Wallbrecher 1984). However, close inspection of the unit reveals that the 'clasts' were in fact large albite porphyroblasts (up to 2 cm in diameter) and thus this unit forms the Trikeri quartzofeldpathic gneiss. The quartzofeldspathic gneiss/schist on the southwestern Pelion Peninsula is correlated with quartzofeldspathic gneisses/schists to the west (south of Sourpi).

At the highest structural levels are outcrops of ultramafic- and limestone-rich conglomerates. This volumetrically small unit is identified primarily on the basis of its paraconformable position above schists of eastern Thessaly and comprises a sheet of ultramafic, phyllitic and Cretaceous marble-rich lithologies. The most distinctive members of this unit are ultramafic- and limestone-rich conglomerates resting unconformably on schistose units on Mt. Pelion and at high structural levels on the southwestern flanks of Mt. Ossa (Figure 3.09a). As these lithologies are intercalated with underlying schists, phyllites and marbles, it is hard to distinguish this unit from other ultramafic schists and marble. The conglomerates on the southwestern flanks of Mt. Ossa are correlated with the Agia phyllites whereas the conglomerates on Mt. Pelion are tentatively correlated with the South Pelion phyllites. The relationship between these two units is discussed in Section 3.7.2.

In summary, careful mapping of lithological units and lithological associations in the Thessaly region has highlighted the complexity of the relationship between lithological units and/or lithological associations.

3.4.3 Age of lithologies

The estimated age of formation of the basement lithologies, that is the crystallisation age of igneous rocks and the deposition age of sedimentary rocks, are summarised in Figure 3.02. Unfortunately, the available data are mainly confined to marbles, quartzofeldspathic schists/ gneisses and ultramafics. The only (other) schists dated (by paleontological and whole Rock U/Pb methods) are quartz phyllites of Mt. Olympos and Ossa (Figure 3.02).

Mappable units of schist contain a wide variety of lithologies (e.g. West Ossa schists, Figure 3.08). In many cases the schists are uniformly interpreted as pre-Hercynian in age (Mountrakis 1986). However, some may be derived from sediments developed during the

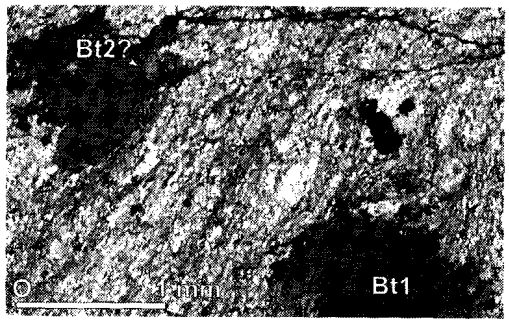

Figure 3.11a
Relic biotite (Bt1) grains are rimmed by finer biotite (Bt2). Most of the biotite, however, has been replaced by fine-grained phengitic white mica. Sample from quartzofeldspathic schist from western Thessaly.

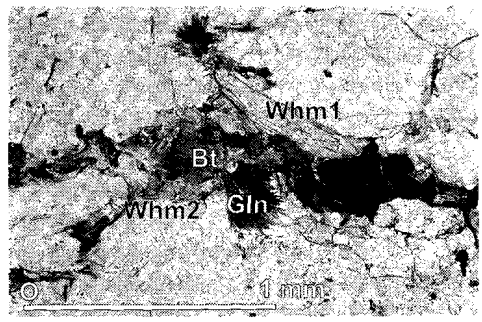

Figure 3.11b Relic biotite (Bt) and white mica (Whm1) have been partially overprinted and replaced by a second fine-grained white mica (Whm2). The secondary white mica has grown synchronously with the radial fibres of glaucophane (Gln). Sample from quartzofeldspathic gneiss, western flanks of Mt. Ossa.

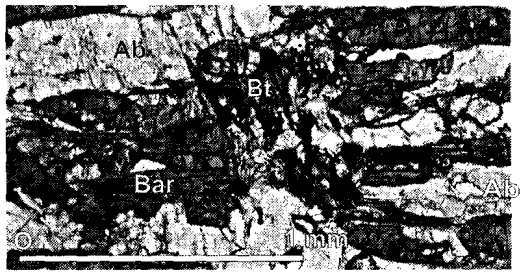

Figure 3.11c
Barroisitic amphibole (Bar), associated with albite (Ab), is surrounded by biotite (Bt). Sample from albite-amphibole gneiss on the western flanks of Mavrovrouni.

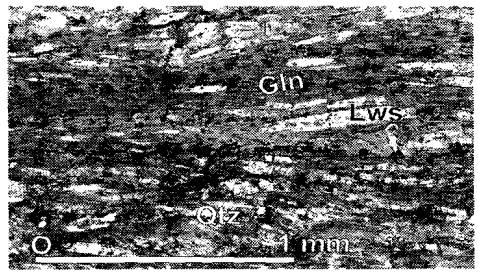

Figure 3.11d
Lawsonite (Lws), albite (Ab) and glaucophane (Gln) assemblage from amphibolite in the West Pelion schists.

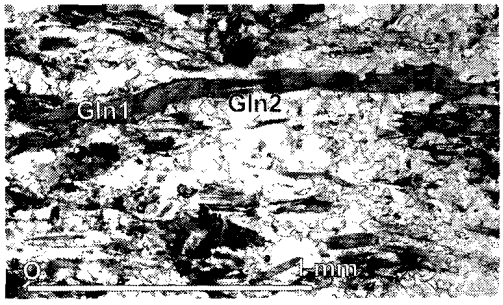

Figure 3.11e: Two stage growth of glaucophane (Gln1 and Gln2). Gln2 grows in pull apart fractures in Gln1. Sample from quartzofeldspathic-mica gneiss from West Ossa schists on the northwestern flanks of Mt. Ossa.

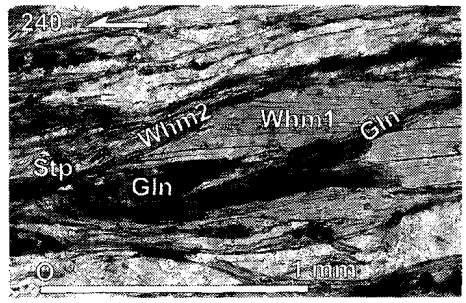

Figure 3.11f: Large grains of phengitic white mica (Whm1) have been cross-cut by finer grained phengite (Whm2), which has grown in association with glaucophane (Gln). Glaucophane has grown along shear planes which defined a sinistral sense of shear. The shear have then been cross-cut by fibres of stilpnomelane (Stp).

Alpine Orogeny, e.g., the Eocene/Paleocene quartz phyllites. Therefore, using the geochronological data available (see Figure 3.02), Thessalian basement can only be subdivided into the following regional chronolithological units: (1) Hercynian (and older) quartzofeldspathic gneiss, (2) Mid-Jurassic ultramafic units, (3) early Mesozoic marbles, (4) early Tertiary phyllites and (5) undifferentiated schists and phyllites (a general name referring to the remaining schists and phyllites of unknown age).

Despite this, it is clear from the distinct composition and age (see Figure 3.02), that the first three lithologies provide important marker horizons. The significance of these horizons is discussed in Section 3.7.4.

3.5 Metamorphic Petrology

3.5.1 Introduction

This section focuses on the metamorphic evolution of the basement in Thessaly, concentrating in particular on the Titaros and Pierien Mountains, and the Pelion Peninsula areas. Incomplete reconstitution of the basement during regional metamorphic events has resulted in complex overprinting sequences of minerals. This is particularly evident in the sequence of amphiboles and phyllosilicates. The mineral analyses of important index minerals are shown in Appendix B.

Unfortunately, the lithologies which are particularly useful for determining metamorphic grade, such as metapelites and metabasites, are not common across the whole Thessaly region. Metabasites (commonly albite amphibole schist/gneiss) are largely confined to northeastern and eastern Thessaly, whereas true Al-rich, Ca-poor metapelitic lithologies are extremely rare. Furthermore, much of the region is occupied by marble which contains very few indicative minerals, although mica-rich inclusions within the marble can be useful. Therefore, the description of the

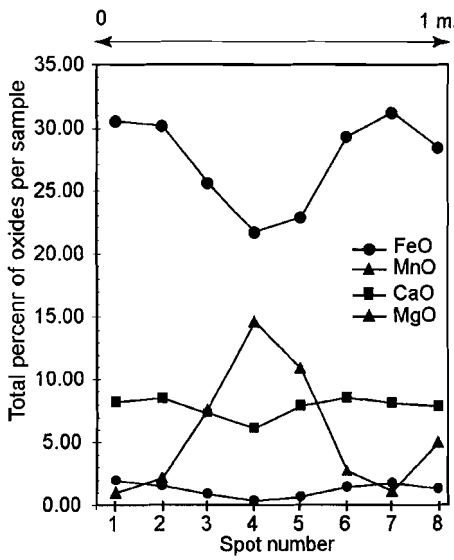

Figure 3.12
Garnet grains in quartzofeldspathic gneiss from the eastern flanks of Mavrovrouni have almandine-rich (Fe) rims and spessartine-rich cores. The increase in almandine (Fe) content is compatible with an increase in pressure (Deer et al. 1992).

regional variation in the metamorphic evolution starts with the oldest (dated) and one of the most widespread lithologies of the region, quartzofeldspathic gneisses/schist, which has a similar general composition (in hand specimen) across the region (Figure 3.10). The sequence of overprinting minerals in this lithology provides a useful regional framework for discussion of overprinting relationships observed in other more mafic lithologies (Section 3.5.3).

3.5.2 Variation in the metamorphic evolution of quartzofeldspathic gneisses across Thessaly

Across the whole Thessaly region, quartzofeldspathic gneisses/schists contain relatively coarse-grained grains of biotite, up to 3 mm in diameter (Figure 3.11b) albeit in small amounts. In this and following sections north Thessaly refers to the Pierien and Titaros Mountains, northeast Thessaly refers to the Mt. Olympos region, east Thessaly refers to the Ossa to Pelion range, south Thessaly refers to the area near Trikeri (SW Pelion Peninsula) and west Thessaly refers to the region west of the north Larissa Basin.

South and west Thessaly

In the west and south of Thessaly, quartzofeldspathic schists and gneisses also contain relic (igneous) K-feldspar. The biotite is often associated with similarly coarse-grained phengitic white mica (Figure 3.11b). Most schists in this region are overprinted by shear zones which contain very fine-grained (secondary) phengitic white mica, sericite, chlorite and rarely rutile.

East Thessaly

Towards east Thessaly (from Ossa to the Pelion Peninsula), the large, early phengitic white mica and rare biotite grains are also overprinted by secondary, fine-grained phengite (0.1-0.3 mm) and glaucophane (Figure 3.11b, 311e). In the Mavrovrouni region porphyroblasts of garnet have grown in association with chlorite, phengitic white mica and rutile (Figure 3.10b). The garnet typically contains a spessartine-rich core and almandine-rich rims (Figure 3.12) and is associated only rarely with very fine-grained, possibly secondary, (~0.1 mm) biotite. An overprint of phengitic white mica, chlorite and stilpnomelane is particularly common in the Mavrovrouni-Agia Valley and southern Pelion Peninsula areas (Figure3.10d, 3.11f).

North Thessaly

In the Titaros and Pierien Mountains of north Thessaly, the preserved metamorphic evolution of the quartzofeldspathic gneisses varies yet again. The relic biotite clasts in this region are overprinted by a fine-grained association of barroisite, white mica and secondary biotite. The relationship between biotite and barroisite is often difficult to determine and thus is interpreted to be coeval. This association is locally overprinted by an association of biotite-white mica-epidote, which in turn is locally overprinted by glaucophane. The presence of glaucophane/ crossite is relatively rare in north Thessaly, compared with rocks of similar composition in east Thessaly (Figure 3.10c).

In summary, quartzofeldspathic schists across the Thessaly region, preserve a sequence of overprinting mineral assemblages. These assemblages are summarised in Figure 3.10 and are as follows; (1) relic biotite ± feldspar , (2) barroisite-albite±white mica±biotite, (3) garnet-white mica-rutile, (4) biotite-white mica-epidote, (5) glaucophane-albite-white mica, and (6) white mica-stilpnomelane-chlorite.

3.5.3 Variations in the metamorphic evolution of other lithologies across Thessaly

The metamorphic sequences in quartzofeldspathic gneiss/schist suggest that the most complex evolutions are in the north and northeast of Thessaly, the area which comprises the most mafic lithologies of the region.

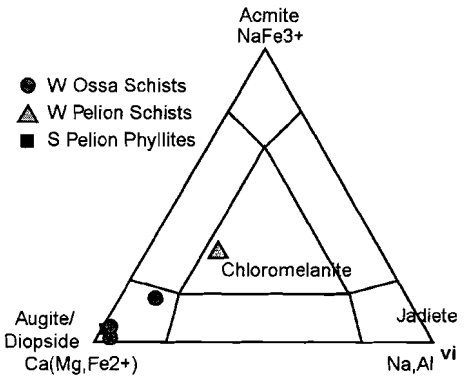

Figure 3.13
A triangular diagram of the composition of pyroxenes from pyroxene-epidote schists expressed in terms of jadiete, acmite and augite/diopside components. The composition is mostly pure augite/diopside (i.e. not a mineral indicative of high-pressure), however, locally the jadiete component is higher.

Albite-amphibole schist/gneisses

The oldest mineral preserved in albite-amphibole schists/gneiss of the Titaros Mountains to Mavrovrouni region is relic green hornblende, which was consistently rimmed by barroisitic amphibole. The barroisite is one of the main rock forming minerals of mafic rocks in this region. Although biotite was often associated with the barroisite as in Figure 3.11c, in the Titaros Mountains, biotite also was concentrated in shears which *cross-cut* barroisite (Figure 4.09a). In most regions biotite is not in equilibrium and the cleavage planes are filled with opaques and plagioclase.

Rare occurrences of glaucophane are reported in the mafic rocks in the Titaros Mountains and overprint the barrosite. This glaucophane overprint appears not to have affected units to the west, e.g. near the Kranea window as only a minor amount of barroisite is reported from this region (Figure 3.10c: Sfeikos et al. 1991). The most widespread development of glaucophane is further towards the east, in the Olympos-Pelion range. In northeastern Thessaly, glaucophane tends to form thin rims around the barroisitic amphibole in albite-amphibole schists. In rocks which contain glaucophane (usually fresh), the relic biotite has been replaced by finely interlayered iron-rich chlorite and stilpnomelane. Barroisite is particularly rare in the albite-rich schists of the Pelion Peninsula, although it has been observed in inclusions within the south Pelion phyllites where it is usually replaced by chlorite and actinolite.

The gneissic texture in albite-amphibole schists (and less commonly in epidote-chlorite-albite and pyroxene-epidote schists) is formed by the porphyroblastic growth of albite. Albite porphyroblasts are typically 1-2 mm wide although in the Mavrovrouni area they are between 3-20 mm wide. The porphyroblasts are full of inclusions of glaucophane (e.g. Figure 4.13), epidote, and/or zoisite which sometimes define a previous foliation. The inclusions in the albite porphyroblasts are often of barroisite and quartz, but epidote, glaucophane, sericite and opaques were also observed. In the West Pelion schists glaucophane is only preserved within the porphyroblasts and not in the matrix.

Other lithologies

Other mafic schists such as, pyroxene-epidote schists, amphibolites and mica-rich schists of east Thessaly, contain some of the best preserved relics of glaucophane (e.g. Figure 3.11d). A range of mineral assemblages is observed with the glaucophane. In most units, glaucophane laths, which locally can be up to 1 cm in length, are associated with epidote and albite. However locally, the main associated minerals are lawsonite (e.g. Figure 3.11d) and albite or orthoclase. In both the Mt. Ossa and the Pelion areas, some lithologies exhibit two phases of glaucophane growth (Figure 3.11e). In most other regions, only a single phase of glaucophane is observed, and is in most cases pervasively overgrown by chlorite and/or actinolite (Figure 4.11). Relic,

	Northern Thessaly	Western Thessaly	Eastern Thessaly
1	relic biotite+hornblende (QF,MB)	relic biotite (QF)	relic biotite and hornblende (QF, MB)
2	barroisite+albite±biotite (MB)	white mica of uncertain affinity ± chlorite (QF)	barroisite+albite+white mica (QF)
3	biotite-white mica (MB)		garnet+white mica+ rutile (?) (QF)
4	glaucophane+albite+white mica (MB,QF)		glaucophane+epidote/lawsonite (QF, MB)
5	white mica+chlorite (MB, QF)		white mica+ chlorite ± stilpnomelane ± pumpellyite (MB, QF)

Table 3.2
A summary of the sequence of mineral assemblages found in three different regions across Thessaly. QF = quartzofeldspathic rocks, MB = metabasite lithologies.

pre-glaucophane minerals in pyroxene-epidote schists include augite (with a minor jadiete component, Figure 3.13). The fine-grained lithologies of the Pelion Peninsula are more pervasively overprinted by chlorite-white mica-actinolite than the lithologies observed further north.

Metabasite inclusions in the Ossa marble and Veneto marble also contain glaucophane and epidote whereas 'impure' horizons in the host marble contain only white mica, chlorite, fine-grained epidote and graphite. Two samples, one from Ossa and one from northwest Pelion Peninsula, were tested for the presence of aragonite by soaking powdered samples in bromoform and by XRD analysis. The tests revealed that the only carbonate present in these samples was calcite.

Calc and quartz phyllite lithologies of eastern Thessaly rarely contain glaucophane. Relic minerals include feldspars (always partly retrogressed to sericite). In both the Agia, Veneto and South Pelion phyllites/schists, local occurrences of glaucophane were observed. The ultramafic and mafic lithologies associated with this unit were mostly composed of tremolite, calcite and serpentinite. Rare, euhedral glaucophane grains, however, were observed in marbles associated with an ophiolitic breccia on the southwestern Trikeri Peninsula.

The most recent overprint of almost all lithologies across the eastern Thessaly region is by fine-grained phengitic white mica grown in association with chlorite. Along the eastern board of the Olympos-Pelion range, stilpnomelane is particularly abundant (Figure 3.10d).

3.5.4 Summary

The lithologies of the Thessaly region show a regional variation of preserved mineral assemblages and overprinting relationships (Figure 3.10). The consistent overprinting sequence of index minerals (e.g. if both glaucophane and barroisite are present, then glaucophane invariably overprints the barroisite) allows a *sequence* of mineral assemblages to be identified which are summarised in the table below. Temporal constraints and the spatial relationships between these overprinting events are discussed in Section 3.6.

The early stages of the metamorphic evolution are best preserved in quartzofeldpathic gneisses and schists of Western Thessaly whereas the later sequences of metamorphic overprints

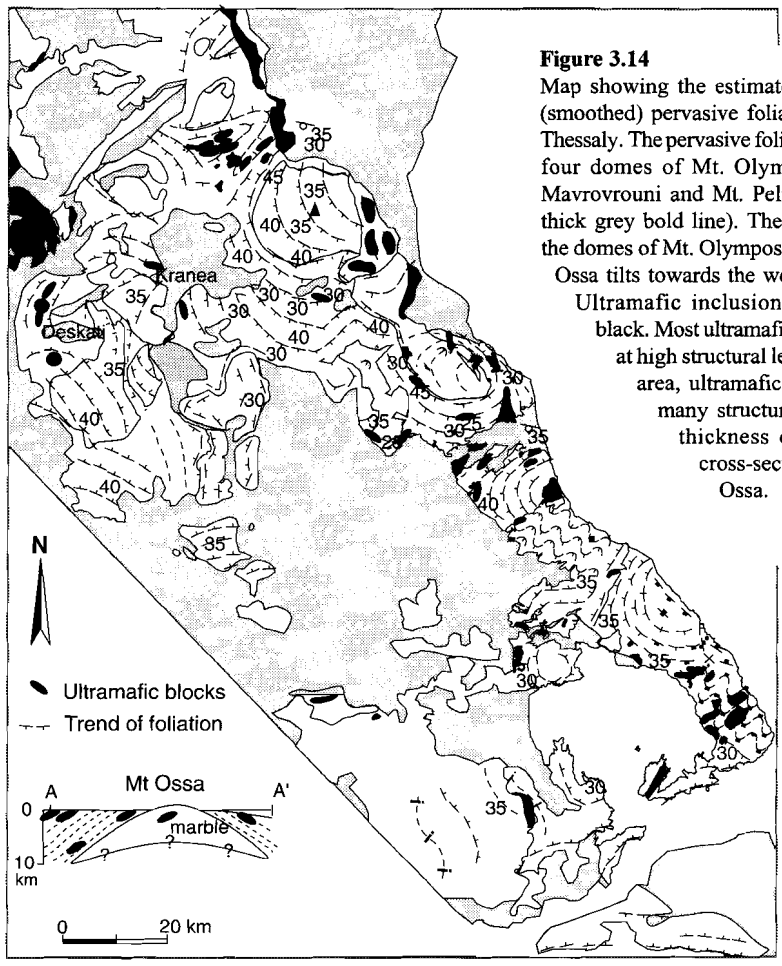

Figure 3.14
Map showing the estimated trends of the (smoothed) pervasive foliations across the Thessaly. The pervasive foliation outlines the four domes of Mt. Olympos, Mt. Ossa, Mavrovrouni and Mt. Pelion (shown as a thick grey bold line). The foliation within the domes of Mt. Olympos, Kranea and Mt. Ossa tilts towards the west to northwest. Ultramafic inclusions are shown in black. Most ultramafic blocks crop out at high structural levels. In the Ossa area, ultramafic blocks occur at many structural levels over a thickness of ~8 km (see cross-section through Mt. Ossa.

tend to be better preserved in mafic schists of north and northeast Thessaly. Although the last mineral assemblage (chlorite-phengitic white mica) occurs across much of Thessaly region, it is most strongly developed in the southern Pelion Peninsula and Agia Valley areas.

3.6 Trend of the pervasive foliation

The pervasive foliation is defined in this thesis as the planar fabric observed when standing several metres from an outcrop (i.e. it is not affected by small scale folds). The foliation may be a phyllitic, schistose, gneissic or rarely fold axial planar foliation (Figure 3.14) . The latter foliation is confined to the central Pelion Peninsula and local occurrences in eastern Ossa and is discussed in Chapter 4 (see Section 4.4.5.2). As the contacts of major lithological units are parallel to this fabric, the pervasive foliation is one of the most important frameworks available with which to gain a 3-D impression of the regional geology.

The minerals which define the phyllitic, schistose, gneissic foliation are predominantly

mica and feldspars but also include some of the key minerals described in the section above. Thus, the age of the fabric forming minerals provides a broad indication of the relative age of the fabric. Although the age/s of the pervasive foliation across the region are discussed in detail in the following chapter, it should be noted that the pervasive foliation direction across much of southeastern and western Thessaly is defined by actinolite, and chlorite.

Figure 3.14 depicts the regional variation in the trend of the pervasive foliation across Thessaly. The foliation is generally shallow to moderate dipping (~35°). In particular, note that the pervasive foliation defines the four anticlinoriums in Mt. Olympos, Mt. Ossa, Mavrovrouni and Mt. Pelion areas. Within these anticlinoriums are marble units which generally tilt to the northeast in western Thessaly, and to the southwest in eastern Thessaly. Also shown are the locations of ultramafic lithologies (in black). The ultramafic units are most abundant at high structural levels but blocks 10-100's m long occur at a range of other structural levels (e.g. within Mt. Ossa, see cross section at bottom left of Figure 3.14). The significance of the wide distribution of the ultramafic blocks throughout the basement is discussed in Section 3.7.3.

3.7 Discussion

3.7.1 Introduction

This chapter started with a discussion of published large (Pelagonian Zone) and small (tectonostratigraphic) subdivisions of the metamorphosed basement in Thessaly. It was concluded that, errors in mapping aside, the current lack of consistency in the definition and boundaries of the subdivisions is largely a function of the application of multiple and poorly defined criteria, both within and between each study. To avoid perpetrating these problems, in this study the basement of Thessaly was examined systematically, first by subdividing the basement into minimum workable units (lithologies distinguishable on a >10 cm scale) based on composition and grain size alone, then by individually examining these lithologies using clearly defined temporal and metamorphic criteria (e.g. age of crystallisation/deposition, preserved metamorphic history).

In this section the geochronological constraints on the regional metamorphic evolution of these lithological unis are examined, and the conditions of metamorphism discussed. As a result, the spatial variation of the preserved metamorphic history allow three distinct regional metamorphic units to be identified (Section 3.7.2). These metamorphic units provides a framework with which to examine the lithological evolution, discussed in the following section (Section 3.7.3). To do this, the quartzofeldspathic and ultramafic horizons are used. These lithologies demonstrate the lithological complexity of the Thessalian metamorphic basement. The cause of which is discussed below.

3.7.2 Correlation between lithological associations

In this section the relationship between the lithological associations presented in Section 3.4.2.3 is examined in terms of the regional pervasive foliation. Available pervasive foliation data of the Thessaly region suggests there is no major tilt in foliation attitude between the Mt. Olympos and Pelion Peninsula.

The West Ossa schists exhibits the most similarities with the West Pelion schists as these are the only associations in east Thessaly which are dominantly composed of epidote-rich

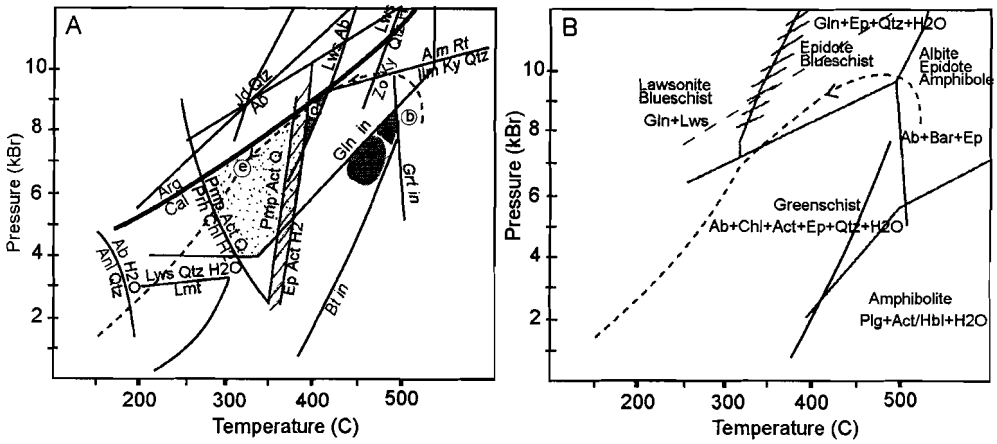

Figure 3.15: Estimates of the maximum preserved metamorphic conditions in east Thessaly from metamorphic assemblages preserved in metabasites. The petrogenic grid in Figure 3.15a also shows the stability field for biotite from a petrogenic grid for pelitic lithologies. Petrogenic grid in Figure 3.15a from Yardley (1984), Figure 3.15b is a petrogenic grid from Evans (1990) showing the nomenclature of subdivisions for high pressure lithologies used in this thesis.

schist and gneisses intercalated with marble. The West Ossa schists, however, contain more albite-amphibole schist and quartzofeldspathic gneiss whereas the West Pelion schists are more marble-rich, particularly towards the south.

The Mavrovrouni quartzofeldspathic gneiss are similar in composition (in hand specimen) to gneisses intercalated with West Ossa schists (particularly towards the south). Thus there may be a very gradational boundary between these two units. The Mavrovrouni gneiss is interpreted to overly the West and East Ossa schists.

The East Larissa marble unit is very similar to the Ossa marble, and contains inclusions of similar composition but occurs at different structural levels and therefore may not be correlated.

The inclusions in East Larissa marble consist of albite-amphibole schist, quartz phyllites and ultramafics. This broad range of lithologies has many similarities with the schist and ultramafics within Agia and South Pelion phyllites. The Agia phyllites contain fewer intercalated epidote-rich schists and is dominated by quartz phyllite unlike the South Pelion phyllites. Furthermore, no large marble unit lies between the Ossa schists and Agia phyllites. Thus, while many lithological associations bare many similarities across the region, the similarities are too few to allow a meaningful correlation between the units.

3.7.3 The metamorphic evolution of Thessaly

Despite the dearth of lithologies suitable for detailed pressure-temperature estimates such as pelite, the mineral assemblages in metabasites of eastern Thessaly (pyroxene-albite gneiss, albite-amphibole schist/gneiss) enable medium to low grade metamorphism to be reasonably well constrained.

Conditions of metamorphism

The regional petrographic study presented in Section 3.5 revealed that relic biotite and

hornblende in metabasites were pervasively overprinted by barroisite in conjunction with albite (± biotite). The overprinting mineral assemblage is typical of moderate temperature (>500°), moderate to high pressure (>6 kbr) conditions of the albite-epidote amphibolite metamorphic facies (Figure 3.15). The almandine rim of garnet in the Mavrovrouni quartzofeldpathic gneiss (Figure 3.12) and higher jadiete components of some pyroxenes in southern Thessaly (Figure 3.13) are interpreted to reflect this increase in pressure (see Deer et al. 1992).

As the conditions are similar to those required for the development of the biotite observed in cross-cutting shears in quartzofeldpathic rock (Figure 3.15; Yardley 1989), both mineral assemblages are tentatively interpreted to have developed during similar metamorphic conditions. This metamorphic event is referred to as M1.

Both quartz- and mica-rich lithologies across northeastern and eastern Thessaly region were then overprinted by an assemblage of glaucophane-albite-epidote/lawsonite. The local occurrences of glaucophane-albite-lawsonite in conjunction with the lack of aragonite constrain the conditions of this metamorphic event in eastern Thessaly to ~ 400° C and ~ 8 kbar (Figure 3.15). This phase lies within the epidote-blueschist facies (Figure 3.15) and is termed M2.

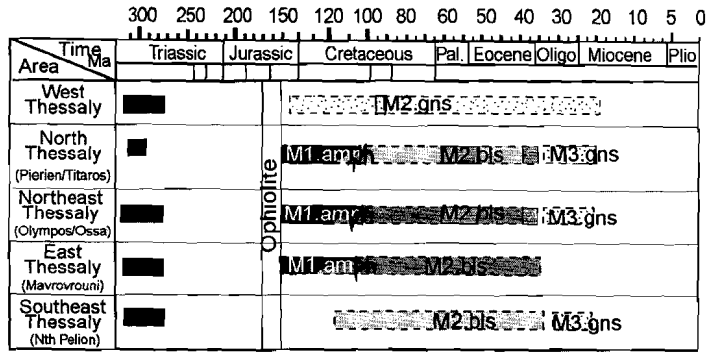

Figure 3.16
A figure summarising the overprinting relationships of minerals across regions in Thessaly discussed in the text. The regions enclosed in bold lines are those with geochronological constraints (see text for discussion). The regions enclosed with dashed lines are for events which have few geochronological constraints.

The progression from M1 to M2 represents cooling of the metamorphic pile. Although cooling may have occurred in conjunction with decompression, there are few constraints on the pressure of M1.

Schermer et al. (1990) note several phases of blueschist facies metamorphism in the Mt. Olympos area, and two distinct episodes of glaucophane growth were locally observed in Mt. Ossa (Figure 3.11e). However, multiple phases of glaucophane growth were not observed in units south of Ossa. This may be due to a more pervasive overprint of the later greenschist facies metamorphism in this area. In all cases where two episodes were apparent, no change in metamorphic grade (e.g. epidote altering to lawsonite) could be detected. Therefore, a conclusion of this study is that (epidote) blueschist facies metamorphism best represented by a single phase (M2).

Finally, the development of an overprinting pumpellyite-actinolite-quartz assemblage allows the retrogressive path of eastern Thessaly mafic lithologies to be broadly estimated (Figure 3.15). The lack of useful PT minerals in the retrograde assemblage precludes a refined estimate of the metamorphic conditions beyond low grade greenschist facies (M3). Since no blueschist facies minerals are overprinted by higher temperature minerals in the Thessaly region, the

resulting PT loop is interpreted to follow an anticlockwise path (Figure 3.15).

The pressure-temperature conditions determined from this study for eastern Thessaly are similar (within ± 50°C) to those determined from the closure temperatures of dated minerals in the Mt. Olympos region (Figure 10 in Schermer et al. 1990). Note that the classification of high pressure metamorphic facies used in this study is after Evans (1990) and thus, differs to that used by Schermer et al. (1990).

Temporal constraints on metamorphic events

Detailed geochronological studies by Schermer et al. (1990) and Lips et al. (1998) allow some temporal constraints of the metamorphic events/evolution to be established across much of the region (summarised in Figure 3.16).

The earliest phase of metamorphism of Schermer et al. (1990), 'M1' metamorphic phase, has a cooling age >100 Ma. The dates of metamorphism in Figure 3.03 show that a variety of of conditions occurred between the Hercynian (~300 Ma) and 100 Ma period. The oldest cooling ages of biotite, hornblende and phengitic white mica in the quartzofeldspathic gneiss cluster around 300 Ma and are interpreted to be cooling ages after Hercynian igneous crystallisation (Schermer et al. 1990). Thus, the relic biotite described in section 3.5 are interpreted to be Hercynian in age. The large phengitic white micas may also be this age but due to the large number of episodes of phengitic growth (observed as fine-grained phengitic white mica) the cooling age of this mineral is ambiguous.

The next cluster of cooling ages is in amphibolite grade mafic lithologies (see Figure 3.16), starting from 135-100 Ma (figure 3.03). Lithologies with this metamorphic age are observed in southeastern Titaros Mountains and around Mt. Olympos and represents the M1.amph metamorphic event. In this study, no barroisite was observed to overgrow low-grade greenschist (chlorite-epidote-white mica) assemblages in metabasite in constrast to observations of Schermer (see Table 2 in Schermer 1993). Rather, barroisite (M1) was observed overgrowing relic (Hercynian) biotite and relic hornblende. Thus, albite-epidote amphibolite event is interpreted to be the first major post-Hercynian event and is thought to be early Cretaceous in age. The very localised development of secondary metamorphic biotite is interpreted to be contemporanous with the waning stages, or immediately postdating, the albite-epidote amphibolite facies metamorphism (also M1).

Albite-epidote amphibolite facies metamorphism observed in the metabasites of northern Thessaly was followed by the epidote blueschist facies metamorphism/s (M2.bls) between 64-36 Ma (Figure 3.16: Schermer et al. 1990). Schermer et al. (1990) suggested that marginal blueschist facies metamophism occurred at low structural levels contemporaneous with 'upper greenschist' (albite-epidote amphibolite) facies metamorphism at higher structural levels (Figure 10 in Schermer et al. 1990). However, as the cooling age of blueschist facies rocks is much younger (~115 Ma) than the oldest cooling ages in the albite-epidote amphibolite facies lithologies (135 Ma, figure 3.03). This suggests that the temporal overlap between the two events (M1 and M2) was relatively short (Figure 3.16).

Schermer et al. (1990) estimated that retrogressive low grade greenschist metamorphism probably started in the Oligocene (Figure 3.03). However, the presence of detrital glaucophane in the Eocene sediments of the Meso-Hellenic Trough (Faupl et al. 1996) indicates that portions of the blueschist facies lithologies must have been completely exhumed prior to much of the greenschist facies metamorphism (M3.gns). This indicates that greenschist of southeast Thessaly must be one of the youngest phases of metamorphism in the region (<35 Ma, Figure 3.03).

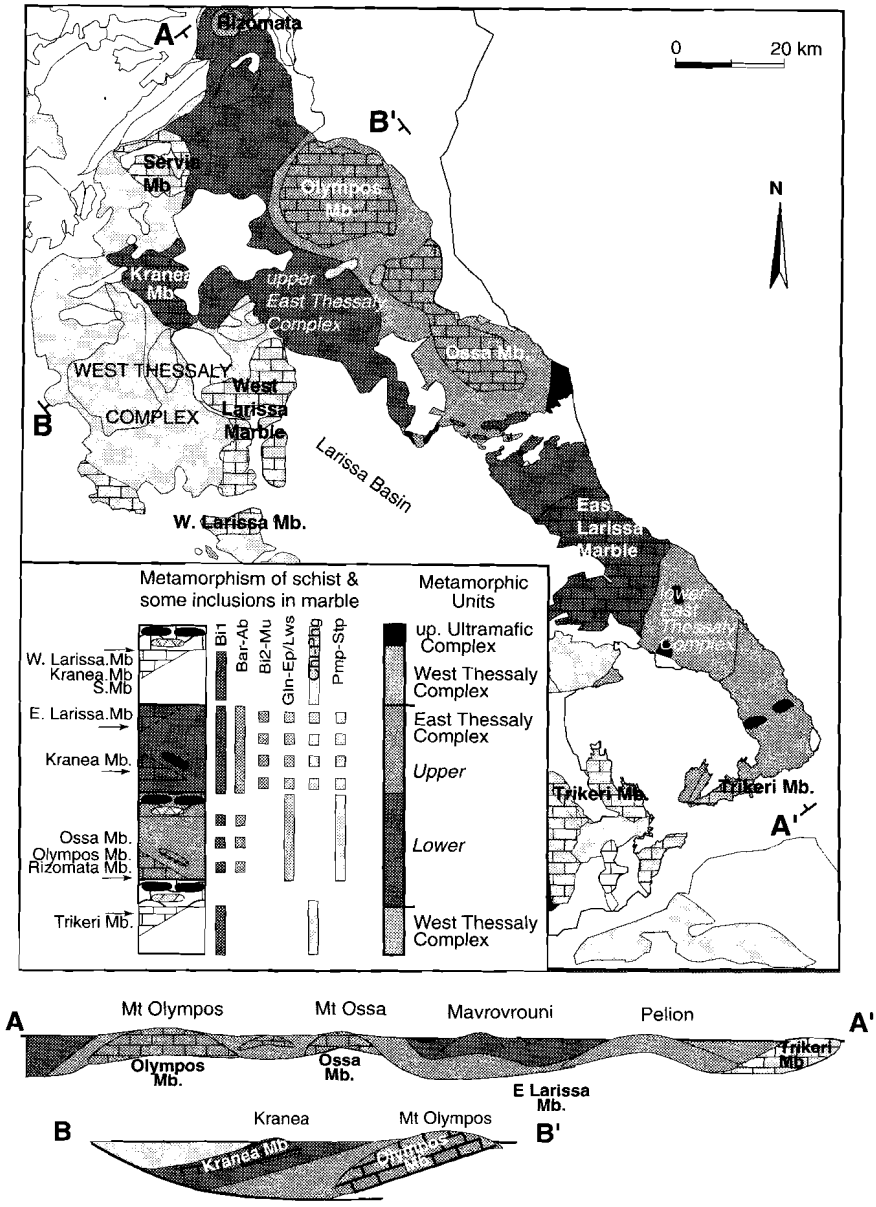

Figure 3.17

A map of the Thessaly region summarising the location and structural relationships between the major metamorphic complexes. The preserved metamorphic assemblages allow the basement of the Thessaly region to be subdivided into two major metamorphic units: the West and East Thessaly Complex respectively. The metamorphic evolution used to define each complex is summarised at the bottom left of the diagram. The West Thessaly Complex largely comprises Hercynian schists and gneisses and has only experienced pre mid Cretaceous low grade metamorphism. The East Thessaly Complex comprises a range of

Greenschist facies rocks near the town of Longa in western Thessaly give Cretaceous (120 Ma and 80 Ma) cooling ages (pers. comm. Lips 1998), and thus are contemporaneous with the early stages of blueschist facies metamorphism in eastern Thessaly. This greenschist facies event occurred at relatively high structural levels (see Figure 3.14) and is therefore termed M2.gns. Without more geochronological data it is difficult to ascertain whether the greenschist facies metamorphism in other areas of western Thessaly was contemporaneous with the greenschist facies metamorphism in the east Thessaly. Structural data provides further constraints and is discussed in the next chapter (Chapter 4).

Regional Tectonothermal Units

The three metamorphic events identified in this study are similar to those identified by Schermer et al. (1990). This study provides additional, detailed information on the spacial variation of these metamorphic events. In conjunction with estimates of the regional pervasive foliation direction, the metamorphic history in mafic and quartzofeldspathic lithologies allow 3 tectonothermal complexes to be identified (one of which may be subdivided into two) which are characterised as follows.

The *West Thessaly Complex* is characterised by very low grade metamorphism (shown in white in Figure 3.17). The *East Thessaly Complex* is composed of a wide range of lithologies which are characterised (on a regional scale) by the presence of high pressure assemblages (i.e., albite-epidote amphibolite (M1.amph) or epidote blueschist (M3.bls), shown in white in Figure 3.17). Note that the available structural data indicate that the West Thessaly Complex occurs both structurally above and below the East Thessaly Complex, in the western and southern Thessaly regions respectively (Figure 3.17).

The East Thessaly Complex may be subdivided into two on the basis of structural position and of metamorphic evolution preserved in its mafic lithologies. The highest structural level is occupied by the *upper East Thessaly Complex* which is characterised by the widespread preservation of albite-epidote amphibolite facies. The *lower East Thessaly Complex* comprises a complex range of lithologies (epidote-rich schists, phyllites, marbles) and is characterised by relic epidote (or lawsonite)-blueschist facies metamorphism but only sparse albite-epidote amphibolite facies metamorphism.

Due to the relatively small number of samples analysed, these metamorphic complexes reflect only major regional-scale subdivisions of the rocks. When examined in terms of the quartzofeldpathic gneiss and ultramafic marker horizons, the composition is clearly more complex (see lithotectonic column in bottom left of Figure 3.17).

3.7.3 Lithological Evolution of Thessaly

As mentioned in Section 3.4.3, serpentinites and quartzofeldspathic gneisses, in particular, provide useful lithologies with which to examine the lithological structure of the metamorphic

---

compositions and includes lithologies as young as Eocene quartz phyllites and largely records late Cretaceous to Tertiary metamorphic events. The upper East Thessaly Complex *dominantly* comprises mafic and quartzofeldspathic gneisses and the lower East Thessaly Complex *dominantly* comprises epidote-rich schists, quartzofeldspathic schist and marbles but many lithologies crop out within all metamorphic complexes and at all structural levels (see figure 3.08). This is demonstrated by the early Mesozoic marble and ultramafics in simplified lithotectonic column for Thessaly at the bottom left of the diagram. Ol.M = Olympos marble, Os.M = Ossa marble, K.W = Kranea marble, V.M = Verdikoussa marble, T. M = Trikeri marble, and R.M = Rizomata marble.

basement. When examined in terms of structural position the lithologies form complex units interlaminated at all levels (Figures 3.07 and 3.14). Although ultramafic blocks are largest at high structural levels, there is little evidence that the ophiolites are confined to a single or two discrete horizons as suggested by previous workers (see Figure 3.05); ophiolite blocks are scattered throughout the region. Thus, the distribution of ophiolite blocks is not necessarily indicative of the 2-discrete obduction events as has been suggested, e.g. Jacobshagen and Wallbrecher (1984).

The differing ages obtained from ultramafics and quartzofeldpathic rock, plus the obviously different sources of these lithologies (oceanic, and continental respectively), suggests that the incorporation of the mid-Jurassic ultramafics *into* Hercynian quartzofeldspathic gneisses is unlikely to have occurred by sedimentary or intrusive means and therefore is most likely to be the result of tectonic processe(s). Without the benefit of kinematic criteria (discussed in the following chapter), it is difficult to eastablish whether this tectonic process involved one or more obduction events. However, the estimated age of formation (Section 3.4.3.2), is similar in all cases. It is suggested that distribution of ultramafics, through at least ~8 km of crust (see cross-section in Figure 3.14) is the result of a tectonic 'mixing' process that primarily affected the intermediate to lower structural levels of the East Thessaly Complex. Furthermore, the lensoidal shape of ultramafic bodies at low structural levels, which were presumably once part of oceanic sized blocks, suggests that there has been physical and chemical erosion of the margins of the blocks during tectonism.

Such 'blending' of one lithology with another (or mix of lithologies) was also observed on a small scale in the Pelion Peninsula. Although it is difficult to estimate the role of both physical and chemical mixing processes, if it has affected relatively competent lithologies such as ultramafic and mafic lithologies then similar processes presumably have affected less competent units. For example, such tectonic mixing processes may be the origin of the numerous marble horizons ~1-10 m that are apparent in the vicinity of large marble units, e.g. the southern margin of the Mavrovrouni quartzofeldspathic gneiss (Figure 3.09).

Tectonostratigraphic evolution of Thessaly

The lithological sequence of metamorphic basement (in particular the schistose and phyllitic units of the lower East Thessaly Complex) is therefore best described as ductile melange (summarised in the tectonostratigraphic column at the bottom left of Figure 3.17). This melange, however, has been subject to regional (syn-tectonic) metamorphism that resulted in a sequence of discrete and mappable (on a 10-100 km scale) *metamorphic* units. The boundaries of each metamorphic slice are diffuse on a smaller scale (100 m scale).

Although the tectonothermal complexes are primarily based on the evolution of the meta-basite lithologies, each metamorphic unit consists of different dominant lithologies. The West Thessaly Complex is primarily composed of quartzofeldspathic gneiss and schist with minor intercalated micaceous schists and amphibolites and rare ultramafic units; the upper East Thessaly Complex is dominanted by mafic lithologies and quartzofeldspathic gneiss, whereas the lower East Thessaly Complex is dominanted by calcareous, phyllitic and mafic lithologies and contains the most ultramafic units. On the basis of lithological content, the West Thessaly Complex represents a relic slice of Hercynian basement whereas the wedge of East Thessaly Complex contains a higher proportion of lithologies related to subduction (e.g., ophiolite and phyllite, Ernst 1975) and thus is interpreted to represent a ductile melange.

As the upper East Thessaly Complex contains ultramafic units and has undergone albite-

epidote amphibolite (M1.amph) metamorphism (Figure 3.09), the assembly of this melange in this region is most likely to have begun in the early Cretaceous (between 135-100 Ma). Most ultramafic units however are associated with the M2.bls units (although they are also observed in M2.gns units east of Kranea, Figure 3.14). The Eocene-aged, quartz phyllites of Mt. Ossa (Figure 3.02) are the youngest lithologies to contain ultramafic bodies, hence the assembly of the ductile melange in this area did not cease until after the Eocene. As this unit is covered by Neogene gravels in the Agia Valley (Caputo and Pavlides 1993), the age of this complex must be between Eocene and Miocene. The variable metamorphic history preserved in the units which contain ultramafic blocks (ultramafic lithologies form few index minerals), suggests that not all ultramafic blocks followed the same obduction and subduction (and therefore metamorphism) path. Rather, mixing of ophiolite blocks into the Thessalian basement appears to have occurred over a long time span (~ 100 Ma).

Thus, the lithologies and metamorphism of the Thessalian basement records the initially moderate temperature metamorphism (M1) and cooling during decompression (M2-M3) of melange which developed during all stages of Alpine Orogeny. M2 is subdivided into M2.gns and M2.bls, which represent different structural levels of the same event. The regional evolution of the Thessaly region is discussed in Chapter 6 in conjunction with the strucutural and kinematic results presented in Chapter 3.

The complexity of the tectonostratigraphy of the Thessaly region may be one of the major causes of difficulties faced in trying to correlate units across the Aegean (see Section 2.4.2.3)

3.8 Summary and Conclusions

1. A thorough review of the literature concerning the lithological and metamorphic development of the basement of the Pelagonian Zone in the Thessaly region and the definition of the Pelagonian Zone is presented. The review revealed an enormous variation in definitions of the units/zones and it was concluded that this is in part due to confusion induced by the application of variable criteria when defining units in metamorphic complexes.
2. A new system for subdividing the basement of east Thessaly is presented. This system involved the identification of 12 lithological units based on the dominant mineral constituents and mineral size (e.g. phyllitic, schitose, gneissic). The lithological units were examined separately in terms of three criteria; (1) age of formation, (2) preserved metamorphic evolution, (3) pervasive schistosity level. This examination led to conclusions 3-6 outlined below.
3. A detailed metamorphic study across Thessaly identified a sequence of three Alpine metamorphic events which overprint relic Hercynian minerals:
   M1: An early, early Cretaceous, albite-epidote amphibolite facies event (>6 kb, >450° C) (M1)
   M2: A late, early Cretaceous to early Tertiary, epidote/lawsonite blueschist facies event (M2.bls, ~400° C, 8 kbr) in conjunction with an upper greenschist event in west Thessaly at high structural levels (M2.gns),
   M3: A greenschist facies event (M3.gns), mainly in east Thessaly.
4. Variation in the preservation of these events allows the basement to be subdivided into 3 major lithological complexes:
   The West Thessaly Complex comprises rocks affected by only by greenschist facies

metamorphism (locally of M2.gns).
The East Thessaly Complex is composed of 2 subcomplexes: the upper and the lower East Thessaly Complex which best preserve M1.amph and M2.bls metamorphic events, respectively.

5. The boundary between units that exhibit high-pressure mineralogies and those that have not is gradational.
6. Comparison of the ages of crystallisation of some units (chiefly quartzofeldspathic gniess, and ultramafics) suggests that these units are important marker horizons. They crop out at all levels in the structural sequence, and thus, are one of the key indicators of intense (tectonic) mixing in the region.
7. The metamorphosed basement of the Thessaly region is best described as a ductile melange, assembled during the Cretaceous to Miocene period, which is the most intensely developed in the southeast of the region.

Chapter 4:
Structural evolution of the Thessaly region

4.1 Introduction

Late Tertiary syn- to post- orogenic extension in the Aegean, as the name implies, is centered on a region which had previously undergone orogenesis. Although in many areas deformation related to extension has largely obliterated the earlier structures, the Thessaly region, which is located near the northern and the outer margin of this stretched region (Figure 4.01), provides an important insight into all stages of development and collapse of the Alpine orogen.

Many tectonic windows, the most famous of these being the Olympos window, have been identified in northern Thessaly (Figure 4.01). These windows are thought to expose the units that underlie a major Alpine thrust sheet (Godfriaux 1968). As a consequence, most structural

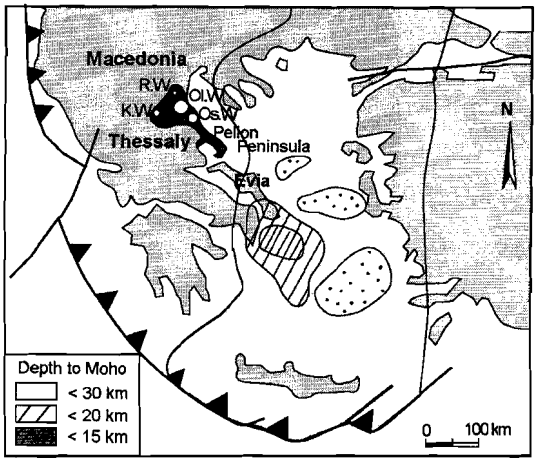

Figure 4.01
Basement rocks of the Thessaly region (shown in dark shade) comprise sheets which were thrust over low grade calcareous platform sediments during the Eocene. These calcareous units are now exposed as tectonic windows (shown as white spots). The thrust sheets now lie to the northwest of the locus of Aegean extension as represented by region of crust less than 30 km thick. Moho depth from Tsokas and Hansen (1997). K.W. = Kranea window, R.Z. = Rizomata window, Ol.W. = Olympos window, Os.W. = Ossa window.

studies in Thessaly have focused on the kinematics of (ductile) deformation in and around these 'windows'. The area to the south of the Olympos window has received considerably less attention (Figure 4.02). This chapter presents a detailed structural study of the Thessaly region concentrates in particular on the area between Mt. Olympos and the southern Pelion Peninsula (shown as a thick bold line Figure 4.01). This detailed study is combined with a study of other areas in Thessaly (namely western and northern Thessaly) to determine the metamorphic and structural evolution of the region throughout the development and collapse of the Alpine Orogeny.

In this chapter, the following terms are used: a 'kinematic unit' is defined as the region in which kinematic and structural features have a consistent orientation, within a single metamorphic grade; a 'deformation phase' is defined as the period of time during which kinematics of deformation demonstrate a consistent orientation. Hence, a single deformation phase may effect different crustal levels and therefore be recorded in lithologies of different metamorphic grades. The distinction between these definitions is important as, in the Thessaly region, deformation phases have affected lithologies of different metamorphic grades both synchronously and diachronously. The structural data of Thessaly is presented first in terms of

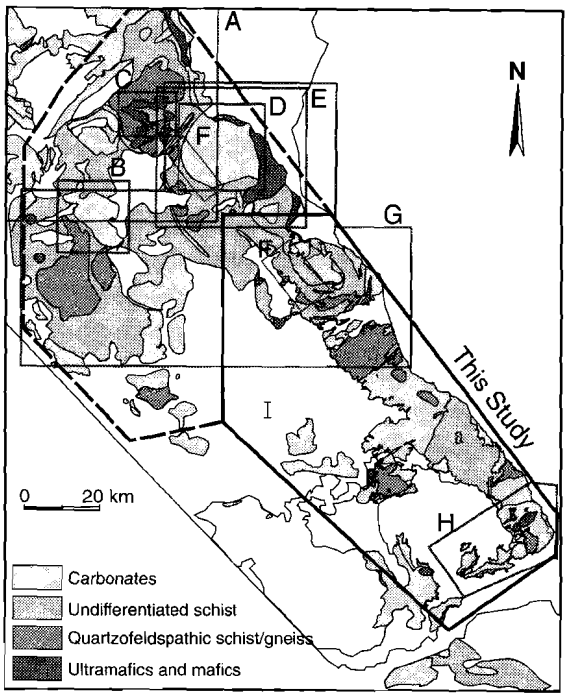

Figure 4.02
The outlines of areas covered in the published studies concerning the structural evolution of Thessalian basement are superimposed on a simplified lithological map of Thessaly. Note that carbonates are one of the most widespread lithologies of the region. A = Kilias et al. (1991), B = Sfeikos et al. (1991), C = Nance (1981), D = Barton (1975), E = Schermer (1993), F = Vergély and Mercier (1990), G = Doutsos et al. (1993), H = Jacobshagen and Wallbrecher (1984), I = Caputo and Pavlides (1991).

the different 'kinematic units', then, by examining the temporal and overprinting relationships between kinematic units, deformation phases are determined. Using this method, kinematic units within greenschist facies lithologies allow temporal variations in greenschist facies shear zones to be ascertained in areas lacking geochronological data.

The chapter is subdivided into three sections. The first section discusses the results of previous structural studies in Thessaly. Second, the structural evolution of the region is discussed in terms of the metamorphic events defined in Chapter 3. Meso- and microstructures of shear zones developed in each metamorphic event are summarised. The structural significance of a previously undescribed unusual 'fibrous' calcite fabric found in greenschist facies marbles in eastern Thessaly is also examined. In the last section of this chapter, temporal constraints on the kinematic units are used to identify deformation phases, and a 3-D structural evolution of the Thessaly region is presented. The significance of the Thessalian kinematic data is discussed in a regional (Aegean-scale) context in the following chapter (Chapter 5 and 6).

4.2 Background

Early reconnaissance studies interpreted the basement rocks of the Thessaly region as part of a relatively stable craton (the Thessaly Massif; e.g. Kober 1952). However, active involvement of the basement rocks in the Alpine Orogeny was confirmed by the discovery of Eocene fossils in the low grade quartz phyllites (metaflysch) that lay structurally below >4 km of metamorphosed basement (Godfriaux 1968). Since this discovery, it has been well established that the basement of Thessaly is pervasively traversed by numerous low (0-30°) to moderate (30-60°) angle shear zones which range from ~120 to 16 Ma in age and which developed in a variety of metamorphic conditions (Barton 1975; Yarwood and Aftalion 1976; Yarwood and Dixon 1977).

The Alpine Orogeny is interpreted to be the result of closure and obduction of the Neotethyan

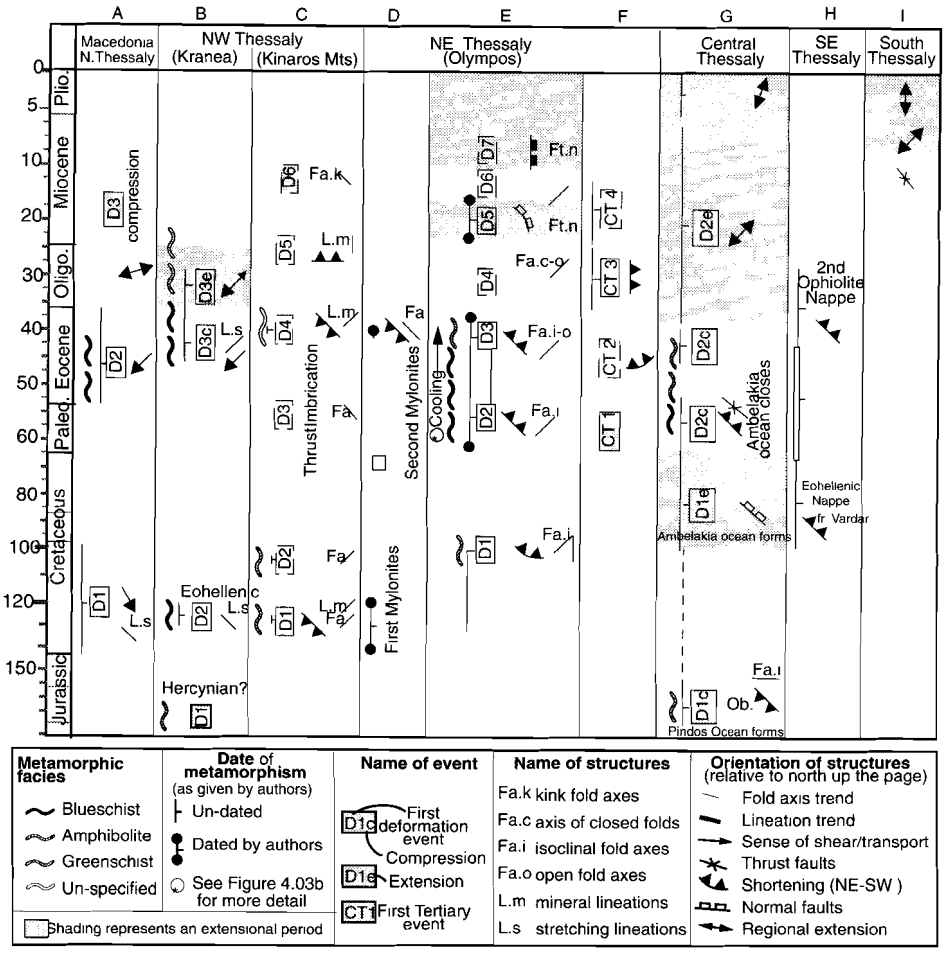

Figure 4.03a: A figure summarising the structural evolution of each of the regions shown in Figure 4.02 (see caption of figure for references). Note that while most workers favour a NE-SW direction of transport during the Tertiary, there is little agreement about the *sense* of transport. See text for discussion. A to E refer to authors in Figure 4.02. Shaded areas represents periods of extension.

oceans now preserved as fragments of ophiolite (see Section 2.4.3.2 and 2.4.3.3). As one of the few areas where the base of the Alpine nappes was thought to be exposed, much of the literature on the regions structural evolution has been largely concerned with the sense of tectonic transport during the early stages of Alpine Orogeny. The upper age of obduction is thought to be constrained by the deposition of upper Jurassic (150-169 Ma) oceanic sediments on top of the ophiolites (Robertson et al. 1991), but as no dated ductile fabrics in the continental basement are of this age (Figure 4.03a), the obduction direction has largely been determined from the kinematics of later ductile shear zones.

The structures within the shear zones define deformation events (D1-Dn), the number of which varies between each region and study (Figure 4.03a). The events, however, are often

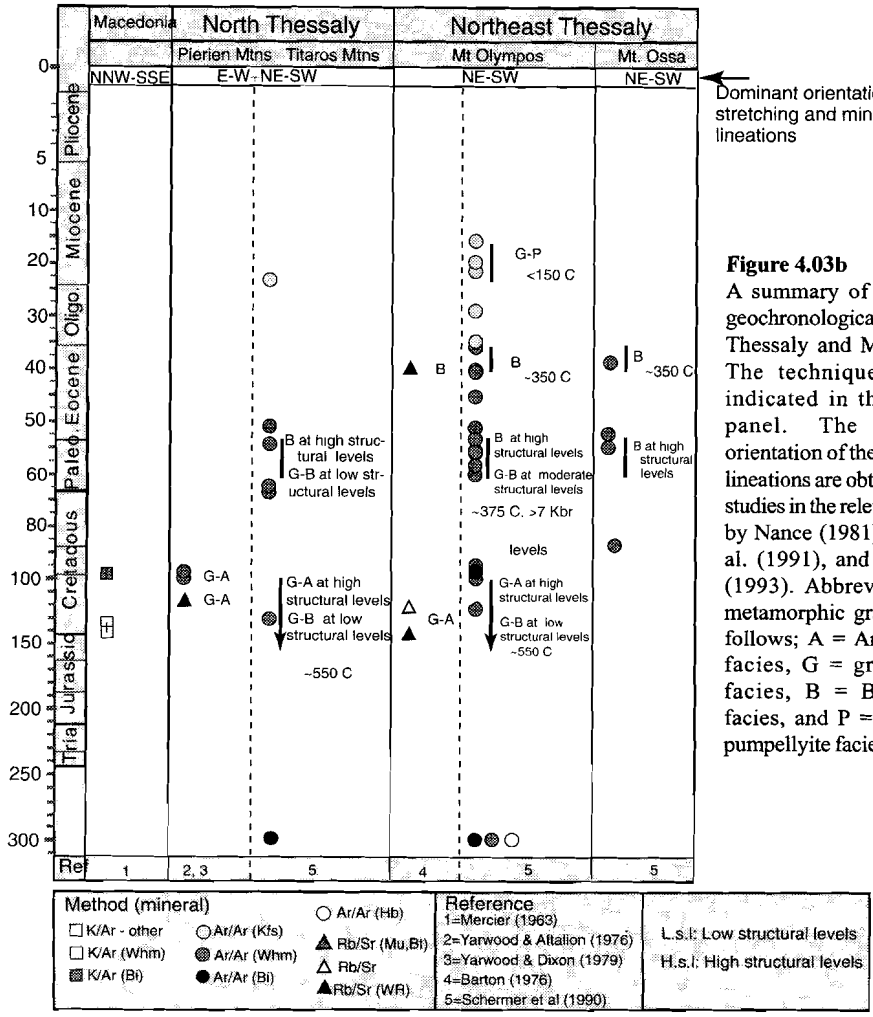

Figure 4.03b
A summary of published geochronological data from Thessaly and Macedonia. The technique used is indicated in the bottom panel. The dominant orientation of the stretching lineations are obtained from studies in the relevant region by Nance (1981), Kilias et al. (1991), and Schermer (1993). Abbreviations of metamorphic grade are as follows; A = Amphibolite facies, G = greenschist facies, B = Blueschist facies, and P = Prehnite-pumpellyite facies.

interpreted as part of two major periods of deformation, one in the early Cretaceous and one that spans the Paleocene and Eocene to the present (Figure 4.03a and b). Some workers have interpreted the two periods to be the result of two ophiolite obduction events. This is largely based on the observation that some, but not all, ophiolite-rich lithological units contain high pressure mineral assemblages (e.g., Jacobshagen and Wallbrecher 1984). Jacobshagen et al. (1978) termed the first and second obduction events as the 'Eohellenic' and 'Mesohellenic' events respectively. The Eohellenic event was defined to incorporate the intrusions, metamorphism and structures associated with SW directed obduction of oceanic crust between 120-160 Ma. The term 'Eohellenic', however, has also be used to describe an NE directed obduction event (Doutsos et al. 1993). Both Jacobshagen et al. (1978) and Doutsos et al. (1993) suggest that the two major periods of deformation are separated by an extensional or tectonically quiet period. Most workers to date, however, do not recognize a gap in tectonism,

and hence favour a single phase of obduction and do not follow the above terminology (e.g., Schermer 1993).

To the north of the Thessaly region, in the basement of the Macedonian Massif (see Figure 4.01a), a early Cretaceous period of deformation is thought to have involved greenschist facies, SSE directed thrusting (Kilias et al. 1991). The sense of thrusting is inferred to have gradually rotated clockwise, so that by the Eocene it was towards the SW. South of the Macedonian Massif in the Thessaly region, indicators of a SSE sense of shear are less common. Near the Kranea window (Figure 3.01), Sfeikos et al. (1991) have stated that NNW-SSE trending mineral lineations predate the more dominant NE-SW trending fabrics, but provide no supporting evidence. In the Titaros Mountains of north Thessaly (Figure 4.02), Nance (1981) observed that N-S trending lineations occur within ultramafic units only, and suggested that these are the result of later intra-continental thrusting during the final (Miocene) stages of the Alpine Orogeny (Figure 4.03a).

Most of the ductile shear zones in east Thessaly have a NE-SW direction of shear (see caption of Figure 4.03a for references). Despite numerous studies, little consensus has been reached on the *sense* of displacement. For example, Nance (1981) suggests, on the basis of vergence direction of folds, that thrusts were largely directed towards the NE (column C in Figure 4.03a), whereas Schermer (1993) favours the opposite (SW) sense of transport throughout the Alpine Orogeny (column E in Figure 4.03a). Doutsos et al. (1993), on the other hand, observed both senses of shear (first top-to-the-NE followed by top-to-the-SW, column G in Figure 4.03a). In some cases similar data have been interpreted by different workers to indicate different senses of transport. For example, the vergence direction of folds observed on the western flanks of Mt. Olympos have been interpreted to indicate both a NE sense of transport (Barton 1976) and a SW sense of transport (Vergély and Mercier 1990).

Temporal constraints on deformation phases in the region are largely based on the results of greenschist to amphibolite facies deformation in the Pieria-Titaros Mountains and from the blueschist to prehnite-pumpellyite facies lithologies of Mt. Olympos and Mt. Ossa (see Figure 4.03b for dates and references).

In a detailed combined structural and geochronological study in the basement surrounding Mt. Olympos, Schermer (1993) distinguished 3 tectonic events that developed during what she interpreted as consistent top-to-the-SW shortening. Although these events involved the development of many similar sets of structures (e.g., NE-SW trending open to close folds), she observed that the early deformation phases (her D1-D2) synchronously affected different structural levels and synchronously occurred in rocks deforming in different metamorphic conditions (Figure 4.03b). In general, the lower structural levels involved of a lower grade metamorphism although the boundaries between the different metamorphic grades migrated upwards (in structural level) with time. For example, while the lower structural levels started to undergo greenschist/blueschist facies metamorphism during her D1, the higher structural levels did not start to undergo blueschist facies metamorphism until her D2. Without the benefit of such detailed geochronological constraints, and noting the similarity in structures developed in blueschist facies, other workers have interpreted these structures as part of a single event (e.g.,' D1' Sfeikos et al. 1991).

Regional extension is generally thought to have begun in the Oligocene with the development of low angle normal faults (Schermer 1993, Doutsos et al. 1993), relative to the present reference frame. Interpretations differ as to the conditions prevailing during the early extensional events. Schermer (1993) proposed that extension in the Olympos area involved entirely brittle faults,

and therefore was unrelated to any metamorphism. Doutsos et al. (1993), on the other hand, suggest that the extension affected the last stages of ductile (greenschist facies) deformation.

Schermer (1993) and Caputo and coworkers (Caputo 1990; Caputo et al. 1994; Caputo and Pavlides 1993) all note that the orientation of normal faults has changed since the first NW-SE trending faults developed in the early Miocene (Figure 4.03a). However, the orientation of the new structures differs between the workers. Schermer (1993) suggested that the early faults were first overprinted by NE-SW trending folds (a result of NW-SE directed shortening) and again by a set of N-S trending normal faults (column E, in Figure 4.03a). In contrast, Caputo and coworkers suggested that the first cross-cutting faults were orientated NE-SW (i.e. at right angles to the old faults) and that these have been cross-cut again by late Pliocene, WNW-ESE trending faults (column I, in Figure 4.03a).

To summarize, previous studies have established that, in the Thessaly region, ductile deformation began in the early Cretaceous and involved largely NE-SW directed transport during the height of the Alpine Orogeny. There is less consensus on the orientation of both the *earliest* and the *latest* Alpine structures and very little consensus on the *sense* of transport throughout the orogenic development and collapse. Schermer (1993) demonstrated that in the Olympos area early deformation phases affected lithologies that exhibit different metamorphic grades. Few structural studies elsewhere in the Thessaly region have discussed such a possibility. Thus, the study reported in this chapter aims, in part, to expand on the findings of Schermer (1993) and determine the spatial distribution of major metamorphic and deformation phases across the Thessaly region as a whole.

4.3 Method of kinematic analysis

Early structural studies in Thessaly largely based their kinematic analysis on the vergence direction of folds (Barton 1975; Doutsos 1984). However, as demonstrated by the geochronological results of Schermer (1993), many similar styles of folds formed during different events. Furthermore, as folds do not necessarily involve the growth of new minerals, it is often hard for the conditions and timing of folding to be unequivocally constrained. In this study, the kinematic evolution was determined primarily from structures in which the conditions of formation can be readily determined.

It has been well established that most strain is concentrated along broadly planar regions which form brittle faults at shallow levels and ductile shear zones at depth, and that these structures accommodate largely pure shear strain (Sibson 1975; Lister and Snoke 1984). Experimental and detailed field studies have shown that during such intense deformation, lithologies within the shear zones synchronously develop a range of planar and linear fabrics (Tchalenko 1968; Ramsay and Graham 1970; Berthé et al. 1979; White et al. 1980; Platt and Vissers 1980; Platt 1984; Sylvester 1988). During favourable conditions many of these fabrics involve the growth of (datable and/or index) minerals which allow the timing of the shear displacement to be determined. The most common fabrics to develop are shown in Figure 4.04 and include; (1) a mylonitic foliation (S.m) defined by the alignment of minerals such as mica and feldspars (see note below), (2) an extensional shear band foliation (S.h) which cross-cuts the mylonitic foliation at a low (10-35°) angle often forming regularly spaced sets, and (3) stretching (and mineral) lineations (L.m and L.s) which develop in the mylonitic foliation plane.

The important conclusion from the above studies, is that these structures have rather consistent geometrical relationships with each other, irrespective of the metamorphic conditions

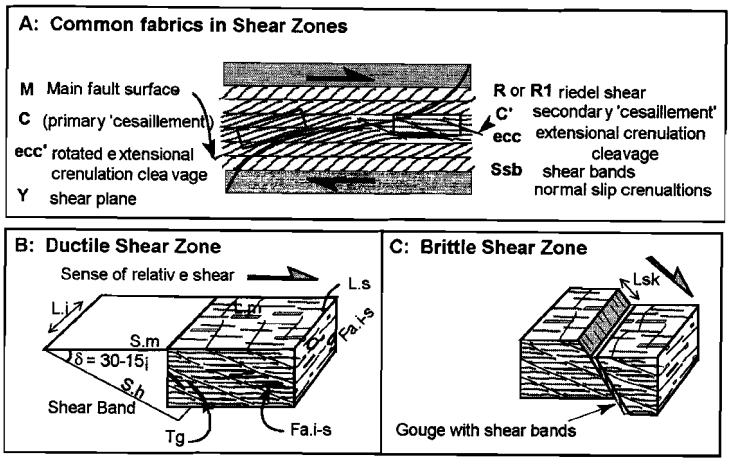

Figure 4.04
A cartoon depicting the geometrical relationships between commonly developed fabrics in shear zones of the Thessaly region, with a summary of the nomenclature for such fabrics in the published literature. The variation in terminology is, in part, derived from studies of ductile shear zones (Figure 4.04b) and, in part, from studies of brittle shear zones (see Figure 4.04c). Abbreviations of these fabrics are as follows: S.m = main (mylonitic) foliation formed by aligned minerals, S.h = extensional shear band foliation, Fa.s = sheath fold axis, Fa.i = isoclinal fold axis, Fa.o open fold axis. L.i = intersection lineation, L.s. stretching lineation, L.sk = slickenline lineation, L.m = mineral lineation, and Tg = tension gash.

under which the shear zone developed (Figure 4.04b and c). Ideally, the poles of associated planar fabrics (including tension gashes, Figure 4.04b), and the linear fabrics lie in the same plane, perpendicular to the mylonitic foliation and parallel to the stretching lineation. The asymmetrical geometry of these fabrics enables the sense of shear, hanging wall relative to footwall, to be determined within a local reference frame. The regional integration of the kinematics of shear zones of the same age enables a *regional* sense of shear to be estimated.

Note that there is an enormous variation in the nomenclature for the foliations described above (see Figure 4.04a). In this chapter, the terminology of shear zones follows that proposed by White et al. (1980). The term 'lineations' refers to stretching and mineral lineations unless stated otherwise. For clarity, 'direction of shear' is used in the scalar sense of the word (e.g. in a north-south direction), whereas 'sense of shear' is used to refer to the vector (e.g. towards to south or towards the north). Note also, in Thessaly, a lack of protoliths and incomplete development of shear indicators means that a common problem is how to distinguish mylonites from schists and phyllites. In such cases, a strongly attenuated rock with a pronounced stretching lineation (or kinematic indicators where available) is termed a mylonite.

4.4 Results

4.4.1 Introduction

In this section, the structures and kinematics associated with shear zones developed in the West and East Thessaly Complexes (Figure 4.05) that formed during different metamorphic events and under ductile, semi-ductile and brittle regimes are presented. Within each metamorphic event the structures, where possible, are separated into groups of shear zones that share a common shear direction (thus forming a kinematic unit, see introduction to this chapter, Section 4.1). In the Thessaly region, shear zone foliations dip in all orientations (Figure 4.06), on a small (1-10 m) to medium (10-1000 m) scale, whereas the orientation of associated mineral and stretching lineations is typically consistent. Therefore, the kinematic units are

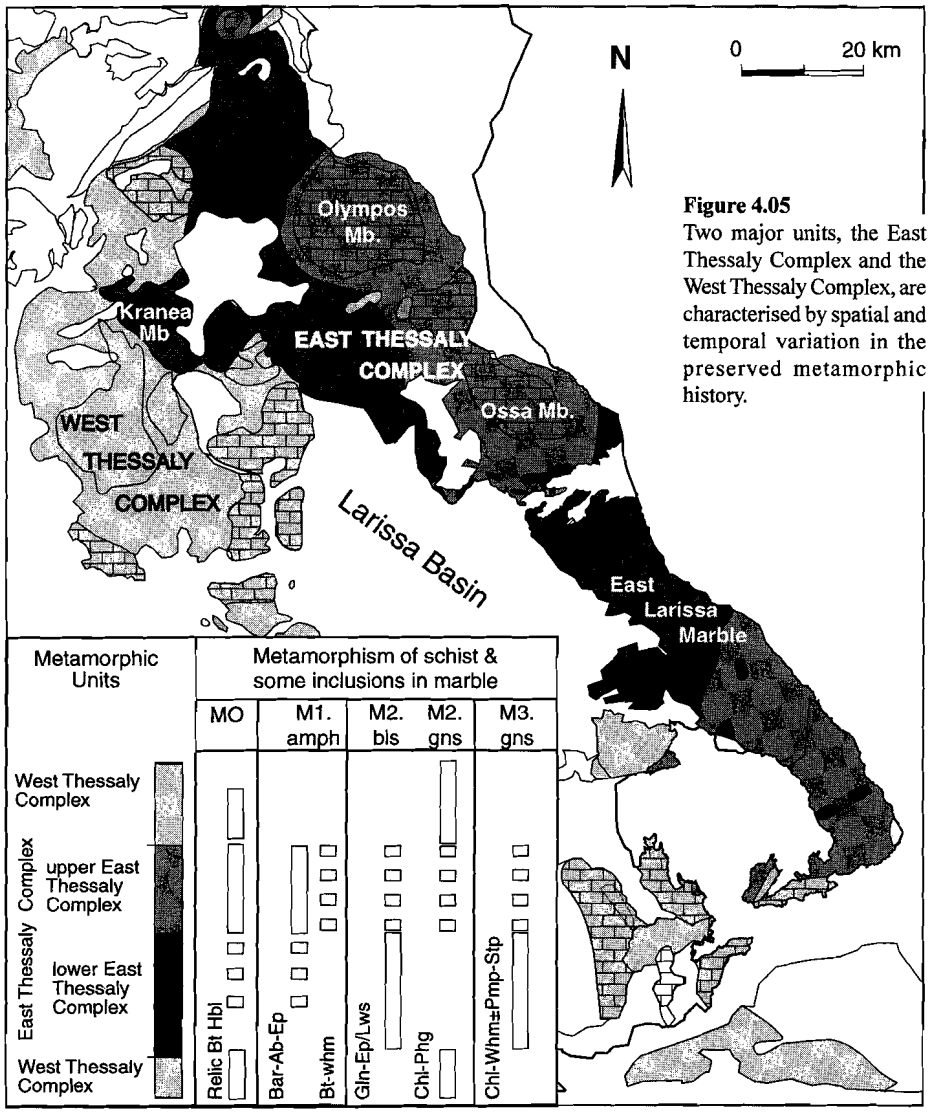

Figure 4.05
Two major units, the East Thessaly Complex and the West Thessaly Complex, are characterised by spatial and temporal variation in the preserved metamorphic history.

most usefully characterised by the orientation of the lineations; and the orientation of the mylonitic foliation is not discussed in great depth. The tectonic significance and the relationship between the shear zones within each kinematic unit is discussed in the following section (Section 4.5).

The metamorphic facies described below are based on mineral assemblages in metabasite lithologies, using the definitions of Evans (1990), and are described in detail in the previous chapter (Chapter 3). The kinematic units described in this chapter are based on observations made during this study only, unless otherwise stated. Because the temporal sequence of deformation is determined from the associated metamorphism (see Figure 4.05), they are described as 'M' events rather than as 'D' events.

4.4.2 Deformation during the Hercynian event

Hercynian metamorphism is preserved as relic biotite and white mica in quartzofeldspathic gneisses and schists, and is found in both the West and East Thessaly Complexes (Figure 4.05). In all observed cases, rocks containing relic Hercynian minerals have been overprinted and deformed at albite-epidote amphibolite, epidote blueschist or greenschist facies conditions (e.g., Figure 4.05). Available geochronological data suggest deformation at these conditions is related entirely to the Alpine Orogeny (Figure 4.03b). Unfortunately, very little evidence of Hercynian deformation fabrics have been preserved.

4.4.3 Deformation during the amphibolite facies metamorphic event, M1

4.4.3.1 Introduction

The earliest metamorphic event to overprint Hercynian assemblages occurred during the early Cretaceous and involved albite-epidote amphibolite facies conditions (termed the M1.amph event). The M1 amphibolite facies event is best preserved in the upper East Thessaly Complex northwest of Mt. Olympos (Figure 4.05). Rocks exhibiting this metamorphic grade comprise

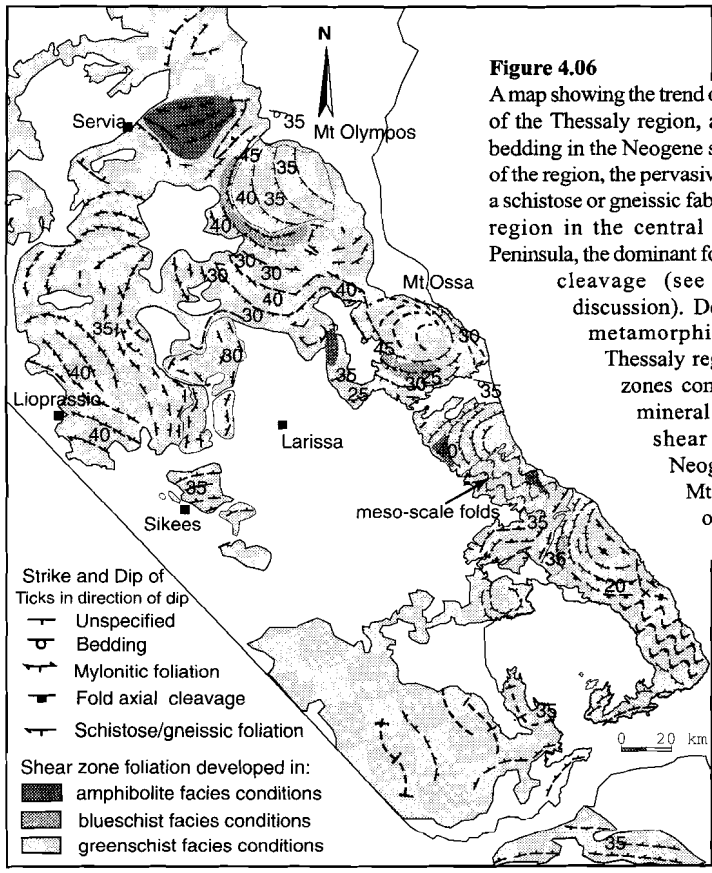

Figure 4.06
A map showing the trend of the pervasive foliation of the Thessaly region, along with the trend of bedding in the Neogene sediments. Across most of the region, the pervasive foliation is defined by a schistose or gneissic fabric. However, in a small region in the central and southern Pelion Peninsula, the dominant foliation is an axial planar cleavage (see section 4.4.5.1 or discussion). Despite the variation in metamorphic grades across the Thessaly region, most of the shear zones contain greenschist facies mineral assemblages in their shear fabrics. Note that Neogene sediments east of Mt. Olympos and southeast of Mt. Ossa tilt towards the SSW.

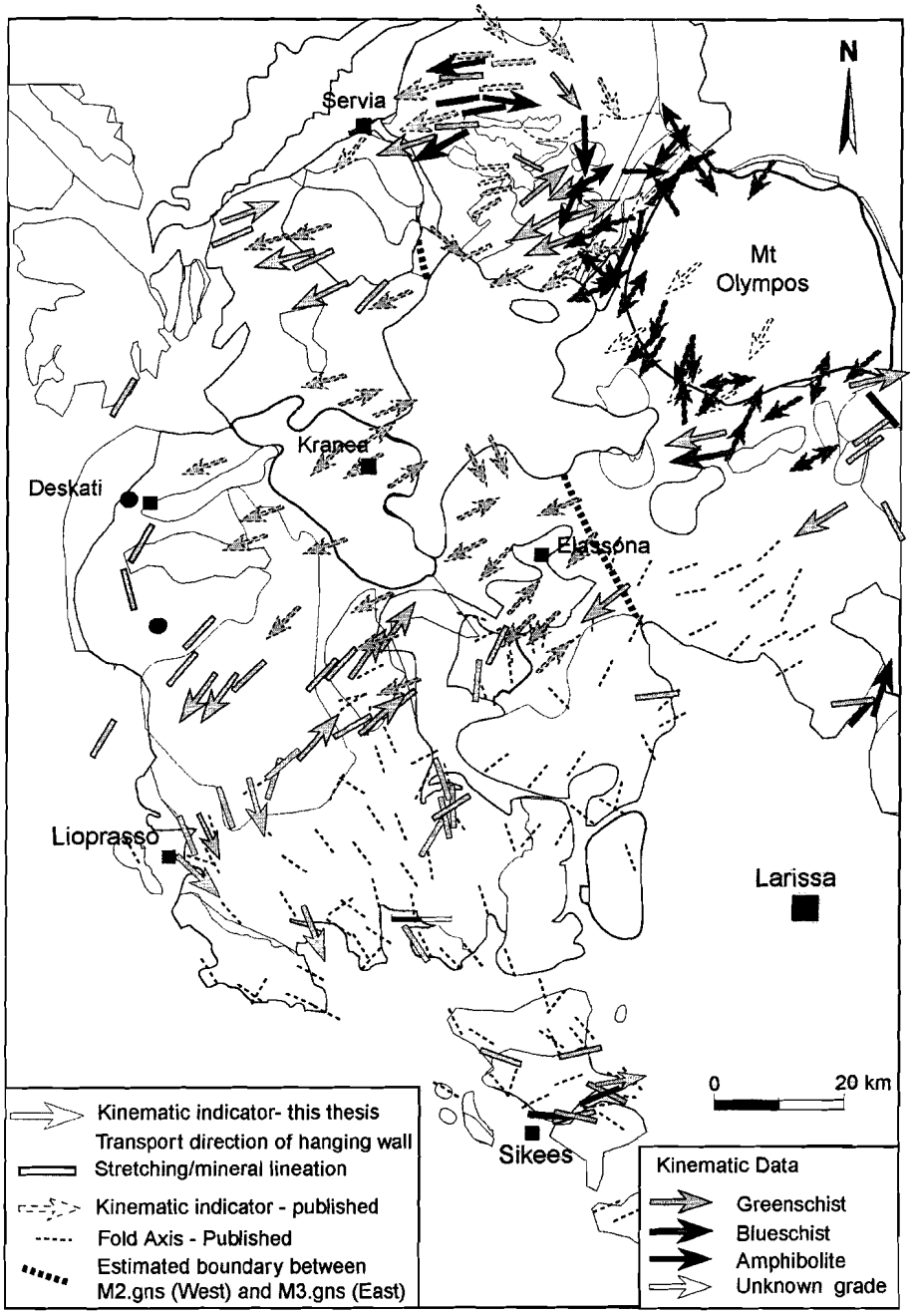

Figure 4.07: A kinematic map of north Thessaly. Most deformation fabrics developed in greenschist facies conditions. Rare occurrences of albite-epidote amphibolite grade mineral lineations defined by barroisite have a ~N-S trend (middle right side of map) and E-W trend in the Pierien-Titaros mountains. Blueschist

some of the least deformed lithologies in the region and most shear zones within these lithologies have deformed during retrogressive greenschist facies conditions (Figure 4.06). Nevertheless, shear zones developed during the M1 amphibolite facies event allow two kinematic units to be identified. The most common and best defined structural feature (kinematic unit) comprises shear zones with E-W trending lineations. These are found in the Pierien Mountains and on the western flanks of Mavrovrouni (Figures 4.07 and 4.08). The other kinematic unit is only locally preserved and is characterised by M1 amphibolite facies shear zones with broadly N-S (NNW-SSE) trending lineations. This kinematic unit is best developed northeast of the Larissa Basin, but it is also found in the Titaros Mountains (Figure 4.07) and Mavrovrouni areas (Figure 4.08). M1 kinematic units exhibit many similar meso and microstructures and hence are discussed together.

4.4.3.2 Mesostructures associated with deformation during M1

The foliation in albite-epidote amphibolite facies shear is defined by biotite and phengitic white mica (see Figure 4.09a). Mineral lineations, where developed, are defined by barroisite, whereas stretching lineations are defined by elongate quartz and by the pressure shadows around feldspars. Shear bands are confined largely to mica-rich lithologies, whereas tension gashes are rarely developed. Shear zones that developed during this metamorphic facies have foliations that typically dip at moderate to shallow angles (0-35°) in all directions, e.g. Pierien/ Titaros Mountains (Figure 4.06). Stacks of *en echelon* north-dipping lithological slices were commonly observed in Titaros Mountains, which confirms a similar observation of Nance (1981).

Shears zones with E-W trending lineations are typically defined by biotite but are often overgrown by lower grade greenschist facies minerals (Figure 4.09b, Section 4.4.5). Such an overprint was not observed in the shear zones with ~N-S lineations. The relationship between the shear zones with E-W and ~N-S lineations developed during albite-epidote amphibolite facies metamorphism was not observed due to the sporadic preservation of these structures.

Shear zones with N-S lineations developed during albite-epidote amphibolite facies metamorphism have few kinematic indicators, and those present indicate both senses of displacement. Shear zones with E-W albite-epidote amphibolite facies lineations generally exhibit a top-to-the-E sense of shear (e.g., Figure 4.09a & b), although the opposite sense of shear was also observed in the Pierien-Titaros Mountains (Figure 4.08).

4.4.3.3 Microstructures associated with deformation during M1

Finely developed tensions gashes (0.5 mm) filled with biotite, barroisite, quartz and albite are common. Mica occasionally forms mica-fish (sensu Lister and Snoke 1984). Feldspars exhibit carlsbad twins and subgrain development. They form rounded grains with distinct strain shadows. Quartz forms ribbons, subgrains and occasionally exhibits a clear dimensional preferred

---

facies shear zones are largely confined to the Mt. Olympos region, and exhibit a top-to-the-SW sense of shear. Greenschist facies shear zones form three structural units; 1) shear zones with a NNW-SSE sense of shear (e.g. east of Lioprasso), 2) shear zones with a E-W sense of shear (e.g. east of Sikees), and 3) shear zones with top-to-the-SW sense of shear (observed across most of the region). Data from this study shown as large arrows, other data (shown as smaller arrows) from Doutsos 1984 (folds), Sfeikos et al 1991, Kilias et al 1991, Schermer (1993), and fourth year students of University of Utrecht (Brouwer 1994; Meijer 1996; Tromp 1996).

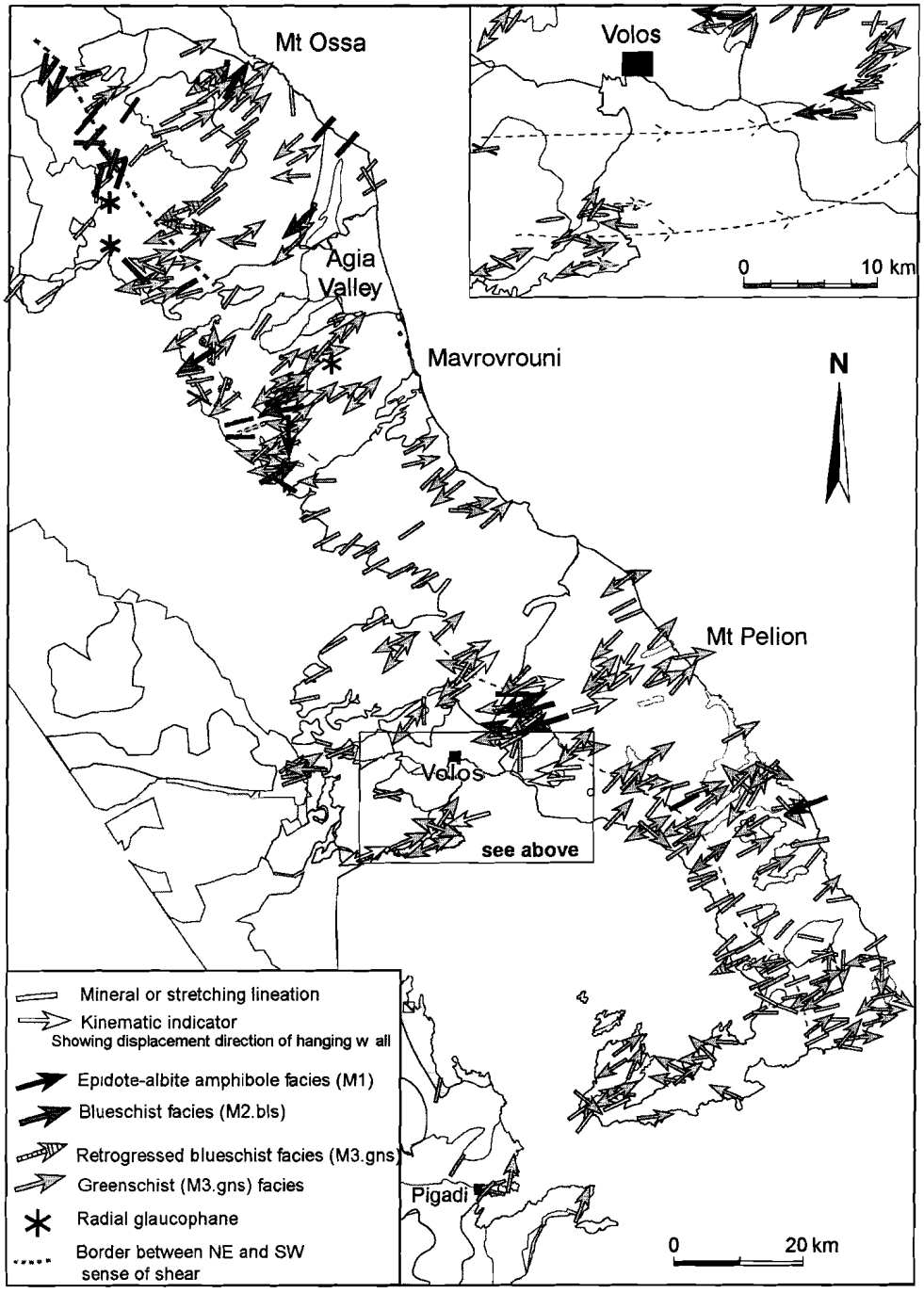
Mt Ossa
Volos
0 10 km
Agia Valley
Mavrovrouni
N
Mt Pelion
Volos
see above
Mineral or stretching lineation
Kinematic indicator
Showing displacement direction of hanging w all
Epidote-albite amphibole facies (M1)
Blueschist facies (M2.bls)
Retrogressed blueschist facies (M3.gns)
Greenschist (M3.gns) facies
Radial glaucophane
Border between NE and SW sense of shear
Pigadi
0 20 km

orientation. In the Titaros Mountains, recrystallised grains are entirely annealed, forming a foam texture, elsewhere the albite-epidote amphibolite facies shears exhibit only a partially annealed texture.

4.4.4 Shear zones developed during blueschist facies M2 metamorphism

4.4.4.1 Introduction

Although relic minerals indicative of epidote blueschist facies metamorphism (M2.bls) occur in the East Thessaly Complex (Figure 4.05), areas which preserve structures developed *during* high pressure conditions are rarely continuous for more than a few meters normal to the pervasive mylonitic foliation, and 100's m parallel to the pervasive mylonitic foliation. The strong degree of greenschist overprint means that almost all of the blueschist facies kinematics have been obliterated, thus to be confident of the conditions under which deformation occurred, the kinematics were determined from thin sections cut from orientated samples.

Two kinematic units are identified which developed during this metamorphism event; one is defined by NE-SW trending lineations and another small unit which is characterised by E-W trending lineations.

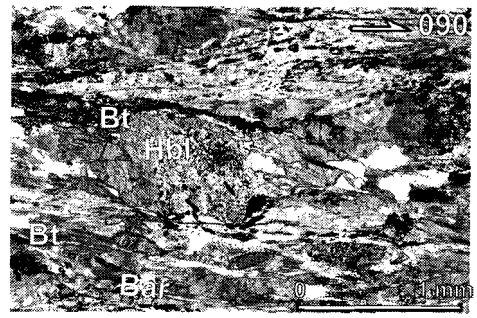

Figure 4.09a: Albite-amphibolite schist from the Pierien mountains, 5 km east of Servia. Biotite (Bt) grows along the mylonitic foliation and indicates a top-to-the-E sense of shear.

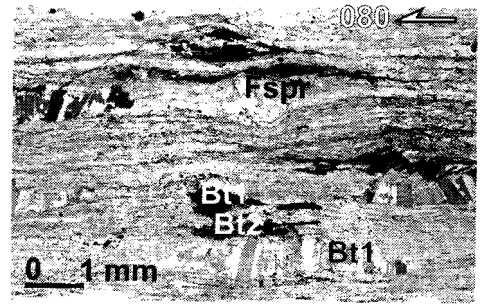

Figure 4.09b: E-W directed shears from quartzofeldspathic schist east of Sikees, northwest Thessaly. Movement started in mid-greenschist to albite-epidote amphibolite facies, now represented by biotite grains (Bt1 and Bt2). Deformation, however, continued in largely mid to lower grade greenschist facies as exhibited by predominance of phengite in the shear matrix overprinting the biotite.

4.4.4.2 Mesostructures of M2 blueschist facies shear zones

Although some of the best examples of blueschist facies metamorphism are preserved in epidote-rich lithologies of the lower East Thessaly Complex (Figure 3.11d), these rocks are (relatively) least deformed rocks that are affected by blueschist facies metamorphism, and hence exhibit only a weakly to moderately developed foliation and lineation. Furthermore, the quartzofeldspathic gneisses of the central Mavrovrouni and Ossa mountains contain thin, radiating needles of glaucophane that overprint the gneissic foliation (e.g., Figure 3.11b). This

Figure 4.08: A kinematic map of southeast Thessaly demonstrates that the direction of shearing is very consistent despite variations in metamorphic grade and variations in the trend of the pervasive foliation direction (compare with figure 4.05b). Blueschist facies lithologies dominantly exhibit a top-to-the-SW sense of shear. In greenschist facies both senses of shear are observed. Note, however, that NE of the thick dashed grey line *most* greenschist facies shears exhibit a top-to-the-NE sense of shear whereas to the southwest of the line the opposite sense dominates.

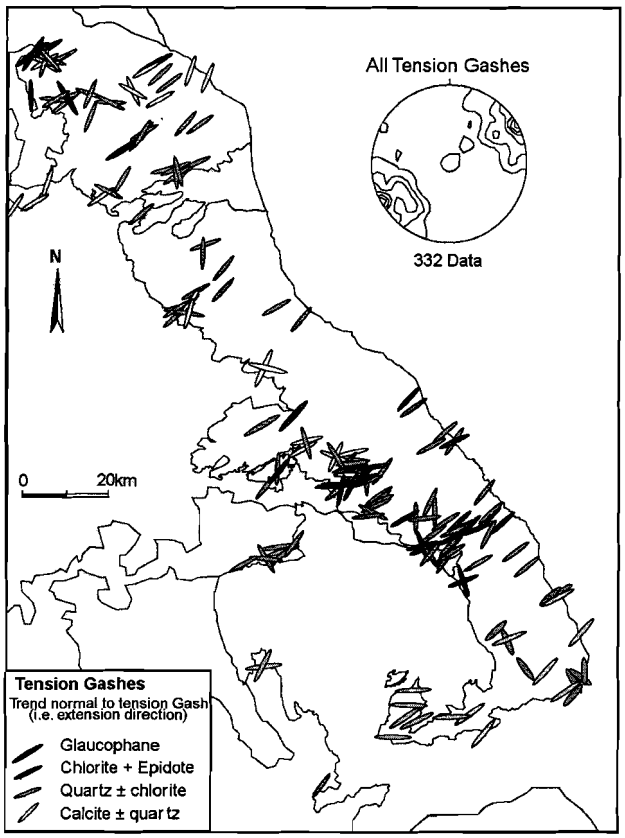

Figure 4.10: Map of the poles to tension gashes in east Thessaly, showing that the tension gashes dominantly trend NE-SW irrespective of the metamorphic conditions at the time of vein development. The poles to greenschist facies tension gashes west of Volos and on Trikeri trend in a NE-SW direction, although lineations in these regions trend E-W (see Figure 4.07). Blueschist facies tension gashes often contain greenschist facies minerals assemblages in their centres (indicated here by a lighter shade).

suggests that, in these regions, this gneissic foliation formed prior to blueschist facies metamorphism. The more amphibole- and mica-rich blueschist facies rocks typically have a well developed LS mylonitic fabric (Davis and Reynolds 1984). However, these shear zones have commonly been overprinted by greenschist facies shear zones (compare Figures 4.05 and 4.06).

Shear zones that have developed during M2 blueschist facies metamorphism have foliations which are defined by phengitic white mica, lawsonite, quartz, epidote and glaucophane, and which dip at moderate angles (10-50°) in all directions (Figure 4.06). The stretching lineation is defined by quartz and by pressure shadows around albite, whereas mineral lineations are defined by glaucophane and lawsonite. Blueschist facies lineations across Thessaly dominantly trend NE and overprint earlier E-W trending lineations. An exception to this is found in a small area in northwest Pelion Peninsula where E-W trending lineations rotate into a NE-SW orientation over a distance of ~ 300m (as indicated by a dashed line in the inset of Figure 4.08).

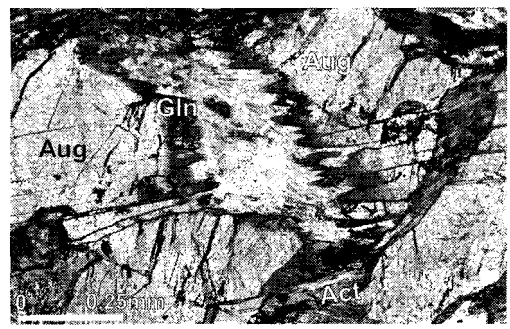

Figure 4.11
Photomicrograph of pyroxene-albite schist from the northern flanks of Mt. Ossa that has deformed under blueschist facies conditions. The pyroxene (Aug) has fractured along and across cleavage planes. The fractures are filled with glaucophane (Gln), albite and quartz. Glaucophane in the shear on the right hand side of the diagram is overprinted by actinolite (Act), suggesting that deformation continued in retrograde greenschist facies conditions.

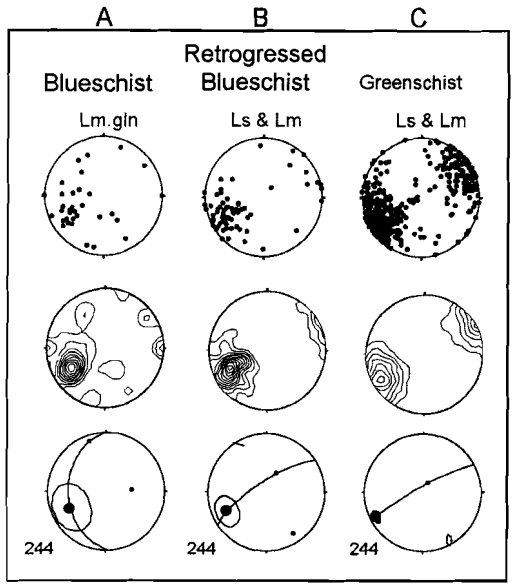

Figure 4.13
Photomicrograph of an albite-amphibolite schist with syntectonically incorporated calcite (Cal) deformed during blueschist facies conditions from the southern flanks of Mt. Ossa. Stretching and mineral lineations in this lithology trend NE-SW. Some albite porphyroblasts (Ab) have a previous foliation defined by the alignment of glaucophane (Gln). Note that calcite forms grains with a preferred orientation (indicated by a double headed arrow).

Although E-W trending lineations occupy only a small area, shear zones with such lineations are important in the following discussion (Section 4.5).

Evidence for folding during the progressive decrease in the intensity of blueschist facies metamorphism was observed in the lower East Thessaly Complex from the Mt. Olympos area south to the Pelion Peninsula. Near Mt. Olympos, isoclinal to open folds (limbs spaced up to 15 mm apart) that developed in blueschist facies conditions are well preserved. South of Mt. Olympos, the folds tend to be more recumbent (limbs spaced ~5 mm apart) and are locally well preserved (particularly on the northeastern flanks of Mt. Ossa). Further south in the Pelion Peninsula area, folds (limbs spaced ~2 mm apart) in blueschist facies lithologies have all but been obscured by overprinting metamorphism and shearing.

Tension gashes, ~1 cm wide by ~10 cm long, are not uncommon in blueschist facies rocks, particularly in epidote-rich lithologies (e.g. epidote-chlorite-albite schists of the northern Pelion Peninsula and western Mt. Ossa areas). These tension gashes typically have irregular vein walls and have developed at a steep angle to schistosity. Both the fibres in the veins and the pole to tension gashes trend NE-SW (Figures 4.10 and 4.11).

Shear bands and the offset across boudins demonstrate a predominantly top-to-the-SW sense of shear during blueschist facies conditions, although the data are limited in the Pelion region. The opposite sense of shear is observed, particularly on the east side of the Olympos-Pelion range (Figure 4.08). The average orientation of the NE-SW trending mineral lineations is 064°-244° (Figure 4.12).

4.4.4.3 Microstructures of M2 blueschist facies shear zones

Two generations of glaucophane are observed; glaucophane is present both in the fold axial planes of recumbent folds and between the boudinaged laths of earlier glaucophane. Barroisite grains have also been boudinaged in blueschist facies conditions. Pyroxenes (augite; see Figure 3.13) are relatively rare but where observed are pervasively fractured across and along their cleavage planes (Figure 4.11). Albite is one of the most widespread minerals in this metamorphic facies and often forms porphyroblasts (Figure 4.13). Albite grains exhibit brittle fracturing, undulose extinction, subgrain development, and carlsbad twins. Quartz forms ribbons and exhibits intense subgrain development, a crystal preferred orientation, grain boundary migration

undulose extinction, subgrain development, and carlsbad twins. Quartz forms ribbons and exhibits intense subgrain development, a crystal preferred orientation, grain boundary migration and undulose extinction. Evidence for the introduction of calcite into schists during blueschist facies deformation is locally observed (e.g., Figure 4.13). Tension gashes developed in this facies are infilled with glaucophane and epidote and often exhibit a crack-seal morphology.

4.4.5 Shear zones developed during M2 and M3 greenschist facies metamorphism

4.4.5.1 Introduction

Most of the shear zones of Thessaly have been deformed under greenschist facies conditions (Figure 4.06). However, the age of this facies of metamorphism differs between western and eastern Thessaly (Lips et al. 1998) and thus, the greenschist facies deformation is subdivided into two events (M2.gns and M3.gns). The M2 greenschist event is confined to the West Thessaly Complex, and has a late Cretaceous cooling age. The M3 greenschist event is found across the East Thessaly Complex (Figure 4.05) and have cooling ages younger than Eocene.

Four kinematic units are recognised in these greenschist facies lithologies, which are defined by: 1) M2.gns, NNW-SSW trending stretching lineations; 2) M2.gns, E-W trending stretching lineations; 3) M2.gns, NE-SW trending stretching lineations; and 4) M3.gns, NE-SW trending stretching lineations (Figure 4.07 and 4.08). Unfortunately, only shear zones with NE-SW trending lineations have been dated. The other two kinematic units lie in west Thessaly and are only tentatively interpreted to have developed during the M2 greenschist facies metamorphic event (see Section 4.5 for discussion). In all cases, the greenschist facies shear zones have mylonitic foliations defined by chlorite, fine-grained phengitic white mica and epidote, whereas the mineral lineations are defined by feldspar grains, calcite grains and actinolite laths.

One of the most abundant rock types in the region, marble, is often very homogenous in composition and exhibits few of the kinematic indicators usually found in more mica- or quartz-rich rocks. However, in the East Thessaly Complex, an area dominated by NE-SW trending (and to a lesser extent E-W trending) stretching and mineral lineations, marble exhibits a finely developed and elongate or 'fibrous' fabric. Few references to such regional development of this fabric are available in the literature. Therefore, a detailed microstructural examination of this fabric was carried out to determine its origin and in particular the structural implications of its development.

4.4.5.2 Mesostructures of M2 greenschist facies shear zones

(A) Shear zones with a NNW-SSE sense of shear

Shear zones with NNW-SSE trending, greenschist facies lineations are typically, 1-10 m wide, anastomosing, and weakly defined. Stretching lineations are defined by disseminated epidote, stretched quartz and the pressure shadows on feldspars. Tension gashes are relatively rare (compared to later kinematic units) but where observed were filled with quartz.

In the quartzofeldspathic schist and gneisses of the West Thessaly Complex, east and south of Lioprassio (Figure 4.07), greenschist facies shear zones exhibit strongly developed NNW-SSE trending stretching lineations. NE-SW trending greenschist facies (M2.gns) shears are interleaved with, and rotate into, the N-S trending lineations (Figure 4.07). Shear zones exhibiting a NNW-SSE sense of shear have foliations that typically dip at moderate angles (15-50°) towards the NE (Figure 4.06). The poles to tension gashes (i.e. the extension direction) are

parallel to the stretching lineations. Isoclinal to open folds also trend parallel to the stretching lineations. Shear bands highlighted by 3-4 mm wide quartz ribbons indicate a dominantly top to the SSE sense of relative shear (Figure 4.07).

(B) Shear zones with an E-W sense of shear

Rocks containing a strongly developed mylonitic fabric with relic E-W trending stretching lineations are found in small areas, approximately 10 km in width, east of Sikees and Servia (Figure 4.07), west of Volos (Figure 4.08 inset), and south of the Trikeri Peninsula (southwest corner of the Pelion Peninsula). Lineations are defined by attenuated books of biotite as well as stretched quartz and the pressure shadows on feldspars (Figure 4.09b). The presence of biotite in zones of shearing suggests that this generation of structures may have initiated in upper greenschist facies conditions (Figure 4.09b: see also Figure 3.11a). Other structures associated with this phase include isoclinal folds and tension gashes infilled with quartz and chlorite (Figure 4.12).

The mylonite foliation associated with these shear zones dips at a shallow angle in all orientations (Figure 4.06). As with the NNW-SSE greenschist facies lineations (see above), the E-W lineated fabric both rotates into, and is cross-cut by, greenschist facies shear zones with NE-SW trending lineations (e.g., west of Volos Figure 4.08 inset). Hence, the E-W lineations are interpreted to predate the NE-SW lineations.

The Bingham mean orientation of all data from these zones of E-W M2.gns trending lineations is 262° with an $\alpha 95\%$ confidence level of 25°. The isoclinal folds and poles to tension gashes trend parallel to the stretching lineations. East of Servia and Sikees (Figure 4.07), the sense of shear is predominantly top-to-the-E. West of Volos, however, the sense of shear is in both directions (E and W).

(C) Shear zones with a NE-SW sense of shear

Greenschist facies shear zones with an NE-SW sense of shear which developed during M2 greenschist facies metamorphism dominate the northwest Thessaly region (Figure 4.07). The mylonitic foliation in the M2 shear zones typically dips towards the NE, and is more weakly developed than in M3 greenschist facies shear zones. The kinematic sense of shear is dominantly towards the west (Figure 4.07). There is no discrete break in greenschist facies shear zones between east and westThessaly, and hence, the

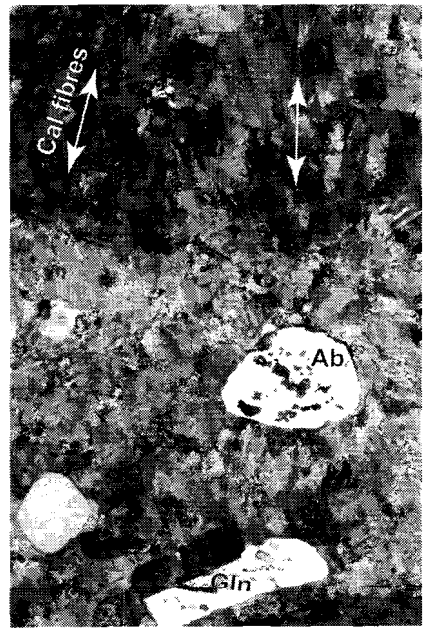

Figure 4.13: Photomicrograph of an albite-amphibolite schist with syntectonically incorporated calcite (Cal) deformed during blueschist facies conditions from the southern flanks of Mt. Ossa. Stretching and mineral lineations in this lithology trend NE-SW. Some albite porphyroblasts (Ab) have a previous foliation defined by the alignment of glaucophane (Gln). Note that calcite forms grains with a preferred orientation (indicated by a double headed arrow).

shear zones with M3 greenschist facies NE-SW trending stretching lineations may represent a reworking under greenschist conditions of similarly orientated M2 greenschist facies shear zones.

(D) Shear zones with a NE-SW sense of shear

Most lithologies within the East Thessaly Complex, in particular the lower portion, exhibit a very strongly developed LS mylonitic foliation which dips at moderate to shallow angles (0-50°) in all directions (Figure 4.06), and which contains very consistently orientated NE-SW trending stretching and mineral lineations (Figure 4.08). In the Pelion Peninsula, the M3 greenschist facies mylonites together form a sheet of approximately 1 km thickness (based on the width of outcrop and the dip of the mylonitic foliation). Near the margins of the area affected by this NE-SW M3.gns shearing, the NE-SW stretching lineations developed during greenschist facies overprint the E-W or NNW-SSE lineations (Figure 4.07 and 4.08). The border between M2.gns NE-SW trending lineations and M2.gns NE-SW trending lineations is difficult to locate accurately without more geochronological data. The estimate of the border is shown as a dashed line in Figure 4.07.

Many M2.bls blueschist facies rocks and assemblages exhibit a M3 greenschist facies overprint. The contact between rocks affected and unaffected by this overprint is gradational on all scales observed, and hence appears to represent a progressive rather than an abrupt change in metamorphic and structural conditions (e.g., Figure 4.11).

The mean orientation of M3 greenschist facies structures is 244° with an α95% of 7°. In retrogressed blueschist facies lithologies of east Thessaly, the trend is similar but there is a slightly greater spread in the data (Figure 4.12). The M3 greenschist facies shear zones of eastern Thessaly exhibit a regional divergence in the sense of shear about an axis which runs down the centre of the Olympos-Pelion range (shown as a dashed grey line in Figure 4.08). East of this dashed line, the sense of shear is dominantly top-to-the-NE whereas to the west it is dominantly to the SW.

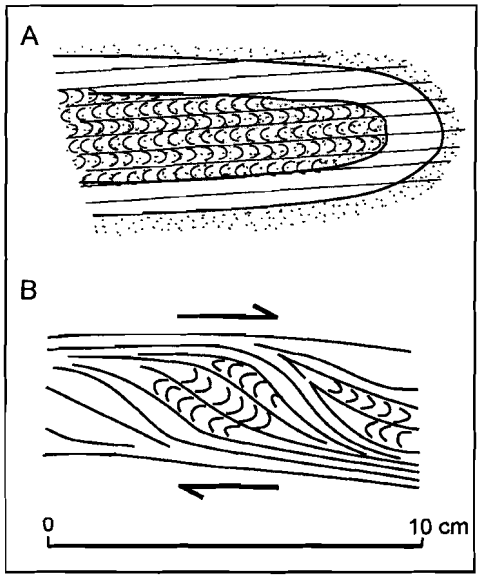

In the central Pelion Peninsula region, the shear zone foliation has been progressively overprinted by a finely-spaced, axial planar cleavage (Figure 4.14a). The orientation of the pervasive cleavage foliation is broadly parallel to, and interlaminated with, the pervasive mylonitic foliation in the rocks (Figure 4.06). In the more micaceous lithologies, 10-50 cm wide lensoidal remnants of axial planar cleavage have been enveloped by shears bands (Figure 4.14b). The sense of folding in these packets is often verges towards the SW whereas the sense of displacement exhibited by the enveloping shears is towards the NE.

Figure 4.14
A sketch of a typical fold axial cleavage fabric in quartz-rich lithology (Figure 4.14a). In mica-rich lithologies these fabrics have progressed into a (dextral) shear fabric (Figure 4.14b).

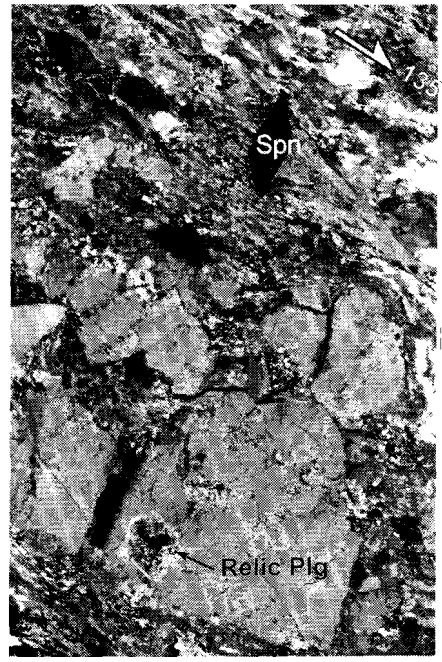

Figure 4.15: A photomicrograph of quartzofeldpathic schist from Lioprasso in northwest Thessaly. The schist deformed under greenschist facies conditions and has N-S trending stretching lineations. Thin reaction rims of alkali feldspar rim relic plagioclase (Plg) grains. Sphene (Sph) has partially overgrown the deformation fabric. Such overgrowths of sphene are not observed in any other kinematic unit.

Both the shears and the fold axial cleavage fabric are broadly flat lying and parallel to the mylonite foliation in the central to west Pelion Peninsula (Figure 4.06).

Rocks in which random stilpnomelane or actinolite have grown are primarily confined to Mt. Ossa area and indicate that deformation ceased in these areas prior to exhumation of the rock above greenschist facies conditions.

4.4.5.3 Microstructures of M2 and M3 greenschist facies shear zones

The microstructures observed in the shear zones formed during the M2.gns and M3.gns metamorphism are similar to each other and have many similarities to blueschist facies (M2.bls) shear zones. Large relic phengitic white micas form 'mica fish' (Lister and Snoke 1984) and recrystallised grains. Quartz forms ribbons which have often undergone intense grain boundary migration. It has a preferred crystallographic orientation, deformation bands and exhibits undulose extinction.

In the NNW-SSE and E-W directed greenschist facies shear zones, relic igneous plagioclase grains have alkali feldspar overgrowths (Figure 4.15). Such a reaction texture is also observed locally in quartzofeldspathic gneisses near the schist-marble contact on Mt. Olympos. Across the whole region feldspars have deformed by brittle fracturing (Figure 4.15) with dislocation glide along with induced dynamic recrystallisation, and subgrain growth. Note that the sphene has partially overgrown the mylonite foliation. Such a mineral overgrowth was only observed in shear zones with NNW-SSE trending lineations.

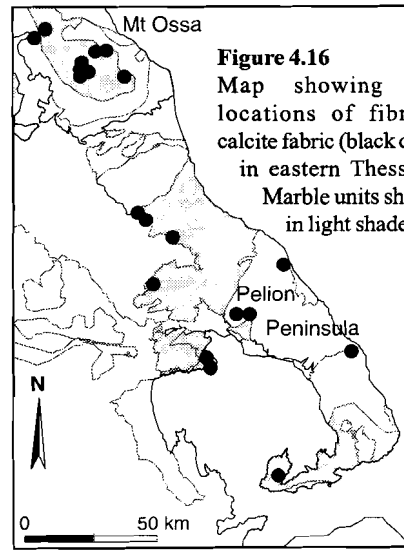

Figure 4.16 Map showing the locations of fibrous calcite fabric (black dots) in eastern Thessaly. Marble units shown in light shade.

4.4.5.4 Fibrous calcite fabric

Detailed mapping of the basement in Thessaly has demonstrated that much of the regions calcareous units exhibit a fibrous calcite fabric. This fabric was observed throughout the lower East Thessaly Complex (Figure 4.16). Marble that

exhibited this fabric varied from one cm (e.g., in banded mica schists and marble) to possibly 100's of metres in thickness (e.g., within the marble of Mt. Ossa). A similar fabric has been described as 'I1b' calcite lineations from Mt. Olympos (Vergély and Mercier 1990), no other references of such a regionally developed fibrous calcite fabric has been recorded in the literature. The fibrous calcite fabric cross-cuts older mylonite fabrics (Figure 4.17a). The development of the fabric over large areas suggests that it is may be related to the exhumation process. Therefore, a study was undertaken to determine the origin of development of the fabric and the conditions under which the fabric developed.

The fibrous calcite occurs in two orientations: 'steep' and 'flat' (Figure 4.17b, c and d). Steep fibres generally form an angle of 60-70° to the pervasive schistose or phyllitic foliation (defined by layers of impurities such as mica, quartz, feldspars and dolomite; Figure 4.17a, b and c). Locally, the steep fibres rotate into and are cross-cut by thin (0.1 to 1 mm) horizons of flat calcite fibres that are orientated parallel to schistosity (Figure 4.17b). Not all flat fibres

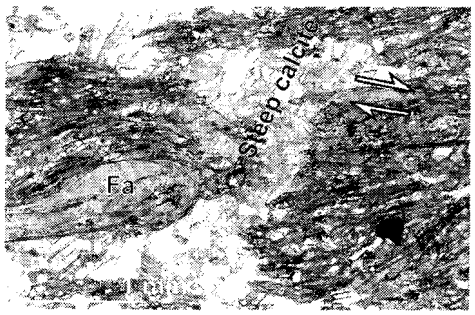

Figure 4.17a: Fibrous calcite fabric in micaceous marble; a relic fold hinge (Fa) is defined by chlorite. The calcite fabric is unaffected by the fold and maintains a steep and constant angle throughout the sample.

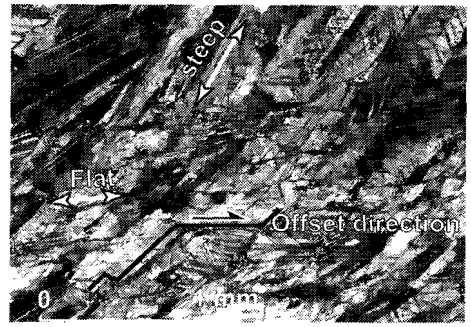

Figure 4.17c: Photomicrograph of steep and flat fibrous calcite fabric exhibiting an offset in the direction of the flat fibrous calcite (direction indicated by a black arrow). Note the primary twins in the top right hand side of the photo indicated by the presence of symmetrical secondary twins.

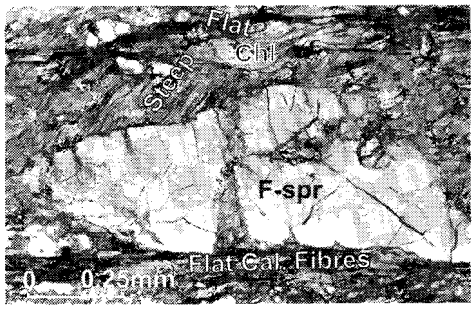

Figure 4.17b: Photomicrograph of steep and flat fibrous calcite fabric in an impure marble. The schistose foliation is indicated by chlorite-rich horizons (Chl) and boundinaged feldspar grains (Fspr). Flat calcite fibres grow in the pressure shadow of these impurities.

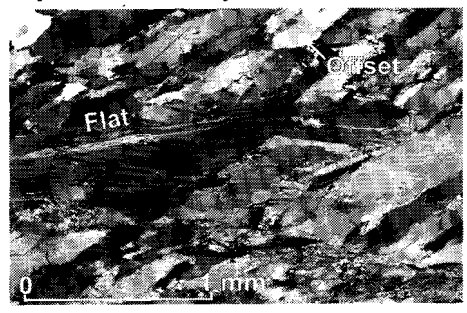

Figure 4.17d: Photomicrograph of steep and flat fibrous calcite fabric. Note the large grain in centre left cross-cut by a flat calcite fibre which lies sub-parallel to a zone of intense recrystallised grains (bottom of photo). Secondary twins in the steep calcite fibres are orientated parallel to the flat calcite fibres.

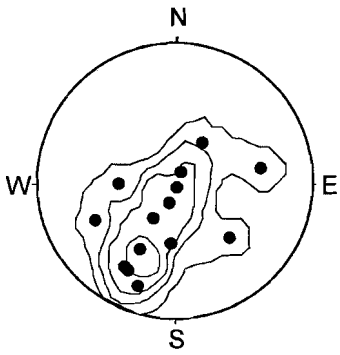

Figure 4.18: A lower hemisphere stereoplot showing that the calcite fibres (both steep and shallow) trend in a broadly NE-SW direction.

cross-cut steep fibres. Flat fibres also are commonly developed in the pressure shadows of relatively competent grains such as feldspars (Figure 4.17b) or magnetite, and typically exhibit a much higher aspect ratio than steep fibres (1:20 versus 1:4 respectively).

The geographical orientation of the steep and flat fibres is NE-SW (Figure 4.18), thus they lie in the same vertical plane. The trend of the calcite fibres were observed to trend parallel to the M3.gns stretching and mineral lineations preserved in associated dolomite-, quartz-, or mica-rich layers in the field.

EBSP analysis

Many of the steeply inclined calcite fibres exhibit a twin relationship with neighbouring fibres (Figures 4.17c and 4.19). These 'steep' twins are termed 'primary twins'. Within any one steep fibre, several 'secondary' twins were also observed and typically form at a high angle to the primary twin (e.g., Figure 4.19). Many secondary twins in steep fibres are orientated parallel to flat fibres (Figure 4.17d). Twins within the flat calcite fibres are typically orientated parallel to the margins of the fibre.

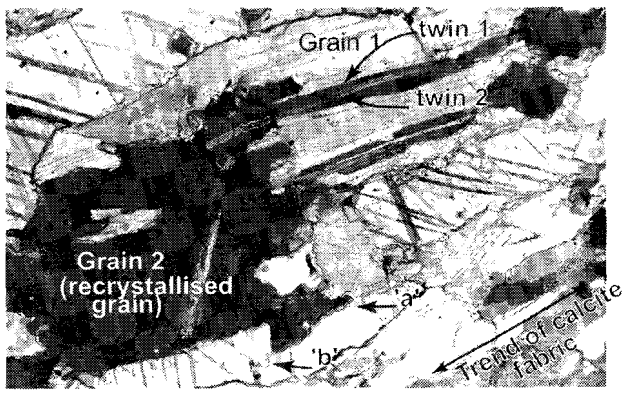

Figure 4.19: Photomicrograph of weakly developed fibrous calcite. Primary twins (twin1) merge near the grain boundary contact (which runs from top left to bottom right of the photograph) of Grain 1 where they form Grain 2, a 'recrystallised grain'. The recrystallised grain has irregular contacts and has preferentially grown along grain boundary (indicated by an 'a') and twin plane contacts (indicated by a 'b'). The result is that the recrystallised grain is elongate in the same direction as observed in other calcite grains (bottom right hand side of diagram). Note the secondary twins (twin 2) within the recrystallised grain/primary twin.

Crystallographic analysis by EBSP (Electron Backscatter Patterns, see appendix D for details) demonstrates that steep fibres comprise a range of low (2-3°) through to high (15-20°) angle subgrains (Figure 4.20). Subgrains and recrystallised grains are more readily optically visible in flat fibres than in steep fibres (Figure 4.17d). The angle between many steep fibres is approximately 52° about an a-axis (e.g., between grain 11 and 12 in Figure 4.20). The contact between many fibres is, in many cases, highly irregular, suggesting the occurrence of grain boundary migration.

The c-axes of both the steep and flat fibres trend cluster at a steep angle to the schistosity plane (Figure 4.21) with a slight tilt towards the NE.

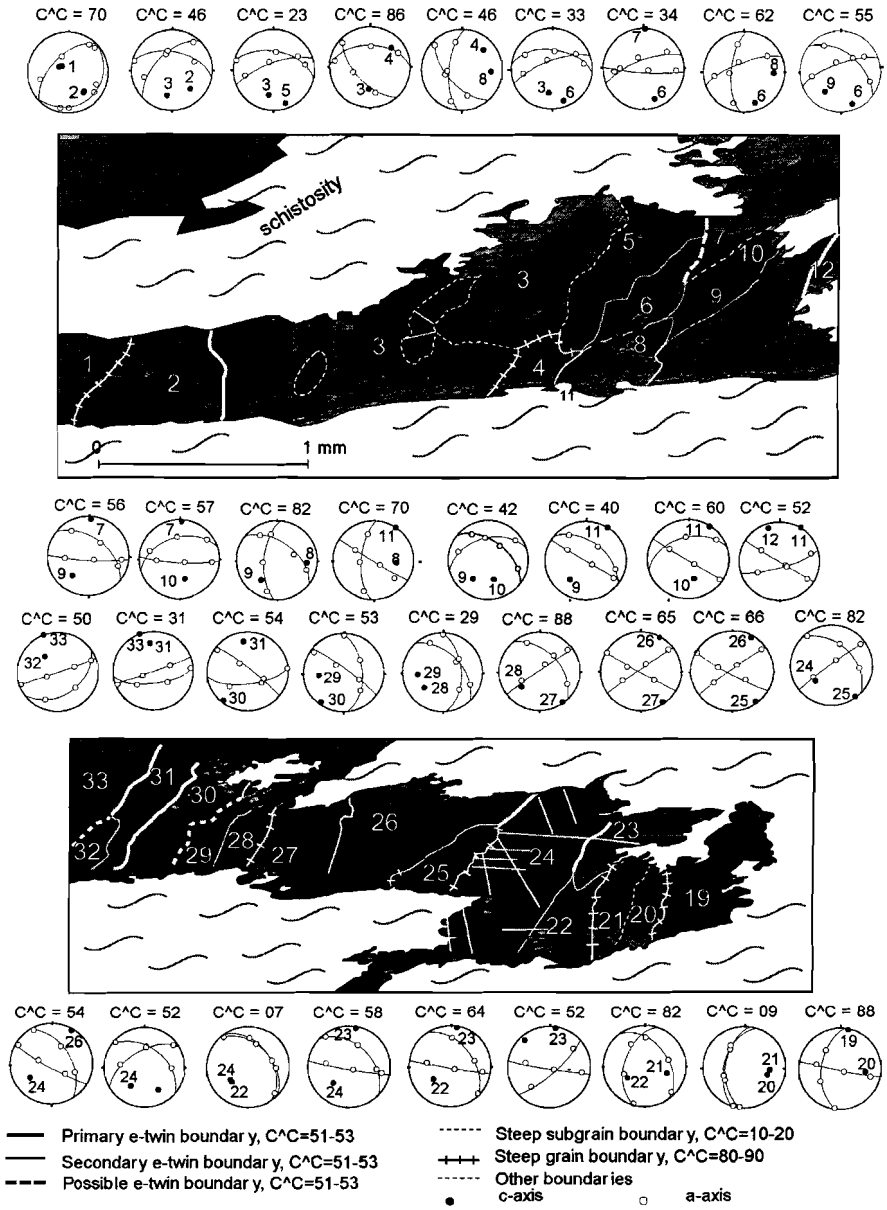

Figure 4.20: Detailed electron back scatter probe (EBSP) crystallographic analysis of the impure fibrous marble shown in Figure 4.17b. Most grains are 'steep' fibres and are composed of numerous low angle (0-5°), and moderate angle (5-15°), often elongate, subgrains. Some of the steep grains are e-twins (e.g. between grain 11-12), as are secondary twins which lie parallel to the schistosity direction (e.g. grain 23). C^C = minimum angle of the c-axes between neighbouring grains. See text for discussion. The orientations in the stereographic projections shown are the average crystallographic orientation per grain. The E-W orientation of each stereoplot is parallel to the foliation plane, whereas the N-S direction is at right angles to the foliation plane.

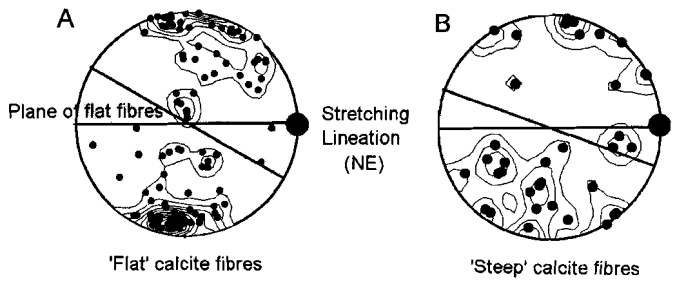

Figure 4.21
Lower hemisphere stereoplots depicting a similarly preferred orientation of the c-axes in both steep and flat fibrous calcite fabrics. The orientation of the c-axis maxima are at a high angle relative to the interpreted shear plane.

4.4.6 Post M3 semi-ductile deformation

Shears and faults that are dominantly brittle but that have rotated the fabrics at the margins of schist they cross-cut are defined as 'semi-ductile' structures. In southern and eastern Thessaly, greenschist facies fabrics are intensely cross-cut by semi-ductile shears (see Figure 4.22). The areas most affected are the eastern flanks of the Ossa-Pelion range and the southern and central Pelion Peninsula areas. Such shears also exhibit an extensional displacement but are generally longer (>30 cm) and more widely spaced (typically 10-30 cm apart) than extensional shear bands (typically only 1- 30 cm long and spaced 1-3 cm apart). In these areas, calcite is often concentrated between boudins (Figure 4.17b) and along shears. Other structures that developed during semi-ductile conditions include slickenlines defined by streaked quartz that have developed on the warped schist surfaces of shear zone/faults.

The kinematics of semi-ductile deformation have been determined from the direction of slip observed on semi-ductile shear surfaces (Figure 4.23). The direction of slip is invariably dip-slip. The shear directions cluster in two conjugate orientations (Figure 4.24) with an extension direction trending in an 064° direction. This direction is parallel to that determined from stretching lineations in greenschist and blueschist facies shear zones in eastThessaly (see Figure 4.12).

4.4.7 Brittle deformation

Brittle faults are observed throughout eastern Thessaly but are most abundant in the Pelion Peninsula area and along the western and eastern flanks of Mt. Ossa and Mavrovrouni. Although the faults trend in a range of orientations, the largest faults tend to trend NW-SE or WSW-ENE. All faults in which the displacement direction could be determined either through slickenlines, secondary shears or folds, indicate almost pure dip-slip displacement (see Figure 4.25). Most faults are small and have a displacement of a few centimeters. However, several faults were observed with displacements of more than one meter (Figure 4.25), some

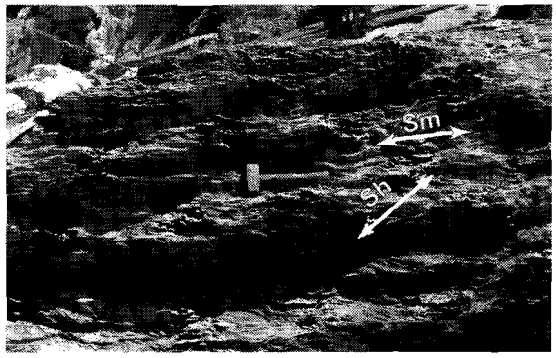

Figure 4.22
A photograph of semi-brittle extensional shear bands in an impure marble from southeast Pelion Peninsula. The angle between the main mylonitic foliation (Sm) and the shears bands (Sh) is 35-45°.

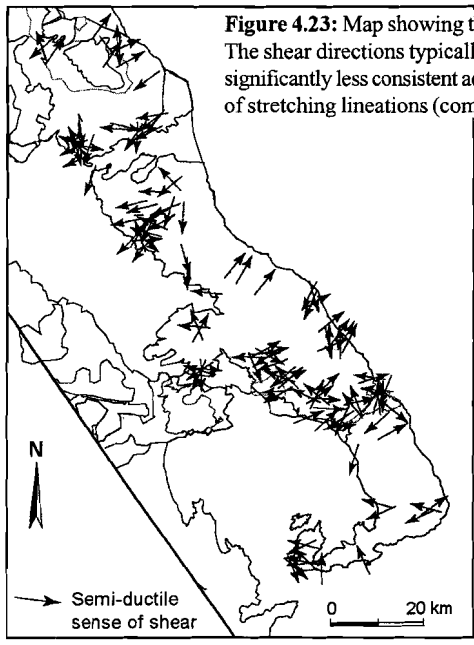

Figure 4.23: Map showing the sense of shear determined from semi-brittle shears. The shear directions typically trend in a NE-SW direction, but the orientations are significantly less consistent across the whole east Thessaly region than the orientation of stretching lineations (compare with Figure 4.07).

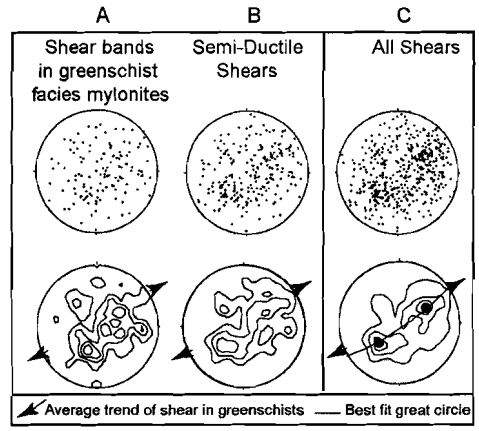

Figure 4.24
Lower hemisphere stereoplots of poles to shear bands associated with shear zones of greenschist facies grade (Figure 4.24a) and overprinting semi-ductile shears (Figure 4.24b). Together the shears bands (Figure 4.24c) form conjugate sets that are orientated parallel to the stretching lineations observed in greenschist facies lithologies.

even juxtapose gravels onto metamorphosed basement (Figure 4.26). Regularly spaced (1-10 mm), small amplitude (0.5-1 mm) crenulation folds and kink folds are locally developed and can sometimes be traced to a nearby fault.

Although slickenline orientations do not cluster nearly as tightly as ductile stretching lineations, the mean is clearly towards the NNE-SSW (032°, Figure 4.24). This indicates a significant rotation of the shear direction between brittle deformation and the preceding ductile deformation.

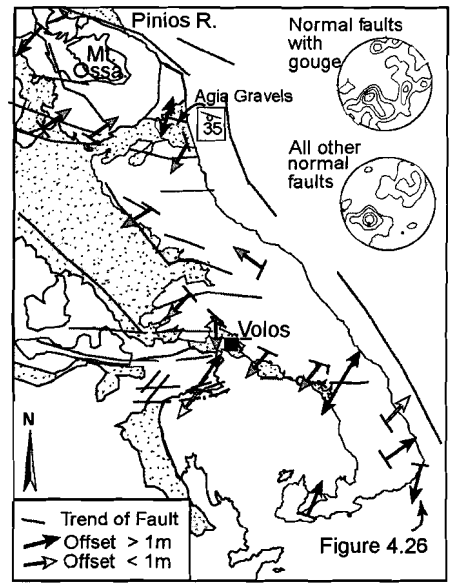

Figure 4.25
Map of east Thessaly showing the trend of slickenlines developed in faults with well developed gouge. The trend of slickenlines in faults with the largest offset is typically NE-SW, however note the large spread in orientation. Many faults have an WNW-ESE orientation. These faults form important geomorphological boundaries, e.g. the northern margin of Mt. Olympos and south of Volos. The tilt of the Neogene gravels in the Agia valley is compatible with dip slip along faults of an WNW orientation.

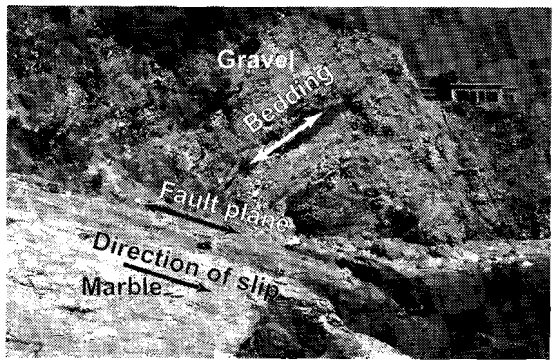

Figure 4.26
Photo of a major normal fault in the southern Pelion Peninsula. Marble in the footwall shows dip slip slickenlines. Note the 45° tilt of gravels in the hanging wall.

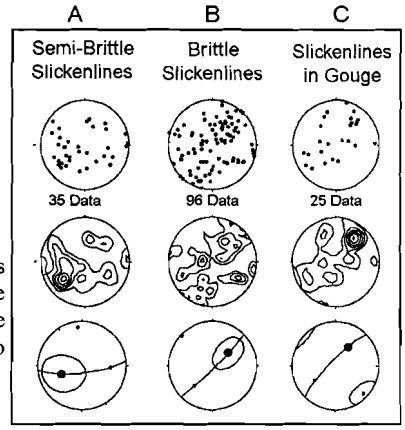

Figure 4.27
Lower hemisphere stereoplot of the orientation of slickenlines developed in: a) on semi-brittle normal shears/faults, b) in brittle faults, and (c) in thick gouge zones of normal faults. The average orientation of the three sets rotates from 064° (i.e., parallel to the stretching lineation in greenschist facies rocks) to 032°.

4.5 Discussion

4.5.1 Introduction

In the previous section the meso- and typical microstructures associated with deformation in different metamorphic events (M1.amph, M2.bls, M2.gns, and M3.gns), and under non-metamorphic conditions, were presented. It was shown that within any metamorphic event, several kinematic units could be identified. Although kinematic units developed in a variety of metamorphic conditions, four distinct sets of kinematic units may be recognised; two sets (sets 1 & 2 below) developed in entirely ductile conditions and further set of structures in both ductile and brittle conditions (set 3) and a fourth developed in entirely brittle conditions (set 4).

		M1.amph 135-100 Ma	M2.gns 120-80 Ma	M2.bls 80-36 Ma	M3.gns <36 Ma	Semi-ductile < 25 Ma	Brittle < 25 Ma
1	NNW-SSE	Variable	to SSE				
2	E-W	indeterminate	to E?	to W?			
3	NE-SW		to SW	to SW	SW & NE	SW & NE	SW & NE
4	NNE-SSW						NNE & SSW

Table 4.1: Table showing the dominant kinematic shear direction (movement of top indicated) developed during each metamorphic event. Shading indicates that the structures have been dated.

In this section, the temporal and spatial relationships between the sets of kinematic units and units themselves are examined using available geochronological data in conjunction with the observed overprinting relationships (Section 4.5.2). The conditions, development and significance of the regionally developed fibrous calcite fabric is also discussed (Section 4.5.3). This is followed with a discussion of the tectonic significance of the different deformation events and the structural evolution of the Thessaly region (Section 4.5.4).

4.5.2 Relationships and temporal constraints between kinematic units

(A) Shear zones with NNW trending lineations

A NNW-SSE orientation is only observed in shear zones of albite-epidote amphibolite facies (with an indeterminate sense of shear) and greenschist facies conditions in the northern and western margins of Thessaly (with a top-to-the-SSE sense of shear). Although the age of shear zones with NNW-SSE trending lineations is unknown (Table 4.1), this unit is cross-cut by early Cretaceous, M2 greenschist facies shear zones with NE-SW trending lineations (Figure 4.07) and hence represent a pre-M2.gns deformation event (see Table 4.1)

As no overprinting relationships between shear zones with E-W and NNW-SSE trending lineations, and no dates of the NNW-SSE trending fabric are available in the Thessaly region, the examination of temporal constraints of this fabric is based on an extrapolation of structures observed in the Macedonia Massif region, north of Thessaly.

In the basement of the Macedonian Massif, lineations have a very consistent top-to-the-SSE sense of shear (column A in Figure 4.03). The Macedonian basement has deformed in amphibolite to upper greenschist facies conditions at low structural levels and greenschist facies conditions at higher structural levels (Kilias et al., 1991). The deformed rocks have early Cretaceous, K-Ar cooling ages, which range from 140-133 Ma (3 samples) to 100 Ma (one sample; Mercier 1963).

The NNW-SSE trending stretching lineations in this region are consistently observed on moderate (10-50°) southward dipping shear zones, and span an 80 km wide area. Thus, these shear zones appear to represent a regionally important tectonic event. If the Thessalian basement was adjoined to the basement of the Macedonian Massif in the early Cretaceous (there is no known evidence to the contrary), this event is likely to have affected the Thessaly region too. The similarity between the metamorphic grade (amphibolite facies with a greenschist facies overprint), and the direction of shear (NNW-SSE) suggests that the NNW-SSE trending lineations west of Larissa were formed in the same, early Cretaceous deformation phase, as the lineations of Macedonia. Importantly, on the basis of structural relationships, the M3 greenschist facies metamorphism observed west of Larissa is temporally unrelated to the M2 greenschist facies tectonothermal event. Geochronological data are required to test this hypothesis.

(B) E-W trending shear zones

Unlike the relatively large area encompassed by NNW-SSE trending lineations (i.e. the Macedonian Massif and pockets within the Thessaly region), areas that exhibit E-W trending lineations tend to form small (10 km by 10 km), scattered enclaves. Shear zones with E-W trending lineations developed in a range of metamorphic conditions (albite-epidote amphibolite, blueschist and greenschist facies: Table 4.1) and have cooling ages that vary from 120-115 Ma in the Pierien Mountains (Yarwood and Aftalion 1976; Yarwood and Dixon 1977), and 100 Ma (Schermer et al. 1990) in the NW Olympos region (Figure 4.03b), Thus, this spread of cooling ages is younger than that of lithologies which contain NNW-SSE trending lineations. This kinematic unit is cross-cut by early Cretaceous M2 greenschist facies shear zones with NE-SW trending lineations east of Lioprasso (Figure 4.07), and hence must, like the NNW-SSE trending lineations, represent a pre-M2.gns deformation event, D1 (see Table 4.1).

Relatively few kinematic data are preserved in these rocks, and within each area regionally divergent senses of shear are observed. However, where kinematic structures are observed,

they dominantly show sense of shear is towards the east. Thus, shear zones with an E-W trending lineation are tentatively interpreted to have formed during the same deformation phase. This deformation event is interpreted to post-date shear zones with NNW-SSE trending lineations (D1). On the basis of generally younger ages preserved in its fabrics and the different orientations of the shear directions, shear zones with an E-W orientation is interpreted to represent D2.

The enclaves of E-W lineations are typically situated between the areas of NNW-SSE (D1) trending lineations and NE-SW trending lineations. Overprinting relationships between the E-W and NNW-SSE trending lineations were not observed. However, on a large scale the NNW-SSE trending lineations appear to rotate into an ~E-W orientation (e.g., Figure 4.07). The sense of shear in shear zones with E-W trending lineations is dominantly top-to-the-E which is compatible with a 60° anticlockwise rotation of the shear zones with a top-to-the-SSE sense of shear, into the shear zones with E-W trending lineations.

The large scale rotation of the NNW-SSE trending lineations towards an E-W may represent a progressive (rather than abrupt) change of tectonic conditions. This suggestion is supported by the similarities in metamorphic conditions observed in the two deformation phases. West of Larissa, the D1 deformation occurred in low grade greenschist facies conditions. Although earlier phases of E-W shearing in Pieria-Titaros Mountains and Sikees areas started in albite-epidote amphibolite facies (e.g., Figure 4.07), deformation continued into low grade greenschist facies conditions as evidenced by the replacement of biotite by phengitic white mica. Furthermore, plagioclase in quartzofeldspathic gneisses in both D1 and D2 deformation phases commonly has a reaction rim of albite (e.g., Figure 4.15). Although no detailed estimates of the pressure-temperature conditions of deformation can be gleaned from such a texture, the development of this reaction a fabric is confined to these deformation phases.

The orientation of stretching D1 and D2 stretching fabrics (120° angle), on similarly dipping mylonitic foliation planes suggest that the fabrics did not developed coevally (e.g., as shortening fabrics which develop contemporaneous with extensional extrusion fabrics may be expected to form a 90° angle to each). Localised block rotation of D1 fabrics and D2 fabrics (see Table 4.1) may explain the similarity of cooling ages.

(C) Shear zones with NE-SW trending stretching lineations

Shear zones with NE-SW trending directions of shear developed in a range of metamorphic conditions of late Cretaceous age and younger (Table 4.1). Deformation in M2 blueschist and greenschist facies conditions involve a dominantly top-to-the-SW sense of shear, whereas deformation in M3 greenschist facies conditions exhibit both senses of shear (Figure 4.08), Therefore, deformation during M2 and M3 metamorphic events are thought to reflect different deformation events, and are termed D3 and D4 respectively.

Although the average orientation of glaucophane mineral lineations (D3) and greenschist mineral lineations (D4) is the same (Figure 4.12), the spread of lineation data is significantly greater in the blueschist facies rocks. This suggests that either some reorientation of D3 lineations may have occurred during later stages or that blueschist facies deformation was originally more complex. The possibility of rotation during later stages is discussed in Chapter 5.

The sense of shear observed in D3 blueschist facies shear zones in this study is compatible with the sense of shear observed in the blueschist shear zones of Schermer (1993) in the Olympos region.

Although, E-W trending, blueschist facies D2 lineations were observed locally rotated into, NE-SW trending blueschist facies D3 lineations (e.g. Figure 4.08 inset), the sense of shear observed in both deformation events is not compatible with a dynamic rotation; D2 has a dominantly top-to-the-E sense of shear whereas D3 has a dominantly top-to-the-SW sense of shear. Moreover, in most regions or areas D3 structures cross-cut D2 structures. Thus, there appears to be a major change in regional kinematics between these two events.

Greenschist facies shear zones of *eastern* Thessaly, in particular the southern Pelion Peninsula, are progressively overprinted by shear bands of decreasing ductility which exhibit the same regionally divergent senses of shear (Figure 4.08). In semi-ductile conditions, however, the divergent sense of shear is observed on a smaller 1- 10 m scale that is commonly observed in greenschist facies conditions (Figure 4.27). Shears with a normal sense of displacement in D3 demonstrate a range in orientation, which together show that the region has undergone overall conjugate shearing with a subhorizontal direction of extension (Figure 4.20).

(D) Brittle deformation

The trends of brittle normal faults in the Thessaly region broadly cluster into two groups; a NW-SE group and a ~E-W group (e.g., Figure 4.24). Few geochronological data associated with the faults are available. The NW-SE trending normal faults lie at right angles to the dominant stretching direction of the D4 deformation phases, thus, these faults are interpreted to represent a brittle progression of D4 deformation, and are defined as the fifth deformation phase. The ~E-W trending brittle normal faults, which are unrelated to the early ductile deformation events and are interpreted to represent the most recent event D6. It is assumed that faults exhibiting fresh gouge exhibit displacements related to D6 event. Note that the directions of D5 and D6 slickenlines are orientated (6° and 32° respectively) anticlockwise of trend of D3-D4 stretching lineations (which are also shear directions).

Neogene gravels dip approximately 35° towards the SSW (Figure 4.07). This suggests that there has been a general rotation of the Olympos-Pelion range towards the west-southwest since the Neogene. The tilt of such gravels is compatible with top-to -the-NNE normal displacement on the late Pliocene WNW -ESE trending faults. A fault of such an orientation forms the northern boundary of Mt. Ossa. As the Pinios river, which has a delta of only 1 Ma old, cuts a gorge between Mt. Ossa and Mt. Olympos, these Pliocene faults are interpreted to have been associated with significant uplift.

4.5.3 Significance of the fibrous calcite fabric

In impure marbles, twinned calcite grains are orders of magnitude larger than grains in the encompassing quartz, feldspar and mica-rich matrix (Figure 4.17a). This indicates that the twinned grains developed from large recrystalised calcite grains. Since the attitude of the calcite fibres is unaffected by the folds in the mylonitised matrix, the recrystallisation must have occurred post-mylonitisation.

EPSB measurements demonstrated that many of the boundaries of the fibrous calcite fabrics are have a c-axis offset of approximately 52° about a common a-axis and are therefore likely to be e-twins (Figure 4.20). Such regular spacing of a e-twins is typical of calcite deformed between 250-350°C (Passchier and Trouw 1996). This temperature range is compatible with the association of chlorite and phengitic white mica observed in most impure marbles with fibrous calcite fabric (e.g., Figure 4.17a). Thus, the microstructure of fibrous calcite is likely to

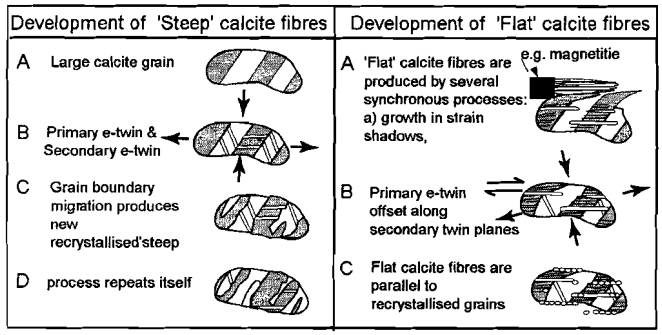

Figure 4.28: A figure outlining the interpreted stages in the development of steep and flat calcite fibres. Steep calcite fibres develop initially from primary e-twins. Through the development of secondary twins and grain boundary migration, these primary twins become replaced and overgrown by recrystallised grains which are orientated in the same direction as the primary grains. Steep fibres represent the pure shear component of strain. Flat fibres developed primarily from secondary and growth twins, and accommodate slightly more (shear) strain. As a result flat fibres are more finely twinned and comprise of more recrystallised grains. This shear strain is exhibited by offset and warping of the primary calcite fibres. Thus, steep and flat fibres have similarity with S-C fabrics developed in mylonites, but probably develop in conditions of low differential stress and high plane strain conditions.

have developed during M3 retrogressive greenschist facies conditions.

Flat fibres do not cross-cut all steep fibres, therefore the flat fibres are interpreted to develop broadly coevally with the steep fibres. The flat fibres exhibit shear strain in a direction parallel to the flat fibres (e.g., Figure 4.17c), thus the relationship between flat and steep fibres, exhibit a similar relationship as S-C fabrics in mylonites. The amount of shear strain along the flat fibres, however, rarely was observed as a sharply defined boundary and hence the amount of shear along flat boundaries may not be large.

A few of the steep grains are marked by e-twin boundaries. Most grains exhibit intense development of subgrains and recrystallised grains. The crystallographic preferred orientations of both 'steep' and 'flat' fibres suggest that the fibres developed in the same stress field of constant orientation.

Figure 4.28 shows how the S-C type relationship between steep and flat fibres may occur. First, large recrystallised grains of suitable orientation form primary twins at a steep angle to the compression direction. Then, under continued stress, subgrains develop and grain boundaries of grains migrate preferentially along grain or pre-existing twin boundaries to form new (smaller), recrystallised grains with long axes parallel to the trend of pre-existing 'fibres'. As the recrystallised grain becomes larger, the grain becomes twinned and the process repeats itself. The end result is that although 'steep' fibrous calcite fabric may have originally developed as a result of twinning and subsequent grain boundary migration, the new (sub)grains may have developed along preexisting boundaries and thereby obscure the original twin relationship. Flat formed from secondary twins in the steep grains and subgrains. It is suggested that these grains formed to accommodate the shear component of deformation.

The c-axes of both 'steep' and 'flat' calcite fibres cluster at a steep angle to the estimated shear plane (shown in Figure 4.21). The orientation of the c-axes in both cases suggests a slight left-lateral (top-to-the-west) sense of shear. Note that this sense of shear is opposite to that determined from shears in the mica-rich of the sample (see top right of Figure 4.17a). This suggests that the shear plane associated with the development of the elongate calcite fabric in Figure 4.17 may not coincide with the schistosity plane defined. However, as the c-axes of both flat and steep fibres in the samples examined exhibit a similar mean orientation relative to

the estimated shear plane (foliation plane), it is suggested that both fabrics developed in the same tectonic regime. The orientation of the c-axis fabrics relative to the shear plane suggests deformation was associated with predominantly plane strain (Figure 4.21).

The orientation of the steep fibres, in combination with the orientation of associated phyllosilicate horizons suggest that the compressive orientation is sub-vertical in the present reference frame, and conversely the extensional direction is broadly sub-horizontal (Figure 4.28). The regional significance of this suggestion is discussion below, in Section 4.5.4. In summary, steep and flat fibres have a similarity to S-C fabrics developed in mylonites, but develop in conditions of low temperature and low rotational strain.

4.5.4 Tectonic implications of deformation phases

In the following section the tectonic evolution of Thessaly, which is summarised in Figures 4.29a-d is discussed.

Shear zones with NNW-SSE lineations (D1) reveal few clues regarding tectonic conditions prevailing during their development. However, the stacks of *en echelon*, NNW dipping basement slices observed in the southern Pieria-Titaros Mountains (see also Nance 1981) suggest that there was a component of NNW-SSE directed shortening. Although the stacks of *en echelon* basement slices may have developed during (now reorientated) transpressional shear zones, the overprint of both E-W and NE-SW trending lineations suggests that the stack may have developed in an earlier event. It seems most likely that the south verging, NNW dipping stacks were developed as a result of the earlier SSW directed shear zones. Therefore, the SSW shearing is tentatively interpreted as regional thrusting (D1) event (Figure 4.29a).

As with the D1 event, the D2 event is represented by very few structures that can be used to determine regional kinematic or tectonic conditions during its development. Lithologies in the West Volos gneiss that were deformed in greenschist facies contain conjugate shears

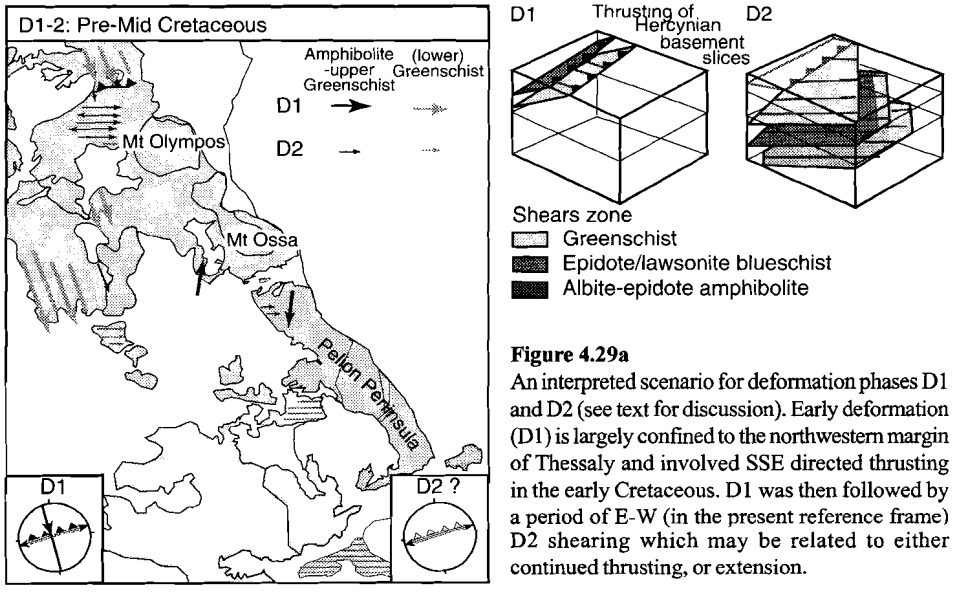

Figure 4.29a
An interpreted scenario for deformation phases D1 and D2 (see text for discussion). Early deformation (D1) is largely confined to the northwestern margin of Thessaly and involved SSE directed thrusting in the early Cretaceous. D1 was then followed by a period of E-W (in the present reference frame) D2 shearing which may be related to either continued thrusting, or extension.

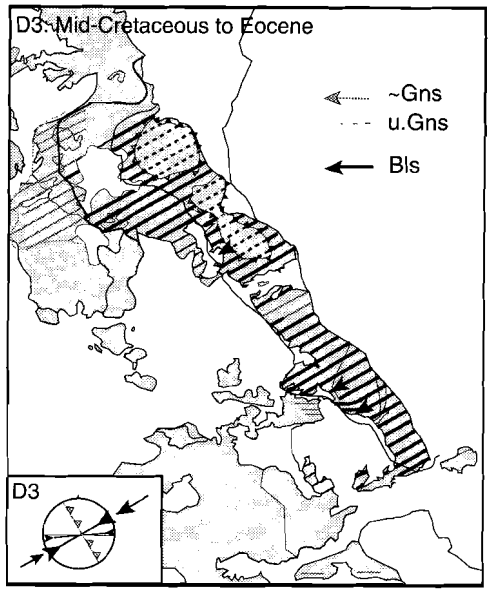

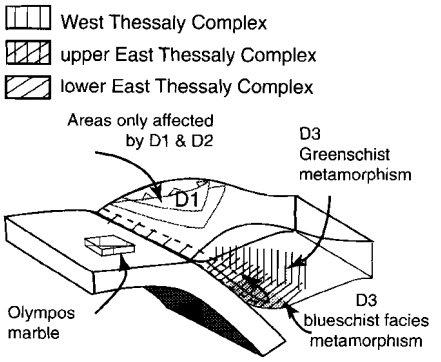

Figure 4.29b
Blueschist facies metamorphism started in the Eocene with top-to-the-W shearing, but rotated into a SW direction during D3 deformation. This event resulted in the development of a melange (East Thessaly Complex) and incorporation of the Ossa and Olympos (and other) limestone units.

suggesting extension occurred parallel to schistosity. Extension (e.g. in the footwall of a normal fault) may also explain the decreasing metamorphic conditions observed in E-W (D2) fabrics of the Pierien Mountains (Figure 4.29a).

The M2 blueschist metamorphic event of Thessaly developed at about 7 kbar, i.e. equivalent to a burial depth of ~20 km for rocks of average density. During exhumation to the earth's surface it seems likely that the mineral lineations may have undergone rotation relative to a reference frame within Thessaly. In the stereoplot of glaucophane mineral lineations

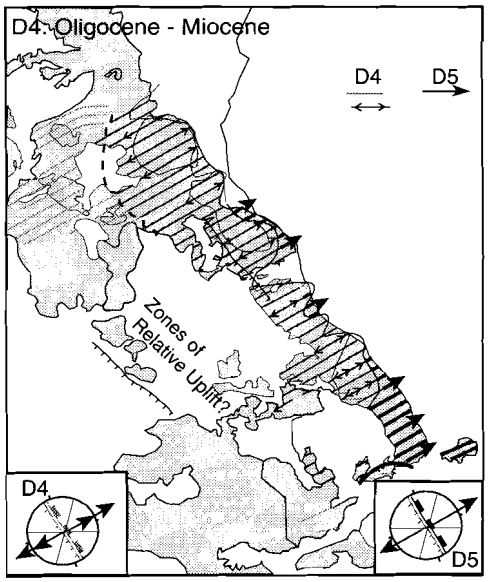

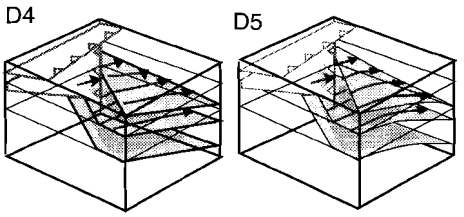

Figure 4.29c
Exhumation of blueschist facies rocks during the Oligocene to Miocene period was associated with retrogressive greenschist facies metamorphism and layer-parallel NE-SW directed extension (D4). Since the Miocene only the southern Pelion Peninsula and eastern board of the Olympos-Pelion range have undergone dominantly top-to-the-NE shearing. These shears were later cross-cut by brittle NW-SE faults (D5) which form the eastern boundary of the range.

(Figure 4.14), the mean orientation is the same as for stretching lineations developed later (244-064°). However, the spread in the data is significantly greater and (α 95% of 20° versus ±7°).

Blueschists exhibit both shortening and lengthening fabrics and hence it is difficult to determine the overall strain regime. Without suitable indicators, such as large-scale repetition of lithological sections, it is pointless to speculate. However, it should be mentioned that blueschist represents an increase in pressure relative to the surrounding rock (all greenschist grade) and therefore an initial component of regional shortening is likely (Figure 4.29c). The most complex lithological units, the East Thessaly Complex incorporated the Ossa and Olympos marble during the later stages of this event. Thus the East Thessaly Complex is interpreted to represent a subduction related melange (Figure 4.29b).

Glaucophane is present in sediments of the External Hellinides from the Cretaceous to the early Miocene (Faupl et al. 1996). As blueschist facies metamorphism was ongoing for up to 30 Ma after deposition of the first detrital glaucophane, the exhumation process must have had a continuous supply either by erosion or in the footwall of normal faults (e.g. within an orogen, see Section 2.5.2.2.).

Greenschist facies fabrics are represented by the widespread development of tension gashes. Although folds are present, they are highly attenuated and there is a progressive overprint by later more brittle extensional shears all with normal displacement. Together these data suggest that greenschist facies deformation, at least in the east Thessaly, was related to a regional extension event (Figure 4.29c). This event largely affected the southern Pelion and eastern margins of the Olympos-Pelion range. In the Olympos area, deformation during this period occurred under brittle conditions (Schermer 1993)

The Pliocene-aged sediments of the Larissa Basin and Pinios delta suggest that the faulting of the Thessaly region is relatively recent (Figure 4.29d) This is also supported by the observation that the Pinios River has cut a 200 m gorge (the Tembi Gorge) through the Olympos-Pelion range even though the western entrance to the gorge is 20-40 m higher than the southern Larissa basin (Caputo and Pavlides 1993). Finally, the recent, WNW-ESE trending

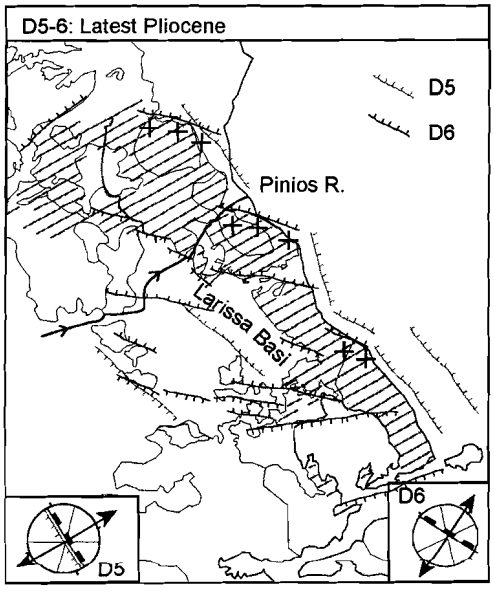

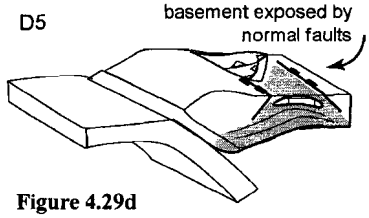

Figure 4.29d
The direction of extension rotated to a NNE-SSW orientation in the latest Pliocene, resulting in development of new WSW-ENE trending faults (D6). These faults are responsible for localised block rotation recorded by tilted gravels, and the uplift of the Mt. Olympos and Mt. Ossa segments of the Ossa-Pelion range. Faults from Caputo and Pavlides (1993).

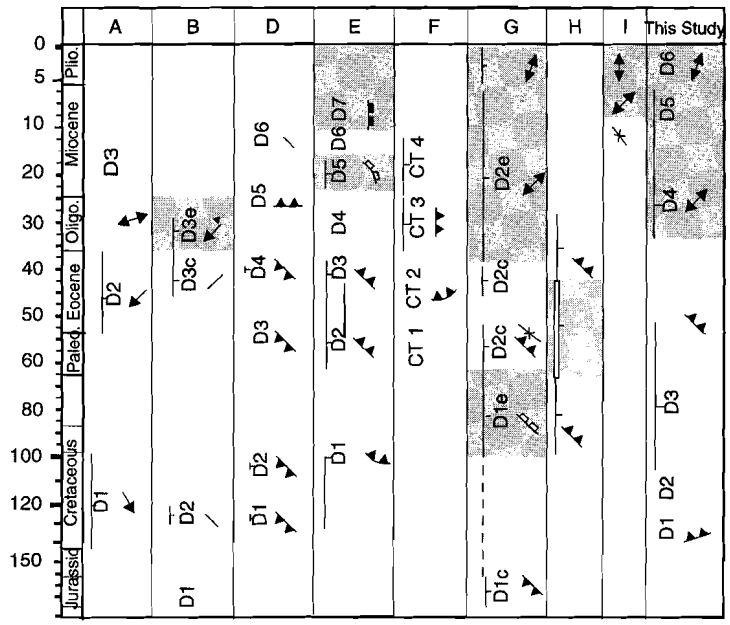

Figure 4.30: A figure comparing the results of this regional study with those of previous workers. See Figure 4.03b for legend and text for discussion:
A = Kilias et al. (1991), B = Sfeikos et al. (1991), C = Nance (1981), D = Barton (1975), E = Schermer (1993), F = Vergély and Mercier (1990), G = Doutsos et al. (1993), H = Jacobshagen & Wallbrecher (1984), and I = Caputo and Pavlides (1991). Grey areas represent periods of extension.

normal faults, in conjunction with the change in orientation of the recent slickenlines suggest that there has been an abrupt anticlockwise rotation of the direction of maximum extension within the Thessaly region since the Pliocene (Figure 4.29d). This important event which affected the Aegean region as a whole and is discussed in a regional context in Chapter 5.

In summary, the basement of Thessaly comprises a melange sheet (the East Thessaly Complex) lying between two sheets of Hercynian basement (the West Thessaly Complex). The West Thessaly Complex records early Alpine evolution and has never been to great depths where as the East Thessaly Complex was subject to blueschist facies metamorphism. Both the structural and metamorphic contacts are gradational. Such a situation may be expected in a sequence which has played an active tectonic role for the last 130 Ma.

4.5.5 Comparison of this study with previous results

In this regional study of the structural evolution of the Thessaly region, a set of six kinematic events (summarised above) were identified that developed in a range of low grade metamorphic through to brittle conditions. In this section, the findings of this thesis are compared with previous results (Figure 4.30), in particular those of the most detailed structural, metamorphic and geochronological study in the region to date, that of Schermer (1993).

Most workers have concentrated on the area outlined in this study that is dominated by M2.gns and M3.gns shear zones with, NE-SW trending lineations. This more regional study also encompassed the area affected by the first (D1) Alpine deformation phase (characterised by NNW-SSE trending lineations). Thus, this study confirms and extends the findings of Kilias et al. 1991 based on a study of the Macedonia Massif north of Thessaly.

The second phase of Alpine deformation (D2) identified in this study (with E-W trending lineations) has not been identified previously. This enigmatic phase may be related to a period of extension as suggested by Jacobshagen et al. (1978) and Doutsos et al (1993) (see columns

H and G in Figure 4.30 respectively). However, as discussed more fully in an Aegean-wide context in Chapter 6, the D2 event of Thessaly may in fact be a localised feature. In this study no major evidence of a period of tectonic quiescence as suggested by Jacobshagen et al. (1978) and Doutsos et al (1993) was unequivocally determined. This may be due to overprints during intense post-Cretaceous deformation.

In agreement with most workers in the Thessaly region, late Cretaceous to mid Tertiary deformation is characterised by NE-SW directed deformation (Figure 4.30). However, this study confirms the observations of Schermer (1993), that the early stages (D3 and D4 of this thesis) involve a dominantly top to the SE sense of shear and occurred during thrust conditions.

It was concluded in this study that brittle structures are orientated 32° anticlockwise of ductile (D2 D3 and D4) structures. This observation is in broad agreement with the results of Caputo and coworkers (summarised in column I of Figure 4.30). Few other workers have addressed the brittle evolution of the region. Schermer (1993) suggested that a phase of E-W fault was the last dominant event in the Mt. Olympos region. E-W faulting however does not appear to be of regional significance.

In summary, while this study confirms many of the observations made in this thesis by other workers (namely Schermer 1993) it provides temporally and spatially wider framework which allows regionally important deformation events to be identified and placed in a 3-D framework (summarised in Figures 4.29a,b,c,d).

4.6 Conclusions

1. Deformation structures of the Thessaly region record a sequence of 3 major ductile fabric forming events (D1, D2, D3) which young and become more intensely developed towards the southeast of the region.
2. On the basis of the orientation and estimated ages of the average direction of shear these events are:
   - An early, (D1) Cretaceous greenschist event (at high structural levels) amphibolite to upper greenschist at low structural levels, characterised by a NNW-SSE shortening with a SSE vergence.
   - This was closely followed by a second Cretaceous greenschist event (D2), characterised by dominantly E verging shearing.
   - The mid-Alpine phase of deformation (D3-D4) are characterised by a NE-SW (064°) trending stretching lineation.
   - Initial shortening during blueschist facies with a dominantly top-to-the-SW vergence (D3).
   - The D3 event was overprinted by a greenschist event during the Oligocene to Miocene, characterised by NE-SW stretching lineations with a regionally divergent sense of shear (D4).
   - Deformation conditions became progressively more brittle until the region start to develop a NW-SE trending 20-30 km spaced horst and graben structure which resulted in the uplift of the Olympos-Pelion Massif (D5) during the latest Miocene to Pliocene.
   - The most recent phase (Pliocene in age?) is characterised by 032° extension which developed only in brittle conditions. The newest brittle faults trend WNW-ESE (D6) and developed during the Pliocene.
3. Rocks involved in blueschist facies metamorphism contain marbles which exhibit a previously

undocumented regional development of fibrous calcite fabric. The fabric is the result of
a) Post deformational grain growth of pure calcite
b) Twinning during 250°-300° C
c) Grain boundary migration and recrystallisation in conditions of low differential stress and plane strain.

Chapter 5:
Constraints on Aegean kinematics

5.1 Introduction

The metamorphosed basement of the central Hellenides has played an important role in Aegean tectonics, both as a central part of the Tethyan suture zone (see Section 2.4.3.3) and as a locus of post-orogenic extension. Consequently this region, often referred to as the Pelagonian Zone (see below), has been the subject of intense geochronological, metamorphic and structural study. To date, most lithological and metamorphic studies in this region have concentrated on the Alpine and post-Alpine evolution of metamorphosed basement in relatively small areas within northern Thessaly (Mt. Olympos area) and the Cycladic islands (e.g. Avigad 1991;

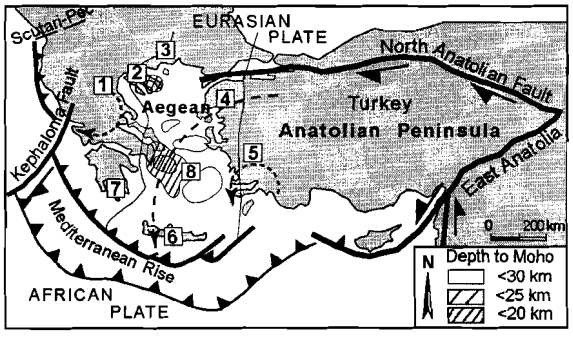

Figure 5.01: Deformed basement of Tertiary age exposed within and around the area of relatively thin crust of the Aegean. (1) Thessaly, (2) Chalkidiki, (3) Rhodope, (4) Kazdag and Kozak Massifs, (5) Menderes Massif, (6) Crete, (7) Peloponnesos, and (8) Cyclades. Note the NE-SW trending boundary between the crust of less than 25 km thickness in the northwestern Cyclades and crust greater than 30 km thickness in the southeastern Cyclades. Also shown are the paleomagnetically determined senses of rotation (shown as finely dashed lines) associated with regional SSW directed extension (Kissel et al. 1986, 1988). The line with larger dashes follows the trace of a small circle published by Jolivet et al. (1994) to describe anticlockwise motion of Turkey. Crustal thickness adapted from Tsokas and Hansen (1997).

Schermer et al. 1990; Vandenberg and Lister 1996). Although these and other studies have highlighted numerous important metamorphic and structural relationships (see Sections 3.3.3 and 4.2), it is demonstrated in this chapter that a lack of a common framework in such a complex region has hindered detailed correlation between studies. The problems encountered when trying to correlate units between the studies have not been highlighted in the past because relatively few studies have tried to integrate lithological, metamorphic and structural data across the entire region.

Post-orogenic extension of the Aegean involved SSW directed extrusion of the crust from a once broadly east-west trending orogen (Le Pichon and Angelier 1979; Le Pichon et al. 1995). This occurred contemporaneously with outward diverging clockwise and anticlockwise rotation of the northwestern and southeastern margins respectively (Figure 5.01: Kissel et al. 1986, 1987; Kissel and Laj 1988; Morris and Anderson 1996). The surface kinematics of this regional extension are not well understood, despite the fact that they provide important constraints on the various models proposed to account for Aegean extension. In particular

they may differentiate between radial spreading and block rotation models (see Section 2.5.3).

The surface exposure overlying and rimming the area of anomalously thin crust in the Aegean (Figure 5.01), largely comprises highly deformed pre-Alpine basement and Alpine intrusives which are covered by extrusives and Neogene sediments. Since Lister et al. (1984) first identified core complex style deformation in the basement of the central Cyclades, a region which now occupies a seismic gap, it has been established that much of the Aegean basement was exhumed in the footwalls of normal faults related to regional extension (Lister et al. 1984; Schermer 1993; Jolivet et al. 1994a; Dinter et al. 1995; Hetzel et al. 1995a, b). Since the pre-

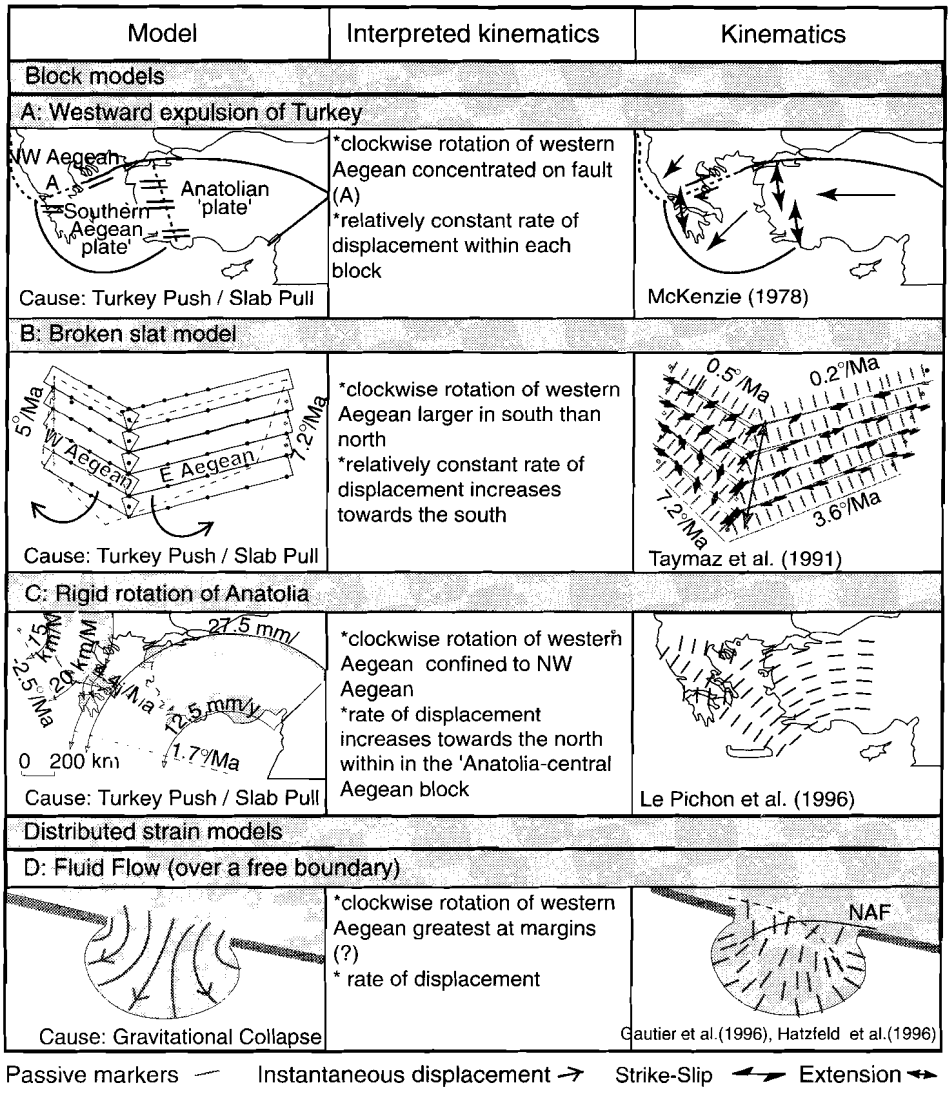

Figure 5.02: Models and interpretations of the kinematics of post-orogenic extension with the observations upon which they are based. See text (and Chapter 2) for discussion.

Schermer 1993; Jolivet et al. 1994a; Dinter et al. 1995; Hetzel et al. 1995a, b). Since the pre-Alpine basement predates extension, it has the potential to record late Alpine kinematics, and their subsequent rearrangement during exhumation. Thus, the aim of this chapter is to present a detailed kinematic analysis of pre-Alpine basement across the Aegean, and to combine this study with published paleomagnetic data, to determine constraints on the surface kinematics involved in post orogenic evolution of the Aegean. To do this, new data is presented from regions with little published data, and published data from elsewhere is reviewed.

This chapter is divided into 4 sections. In the first (Section 5.2), previous studies concerning the kinematic evolution of the Aegean and their implications for surface kinematics are reviewed. This is followed by a discussion of the method and assumptions used to integrate the kinematic data from elsewhere in the Aegean region. The second section (Section 5.3), summarizes published kinematic data from basement across the Aegean region. It begins with a discussion of the spatial, temporal and scalar dependency of Alpine stretching and mineral lineations, and associated kinematics, of the Thessaly region (discussed in detail in Chapter 4). In this section, additional new data, chiefly from northwest Turkey and the Cycladic and Peloponnesos areas are presented. In the third section (Section 5.4), published paleomagnetic data from the Aegean region are reviewed and the results of a reconnaissance study of the central Cyclades are presented. Finally, the paleomagnetic and kinematic data are combined, and the constraints that these data impose on the kinematic evolution of the region are discussed (Section 5.5).

5.2 Background to previous work and method

5.2.1 Published kinematic studies related to the post orogenic evolution of the Aegean

Due to the abundance of geodetic and seismic displacement data, much effort has been devoted to determining active kinematics of the Aegean region (see Jackson 1994 for a review). Kinematic models of the Aegean tend to fall into two categories: (1) models in which deformation is focused on a few narrow regions between relatively coherent units (e.g. block rotation models shown in Figure 5.02-a), and (2) models which interpret deformation as being regionally distributed (Figure 5.02-b). The surface kinematic data, on which the models are constructed, are discussed in more detail below.

Rigid block models

The first block model consists of 3 rigid blocks in which a central Aegean mini-plate is separated from 'northwestern Aegean' and 'eastern Aegean/Anatolian' blocks by zones of dominantly left-lateral slip and N-S extension respectively (Figure 5.02-a: McKenzie 1978). The central Aegean mini-plate is characterised by a lack of seismicity. In this model, the 'northwest Aegean block' moves towards the SW at half the speed of the 'southern Aegean block', whereas the 'Anatolian block' moves towards the WNW at approximately the same rate as the southern Aegean block (albeit in a different direction). The region between the northwest and southern Aegean blocks undergoes dominantly right-lateral slip whereas the area between the southern Aegean and the Anatolian blocks undergoes N-S extension. In this model, most rotation in the northwest Aegean block is concentrated in the narrow zone of left lateral shear (i.e. involving a component of clockwise rotation) between the northwest and southern Aegean blocks (Figure 5.02-a).

A second model is based on 2 uniaxially rigid blocks, and is commonly known as the broken slat model (Taymaz et al. 1991). In this model, the 'western block' is modeled as a series of

NW-SE trending rigid slats, representing crustal blocks, which are linked by hinges to a set of ENE-WSW trending slats that form the 'eastern block' (Figure 5.02-b). In this model, the western and eastern Aegean contemporaneously rotate in opposite directions whilst undergoing extension. The amount of extension is greatest near the hinges of the broken slats, i.e. close to the northern central Aegean region in this model. Stretching lineations of the western Aegean, which developed during the early stages of extension, may be expected to be *progressively* overprinted by later lineations that are rotated anticlockwise with respect to the earlier lineations. It will be shown in this chapter that the bulk of the rotation in the western Aegean occurred with the lineations maintaining a constant orientation relative to each other. Furthermore, recent studies have shown that the most recent active faults and basins developed in the western Aegean have an E-W orientation and not NW-SE as required in the broken slat model.

Finally, the third 'block' model is based on the rotation of a single rigid block (Le Pichon et al. 1995). In this model (Figure 5.02-c) the south Aegean is rigidly coupled to a westward moving Anatolian plate. These regions form a single 'block', bound to the north by the North Anatolian Fault, and together they rotate anticlockwise into the Mediterranean Basin. The contact of the northern margin of the Aegean/Anatolian block with Eurasia is modeled as a wedged-shaped zone of dominantly N-S displacement. This region undergoes translation around a small circle (Figure 5.02-c), and thus stretching lineations developed during different periods may be expected to have the same average orientation. Note that in this model, although the angular velocity is constant, the rate of displacement increases towards the northern Aegean. This contrasts with the broken slat model in which the rate of displacement increases towards the south.

Distributed strain models

Compared to studies of the active kinematics, there have been few detailed studies of pre-Pliocene kinematics of the Aegean region. Jolivet et al. (1994a) compared data for active displacements with stretching lineations preserved in the exhumed basement. They suggested that parallelism between the directions of active displacements and stretching lineations in the northeast Aegean indicate that this area was kinematically linked to Anatolia during regional extension and has since rotated anticlockwise. Recent paleomagnetic results show, however, that the north Aegean basement has rotated in the opposite sense. Hence, this area appears to be more closely linked with the western Aegean (Atzemoglu et al. 1994).

Gautier (1995) suggested that stretching lineations in the central Cyclades form a radiating pattern (Figure 5.02-d), roughly normal to the subduction zone, and that the lineations were formed by the outward spread of a viscous fluid (Gautier et al. 1996). This observation was contested by Morris and Anderson (1996), again on the basis of paleomagnetic data. They showed that the magnetic declinations, which are subparallel to stretching lineations, from two islands (Mykonos and Naxos) in the northern Cyclades form two distinct data sets separated by a NE trending fault. These results were thought to support the broken slat model (block model 2 above) as far back as the Miocene. As discussed in the description of the broken slat model above, there are problems with the model itself, and these are compounded when the model is extrapolated backwards in time.

Many studies have suggested that a major change in the kinematics of the western and northern Aegean occurred in the latest Miocene/early Pliocene (see Le Pichon et al. 1995). This observation is based on the following:

1. extension is currently focused on the northern Aegean near the westward termination of the

North Anatolian Fault (Figure 5.01). However, the region of anomalously thin crust and the present distribution of normal faults across the region indicate that extension was once focused south of its current position (Sonder and England 1989).

2. Miocene basins (typically half-grabens) uniformly trend NW-SE whereas in the Pliocene basins began to develop in an ~E-W orientation (e.g. Caputo and Pavlides 1993).
3. analysis of stress fields determined from displacements on faults show that there have been significant changes in the orientation of the stress field since the late Miocene (Mercier et al. 1989; Caputo and Pavlides 1993).

The reason for the change in kinematics is not known, and is clearly not explained by present day models. In addition, if an abrupt change occurred at this time, models of mid to late Pliocene kinematics should not be extrapolated to the past.

5.2.2 Introduction to Aegean basement

The Aegean basement is composed of slices of Alpine to pre-Alpine lithological units intercalated by shallow-dipping shear zones which record both brittle and ductile deformation (Lister et al. 1984; Schermer 1993; Burg et al. 1996; and Chapter 3 of this thesis). This deformed basement is exposed in several tectonostratigraphic zones, each of which contains one or more of the following lithological units: (1) pre-Alpine gneisses and metasediments; (2) Tethyan meta-ophiolitic sequences; (3) Alpine metasediments, volcanics, syn-extensional granites and gneisses (see Section 2.4.2).

The shear zones within the basement typically have a mylonitic texture in which stretching lineations, chiefly elongated quartz and feldspar, indicate the direction of ductile extension. Mineral lineations defined by glaucophane and/or actinolite develop locally and are usually parallel to the stretching lineations. The direction of ductile shear can be deduced by the geometry of the stretching lineations in conjunction with internal foliations, chiefly shear bands and schistosities. Where ductile shear zones have been progressively overprinted by a more brittle deformation, the direction of semi-brittle shear can be determined from the geometry of the internal brittle shears and tension gashes (see Passchier and Trouw 1996).

5.2.3 Outline of method and assumptions

In the following section (Section 5.3), kinematics indicated by late Alpine deformation fabrics from around the Aegean are examined. In many regions, the timing of the stretching and mineral lineations and/or the kinematic displacement can not be determined precisely due to the lack of geochronological constraints. Therefore, the following method is employed to make this association using the assumptions outlined below.

1. It is demonstrated (Section 5.3.2) that the distribution of late Alpine greenschist facies stretching and mineral lineations in the Thessaly region is approximately independent of length scale of observation. From this, it is concluded that: (i) the mean orientation (within the 95% uncertainty of the mean) of stretching and mineral lineations of known age provides a reliable indicator of the extension direction; and (ii) this extension direction was of regional significance. Therefore, the mean orientation of lineations of similar age may be compared with others elsewhere in the Aegean.
2. Recent studies have demonstrated that much of the Aegean basement was exhumed in the footwall of normal faults since the late to mid Miocene (Section 2.4.3.5). Therefore, compared to the time scale of the decline of the Alpine Orogeny, basement that was exhumed in the

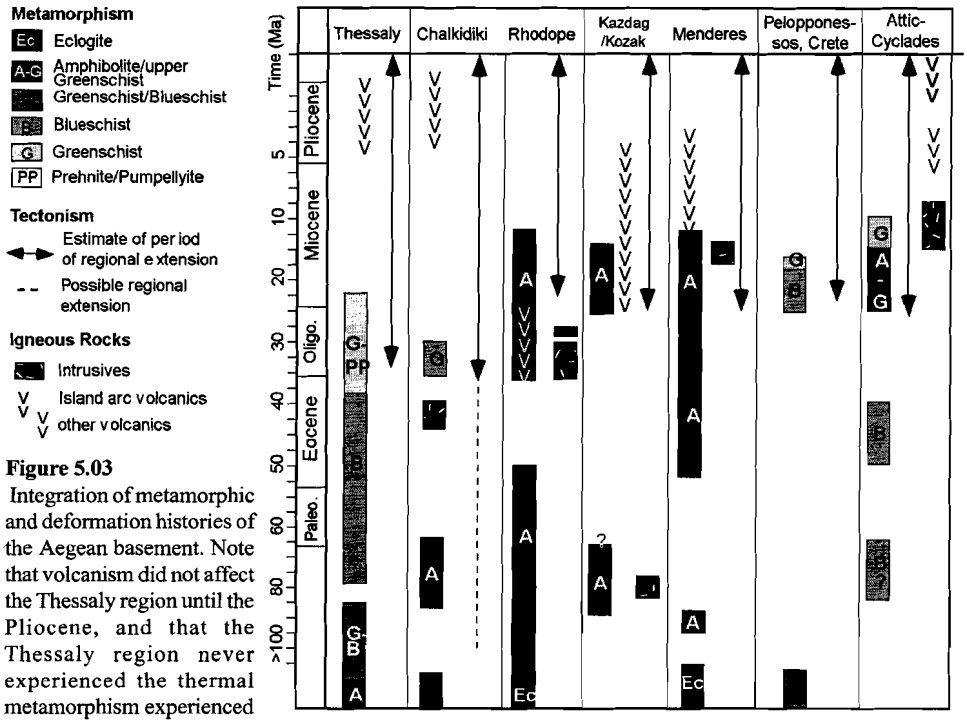

Figure 5.03
Integration of metamorphic and deformation histories of the Aegean basement. Note that volcanism did not affect the Thessaly region until the Pliocene, and that the Thessaly region never experienced the thermal metamorphism experienced in the Rhodope. To date, few data are available from the northern Macedonian Massif (see Figure 5.04 for location). Extension in this region began with the development of low angle faults in the early Oligocene. The anomalous 100 Ma age for the onset of extension in the Chalkidiki suggested by Falalakis et al. (1995), shown as a dashed line, is interpreted here as the exhumation age. The late Tertiary extensional period is marked by the onset of low angle normal faulting. Data are from Altherr et al. (1979, 1982), Andriessen et al. (1979, 1987), Seidel et al. (1982), Wijbrans and McDougall (1988), Pe-Piper and Piper (1989), Schermer et al. (1990) Okay (1989,1991), (1990), Doutsos et al. (1993), Bozkurt et al. (1994), Fassoulas et al. (1994), Falalakis et al (1996), Dinter et al (1995), Gautier (1995), Hetzel et al. (1995a,b), Jolivet et al. (1996), Hetzel and Reischmann (1996), and Burg et al. (1996).

assumed that since the exhumation of the lineations above this transition, the lineations have behaved as passive markers, as brittle deformation was localised along the block margins.

3. In any given region, the mean orientation of the stretching and mineral lineations can be determined in rocks of known late Alpine age (e.g. from syn-extensional plutons). It is assumed that stretching and mineral lineations of a similar orientation in adjacent regions developed, or possibly rotated into parallelism, during the same tectonic regime.
4. Finally, the mean orientation of stretching and mineral lineations is compared to paleomagnetic declinations. Appraisal of the orientations of the lineations and declinations together allow the regional surface kinematics to be analysed in detailed.

5.3 Alpine kinematics of the Aegean basement

5.3.1 Introduction

The Alpine to post Alpine kinematics of the Aegean basement is examined in terms of the following sub-regions: (1) northwestern Aegean, (2) northern Aegean, (3) eastern Aegean

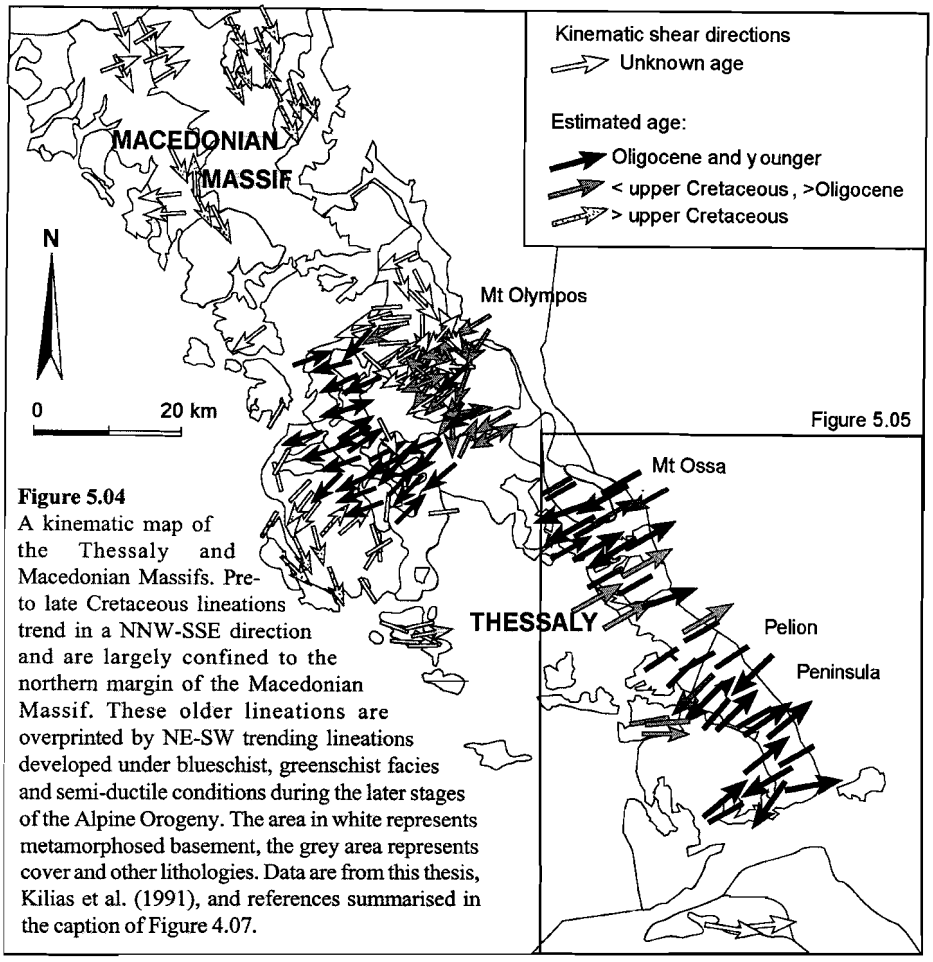

Figure 5.04
A kinematic map of the Thessaly and Macedonian Massifs. Pre- to late Cretaceous lineations trend in a NNW-SSE direction and are largely confined to the northern margin of the Macedonian Massif. These older lineations are overprinted by NE-SW trending lineations developed under blueschist, greenschist facies and semi-ductile conditions during the later stages of the Alpine Orogeny. The area in white represents metamorphosed basement, the grey area represents cover and other lithologies. Data are from this thesis, Kilias et al. (1991), and references summarised in the caption of Figure 4.07.

(NW Anatolian and the Menderes Massif), (4) southwestern Aegean, and (5) the central Aegean. Within each region, the geochronological and metamorphic data, which provide temporal constraints on the ductile fabrics (see Figure 5.03), are examined. The section on the northwest Aegean begins with an analysis of the dependence of Alpine kinematic data from the Thessaly region on the length scale of observation.

5.3.2 Northwestern Aegean

5.3.2.1 Introduction

In the previous chapters (Chapters 3 and 4), a detailed examination of the metamorphism, lithologies and kinematic evolution of the Thessaly region was presented. In this section, these thermal (metamorphic and geochronological) data are summarised and combined with a summary of similar data for the region of the Macedonian Massif. The temporal, spatial and scalar dependency of lineations in the Thessaly region is then examined in detail.

5.3.2.2 Summary of metamorphism and tectonothermal events

Few data are available for the northern, Macedonian Massif, region, therefore the data below concentrate on the Thessaly region. The overprinting relationships, in conjunction with geochronological constraints are summarised in a previous chapter (Chapter 4), hence only a summary of important tectonothermal events is outlined here.

Four major tectonothermal events, which were determined from the regionally developed lineated mylonitic fabric, have affected the basement of the northwestern Aegean (see Figure 4.27). The associated metamorphism is depicted in Figure 5.03. Evidence for the oldest deformation event (D1) is preserved as NNW-SSE trending stretching lineations (see Figure 5.04) which developed in the early Cretaceous. This event was overprinted in the late Cretaceous by E-W trending stretching and mineral lineations (D2) which are now preserved in small areas to the west of the Olympos-Pelion range (Figure 5.04). The third tectonothermal event (D3) resulted in the widespread development of NE-SW trending, blueschist facies fabrics. The best preserved event, however, is D4. This event is represented by NE-SW trending greenschist facies semi-ductile structures, and has been dated as young as the Miocene in the Olympos and Pelion areas (Schermer 1993; Lips et al. 1998).

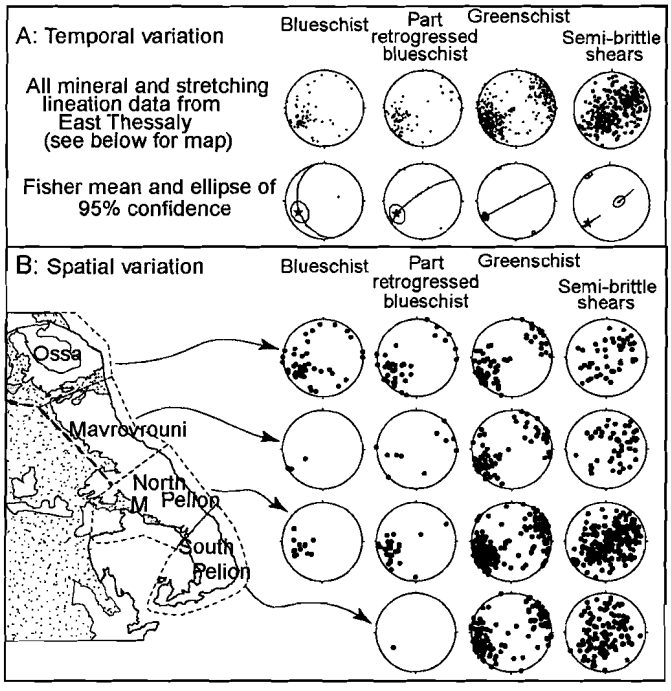

Figure 5.03: Stretching and mineral lineations from Thessaly region of northern Greece.
Figure 5.05a shows the temporal variation in the data, which is indicated by changing metamorphic condition. For example, blueschist lineations broadly represent early Alpine (late Cretaceous to Eocene) deformation whereas semi-brittle shears represent late Alpine (Oligocene to early Miocene) deformation.
Figure 5.05b demonstrates the spatial variation by comparing the variation in lineation orientations from four approximately equal size areas in the Ossa-Pelion range. Lineations formed under all conditions (i.e. blueschist, greenschist and semi-brittle shears) predominantly trend NE-SW.

5.3.2.3 Temporal, spatial and scalar variations of lineations

Temporal variation

In this section, the temporal variation in the orientation of stretching and mineral lineations developed in late Alpine mylonites is analysed. The period in which the lineations were formed is determined by the age of minerals which grew contemporaneously with the deformation

(see Schermer et al. 1990 and Wijbrans et al. 1996). In eastern Thessaly, these are represented by NE-SW trending lineations which mainly developed under greenschist facies conditions. However, remnants of earlier blueschist facies deformation are present in the Mt. Ossa and northern Pelion Peninsula areas. A later *semi-ductile* deformation has pervasively overprinted these early fabrics in the Pelion Peninsula and Agia valley areas. This enables the change in orientation over a range of conditions (which is proportional to a range of time, see Chapter 4) to be estimated. The results are shown in Figure 5.05a. Note that the semi-ductile shears often form conjugate pairs as demonstrated by the two maxima of poles to shears (rightmost stereoplot in Figure 5.05a).

The similarity in the orientation of the Bingham statistical mean for each metamorphic facies demonstrates that the azimuth of stretching and mineral lineations and the extensional direction of the shears trend consistently NE-SW. Hence, direction of shear appears to have maintained the same orientation, relative to a reference frame within the Thessaly region, from latest blueschist facies through greenschist facies to semi-brittle conditions, i.e., from the early Alpine (late Cretaceous and early Tertiary) to mid-late Alpine (Oligocene).

Spatial Variation

Local variation in the direction of Tertiary lineations across the southern Thessaly region is demonstrated by comparing lineation orientations in different areas (Figure 5.04). Towards the northern Thessaly region and within the Macedonian Massif region, stretching and mineral lineations of Tertiary age overprint an *older* SSE trending ductile shear fabric (Figure 5.04). In Figure 5.05b, the orientation of lineations from four sub-regions of the Olympos-Pelion range are examined. The average orientations of greenschist facies stretching and mineral lineations in each area lie within the 95% error margins of each other.

Scalar consistency

Such a spatial consistency is further supported by comparing the mean stretching and mineral lineation orientations from 3 different sized areas (1 km, ~600 km^2 and 2400 km^2: Figure 5.06). Only lineations of greenschist facies, Oligocene and younger (see Chapter 4) are included here. Figure 5.06 demonstrates that the different areas have similar mean orientations and data

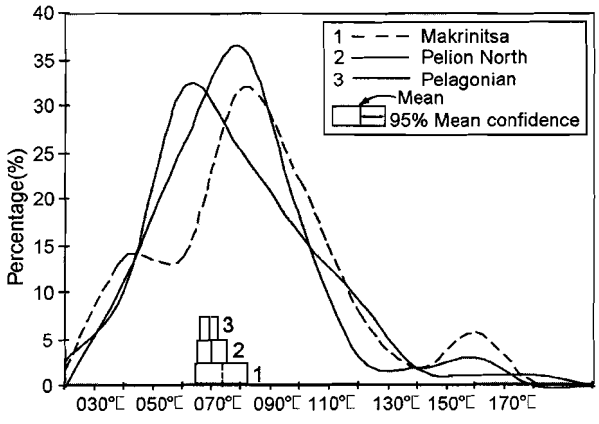

Figure 5.06: A graph showing the distribution curves of stretching and mineral lineation orientations from three areas of different sizes, with the means and the uncertainties shown in the boxes below. Although the distribution curves for the three regions show some variability, the mean orientation of stretching and mineral lineations from all areas is very similar. Areas are of increasing size and are centered west of Volos. The Makrinitsa area is a kilometre-long road section in Pelion North region (location shown as an 'M' in Figure 5.05b). Pelion North covers ~600 km^2. The east Thessaly region, which includes all four areas shown in Figure 5.05b, covers ~2400 km^2. To ensure that data from each subset did not bias the larger sets only the mean of each subset was included in the larger set.

distributions despite the variation in the modal value, and hence are largely scale-independent.

It should be noted from Figure 5.05, that blueschist facies lineations exhibit a broader spread in orientation than the later greenschist facies lineations. This spread may be the result of the rotation of blueschist facies lineations that were originally at a high angle to greenschist facies lineations. This appears to be the case on some islands in the Cyclades, in particular Tinos and Syros (Ridley 1984; Gautier 1995), but not all islands (e.g. Crete and Folengandros, Sowa 1985; Fassoulas et al. 1996). Therefore, lineations developed during retrograde conditions are used wherever possible.

The spatial, temporal and multi-scale consistency in the average orientation of stretching lineations (and their associated direction of ductile shear) suggests that the lineations developed in response to large scale (~10 to 100 km), long term (~10 Ma) forces. Therefore, it might be expected that lineations from other regions in the Aegean, which deformed under similar conditions would reflect similar characteristics.

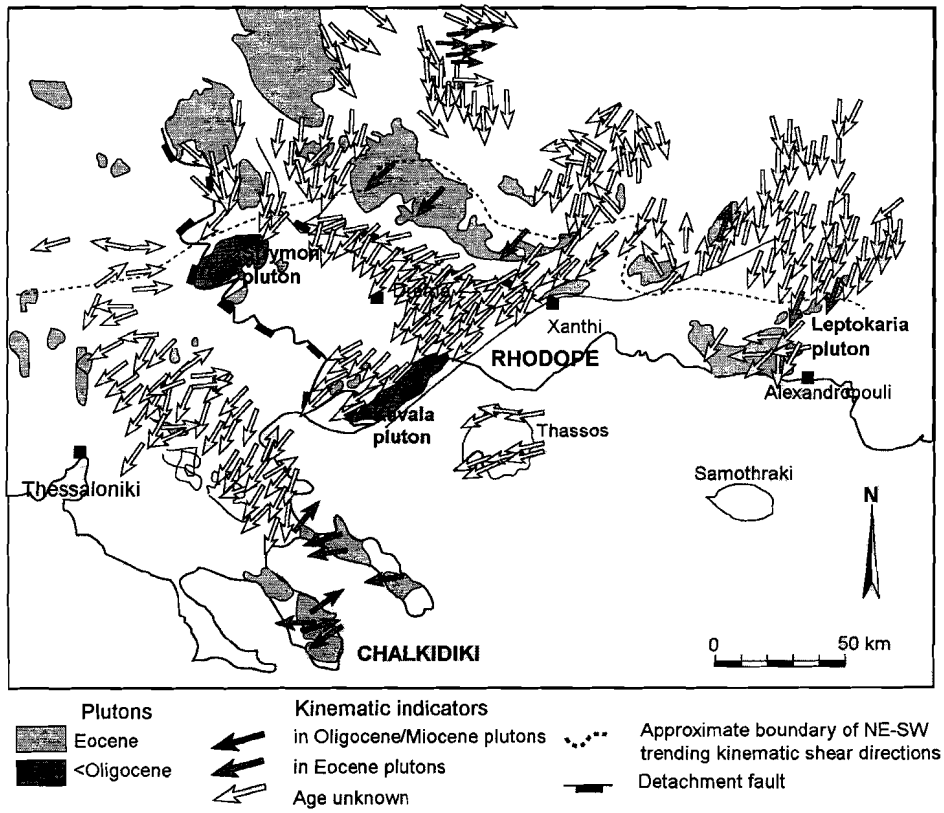

Figure 5.07: A kinematic map of the northern Aegean region. The boundary between two major groups of kinematic orientations present across the northern Aegean region is indicated by a dashed grey line. To the northeast of the line, thelate Cretaceous kinematic indicators typically trend NNE-SSW. Southwest of the dashed line kinematic indicators typically trend towards the SW, parallel to the kinematic indicators in syn-extensional plutons (black arrows). The one exception is the Leptokarya pluton which lies near the transition zone between NNE-SSW and NE-SW trending lineations. Data are from Sokoutis et al. (1993), Dinter et al. (1995), Falalakis et al. (1995), and Burg et al. (1996).

5.3.3 Northern Aegean: Chalkidiki and the Rhodope

5.3.3.1 Introduction

The northern Aegean region consists of two major areas which, from west to east, are the Chalkidiki and Rhodope areas (Figure 5.07). The lithologies in this region are similar to those in the northwestern Aegean, and include a range of Hercynian basement rocks, Mesozoic marbles with intercalated ultramafics (largely confined to the western margin of the Chalkidiki area, see Koukouvelas and Doutsos 1995), metabasites and calc-schists. The Rhodope region was initially thought to represent a stable cratonic platform, 'Zwischengebirge', between two branches of the Alpine orogenic belt (Jacobshagen et al. 1978). However, recent studies have demonstrated that portions of the Rhodope region have been involved in active Alpine tectonics since the late Cretaceous (Burg et al. 1990; Dinter and Royden 1993; Dinter et al. 1995; Burg et al. 1996).

5.3.3.2 Metamorphic history

Most metamorphic studies of the northern Aegean are confined to the Rhodope region (Burg et al. 1990), although many plutons on the Chalkidiki Peninsula have been dated (de Wet et al. 1989). A period of high pressure (eclogite facies) metamorphism, estimated to be late Cretaceous in age (Burg et al. 1990), is observed to be followed by a more moderate temperature, moderate pressure (amphibolite facies) metamorphism in the Rhodope and Chalkidiki regions (Figure 5.03). The moderate pressure, moderate temperature phase of metamorphism is thought to have affected both areas in the late Cretaceous (Figure 5.03), although in the Rhodope region amphibolite facies conditions were maintained until the Eocene (Burg et al. 1990).

The oldest basins of the Aegean (Eocene in age) are preserved in the northern region. However, core complex style deformation occurred along the Strymon Fault in the Miocene (Figure 5.07; Dinter and Royden 1993). This phase of deformation is associated with retrogressive greenschist facies metamorphism (Falalakis et al. 1995).

5.3.3.3 Kinematic orientations

Kinematic indicators in the northern Aegean region fall into two major groups of orientations: NE-SW and N-S. Near the northeastern margin of the Rhodope area (north of the dashed line in Figure 5.07), N-S and NE-SW trending lineations are apparent, whereas to the west (i.e. Chalkidiki and western Rhodope), lineations generally trend NE-SW. An exception to the NE-SW trend of lineations in the Rhodope and Chalkidiki regions, is found in the southern Chalkidiki Peninsula, close to the termination of the left lateral North Anatolian Fault (see Figure 5.01). There the stretching lineations in and/or near the Oligocene plutons (shown in a dark shade, Figure 5.07) trend E-W. The lineations in basement surrounding the Leptokarya pluton trend N-S. Note, however, that the Leptokarya pluton lies at the border between the zone of N-S lineations and NE-SW lineations.

The age of the N-S lineations is estimated to be late Cretaceous, whereas overprinting E-W trending lineations in the northern Rhodope area are estimated to be Eocene in age (Burg et al. 1990). The overprinting sequence of lineations in the border regions (i.e. north and east of the dashed line in Figure 5.07) is similar to those observed in the Thessaly region. The youngest plutons of the region, the Miocene Kavala, Strymon and Xanthi plutons show consistent top-to-the-SW sense of displacement, and therefore this orientation is taken to be most representative

of fabrics related to the extensional event, and the most important orientation to use for documenting post-exhumation kinematics.

5.3.4 Eastern Aegean: NW Turkey and the Menderes Massif

5.3.4.1 Introduction

As in the Rhodope area, the involvement of the SW portion of the Anatolian Peninsula in Alpine tectonics has only recently been established (Verge 1993; Bozkhurt et al. 1994; Hetzel et al. 1995a,b). Hence, relatively few structural studies on the eastern Aegean/western Anatolian region have been published. For this reason, a study was undertaken of the Kazdag and Kozak Massifs, which lie in northwestern Anatolia (Figure 5.08).

The basement of the western Anatolian region examined here generally comprises high grade gneisses, with syntectonically intruded diorites and metabasites. Marble units are intercalated with gneiss throughout northwest Anatolia, and in both the Menderes Massif and NW Anatolia the basement is covered by low-grade ophiolitic melange (Okay 1980).

5.3.4.2 Temporal and metamorphic data

In this section, available metamorphic and geochronological data for the two regions are summarised, then published kinematics results from the Menderes Massif region are followed by a summary of the new structural data from northwestern Turkey.

Few detailed metamorphic and geochronological studies have been published in the European literature on the eastern Aegean. As with the Rhodope area eclogites, estimated to be of late Jurassic to late Cretaceous age are found scattered throughout the basement of northwest Anatolia (Figure 5.03; Okay 1980). High pressure blueschist facies metamorphism preserved

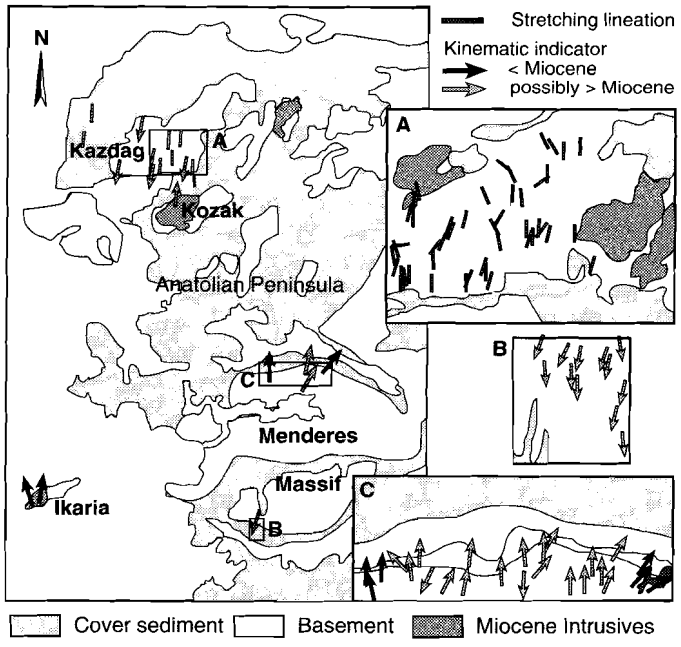

Figure 5.08
A kinematic map of the Anatolia Peninsula in the eastern Aegean. Kinematic indicators in syn-extensional plutons (black arrows) show a divergent sense of shear, although the orientation of these shears is consistently ~N-S. A similar pattern is observed in the surrounding schists of unknown (but younger than Cretaceous) age. White area represents metamorphosed basement, grey area represents cover rocks. Data from Kazdag and Kozak Massifs are from this study, other data are from Okay (1991), Bozkurt et al. (1994), Hetzel et al. (1995a, b).

in northwestern Anatolia is late Cretaceous in age (80-115 Ma, K/Ar on phengite; Okay 1989). Although no blueschist facies metamorphism has yet been recorded from the Menderes Massif, eclogitic rocks of unknown age were recently described by Oberhänsli et al. (1997).

Both northwest Turkey and the Menderes Massif contain amphibolite facies metamorphic rocks. Although the age of this metamorphic event is not known in northwest Anatolia, it affects plutons of late Cretaceous age. In the Menderes Massif, this phase of metamorphism is thought to have occurred between the Oligocene and Eocene (Oberhänsli et al. 1997), and is often referred to as the 'main Menderes metamorphism'.

5.3.4.3 Kinematic evolution of the Menderes Massif

The Menderes Massif has recently been interpreted as a parallel-deforming core complex with top-to-the-NNE sense of shear along its northern flanks and a top-to-the-SSW sense of shear on the southern flanks (Figure 5.08: Hetzel et al. 1995a,b). Mylonites on the southern flanks of the Menderes Massif are latest Oligocene to earliest Miocene in age, and are unconformably overlain by 21 Ma sediments. This constrains extensional deformation in this region to the early Miocene (Bozkurt and Park 1997).

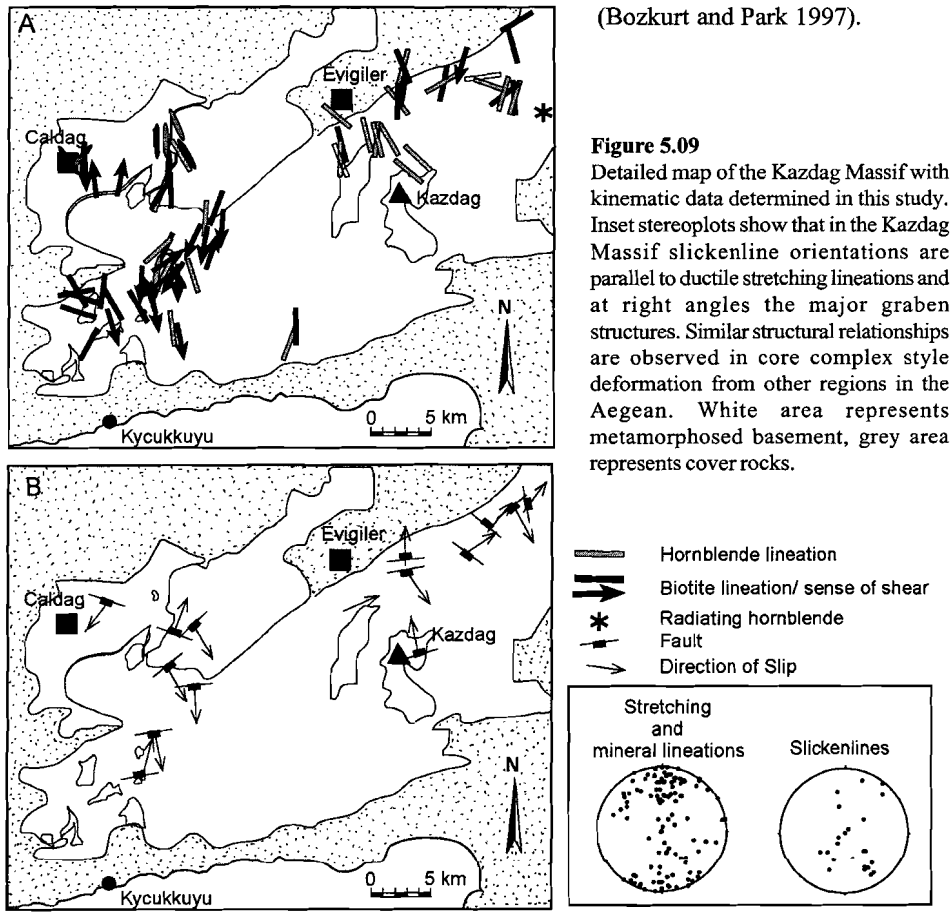

Figure 5.09
Detailed map of the Kazdag Massif with kinematic data determined in this study. Inset stereoplots show that in the Kazdag Massif slickenline orientations are parallel to ductile stretching lineations and at right angles the major graben structures. Similar structural relationships are observed in core complex style deformation from other regions in the Aegean. White area represents metamorphosed basement, grey area represents cover rocks.

5.3.4.4 Kinematic evolution of NW Anatolia

Study of shear zones in the northern and western Kazdag Massif reveal that the high-grade basement and syn-tectonic intrusives have undergone intense ductile deformation, which resulted in N-S (±30°) stretching with a divergent sense of shear (Figure 5.09). Overprinting mineral lineations demonstrate that extension was contemporaneous with cooling/exhumation of basement: the earliest lineations are defined by hornblende which is locally overprinted by biotite and rare chlorite.

Fault zones on the northwest flank of the Kazdag Massif have a variable but generally top-to-the-NW (±20°) sense of displacement (Figure 5.08 and 5.09). Granite dikes in the Kozak Massif typically trend E-W to ENE-WSW, as do the orientations of dominant fractures, small veins, and zones of skarn. In contrast to the recent (Miocene) lineations and kinematic data from the western and northern Aegean, the youngest lineations in the eastern Aegean have a N-E to NNE-SSW orientation. Kinematic indicators in the Kazdag and Kozak Massifs are subparallel to those observed in the Menderes Massif (Figure 5.08). The age of these fabrics is roughly the same as that of lineations in the Rhodope region. No areas of NE-SW stretching lineations occur in western Anatolia.

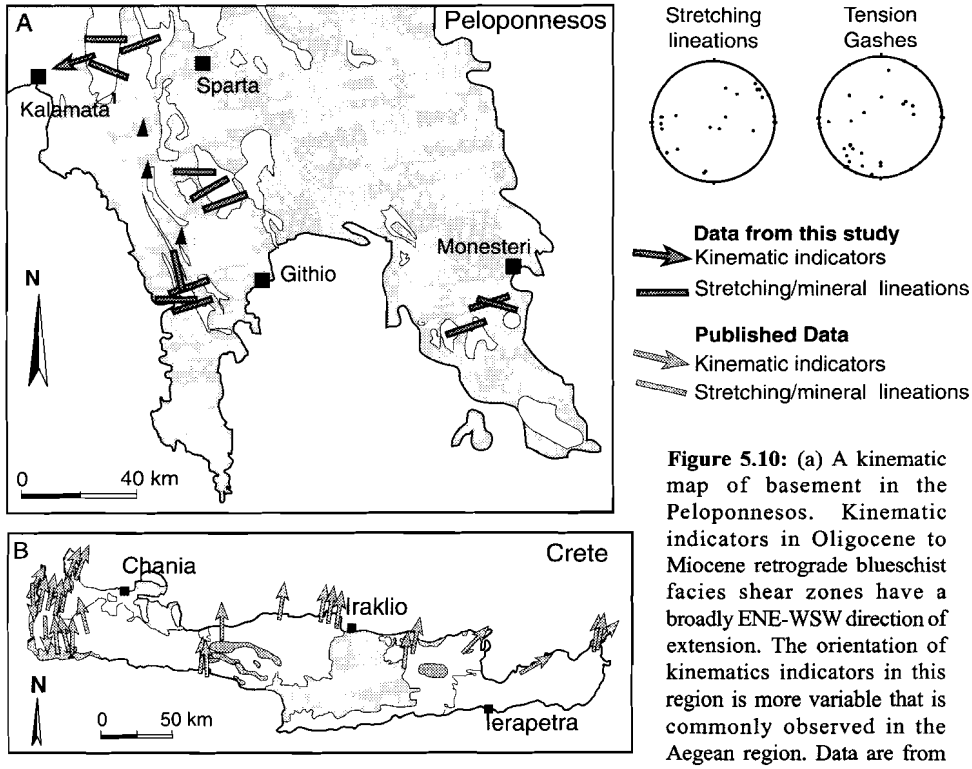

Figure 5.10: (a) A kinematic map of basement in the Peloponnesos. Kinematic indicators in Oligocene to Miocene retrograde blueschist facies shear zones have a broadly ENE-WSW direction of extension. The orientation of kinematics indicators in this region is more variable that is commonly observed in the Aegean region. Data are from this study.

(b) A kinematic map of the Crete. Kinematic indicators in Oligocene to Miocene retrograde blueschist facies shear zones have a top-to-the-north sense of shear, which is parallel to the orientation of glaucophane mineral lineations. Data are from Jolivet et al. (1996) and Fassoulas et al. (1994). In both figures the white area represents metamorphosed basement, grey area represents cover rocks.

5.3.5 Southwestern Aegean: Crete and the Peloponnesos

5.3.5.1 Introduction

The basement of Crete and the Peloponnesos comprises a nappe stack of marble, metapelite, quartzites, quartzofeldspathic schists, calc-schists and phyllites, which include the Pre-Apulian, Ionian, Tripolitsa, Pindos, and Pelagonian (Asteroussia nappe) zones (Jolivet et al. 1996). In the Peloponnesos, the stack of lithologic units is rather more ordered than is found on Crete. Of particular interest is 'quartz phyllite nappe' (also called the 'Arna units'; Jacobshagen et al. 1978), which is found at the base of the Tripolitsa series (Bonneau 1982) in both Crete and the Peloponnesos, and which has undergone Tertiary ductile deformation (Jolivet et al. 1996).

The quartz phyllite nappe has suffered only low grade metamorphism (Figure 5.03). A late Jurassic episode of blueschist to epidote-albite amphibolite facies metamorphism (barroisite-albite-epidote-phengite-calcite) has been dated from Crete. However, few structural fabrics have been attributed to this event. Most ductile fabrics are related to a blueschist facies event of Oligocene to Miocene age which affected the quartz phyllite nappe on both Crete and the Peloponnesos (Figure 5.03; Seidel et al. 1982). The pressures obtained from blueschist facies assemblages in the Peloponnesos area were slightly higher (10-17 kbar (400°C): Theye et al. 1992; Bassias and Triboulet 1994) than those experienced in Crete (8-10 kbar (400° C): Theye et al. 1992). Retrograde greenschist facies metamorphism locally overprinted the high pressure event (Fassoulas et al. 1994).

To date most structural studies have concentrated on Crete (Fassoulas et al. 1994; Jolivet et al. 1994a, 1996) and therefore a study of the Peloponnesos region was undertaken.

Kinematics of the southwestern Aegean

Although pre-Alpine lineations in central Crete exhibit an E-W trend (Fassoulas et al. 1996), kinematic indicators in late Tertiary blueschist facies and retrograde altered rocks on Crete have a dominantly top-to-the-N sense of shear (Figure 5.10b: Fassoulas et al. 1995). Note the local occurrences of top-to-the-NE sense of shear, e.g. north of Ierapetra (Figure 5.10b). The sense of shear observed from shear zones in the Peloponnesos is rather variable but appears to be dominantly towards the NE (Figure 5.10a). The direction of shear is broadly parallel to the extension direction determined from the orientation of the poles of tension gashes. Thus, there is a difference in orientation of kinematic indicators of approximately 50° between the Peloponnesos and Crete.

5.3.6 Central Cyclades

5.3.6.1 Introduction

Of all basement regions in the Aegean, the Attica-Cyclades region has been the subject of the most detailed metamorphic and structural studies (e.g., Papanikolaou 1978, 1980; Lister et al. 1984; Ridley 1984; Sowa 1985; Avigad 1991; Lee and Lister 1992; Gautier 1995; Vanderberg and Lister 1996). Most studies have concentrated on the islands of Naxos, Ios, Mykonos, Paros, Syphnos, and Syros, and hence this study focuses on the kinematics found on the peripheral islands of Kea (Figure 5.11a) and Santorini (Figure 5.12), and the central Cycladic island of Antiparos (Figure 5.11b).

Basement of the central Cyclades is interpreted to represent a continuation of the basement of the Thessaly region (the Pelagonian Zone; Aubouin 1959). Gautier (1995) recognised two units, an 'upper unit' and a 'lower unit'. The upper unit is composed predominantly of

unmetamorphosed rocks, mainly ophiolite blocks and early Cretaceous neritic limestones. Rocks metamorphosed prior to the Cretaceous are locally exposed, which and largely Hercynian gneisses and mica-rich schists and marble. These lithologies are broadly equivalent to the West Thessaly Complex and upper East Thessaly Complex of this thesis (see Chapter 3). The lower unit contains similar metamorphic lithologies to the upper unit, but has experienced two Tertiary metamorphic events (Gautier 1995): an Eocene high pressure event is overprinted by Miocene high temperature, moderate pressure upper greenschist to amphibolite facies metamorphism. The lower unit is the equivalent to the lower East Thessaly Complex defined in this thesis (see Chapter 3).

In the late Miocene, a series of I- and S-type granites intruded the central Cycladic region. Although these are concentrated along a NE-SW trending zone in the central Cyclades (Blake et al. 1981) small volumes are also observed on the Attica Peninsula and Kos (Dürr et al. 1978).

5.3.6.2 Kinematics of Cycladic basement

Kinematic indicators in syn-extensional intrusives in the northwestern Cyclades trend consistently NE-SW (Figure 5.12: Gautier 1985). In contrast, the sense of shear in syn-extensional plutons in the eastern Cyclades (Ikaria and Naxos) is N-S. This difference in shear orientations is also observed in kinematic indicators of late Alpine age found in the surrounding schists, with the exception of Syros which has an overall E-W direction of shear. On the island of Paros this change in orientation coincides with the SE dipping Paros detachment fault (Figure 5.11b), which is interpreted to be one of the oldest faults in the island (Lister and Forster 1996).

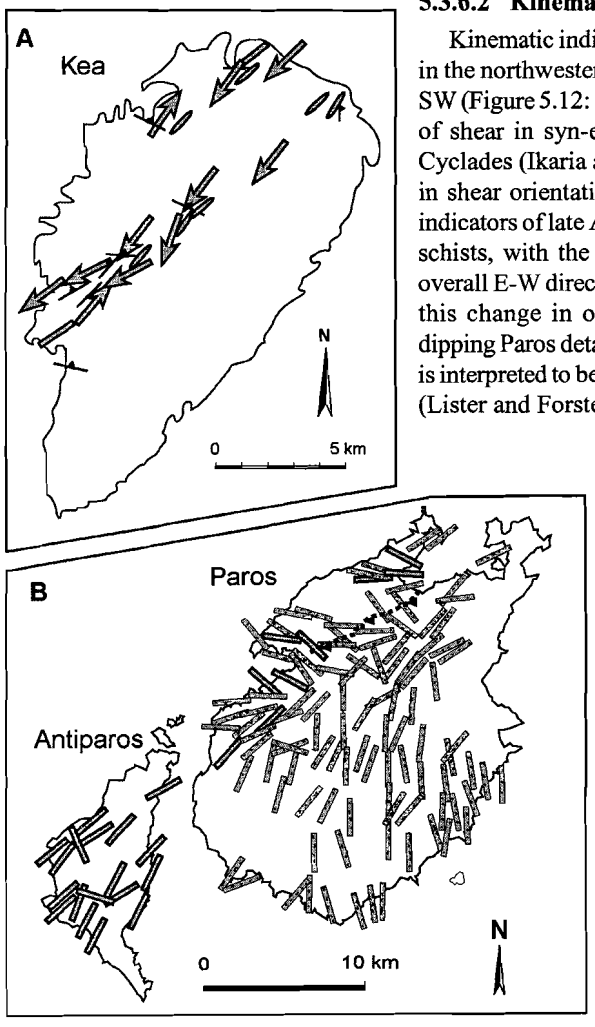

Figure 5.11: (a) A kinematic map of the basement of Kea, which demonstrates that shear directions are consistently NE-SW. The age of the kinematic indicators is unknown.. (b) A kinematic map of the basement of Paros and Antiparos. Note the change in orientation of stretching and mineral lineations across a NE-SW trending zone in northwestern Paros (see text for discussion).

Paros detachment fault
Strike and dip of mylonitic foliation

Data from this study
Kinematic indicators
Stretching/mineral lineations

Published Data
Kinematic indicators
Stretching/mineral lineations

On the islands of Folengandros and Andros, glaucophane mineral lineations are parallel to the later greenschist facies lineations, whereas on Syros and Tinos they are at a high to moderate angle (80° and 30° respectively) to the greenschist facies lineations (Ridley 1984; Gautier 1995). The only blueschist facies lineations used in this study are those that parallel the greenschist facies lineations.

At the inception of this project (1993), this change in shear directions had been interpreted as either: the consequence of a regional radial flow of the crust/lithosphere (Gautier and Brun 1994; Jolivet et al. 1994a); or as two discrete orientation data sets resulting from two separate tectonic (subduction) events (Blake et al. 1981). A study of kinematic indicators on the islands of Kea, Antiparos, and Santorini (Figures 5.11 and 5.12) was undertaken to extend the surface coverage of data, and to clarify the nature of this change in orientation.

The island of Kea is dominated by NE trending greenschist facies shear zones with overall top-to-the-SW sense of shear (Figure 5.11a). The kinematic indicators of Antiparos exhibit a similar direction but different sense of shear (top-to-the-NE, Figure 5.11b). Santorini is dominated by low grade schists and phyllites and therefore stretching lineations are not readily apparent. The most prominent lineation is a N-S trending intersection lineation, which is parallel to rare stretching lineations. Kinematic indicators from Santorini have a dominantly top-to-the-S sense of shear (Figure 5.12).

5.3.7 Summary of the orientation of kinematic indicators in the Aegean

In this section, it will be demonstrated that the stretching lineations and sense of shear directions associated with syn- to post-orogenic extension in the Aegean region exhibit a regional consistency in their orientations, not only outcrop (1 m) to regional (100 km) scale but also

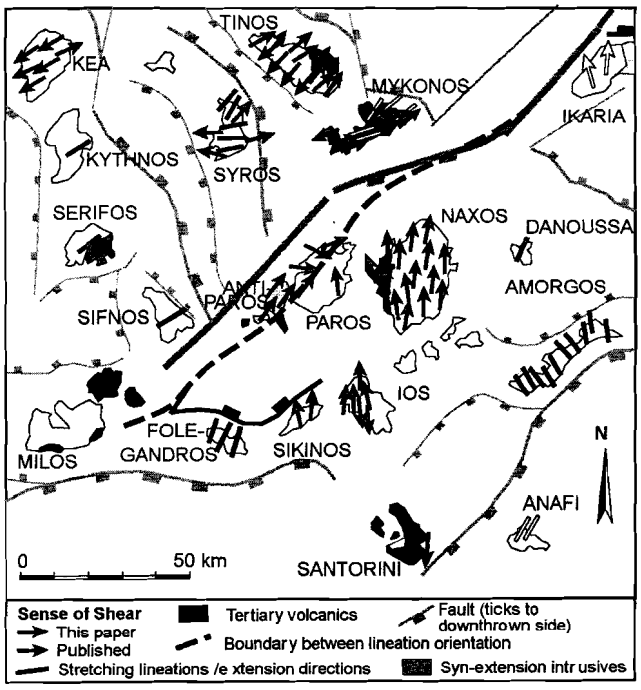

Figure 5.12
Map showing the distribution of the directions of ductile shear (arrows) and of stretching lineations (bars) in the central Cyclades, superimposed on the main brittle fault structures. Black arrows on Kea, Tinos, Santorini, Antiparos are from this study, lighter arrows represent data from Gautier (1995), Sowa (1985) and Faure et al. (1991). Most of the kinematic data are from Gautier (1995). Note that the sharp change in orientation of lineation/ shear directions lies subparallel to a fault (shown in dashed line) in the north but diverges slightly from the fault in the south, and crosses Paros itself (see Figure 5.11b). The boundary on Paros corresponds to the Paros detachment fault (Lister and Forster 1996).

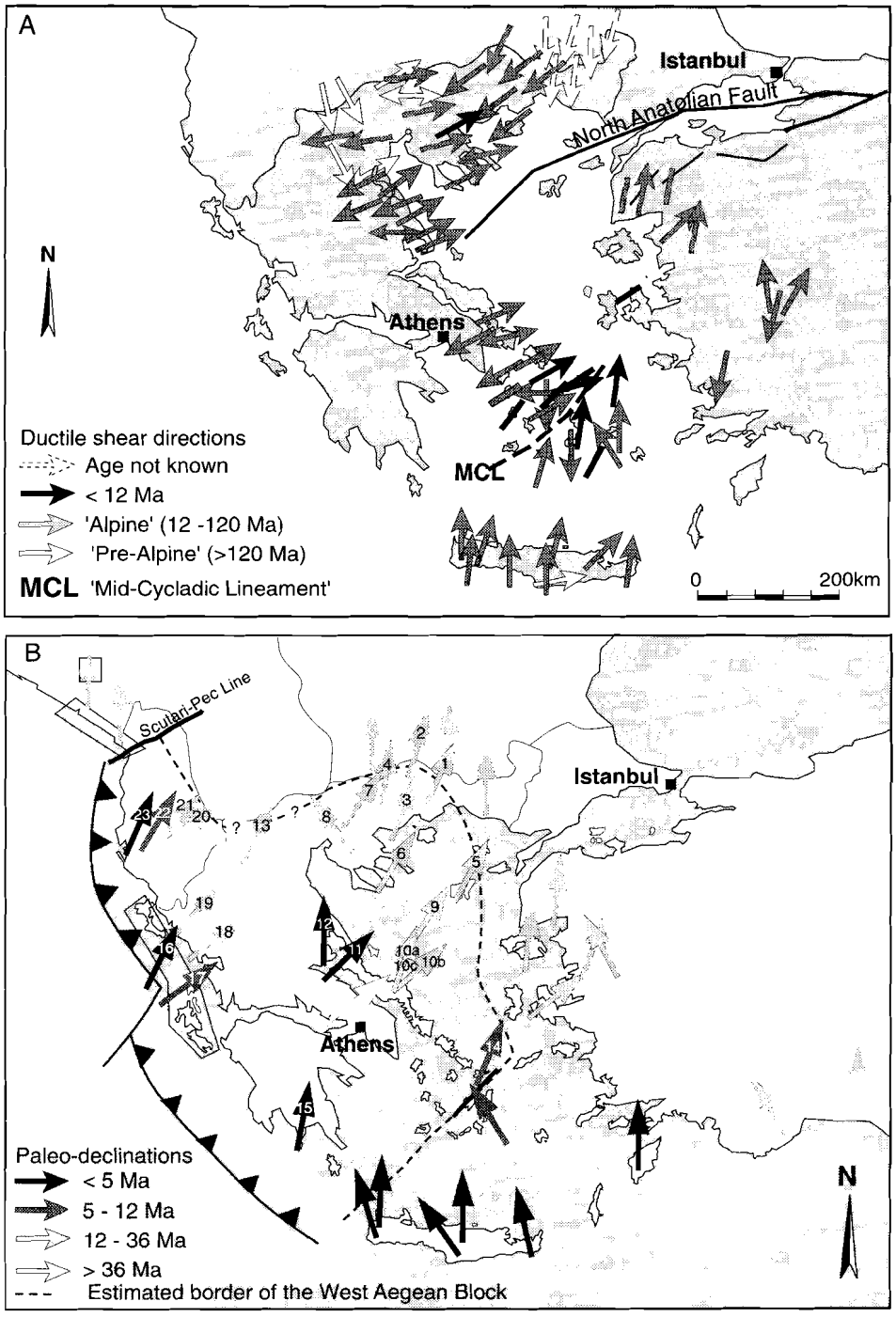
A
Istanbul
North Anatolian Fault
N
Athens
MCL
Ductile shear directions
Age not known
< 12 Ma
'Alpine' (12 -120 Ma)
'Pre-Alpine' (>120 Ma)
MCL 'Mid-Cycladic Lineament'
0
200km
B
Scutari-Pec Line
Istanbul
Athens
Paleo-declinations
< 5 Ma
5 - 12 Ma
12 - 36 Ma
> 36 Ma
Estimated border of the West Aegean Block
N

over a time span of 10's Ma, irrespective of the metamorphic conditions under which they were formed.

Towards the north and west Aegean, NE-SW trending shears of Tertiary age overprint *older* ductile shear zones that have top-to-the-SSE to S directions of shear (see Figures 5.04 and 5.07). Small areas (~10 km by 10 km) of Tertiary E-W trending lineations are observed in the north and west Aegean (e.g., Chalkidiki in Figure 5.07; west Paros in Figure 5.11, southern Syros in Figure 5.12). However, what is most striking is the otherwise consistently orientated NE-SW direction of shear in all lithologies deformed during the Tertiary, from as far east as the Rhodope (Figure 5.07), and as far south as the central Cycladic islands (Figure 5.14).

In contrast, lineations in the eastern Aegean typically trend N-S. A change of 50° in the orientation of Tertiary lineations occurs across a NE-SW trending zone that runs from the southwest to northeast across the Aegean (Figure 5.12) NE through the Central Cyclades (Figure 5.12). In view of the regional scale and relative abruptness of the boundary between the areas of NE-SW and N-S trending extension and shear directions, this zone of transition is termed the 'Mid-Cycladic Lineament'. The regional importance of this observation is discussed below using published paleomagnetic data (Section 5.4). Although samples for paleomagnetic analysis were collected from Paros, Mykonos and Tinos as part of this study, the data proved to be inconclusive. Fortunately, paleomagnetic data from Mykonos and Naxos (Morris and Anderson, 1996) were published during the course of this study.

5.4 Discussion

This discussion begins by comparing the orientations of stretching and mineral lineations with paleomagnetically determined declinations that developed during similar time periods (Figure 5.13a and b). The paleo-north indicators recorded by the declinations provide an important external reference frame with which to examine the orientation of the stretching and mineral lineations through time. This discussion demonstrates that the orientation of the stretching lineations across the whole Aegean is related to the degree of rotation that has occurred since the early to mid-Tertiary. The regional distribution of lineation orientations is then used to define the margins of the (clockwise) rotating block in the western Aegean more accurately than is possible from paleomagnetic declination data alone. It is suggested that this block probably ceased to rotate as a semi-coherent unit in the late-Miocene/early Pliocene, when it subdivided into two parts. The central Cycladic region is discussed first as this area is thought to contain the best record of pre-Pliocene kinematics (in particular the degree of

Figure 5.13

(a) Directions of ductile shear and stretching lineations within Aegean basement. The ages of structures were derived from Figure 5.03. Black arrows represent data from this thesis; grey arrows are published data. The data from central Greece and NW Turkey are from this study, other data are from Gautier (1995), Jolivet et al. (1996), Altherr et al. (1982), Dürr et al. (1978), Faure et al. (1991), Sfeikos et al. (1991), Kilias (1991), Schermer (1993), Brocker et al. (1993), Falalakis et al. (1995), Hetzel et al. (1995a,b), Dinter et al. (1995), and Burg et al. (1996),

(b) Paleomagnetic declinations of Tertiary rocks in the Aegean. The Scutari-Pec Lineament and a fault in the southern Aegean mark the boundaries of an area of predominantly clockwise rotation. The numbers represent the location of declinations plotted in Figure 5.16. Paleomagnetic data are primarily from Kissel and Laj (1986, 1988), but also from Atzemoglu et al. (1994), Speranza et al. (1995), Morris (1995), Morris and Anderson (1996) and Duermeijer et al. (1998).

relative rotation). The area examined is then extended to determine the Aegean-wide pattern of pre to post Pliocene kinematics. Finally, the mechanisms by which the west and east Aegean may have accommodated strain during rotation are discussed, and a chronological kinematic model summarizing the results is presented.

5.4.1 Comparison of the orientation of paleomagnetic declinations with stretching lineations: definition of the West Aegean Block

Stretching lineations and the sense of ductile shear can be used as passive markers (given the assumptions outlined in Section 5.2.3) to document regional kinematics only when the orientation is known relative to an external reference frame at the time of formation. Such a

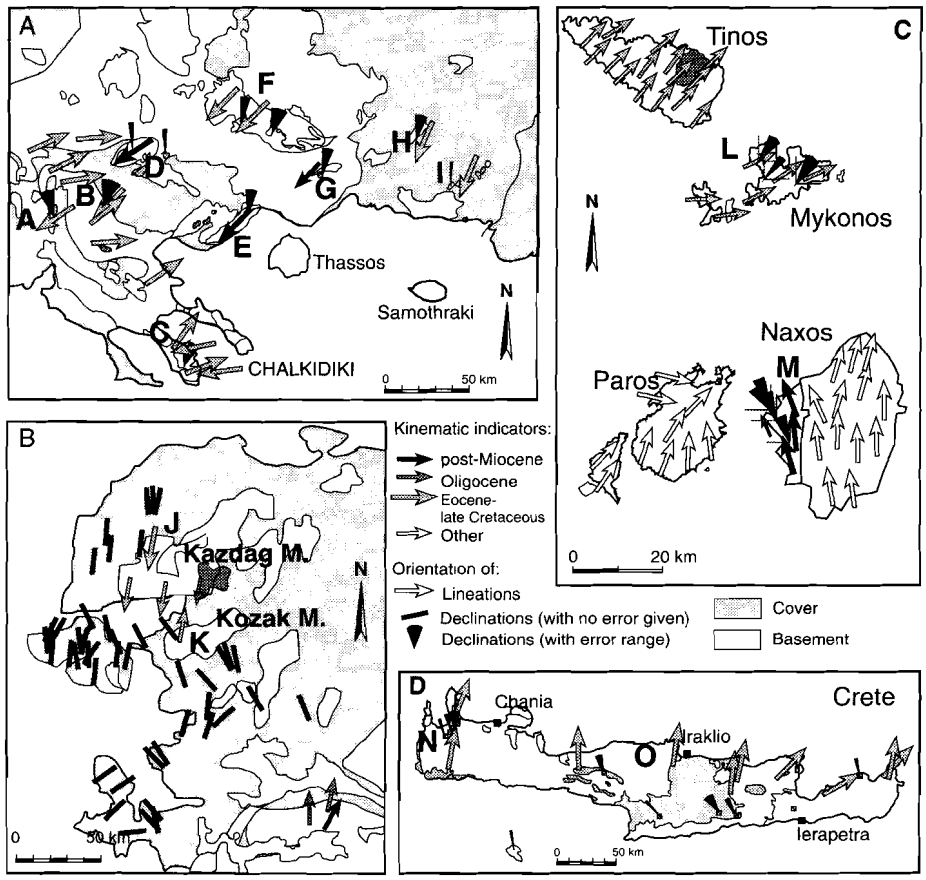

Figure 5.14: Detailed paleomagnetic data from the north Aegean (a), east Aegean (b), and central Aegean (c), and Crete (d) show the relationships between paleomagnetic declinations and ductile kinematic indicators. The declinations in all regions are rotated clockwise from the average stretching direction determined from mineral and stretching lineations. Locations of paleomagnetic data used in Table 5.01 are depicted with a letter. Data are from Atzemoglu et al. (1994), Kissel and Laj (1988) and Morris and Anderson (1996). For orientations of lineations data see references in captions of Figure 5.13.

reference frame can be obtained by examining the relationship between these markers and paleomagnetic declinations of a similar time range. Such a comparison can be made for pre and post mid Miocene declinations and stretching lineations/sense of shear directions (henceforth referred to simply as lineations) (see Figures 5.13a and b). The area in which the lineations trend NE-SW coincides with the area which has undergone some degree of clockwise rotation as determined from the paleomagnetic data (Figure 5.13a and b). Similarly, the area in which the lineations trend N-S has undergone complex (possibly anticlockwise) rotation (right hand side of both Figure 5.13a and b). Thus, the Scutari-Pec Line and the Mid-Cycladic Lineament appear to define northwest and southeast margins, respectively, of the same block, which for simplicity is called the West Aegean Block. The rotation of the West Aegean Block caused initially parallel lineations to diverge. The presence of a clockwise rotating block in the vicinity of the NW Aegean has been proposed by several workers (Kissel and Speranza 1995; Le Pichon et al. 1995; Speranza et al. 1995; Morris and Anderson 1996). However, the incorporation of data presented in this thesis (Section 5.3.2) with previously published data from the north and south Aegean (Figure 5.13a and b) allows the deformational history of the block and the nature of its margins to be determined more precisely than was previously possible from paleomagnetic data alone.

The Scutari-Pec Line has previously been identified as the sharply defined northwestern margin of the clockwise rotating block (Kissel and Speranza 1995; Speranza et al. 1995). The outer (western) margin of the West Aegean Block appears to coincide with the plate boundary, whereas the inner (northeastern) margin is much more diffuse (Figure 5.13a and b). Both paleomagnetic and declination data suggest that the inner margin, which is in the 'lee' of the rotating block, is a gradational boundary occurring over a distance of ~50 kilometers.

The southeastern margin is delineated by the Mid-Cycladic Lineament (MCL). The apparent abruptness of the MCL *on the scale of the Cyclades region*, is one of the more striking aspects of the West Aegean Block and suggests that this margin is a discrete shear zone or fault. A major NE-SW trending fault in the northern Cyclades has been interpreted to mark the boundary between the eastern and western Aegean (Figure 5.12; Morris and Anderson 1996). Although the lineament may coincide with this fault in the northern Cyclades, the change in stretching lineation orientations across island of Paros suggests that the MCL diverges from this fault in the southern Cyclades and crosses Paros itself (Figure 5.12). A boundary on the island of Paros between the two orientations of lineations (the 'Paros detachment fault') has been noted recently by Lister and Forster (1996)(Figure 5.11). Unlike Lister and Forster (1996) who interpret the structure as one of the earlier 'detachments' on the island, this study suggests that the fault may represent, in part, a structure which helped accommodate the rotation of the West Aegean Block. Clearly, more detailed paleomagnetic and geochronological data are required from this region to determine the relationship between this fault and the MCL.

5.4.2 Active deformation and the Mid-Cycladic Lineament (MCL)

Despite the abruptness of the MCL, there is little documented seismic activity in the vicinity (Figure 2.09b). In fact, the whole Cycladic region is most noted for its aseismic behaviour (Jackson and McKenzie 1988a). This suggests that while the MCL has clearly played an important role in the past, it may no longer be active.

Greenschist facies stretching lineations within the West Aegean Block are at right angles to NW-SE trending normal faults. These normal faults are thought to have accommodated the bulk of extension in the region (Gautier and Brun 1994). It is well documented that from

Rotation of the **West Aegean** (clockwise)	Rotation of the **East Aegean** (anticlockwise)	**Relative Rotation**	Reference
25° (0-12 Ma) 25° (>12 Ma)	30° (> 12 Ma)	25°: 0-12 Ma 55°: >12 Ma	Kissel and Laj (1988)
25° (0-5 Ma) 30° (12-30 Ma)	0° (0-12 Ma)	25° (0-12 Ma)	Kissel et al. (1986)
22° (0-12 Ma)	33° (0-12 Ma)	55° (0-12 Ma)	Morris and Anderson (1996)
NWM: 10-15° (0-3 Ma) 30° (3-25 Ma)	SM: ~15 Ma* 19° (3-25 Ma)	~30° (0-~3 Ma) 49° (~3-~25 Ma)	This study

Table 5.1
Estimates of the average total rotation for the western and eastern Aegean region. NWM: northwest margin of Central Aegean Block; SM: southern margin (see text for discussion).

Loc		Lith.	Age (Ma)	Trend of L.dec*	α95	Trend of L.kin	Difference in angle (L.kin-L.dec)	L.dec Ref
A	Kilkis	Vol.	23-28	*-031*	19	48	-	1
B	Metalliko	Vol.	Eo: 36-54	039	19	58	019	1
C	Chalkidiki	Plut.	30-40	037	9	60	023	1
D	Strymon	Plut.	28	*-002*	7	58	-	1
D	Vrondou	Plut.	29-33	011	-	58	047	1
E	Kavala	Plut.	18	024	11	058	034	1
F	Elatia	Vol.	Olig: 24-36	014	12	025	021	1
F	Zagradenia	Vol.	Olig: 24-36	032	-	045	013	1
G	Xanthi	Plut.	28	028	10	048	020	1
H	Leptokarya	Plut.	23-35	023	5	025	002	1
I	Thrace	Vol-Plut	33	007	7	025	018	2
J	Kazdag	Vol	?	000		000	000	2
K	Kozak	Vol	?	-028		010	038	2
L	Mykonos	Plut	14	034		064	030	3
M	Naxos	Plut	12	-032		348	020	3
N	W. Crete	Sed.	6-10	-012		004	016	4
O	Central Crete	Sed.	6-10	-034		004	038	4

Table 5.2
Table showing the trends of paleomagnetic declination (L.dec) and kinematic direction (L.kin) from areas in which both data are available. *Declinations are relative to Africa, and 95% confidence intervals are given in column a95. See Figure 5.14 for locations of sites (indicated by letters A to M). Lithologies (Lith.) consist of volcanic (Vol.) and plutonic (Plut.) rocks. Data in italics have been interpreted as the result of localised block rotation or remagnetisation (see Kondopoulou et al. 1996) and hence are ignored. The data from eastern Crete are also not used as the lineations in this area do not show a consistent trend (see Figure 5.10b). Data are obtained from references (1) = Atzemoglu et al. (1994), (2) = Kissel and Laj (1988), (3) = Morris and Anderson (1996) and (4) Duermeijer et al. (1998).

Pliocene times the NW-SE structural trend of the West Aegean Block started to be overprinted by WNW-ESE trending grabens (see Chapter 3; Roberts and Jackson 1991; Caputo and Pavlides 1993), which are now concentrated around the northern rim of the aseismic central Cycladic region. The widespread development of WNW-ESE trending basins since the Pliocene is interpreted here to be the period in which the MCL ceased to be a regionally important kinematic structure.

Active displacement GPS data from the western and central Cyclades show little east-west variation in displacement rates relative to Europe (Figure 3 in Le Pichon et al. 1995). This lack of variation suggests that the central Cyclades may be responding to currently active deformation as a relatively coherent block, particularly when compared to the margins of the aseismic zone which are extending in a N-S direction (Figure 2.09). It is hypothesized that the currently *aseismic* central Cycladic region has behaved, and is behaving, as a coherent block (termed the Central Aegean Block) since the late Miocene/early Pliocene.

Thus, the observations and interpretations made in this study support the suggestion of Le Pichon et al. (1995) that a major change in the kinematics of central and western Aegean occurred in the Pliocene. In addition, it has been shown that: (1) the boundary between zones of opposing rotation (the MCL) is a sharp, linear feature and not a gradational feature; (2) the

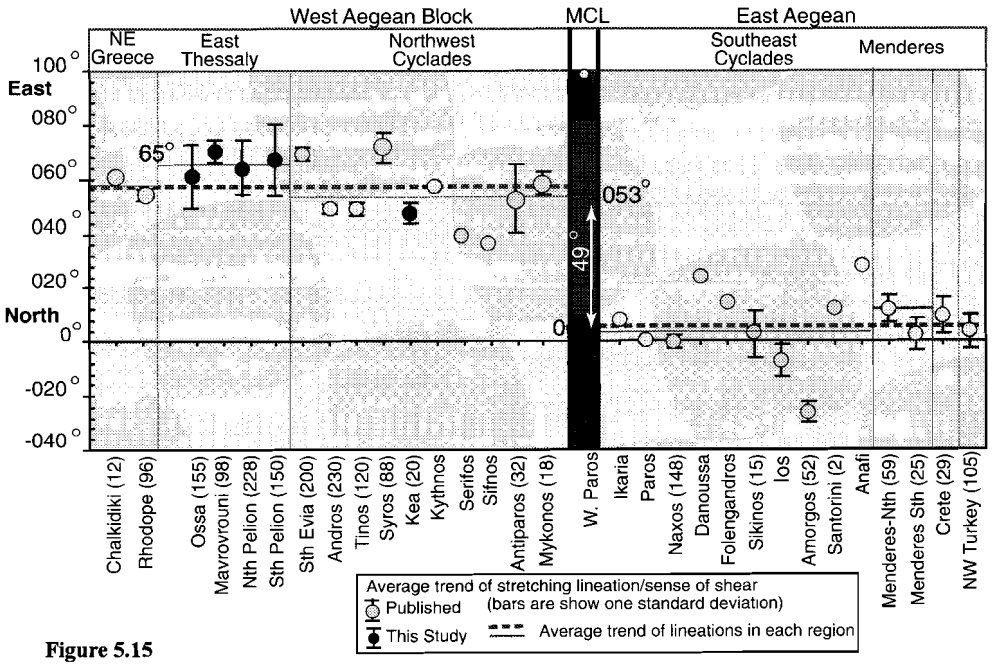

Figure 5.15

A figure of the mean ductile syn- to post Alpine lineation and shear directions from locations west and east of the Mid-Cycladic Lineament. The difference in the mean orientation of lineation/shear directions of northwestern and southeastern Cyclades is ~49°. The number in brackets refers to the number of data points. Published data are derived from maps depicting regional detailed lineation/shear directions published by primarily Gautier (1995), but also include data from Dürr et al. (1978), Sowa (1985), Dinter and Royden (1993), Faure et al. (1991), Brocker et al. (1993), Fassoulas et al. (1994), Bozkurt et al. (1994), Falalakis et al. (1995), Jolivet et al. (1994a), Hetzel et al. (1995a,b), Dinter et al. (1995) and Burg et al. (1996).

MCL does not totally coincide with a fault observed in the Cyclades as was previously supposed by Morris and Anderson (1996); and (3) the location of the MCL does not coincide with a small circle that best fits the North Anatolian Fault scarp and the western extremity of Crete (see Figure 5.01), as has been previously suggested by Le Pichon et al. (1995).

5.4.3 Constraints on Aegean pre-late Miocene/early Pliocene kinematics

Published estimates of the amount of finite rotation of the west Aegean relative to the east Aegean vary widely (Table 5.1). Morris and Anderson (1996) found that the SE Cycladic region underwent 50% more rotation than the NW Cycladic region (part of the West Aegean Block), whereas, during the same time range Kissel et al. (1986) suggest that only the western Aegean rotated (30°).

An important unanswered question is, how much absolute rotation did each block undergo before and after the cessation of activity across the MCL? To answer this question, the orientation of pre-Miocene lineations and declinations (from areas in which both data are available) are compared in order to estimate the initial orientation of the lineations (Table 5.2). Although the amount of paleomagnetic data available for such a comparison is, as yet, limited, the angle between the declinations and lineations is ~23° with a 95% confidence of the mean of 7° (Table 5.2, second to last column).

From the data presented in Table 5.2, it is assumed that, on a regional scale, the lineations were orientated NNE (~023°) relative to paleo-north when rotation started to occur. This assumption can now be used to determine the amount of pre-Pliocene rotation that occurred in the Cycladic region.

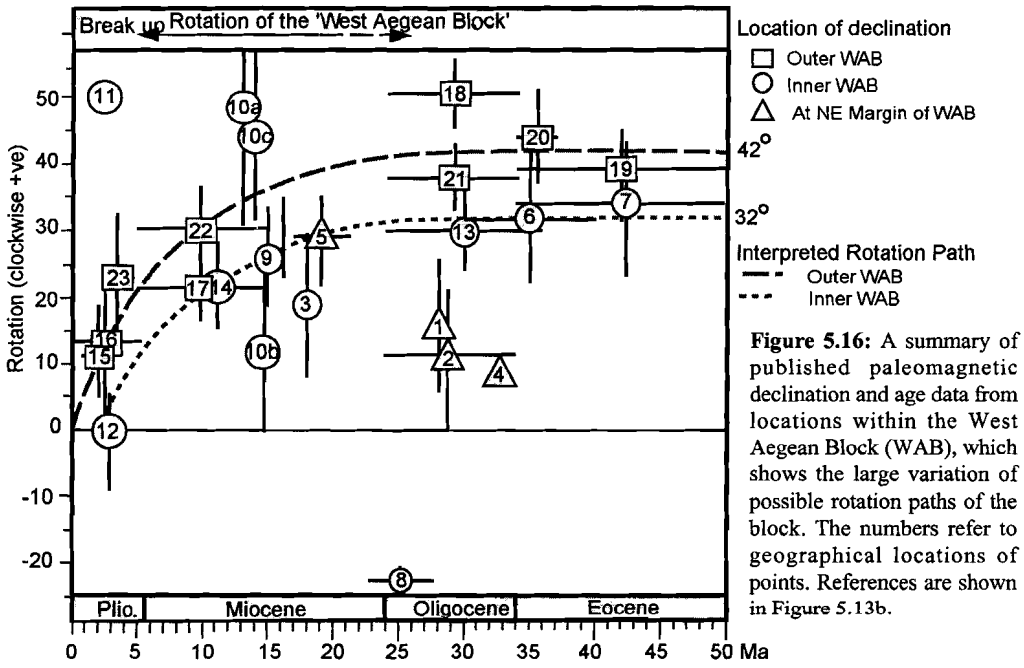

Figure 5.16: A summary of published paleomagnetic declination and age data from locations within the West Aegean Block (WAB), which shows the large variation of possible rotation paths of the block. The numbers refer to geographical locations of points. References are shown in Figure 5.13b.

First, the average orientation of lineations and kinematic directions in the Cycladic region is calculated (this is assumed to represent the paleo-extension direction of the region). The mean orientation of Tertiary lineations is determined by first calculating the mean orientation of areas with the approximate size of crustal blocks (~30 km by ~ 30 km) from published maps, then averaging the mean of 3 approximately equal sized areas (Figure 5.17).

The average paleo-extension direction of the NW Cycladic region calculated by this method is 053°. This suggests the lineations in this region must have rotated ~30° clockwise on average during activity on the MCL, to arrive at their present position. This observation is remarkably similar to the 32° clockwise rotation determined from the estimate of the best fit age-rotation curve of the inner portion of the West Aegean Block (see Figure 5.13). To accommodate the estimated 49° differential rotation observed across the MCL (see Figure 5.13), the southeast Cycladic region must therefore have rotated an equivalent of ~19° anticlockwise. Thus, it appears that the northwest Attic-Cycladic belt underwent almost twice the amount of rotation as the southeast Cycladic region prior to the Pre-Pliocene. Note, however, that these calculations represent true rotations only if there has been no block rotation of the central Cycladic region since cessation of activity across the MCL in late Miocene/pre-Pliocene.

The estimate of 19° degrees anticlockwise rotation of the eastern Cyclades region is significantly less than the 30-33° anticlockwise rotation inferred by other workers (Table 5.1). A 33° anticlockwise rotation (i.e., 14° more than the estimate) was calculated from samples taken from an intrusive body on western Naxos island (shown in Figure 5.16). The orientation of lineations in this intrusive are orientated ~12° anticlockwise of lineations in eastern Naxos, as well as the regional average (Figure 5.16: Gautier 1995). This suggests that the extra anticlockwise rotation apparent on western Naxos may be partly due to localised rotation, and therefore does not reflect a regional average. Paleomagnetic declinations elsewhere in the eastern Aegean also show a wide variation in orientation (Figure 5.12). Hence, the east Aegean region is interpreted to have behaved less coherently, on a small scale, than the west Aegean.

5.4.4 Aegean post early-Pliocene/late Miocene kinematics

By assuming that lineations were initially parallel, and by comparing lineations and declinations from areas outside of the Cycladic region, a constraint can be placed on the amount of relative rotation that may have occurred post latest Miocene/early Pliocene.

During the latest Miocene to the present, different sections of the West Aegean Block appear to have undergone differing degrees of rotation. That is, the smoothed best fit age-rotation curve for the outer or northwestern margin of the West Aegean Block (shown as squares, Figure 5.16) indicates, on average, ~10° more clockwise rotation compared to the inner West Aegean Block (shown as circles, Figure 5.16). Furthermore, the northern portion of the West Aegean Block appears to have also undergone slightly more clockwise rotation than the southern (Cycladic) portion of the block, as lineations of the Thessaly region are orientated slightly clockwise (~12°, Figure 5.15) of the lineations in the northwestern Cyclades.

Two end-member scenarios could account for the 10-15° discrepancy observed between the trend of lineations and declinations from the northern (Chalkidiki/Rhodope), northwestern (Thessaly/west Greece) and southeastern (NW Cyclades) portions of the West Aegean Block. Each scenario requires breakup of the West Aegean Block in the late Miocene/early Pliocene, and the assembly of a Central Aegean Block (see Figure 5.02a), the currently aseismic area. In the first scenario, the Central Aegean Block (coupled to Crete and western Anatolia) rotates

~10-15° anticlockwise relative to an irrotational mainland Greece. In the second scenario, NW Greece rotates ~10-15° clockwise relative to a largely irrotational, but SW translating, Central Aegean Block. These options, and an intermediate scenario, are discussed below.

The first end-member option requires that the outer margin of the Aegean, e.g., the region around the Kephalonia fault (Figure 5.01), remains relatively irrotational. This is in direct contrast to a paleomagnetic study of the region by Kissel et al. (1996), who calculated significant rotation in the last 5 Ma (Table 5.1). Hence, this scenario is unlikely.

The second end-member option involves no rotation of the Central Aegean Block. Thus in this scenario, the relative rotations calculated for this region would represent absolute rotations. Using these values, one would expect the lineations of the east Aegean region, to have rotated 19° anticlockwise from the NNE (023°) and therefore be in a N-S position (004°) today. This is indeed the case (Figure 5.15), and therefore this option is apparently feasible. Most studies of active tectonics suggest that some degree of anticlockwise rotation of the eastern Aegean has occurred, however data supporting such an interpretation is, at present, inconclusive (see Figure 5.13b).

An intermediate option remains possible, which requires the amount of relative rotation to be partitioned between the NW Greece region and the Central Aegean Block, as in the model of Le Pichon et al. (1995). In this case, the NW Greece region would have undergone slightly more clockwise rotation and the Central Aegean Block slightly less anticlockwise rotation, prior to the late Miocene, than was estimated above. Until post to late Miocene/early Pliocene regional anticlockwise rotation of the east Aegean has been unequivocally established, the second end-member option is favoured as this is the simplest model that fits all the regional data.

5.4.5 Role of the Mid-Cycladic Lineament during pre-late Miocene/early Pliocene extension

Few data are available to demonstrate offset along the Mid-Cycladic Lineament (MCL). Rocks of similar age, composition and uplift histories occur on both sides of the lineament (Gautier and Brun 1994). However, a recent study of the crustal thickness of the Aegean shows that there is up to 15 km difference in the depth of the Moho between the northwest and southern Cyclades across a northeast trending slope in the vicinity of the MCL (Figure 2.08). Although this suggests that the MCL may have functioned as a normal fault, the MCL is orientated parallel to, not at right angles to, the inferred extension direction. Thus, it is more likely that the MCL has primarily acted at a dislocation zone, with thinning localised along the NW-SE trending faults/ shear zones identified in the northwestern Cyclades (Figure 5.12: Gautier 1995), and with some, but significantly less, extension of the southeastern Cyclades along ENE-WSW trending shear zones. In this scenario, the relative rotation of either side of the lineament is interpreted to be the result of a decreasing shear gradient away from the MCL. Bourne et al. (1998) recently demonstrated that the movement of coupled crustal blocks act in response to drag on the base of the blocks by the relatively strong, ductiley deforming lithosphere. The movement of the West Aegean Block is interpreted as an assemblage of smaller blocks which have deformed in response to a *lateral* shear gradient in the lithosphere, and that the maximum displacement occurs in the vicinity of the Mid-Cycladic Lineament. Thus, there may be virtually no relative horizontal displacement between two points which span the lineament, despite the large absolute translation of both points and the relative rotation of the blocks on

either side when viewed from an external reference frame (e.g. relative to Eurasia). Hence, the lineament has many of the geometrical characteristics of an oceanic transform fault.

5.4.6 Mechanism of regional rotation

Deformation of the West Aegean Block is thought to have occurred largely along pre-existing, subduction zone-parallel, northeast-dipping faults which sole into a ductile detachment (Gautier and Brun 1994). These faults are interpreted to mark the margins of small crustal scale (~30 km wide) sub-blocks. Although local variations in declination and lineation orientations (Figures 5.15 and Figure 5.16) in the West Aegean Block may partially be due to errors or corrections in the data or of local heterogeneities, the variations may also represent different amounts of rotation and regional strain that was locally accommodated on each internal fault that marks the boundary of these small sub-blocks. This would in turn imply that regional rotation of the West Aegean Block was not a smooth or continuous process on a small scale. It may also explain why there is little evidence that the lull in rotation between 5 and 12 Ma reported in the NW Aegean (Kissel et al. 1996) was of regional significance (Figure 5.18).

In the broken slat model (see Figure 5.02b), favoured by Morris and Anderson (1996) to explain the relative rotation of Naxos and Mykonos, the rotational and subduction zone-normal strain is distributed evenly along faults between the blocks. The study of lineation orientations from the Thessalian region presented in this thesis (Section 5.3.2) suggests there is little evidence for significant changes in the orientation of ductile to semi-ductile extension through time (Figure 5.05). The presence of submarine strike-slip faults in the Cyclades (Figure 5.12), and the consistent orientation of stretching lineations both in the northeast and southeast sections of the West Aegean Block (Figure 5.13a), suggest that the rotational component of the regional strain field may have been discretely partitioned along small, cross-cutting, strike-slip faults (e.g. Figure 4 of Gautier and Brun 1994), as well as along the MCL. Thus, it is suggested that the West Aegean Block comprises a coupled assembly of smaller units which have individually accommodated varying degrees of internal translational and rotational strain while the block itself rotated as an overall entity. The bulk rotation of the West Aegean Block since the late Miocene/early Pliocene is interpreted to be the result of pinning and shortening of the northwest margin whilst the southeast Aegean underwent extension (Figure 5.17b).

5.4.7 Thermal evolution of the region.

A number of syn-extensional plutons, which have developed strong stretching and mineral lineations, crop out in the vicinity of the MCL. These plutons are ~14-9 Ma old (Andriessen et al. 1987; Bröcker et al. 1993) and exhibit lineations with orientations parallel to those observed in the surrounding metamorphic rocks. The granodiorite of Mykonos, which is located within the West Aegean Block, has an uncorrected declination of 30° (i.e. similar to the amount of rotation of the West Aegean Block estimated in this study). After rotation of 27° about a NW-SE (165°) trending fault, i.e. a horizontal axis, Morris and Anderson (1996) estimated that the Mykonos granodiorite rotated only 22° clockwise about a vertical axis since its intrusion. This rotation is less than that observed elsewhere in the inner and outer West Aegean Block (Figure 5.16) and suggests either that a small amount of clockwise rotation (estimated here to be ~8°) may have already occurred within the West Aegean Block prior to the emplacement of the granodiorite, or that there has been no rotation about a horizontal axis and the declinations represent true rotations. In either case, the MCL probably formed prior to 14 Ma.

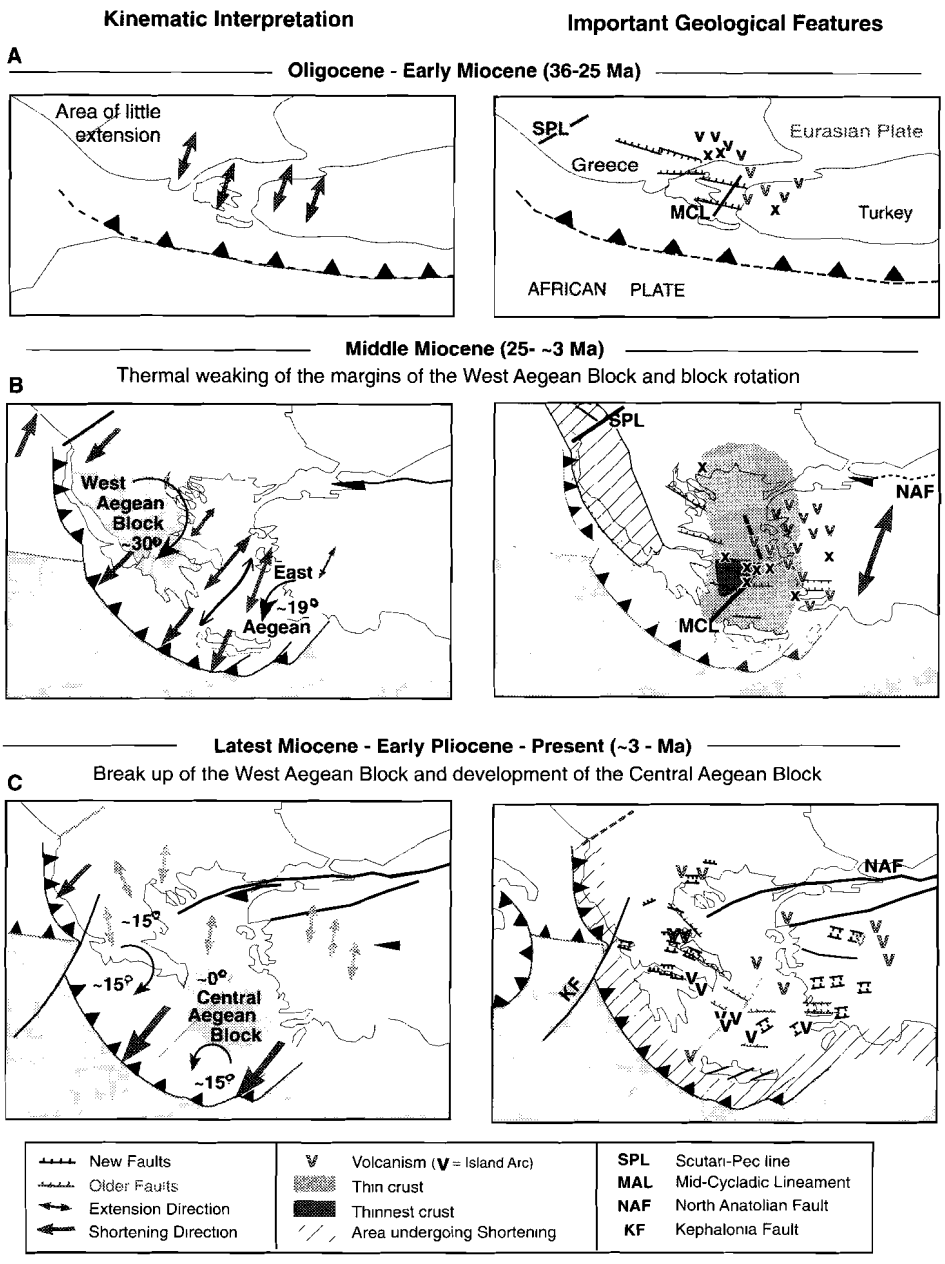

Figure 5.17: A schematic scenario for the evolution of regional extension in the Aegean:
(a) Regional extension trending ~023° initiated in the Oligocene-early Miocene (~35-22 Ma);
(b) Extension took place in the central Aegean whilst the NW Aegean underwent shortening. The resultant coupling forced the west Aegean to rotate 30° clockwise. The semi-coherent block rotation was aided by thermal weakening of the inner margins and the pre-existing zones of weakness near the Mid-Cycladic

Note that the igneous intrusions were emplaced during the final stages of a mid-Tertiary thermal pulse, which is also represented by volcanic extrusives (Figure 2.10: Pe-Piper and Piper 1989) and widespread metamorphism (see Figure 5.03 and references therein). The thermal pulse affected much of the eastern and northern Aegean but only affected the corresponding margins of West Aegean Block. The thermal event, therefore, may have been a factor in defining the MCL as the western boundary of the crust which was weakened prior to and during rotation. In contrast, the interior of the West Aegean Block remained relatively cold, and therefore strong, which enabled it to rotate as a semi-coherent body.

5.4.8 Kinematic scenario for late-orogenic extension of the Aegean

Regional extension in an initially ~023° direction (Figure 5.17a) began in the late Oligocene/ early Miocene. During the mid-Tertiary, this was associated with initiation of the MCL and a thermal pulse (which caused the Oligocene to early Miocene volcanism: Figure 2.10 and 5.03) in the eastern Aegean which weakened the crust in that region.

Stage two began shortly after with subdivision of the crust forming the West Aegean Block which was bound on its northwestern and southeastern margins by the Scutari-Pec Line and Mid-Cycladic Lineaments respectively. Between 25 Ma and ~3 Ma the West Aegean Block underwent ~30° clockwise rotation while the east Aegean (assemblage) underwent an average of ~19° anticlockwise rotation in a much less coherent manner. As the crust thinned and the (now) NW-SE trending faults rotated, the thermal front migrated southwestwards causing onset of volcanism in Thessaly in the Pliocene (Figure 5.03). Contemporaneously, E-W faults began to cross-cut older NW-SE trending faults (see chapter 4). During this time, the Mid-Cycladic Lineament ceased activity. The southeastern portion (NW Cycladic area) coupled with the SW Cycladic area to form the 'Central Aegean Block' and began to translate SW. Areas around the northwestern (and possibly the southern) margins of the Central Aegean Block continued to rotate a further 10° clockwise in the Pliocene.

5.5 Conclusions

1. On a local (1-100 km) scale the *mean* orientation of late to mid Alpine, ductile stretching lineations and their associated directions of ductile shear is constant, irrespective of the age and metamorphic conditions under which they were formed.
2. Stretching lineations, in association with senses of ductile shear, help define the margins of the clockwise rotating portion of the Aegean which is referred to here as the 'West Aegean Block'. The block is bounded by the (previously identified) Scutari-Pec line to the northwest,

---

and Scutari-Pec Lineaments. The Mid-Cycladic Lineament acted as a continental fracture zone (see text for discussion) which extended in length as it accommodated the rotation of the West Aegean Block. The east Aegean region rotated ~19° anticlockwise during this period although in a less coherent manner than the west Aegean;

(c) About 3 Ma ago, the West Aegean Block rotated to such a position that it was more mechanically favourable to form new WNW-ESE trending grabens than to continue reactivating pre-existing structures. These grabens resulted in: (1) the cessation of activity along the Mid-Cycladic Lineament, and (2) the splitting of the West Aegean Block into two portions. The SE portion coupled with a SW portion of the East Aegean Block to form the Central Aegean Block. The margins of the Central Aegean Block are diffusely marked by E-W trending normal faults. As this block translated SSW, its margins rotated away from the block. The geological features associated with each of these events are discussed in the text.

by the subduction zone to the west and by the Mid-Cycladic Lineament to the southeast. The border to the east is gradational and located in the northern Rhodope/northern Aegean sea region.

3. The Mid-Cycladic Lineament is parallel to, but does not coincide with a NE-SW trending fault. Furthermore, the lineament does not coincide with a small circle which best fits the northern trace of the North Anatolia Fault. Both of the small circle and the NE-SW trending fault have been suggested previously to be the boundary between the rotating portions of the Aegean.
4. The Mid-Cycladic Lineament ceased activity in the latest Miocene/early Pliocene.
5. The Tertiary kinematic evolution of the Aegean was not dominated by any single event but involved three stages:
   i. Initial uniform NNE (023°) directed shear over the whole region.
   ii. Between the Oligocene and late Miocene, the crust subdivided into two parts: The western part formed the West Aegean Block which rotated ~30° clockwise, whereas the eastern portion (loosely termed the East Aegean block) contemporaneously rotated ~19° anticlockwise. Thus, both sides of the Aegean underwent similar magnitude of rotation but in opposite senses.
   iii. After the latest Miocene/early Pliocene, the newly developed E-W trending faults caused the West Aegean Block to subdivide into two portions. The southeastern portion (NW Cycladic area) coupled with the SW Cycladic area to form the Central Aegean Block which began to translate coherently to the SW. The NW margin and possibly the Thessaly region continued to rotate ~10° clockwise.
6. Rotation of the West Aegean Block was aided by thermal weakening of its northeastern and southern margins, in conjunction with the pre-existing Scutari-Pec Line and Mid-Cycladic Lineament. Both lineaments are interpreted to be lines of weakness.
7. After a small (~8°) amount of rotation of the West Aegean Block granitoids started to intrude close to the Mid-Cycladic Lineament.
8. Both the West Aegean Block and the Central Aegean Block are comprised of second order rigid sub-blocks (~30 km in diameter).
9. The outward bending of the Aegean Arc during regional extension of the Aegean hinterland has not occurred by radial outward flow of the crust, or by the rotation of a single block, but by successive partitioning of rotational strain on an intermediate to large (100 km) length scale.

Chapter 6: Discussion and Future Work

6.1 Introduction

In the course of this thesis a detailed lithological, metamorphic and structural examination of the Thessaly region in north-central Greece was carried out (Chapters 3 and 4). It was shown that the basement of Thessaly preserves structural and metamorphic events that span the entire temporal range of the Alpine Orogeny (Figure 6.01). Structures related to late orogenic extension of the Thessaly region were then compared to structures in similarly deformed basement elsewhere in the Aegean to determine kinematic constraints on Aegean post-orogenic dynamics (Chapter 5).

The purpose of this chapter is to discuss how the structural, metamorphic and kinematic results presented in Chapters 3 to 5 constrain dynamic models of Aegean evolution summarised in Chapter 2. Firstly, the relationship between the metamorphic and structural evolution of Thessaly and that of the rest of the Aegean is summarised and discussed (further to the discussion in Chapter 5: Section 6.2). Secondly, the role of the West Aegean Block (of which the Thessaly basement forms a major part) is examined in terms of Mediterranean-scale kinematics. Possible causes for the onset of block rotation and late to post-orogenic extension are examined (Section 6.3).

6.2 Relating kinematic structures across Thessaly and the Aegean

Across the northern boundary of the Aegean and over a distance of ~400 km, lower Cretaceous shear zones have broadly N-S stretching lineations (i.e. the D1 event of the Thessaly region) with a similar top-to-the-S sense of thrusting (e.g. Figure 6.01 and 5.15a: Burg et al.

orientation of shear directions	M1.amph 135-100 Ma	Pre M2.gns	M2.gns 120-80 Ma	M2.bls 80-36 Ma	M3.gns <36 Ma	Semi-ductile < 25 Ma	Brittle < 25 Ma
D1: NNW->SSE	to SSE (thrusting)						
D2: E-W			to E extension?	to W			
D3: NE->SW			to SW (thrusting)	to SW			
D4: NE<->SW					SW & NE (extension)	SW & NE	
D5: NE<->SW							SW & NE (extension)
D6: NNE<->SSW							NNE & SSW (thrusting)

Table 6.1
A summary of the relationship between the metamorphic and deformation events determined in Thessaly region. The direction in each box indicates the sense of shear.

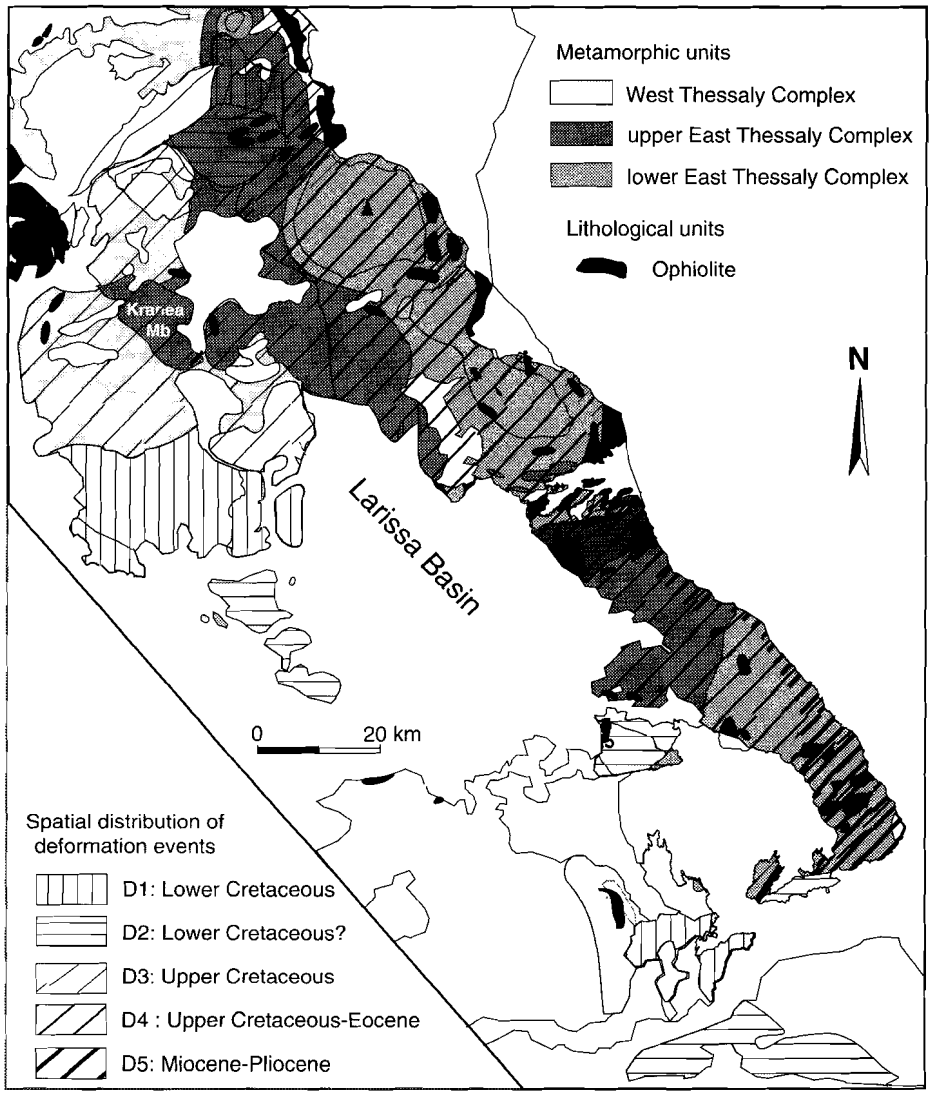

Figure 6.01
A summary of the distribution of deformation events and metamorphic units of the Thessaly area, northern Greece defined in this thesis. The deformation event D6 involved region wide development of ~E-W trending faults (see Table 6.1). Also shown is the location of ophiolite units. The distribution of ultramafics in all metamorphic units is one of the key indicators of tectonic mixing in the region. The most intensely mixed unit is the lower East Thessaly Complex. The age decrease, and intensity of deformation increases, towards the southeast of Thessaly. Note that the many of the boundaries between major metamorphic units and areas affected by the different deformation events do not appear to coincide, this is due to the fact that most of the major Alpine deformation events in the Thessaly region synchronously affected different structural levels (represented here by metamorphic facies).

1990). In the west, lineations trend NNW-SSE (Figure 5.04), whereas in the Rhodope lineations trend broadly NNE-SSW (Figure 5.07). The timing of these shear zones suggests that they developed during the first regionally important tectonic event.

During the lower Cretaceous, Africa was not converging, but was moving left laterally, with respect to Eurasia (Figure 2.01). Thus, this (D1) deformation event may have been caused by the indentation of a small plate unrelated to the African Plate, for example a Pelagonian microcontinent. In this case the Vardar Zone would represent the suture zone between the two plates. The orientation of the D1 stretching lineations is subparallel to the trend of the Africa-Eurasia suture zone. Hence, differential interplate shortening would have had to be associated with a transform fault. The orientation of this fault may not be much different from the present orientation, as clockwise rotation of the region affected by N-S trending lineations has been determined from paleomagentic declination studies (Edel et al. 1992).

Within the area of NE-SW trending lineations there are small areas of E-W trending lineations (e.g. Figure 5.07 and 5.12). The age of the E-W trending lineations varies greatly. In the Thessaly region, available geochronological data suggest that the E-W (D2) lineations may be early Cretaceous in age (Chapter 3). In many areas, however, e.g. on the Chalkidiki Peninsula in the northern Aegean near the North Anatolian Fault (Figure 5.07) and in Syros which lies near the Mid-Cycladic Lineament (Figure 5.12), lineations of this orientation are of late Tertiary age. This suggests that the E-W trending lineations developed throughout the Alpine evolution. As shear zones of both the E-W and the NE-SW trending lineations have similar trends, the two events are unlikely to have developed coevally as a result of strain partioning (e.g. as strike-slip shear zones associated with neighbouring extensional shear zones). Therefore, areas exhibiting E-W trending lineations may represent localised, small scale block rotation within the overall clockwise rotation of the West Aegean Block, probably as the result of small scale strike-slip shear zones.

The N-S kinematic direction appears to have been broadly maintained in the Anatolian region from the Cretaceous until the present. Active normal faulting in the region (Figure 2.09b) exhibits approximately the same direction (but not sense of shear) as the ductile structures in this region (Hetzel et al., 1996). The change in the sense of shear is interpreted to be the result of a change from thrusting to extensional tectonics in the Oligocene. Out of all regions identified in this thesis only the West Aegean Block has undergone a significant change in kinematic deformation since the Cretaceous. The first kinematic change in that region occurred in the mid Miocene when the west Aegean Block started to rotated clockwise, the second in the Pliocene when the West Aegean Block became partioned into two parts (Chapters 3 and 5).

West Aegean Block: Strain components in the vertical plane

Unlike the Menderes Massif in the eastern Aegean which has undergone symmetrically distributed senses of extension (top-to-the-N in the north, top-to-the-S in the south), the western Aegean has undergone dominantly asymmetrical deformation with a largely top-to-the-NE sense of shear (e.g. in the Thessaly region). This asymmetry could have occured by either a top-to-SW block rotation about a NW-SE trending horizontal axis during pure shear as suggested by Gautier and Brun (1994), or by top-to-the-NE shearing during regional simple shear, or a combination of the two. It might be expected that this simple shear could be induced by a bottom-to-the-SW shear traction applied across the base of the continental crust. This, however, would cause the small upper crustal blocks to rotate about a horizontal axis with a

top-to-the-NE sense of rotation and this would cause mineral lineations to be overprinted by brittle lineations with a top-to-the-*SW* sense of shear on SW trending faults bounding each small block. Since there is no evidence for such an overprint (see Chapters 4, 5 and Gautier 1995), regional extension is interpreted to be the result of uniform stretching (i.e. pure shear) in a NE-SW direction. The components of deformation in the horizontal plane are examined below.

West Aegean Block: Strain components in the horizontal plane

Extension of the Aegean has been accommodated by the partitioning and repartitioning of strain into a series of large blocks with a dimension greater than ~100 km, the West and East Aegean Blocks, and later the Central Aegean Block (Chapter 5). These represent coherently deforming amalgamations of smaller (10 km scale) upper crustal blocks. Structures across the West Aegean Block underwent 30° of coherent clockwise rotation during the mid Miocene to Pliocene. This coherency implies that any two marker lines in the block which were parallel in the early Miocene remained parallel during rotation (indeed, this is how the block was defined in Chapter 5, using initially parallel stretching lineations as markers). This rotation appears to have occurred contemporaneously with extension of the SE margin and shortening of the NW margin of the West Aegean Block, corroborated by gravity data which suggests that the northwestern West Aegean Block is significantly thicker than the southeastern portion (Figure 2.08).

The simplest component of strain that both preserves the parallelism of initially parallel lines and produces a consistent rotation of the lines, is simple shear. In this case, since the orientation of the stretching lineations is parallel to the stretching direction of semi-ductile faults which were active during rotation of the block (e.g. post Neogene D5 faults of the Thessaly region), the stretching lineations must be oriented roughly parallel to the direction of maximum extension in the simple shear. This implies that the initial direction of shear would lie at a 45° angle to the initial extension direction (i.e. at an orientation of 065°).

Shear planes do not rotate during simple shear and hence will lie in the same orientation today as at the start of block rotation. The Mid-Cycladic and Scutari-Pec Lineaments are approximately in this orientation and thus are likely to represent the shear planes.

Regional simple shear of the crust, however, does not explain how crustal thickening in NW Greece and crustal thinning in the Cycladic area occurred contemporaneously. Thus, it is proprosed that the horizontal shear strain of the crust may reflect sub-vertical zones of localised shear strain in the upper mantle (e.g. beneath the Mid-Cycladic Lineament and Scutari-Pec Lineament). In this scenario the crust of the West Aegean Block simply responds the different shear strain rates in the underlying lower lithosphere by undergoing relative thinning and thickening.

6.3 Discussion of models of Aegean deformation

Any model of late-Tertiary Aegean evolution must comply with the kinematic constraints presented in this thesis. In particular, it must explain:
why styles of deformation should be coherent over ~100-300 km length scales, with transitions between coherent styles taking place over ~50 km intervals,
why the West Aegean Block has undergone coherent clockwise rotation of 30° during mid-Miocene - Pliocene extension, forming small-scale (~10 km) crustal blocks oriented roughly

NW-SE,
why the east Aegean region has extended with relatively little (~10-15° anticlockwise) rotation,
why the West Aegean Block subdivided during the Pliocene forming the Central Aegean Block,
within which extension takes place on roughly E-W oriented faults.

Of the models summarised in Figures 2.12a and b, only a few can accommodate all of these constraints.

The westwards motion of Turkey from the Arabia-Eurasia collision (dynamic model C, Figure 2.12a; kinematic models G, H and I, Figure 2.12b) may be a significant kinematic factor in active kinematics (for which these models were constructed), but the mid to late Miocene development of the North Anatolian Fault in the northern Aegean suggests that the westward motion of Turkey is probably not significant in pre-Pliocene Aegean extension.

The idea that the western Aegean blocks rotated to accommodate N-S extension (the left-hand section of the model B; Jackson and McKenzie 1983, 1986) does explain how pre-Pliocene ~N-S extension could have resulted in blocks oriented NW-SE. However, neither the

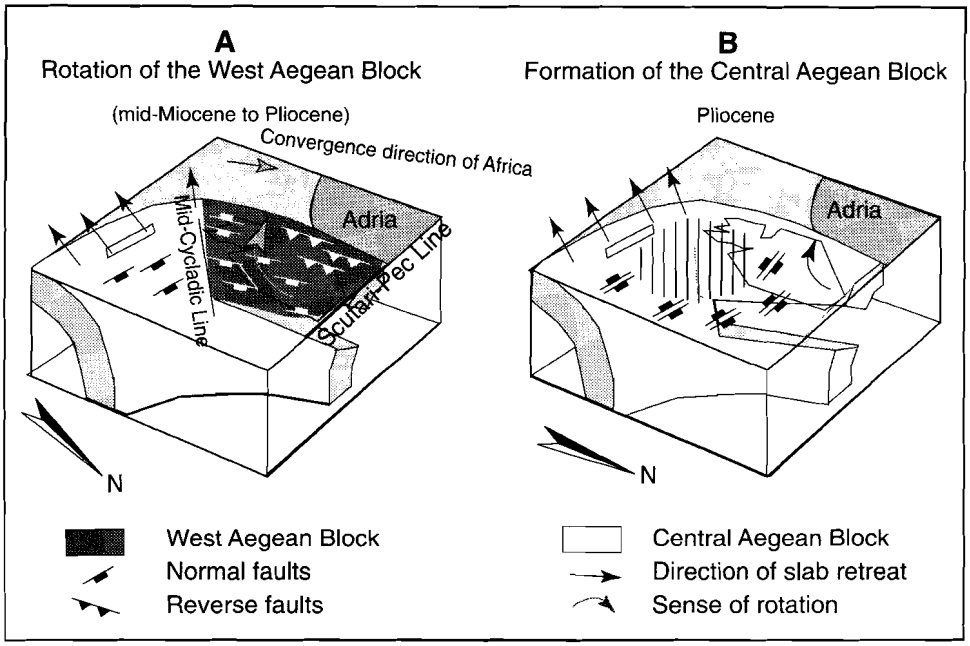

Figure 6.02
A cartoon of the favoured model to account for the late Tertiary deformation of the Aegean. (Figure 6.02a) From the Mid-Miocene to Pliocene this deformation was dominated by block rotation of the West Aegean Block, a lithospheric scale block that is comprised of an amalgamation of smaller fault bounded crustal blocks. The margins of these smaller blocks are schematically represented by normal and reverse faults (see figure) which are linked by transfer faults (not shown). The rotational strain in the West Aegean Block is accommodated along the Mid-Cycladic Lineament and the Scutari-Pec Line. (Figure 6.02b) During the Pliocene this block started to subdivide and now the south east portion forms part of the Central Aegean Block. The margins of the Central Aegean Block is marked by a series of broadly E-W trending normal faults.

models of Jackson and McKenzie, nor the broken slat model (model B) fit the kinematic constraint that Pliocene faults in the West Aegean Block trend roughly E-W and hence cross cut the older NW-SE orientated faults. Hence the broken slat model does not, in fact, provide a comprehensive representation of the active kinematics.

Gautier (1996) suggested that extension across the Aegean may occur in response to pure viscous post-orogenic gravitational collapse of the lower crust/lithosphere (model J, Figure 2.12b). This (dynamic) model was constructed because the authors assumed that current orientations of extensional lineations trace the direction of flow across the Aegean, and ignored the abrupt change in lineations which occurs across the Mid-Cycladic Lineament. However, as explained above, if the West Aegean Block has undergone simple shear, the extensional lineations must be approximately aligned with the direction of maximum extension and therefore at a significant angle (45° during the mid-Miocene) to the direction of flow. Also, the formation of upper crustal blocks of coherent continental deformation with lateral dimension greater than 100 km demonstrated in this thesis (Chapter 5) suggests that the underlying viscous lithospheric deformation must also be partitioned over large distances (see Chapter 1). Such partitioning of strain is not accommodated in the fluid flow model (model J, Figure 2.12b).

Models which involve forces applied at the base of the crust or at the Aegean margin by the subducting slab are summarised in Figure 2.12a. Back arc extension models (model A, Figure 2.12a) explain Aegean extension in terms of back-arc upwelling of mantle material above the subducted slab, whereas the orogenic collapse model (model B, Figure 2.12a) postulates that the delamination of lower lithospheric material would cause the catastrophic collapse of the orogen. Either of these may be contributing causes of Aegean extension but neither model is significantly detailed to fit the kinematic constraints listed above. More specifically, it is difficult to imagine why either model would cause long-term partitioning of lithospheric deformation since in both cases the mantle is replenished.

The subduction pull and slab detachment models (models D and E, Figure 2.12a) concern forces applied along the margins of the over-riding Aegean plate by roll-back, or by a change in velocity of the subducting slab. According to these models, the change in orientation of the subduction zone (~E-W in the south-east, ~NNW-SSE in the west) should cause a significant change in the orientation of stress between the south-eastern and the western Aegean. The additional stress change, which would occur if the subducting slab was tearing, as proposed in the slab detachment model, would accentuate this stress partitioning. The tip of the tear, as inferred from seismic tomography, propagated south-eastwards from NW Greece to adjacent to Crete. The maximum vertical downward force exerted by the subducted slab, and hence the maximum velocity of slab roll-back should occur close to the tear tip, and should have propagated with the tear. This would cause a differential extension which in turn would result in a right lateral shear force between NW and S Greece, and thus may be the one of the causes of the observed clockwise rotation of the West Aegean Block. As the tear approached Crete (see Figure 6.02) a differential in southwards roll-back velocity would occur between Crete and southern Anatolia causing anticlockwise rotation in the east Aegean. In addition, when the locus of maximum roll-back reached Crete, extensional stress in the West Aegean Block would be primarily oriented N-S which could have caused the development of E-W trending extensional faults in the Pliocene (Figure 6.02b). Hence, models involving differential retreat of the subducting slab appear to be the only models which provide a dynamic explanation of why strain and rotation may be partitioned laterally within the over-riding lithosphere over timescales

of ~10 Ma, as observed in this thesis.

Hence, of the models discussed in Chapter 2, models based on forces in the provide the closest fit to the set constraints constructed in this thesis. Subduction pull only represents active kinematics, and the model most favoured is one with subductionward stresses which are partitioned due to the angular geometry of the subduction 'arc', and possibly localised due to slab detachment. Hence, the kinematic model of Chapter 5 in this thesis (Figure 5.17) represents a significant advance in understanding of the regional kinematic evolution, and presents a comprehensive set of constraints (listed above) which discriminate between many of the kinematic and dynamic models which have previously been proposed to explain Aegean evolution. In addition, future dynamic models will be significantly better constrained by the model presented in Figure 5.17, narrowing the diversity of model mechanisms which must be investigated.

6.4 Conclusions of this thesis

As a result of the investigations carried out during the course of this study the following conclusions may be drawn:

1. A fundamental problem with Aegean geology is the use of indescriminate and subjective criteria to define units. It is recommended that units be defined on the basis of a single criteria only (e.g., lithological units defined by lithological criteria, metamorphic units defined using metamorphic units or deformation units defined by structural criteria).
2. The basement of the Thessaly region records synchronous greenschist facies metamorphism at high structural levels, and high pressure, lower temperature metamorphism at low structural levels. Metamorphic events are:
   - an early Cretaceous (M1) epidote-albite amphibolite facies defomation (M1.amph),
   - a late Cretaceous (M2) greenschist facies event at high structural levels (M2.gns),
   - a late Cretaceous to Eocene epidote blueschist facies (M2.bls) event at low structural levels,
   - an Oligocene to Miocene (M3) greenschist facies metamorphism (M3.gns).
3. The basement of Thessaly grades from a complex of Hercynian quartzfeldspathic-rich units in the west to an Alpine, ductiley deformed melange in the east.
4. On the basis of the preserved metamorphic history in these units, two zones are defined:
   - The *West Thessaly Complex* preserves only late Cretaceous M2.gns metamorphism (and another greenschist facies metamorphism of unknown age).
   - The *East Thessaly Complex* preserves early Cretaceous M1.amph, late Cretaceous M2.bls and Oligocene-Miocene M3.gns metamorphism.
5. Five major tectonic periods are recognised, based on the results of Thessaly region:
   - Lower Cretaceous top-to-the-SW thrusting (D1) is preserved only in the West Thessaly Complex but is likely to have been an Aegean-wide event.
   - Lower Cretaceous E-W shearing is preserved along the boundary between the West and East Thessaly Complexes (D2). This may be a local feature related to Tertiary ductile rotation.
   - Upper Cretaceous to Eocene top-to-the-SW (D3) thrusting and erosion, with associated exhumation of blueschists. This is observed in the East Thessaly Complex and part of West Thessaly complex.
   - Oligocene to Pliocene, top-to-the-north Aegean-wide extension (D4 to D5) layer-parallel

extension in Thessaly) with associated exhumation of greenschists observed in the East Thessaly Complex.

- A change to north-south extension of the West Aegean Block in the Pliocene (D6), observed throughout Thessaly.

6. Overprinting of upper Cretaceous and younger deformation over the western early Cretaceous deformation is observed along the boundary between the West and East Thessaly Complexes.
7. Exhumation of the East Thessaly Complex involved low differential stress in the marble units, and the widespread development of a fibrous calcite micro-fabric which is related to low shear strain during uplift of the basement.
8. During the late Tertiary, the Thessaly region formed a central part of a West Aegean Block. This was bounded by the (previously identified) Scutari-Pec Line to the northwest, by the subduction zone to the west and by the Mid-Cycladic Lineament (this thesis) to the southeast. The border to the east is gradational and is located in the Rhodope/northern Aegean Sea.
9. Post-orogenic extension initially occurred in a NNE-SSW direction (023°) across the whole of the Aegean region.
10. Between the Oligocene and late Miocene, the Aegean crust subdivided into two parts: The western part formed the West Aegean Block which rotated ~30° clockwise whereas the eastern portion (loosely termed the East Aegean Block) contemporaneously rotated 19° anticlockwise.
11. After the latest Miocene/early Pliocene, newly developed E-W trending faults caused the West Aegean Block to subdivide into two portions. The southeastern portion (NW Cycladic area) coupled with the SW Cycladic area to form the Central Aegean Block which began to translate SW. The NW margin and possibly the northern Pelagonian Zone continued to rotate a further ~10-15° clockwise.
12. Rotation of the West Aegean Block was probably aided by thermal weakening of its northeastern and southern margins, in conjunction with pre-existing weakness along the Scutari-Pec Line and Mid-Cycladic Lineament.
13. The outward bending of the Aegean Arc during regional extension of the Aegean hinterland has not occurred by radial outward flow of the crust or by the rotation of a single block but by succesive partioning of normal strain and rotation strain on an intermediate to large (100 km) lengthscale.
14. It is suggested that the regional sharply defined boundaries of the West Aegean Block (namely the Mid-Cycladic Lineament) may have represented zones of localised shear strain in the upper mantle induced by roll back and detachment of the subducted Mediterranean slab.

6.5 Future work

During the course of the present study, ductile and semi-ductile fabrics in basement were used to derive constraints on the evolution of the Thessaly region, and on the kinematics of Aegean syn- and post-orogenic extension. The main areas which need to be addressed further are as follows:

1. The system used to catagorise metamorphic rocks must be extended. Now that so much

geochemical, structural and lithological data is readily available, an objective system needs to be established following the guidelines established in this thesis. This is an unglamorous but essential job if large length-scale correlations are to be found efficiently.

2. This thesis suggests that physical mixing processes associated with deformation may form lithologically mappable units and may affect wide regions. Little work has been done on how large a region can become 'mixed' during tectonism, or on the mechanics of how this might occur.
3. Formation of the NNW-SSE lineations preserved in northern Greece needs to be constrained temporally. Further, the relationship between the D1 tectonic event described in Chapter 4 and ophiolite obduction (Chapter 6) is not clear and needs to be examined in more detail.
4. Many questions arise concerning the fibrous calcite fabric observed in Chapter 4. What is the timing of its development? Is it the similar across the whole Aegean, even though the Olympos region appears to have been exhumed prior to the SE Aegean? Can the stress and strain conditions of the fabric formation be determined quantitatively? Why did rapid grain growth of calcite occur at all? How does the mechanism that caused the growth of calcite fibres compare with that which caused the development of the other fibrous fabrics? The calcite fabric has potential for much rewarding study.
5. Paleomagnetic studies of the Miocene plutons of the central and eastern Aegean would reveal whether any independent constraints be placed on the amount and timing of rotation of the east Aegean.
6. The nature and timing of deformation along the margins of the West Aegean Block identified in this thesis are poorly constrained. It is recommended that a kinematic and geochronological study of the boundary zone across Paros be conducted and the Rhodope region.
7. The Peloponnesos region is very complex. A detailed ductile to brittle kinematic and paleomagnetic study is necessary to determine its relationship both with the West Aegean Block during the Miocene, and with the Central Aegean Block during the Pliocene. It is also recommended that a detailed ductile to brittle structural study be conducted to determine whether the structural evolution of this block differs from other regions in the West Aegean Block.
8. Finally, this thesis has demonstrated that the upper crust has deformed as a series of fault bounded blocks0 that with second order rigid sub-block can rearrange during deformation. The question is this behaviour in other orogens and oroclinal belts during collapse.

Samenvatting

Het Egeïsche gebied is een van de best bestudeerde gebieden op aarde waar op dit moment post-orogene extensie plaatsvindt. Verschillende kinematische en dynamische modellen zijn voorgesteld om de actieve tektoniek in dit gebied te verklaren. Meest recent is aangetoond dat , sinds het begin van de extensie in het Mioceen, de regionale kinematiek de laatste 5 Ma een grote verandering heeft ondergaan.

Dit is de reden dat modellen voor de thans actieve deformatie niet gebruikt kunnen worden voor extrapolatie verder terug in de tijd. Tot op heden is er van zowel de Tertiaire kinematische ontwikkeling van het Egeïsche gebied, als van de exacte kinematische samenstelling voor en na de 5 Ma verandering weinig bekend. Dit proefschrift reconstrueert de Alpiene kinematische ontwikkeling van het noordwestelijk deel van het Egeïsche gebied en gebruikt deze informatie om randvoorwaarden aan te geven voor modellen voor de Alpiene tektonische ontwikkeling van het hele Egeïsche gebied. Dit proefschrift concentreert zich op de structurele en kinematische evolutie van Thessalië, een regio in het noorden van Griekenland die zich op de noordwestelijke grens bevindt van het gebied dat Egeische extensie heeft ondergaan.

De lithologische onderverdelingen, en hun kinematische en metamorfe geschiedenis binnen Thessalië zijn door middel van veldwerk bestudeerd, en wel op een schaal die ligt tussen die van eerder uitgevoerd gedetailleerd lokaal onderzoek en grootschaliger regionaal onderzoek. Dit heeft tot gevolg dat deze eerdere studies met dit veldwerk geintegreerd kunnen worden en daarna gecorreleerd kunnen worden in geheel Thessalië en het Egeïsche gebied.

Het veldwerkgebied is gesitueerd tussen de reeds goed bestudeerde gebieden van de Cycladen in het zuiden, en noord Griekenland, zodat de in dit proefschrift gepresenteerde gegevens en modellen een belangrijke geografische en structurele schakel vormen in een synthese voor het hele Egeïsche gebied. Bovendien voorziet dit proefschrift regionale dynamische modellen voor de tektonische ontwikkeling van het Egeïsche gebied van een grote hoeveelheid randvoorwaarden.

Lithologieën en metamorfe geschiedenis

Een van de grootste hindernissen bij de correlatie van metamorfe, kinematische en structurele gegevens uit eerdere lokale onderzoeken, is het gebruik van inconsistente of ongedefinieerde criteria bij het beschrijven van verschillende tektonostratigrafische eenheden of kinematische indicatoren. Om deze reden is hier een nieuw, intern consistent en objectief systeem ontworpen om onderscheid te maken tussen de verschillende lithologieën en hun metamorfe, structurele en kinematische geschiedenis.

Het basement van het Thessalië gebied bestaat uit een gedeformeerde assemblage van Hercynische kwarts-veldspaat gneizen en schisten, Midden-Mesozoische ultramafische ofioliet fragmenten, Laat Paleozoische tot Mesozoische marmers en Vroeg Paleocene flysch sedimenten, alsook mafische en kalkrijke schisten van onbekende ouderdom. In de periode tussen het Vroeg Krijt en het Mioceen worden drie metamorfe gebeurtenissen herkend. De eerste twee vonden plaats in respectievelijk het Vroeg Krijt en Laat Krijt tot Eoceen, en bestonden uit groenschistfacies metamorfose (M1.gns, M2.gns) die tegelijk plaatsvond met hooggradiger epidoot-albiet amfiboliet (M1.amph) tot epidoot blauwschistfacies (M2.bls) metamorfose op

diepere structurele niveaus. De derde metamorfe gebeurtenis is beperkt zich tot oost Thessalië en vond plaats onder groenschistfacies condities.

Het metamorfe deel van het basement bestaat uit twee verschillende eenheden of complexen, een in het westen en een in het oosten. Het West Thessalië Complex bestaat uit groenschistfacies (M1.gns en M2.gns) gesteente. Het Oost Thessalië Complex laat een complexere metamorfe geschiedenis zien, met amfibolietfacies (M1.amph), blauwschistfacies (M2.bls) en groenschistfacies (M3.gns) metamorfose. Het Oost Thessalië Complex is verder onderverdeeld in het Boven Oost Thessalië Complex, waarin metamorfe gebeurtenissen ouder dan het Laat Krijt bewaard zijn, en het Onder Oost Thessalië Complex, waarin metamorfe gebeurtenissen uit het Laat Krijt en jonger bewaard zijn.

De metamorfe, structurele en lithologische relaties tussen delen van de westelijke rand van het Thessalië basement zijn dermate complex dat niet gesteld kan worden dat lithologische, structurele en metamorfe eenheden niet noodzakelijkerwijs samenvallen.

Kinematische geschiedenis

In het West Thessalië Complex is voornamelijk deformatie uit het Vroeg Krijt vastgelegd, terwijl in het Oost Thessalië Complex uitsluited deformatie uit het Laat Krijt e jonger is vastgelegd. De volgende deformatiefasen zijn te onderscheiden:

1. Vroeg Krijt ZZO gerichte overschuivingen (D1) zijn bewaard gebleven in het West Thessalië Complex, maar heeft waarschijnlijk in het hele Egeïsche gebied plaatsgevonden, en is gerelateerd aan het begin van ofioliet obductie.
2. Langs de grens tussen het West en Oost Thessalië Complex zijn Vroeg Krijt O-W extensie structuren (D2) bewaard gebleven. Deze grens zou gerelateerd kunnen zijn aan Tertiaire ductiele rotatie.
3. In de periode van het Laat Krijt tot het Eoceen hadden ZW gerichte overschuivingen (D3), gevolgd door erosie de exhumatie van blauwschisten tot gevolg in het Oost Thessalië Complex en in delen van het West Thessalië Complex.
4. In het Oligoceen tot het Plioceen vond laag parallelle extensie plaats in het hele Egeïsche gebied (D4). Deze structuren hebben een top naar het N transportrichting. Tijdens deze deformatie fase is ook een alomtegenwoordige fibreuze calciet textuur gevormd als gevolg van de lage differentiele spanning tijdens de exhumatie van het basement.
5. Recente N-Z extensionele structuren (D5) zorgden voor een reorganisatie van de Egeïsche kinematiek in het Plioceen (zie onder).

Regionale kinematiek van het Egeïsche gebied

Kinematische indicatoren ((semi-)ductiele extensie lineaties en (semi)brosse wrijfkrassen) van Thessalië zijn gecombineerd en gecorreleerd met vergelijkbare gegevens van gepubliceerde onderzoeken in het hele Egeïsche gebied. Deze zijn aangevuld nieuwe kinematische gegevens van de Peleponnesos, Antiparos en Kea. Deze gebieden waren niet in detail oderzocht en bleken in de regionale context belangrijke kinematische gegevens te bevatten.

De regionale verdeling van orientaties van de extensie lineaties is ruimtelijk gelijk aan die van paleomagnetische declinaties, die de absolute blokrotatie sinds het Mioceen vastleggen. Deze gecombineerde regionale kinematische en paleomagnetische gegevens definieren een deel van het Egeïsche gebied dat 30 graden geroteerd is in het Neogeen.

Thessalië vormt een centraal deel van dit gebied, dat het West Egeïsche Blok wordt genoemd.Het Blok wordt begrensd door de Scutari-Pec Lijn in het noordwesten, door de

subductiezone in het westen en het Midden Cycladisch Lineament in het zuidoosten. De oostelijke begrenzing ligt in het Rhodope / noord Egeïsche Zee gebied en is gradueel.

De kinematische evolutie van het Egeïsche gebied in het Tertiair

De Tertiaire kinematische gechiedenis van het Egeïsche gebied bestaat uit drie fasen:

1. Initiele uniforme NNO (~23°) gerichte extensie in het hele gebied.
2. Tussen het Oligoceen en het Laat Mioceen werd de korst verdeeld in twee delen: het westelijk deel vormde het West Egeïsche Blok, dat ~30° met de klok mee roteerde, terwijl het oostelijk deel (Oost Egeïsche Blok) gelijktijdig 19° tegen de klok in roteerde.
3. Na het Laat Mioceen werd het West Egeïsche Blok verder verdeeld in twee delen. Het zuidoostelijk deel (NW Cycladen gebied) vormt samen met het ZO Cycladen gebied het Centraal Egeïsche Blok, dat naar het ZW schuift. Het noordwestelijk deel dat o.a. het Thessalië gebied en mogelijk de noord Pelagonische Zone omvat, roteert nog 10° verder tegen de klok in.

De rotatie van het West Egeïsche Blok werd vergemakkelijkt door thermale verzwakking van de korst langs de noordoostelijke en zuidelijke rand, zoals blijkt uit de spreiding en timing van magmatische activiteit langs de eerder genoemde Scutari en Mid-Cycladische lineamenten.

De buitenwaartse buiging van de Egeïsche boog tijdens de Miocene tot Pliocene regionale extensie van het Egeïsche achterland is noet ontstaan door radiale naar buiten gerichte vloei van de korst of door rotatie van een enkel blok, maar door verdeling en herverdeling van van de vervorming in een aantal grote (100 km) blokken, elk bestaande uit een gecompliceerde samenstelling van kleinere (10 km) crustale blokken.

Het regionaal gedefinieerde Mid-Cycladische lineament zou een zone kunnen vertegenwoordigen van gelokaliseerde schuifvervorming in de bovenmantel, geinduceerd door terugveren en ontkoppeling van de gesubduceerde Mediterrane oceanische plaat.

References

Altherr, R.; Kreuzer, J.; Wendt, I.; Lenz, H.; Wagner, G. A.; Keller, J.; Harre, W. and Handorf, A. (1982) A late Oligocene/Early Miocene high temperature belt in the Attica Cycladic crystalline complex (SE Pelagonian, Greece). *Geol.Jb.*, **E23**: 97-164.

Altherr, R.; Schliestedt, M.; Okrusch, M.; Seidel, E.; Kreuzer, H.; Harre, W.; Lenz, H.; Wendt, I. and Wagner, G. A. (1979) Geochronology of high-pressure rocks on Sifnos, (Cyclades, Greece). *Contrib.Mineral.Petrol.*, **70**: 245-255.

Andriessen, P. A. M.; Boelrijk, N. A. I. M.; Hebeda, E. H.; Priem, H. N. A.; Verurmen, E. A. and Verschure, L. H. (1979) Dating of events of metamorphism and granitic magmatism in the Alpine Orogen of Naxos (Cyclades, Greece). *Contib. Mineral.Petrol.*, **69**: 215-255.

Andriessen, P. A. M.; Banga G. and Hebeda E. H. (1987) Isotopic age study of pre-Alpine rocks in the basal units of Naxos, Sikinos, and Ios, Greek Cyclades. *Geol.Mijn.*, **66**: 3-14.

Armijo, R.; Meyer, B.; King, G. C. P.; Rigo, A. and Papanastassiou, D. (1996) Quaternary evolution of the Corinth Rift and its implications for the Late Cenozoic evolution of the Aegean. *Geophys.J.Int.*, **126**: 11-53.

Atzemoglu, A.; Kondopoulou, D.; Papamarinopoulos, S. and Dimitriadis, S. (1994) Paleomagnetic evidence for block rotations in the western Greek Rhodope. *Geoph.J.Int.*, **10**: 221-230.

Aubouin, J. (1959) Contribution à l'étude de la Grèce septrionale; les confins de l'Epire et de la Thessalie, *Ann.Géol.Pays Hellén.*, **10**: 1-483

Aubouin, J. and Dercourt, J. (1962) Zone preapulienne, zone Ionienne et zone du Gavrovo en Peloponnese Occidentale. *Bull. Soc.Fr.*, **4**: 785-794.

Aubouin, J.; Bonneau, M.; Celet, P.; Charvet, J.; Clément, B.; Degardin, J. M.; Dercourt, J.; Ferriére, J.; Fleury, J. J.; Guernet, C.; Maillot, H.; Mania, J.; Mansy, J. L.; Terry, J.; Thiébault, F.; Tsofilias, P. and Verriez, J. J.; (1970) Contributions à la géologie des Hellénides: Le Gavrovo, le Pinde, et la zone ophiolitique subpélagonienne. *Ann.Soc. Géol.Nord*, **19**: 4, 277-306.

Avigad, D. (1991) Uplift and exhumation of high-pressure metamorphic terranes: the example of the Cycladic blueschist belt (Aegean Sea). *Tectonophysics*, **188**: 357-372.

Barka, A. A. and Hancock, P. L. (1984) Neotectonics deformation patterns in the convex northwards arc of the North Anatolian Fault zone. *Geol.Soc.London Spec.Publ.*, **17**: 763-774.

Barka, A. A. and Kadinsky-Cade, K. (1988) Strike-slip geometry in Turkey and its influence on earthquake activity. *Tectonics*, **7**: 663-684.

Barton, C. M. (1975) Mt Olympos, Greece: New light on an old window. *J.Geol.Soc. London*, **131**: 389-396.

Barton, C. M. (1976) The tectonic vector, emplacement age of an allochtonous basement slice in the Olympos area. *Bull. Soc.Géol.Fr.*, **18**(2): 253-258.

Bassias, Y. and Triboulet, C. (1994) Tectonometamorphic evolution of blueschist formations in the Peloponnesos (Parnon and Taygetos Massifs, Greece): a model of nappe stacking during Tertiary orogenesis. *J.Geol.*, **102**:697-708.

Bernoulli, D. and Laubscher, H. (1972) The planispastic problem of the Hellenides. *Ecol.Géol.Hell.*, **65**: 107-118.

Berthé, D.; Choukroune, P. and Jegouzo, P. (1979) Orthogneiss, mylonite and non-coaxial deformation of granites: the example of the South Amorican Shear Zone. *J.Struct.Geol.* , **1**: 31-42.

Blake, M. C.; Bonneau, M.; Kienast, J. R.; Lepvrier, C.; Maluski, H. and Papanikolau, D. (1981) A geological reconnaisance of the Cycladic Blueschist Belt, Greece. *Bull.Geol.Soc.Am.*, **92**: 247-254.

Blenkinsop, T. G. and Treloar, P. J. (1995) Geometry, classification and kinematics of S-C and S-C' fabrics in the Mushandike area, Zimbabwe. *J.Struct.Geol.*, **17**(3): 397-408.

Boccaletti, M.; Manetti, P. and Peccerillo, A. (1974) The Balkanides as an instance of a back-arc thrust belt: possible relation with the Hellenides. *Geol.Soc.Am.Bull.*, **85**: 1077-1084.

Bonneau, M. and Kiesnast, J. R. (1982) Subduction, collision, et schistes bleus: exemple de l'Egée, Grece. *Bull.Soc.Géol. Fr.*, **7**(14): 785-791.

Bourne, S. J.; England, P. C. and Parsons, B. (1998) The motion of crustal blocks driven by flow of the lower lithosphere and implications for the slip rates of strike-slip faults. *Nature*, **391**: 655-659.

Bozkurt, E.; Winchester J. A., R. G. and Park, R. G. (1994) Geochemistry and tectonic significance of augen gneisses from the southern Menderes massif (West Turkey). *Geol.Mag.*, **3**: 287-301.

Bozkurt, E. and Park, R. G. (1997) Evolution of a mid-Tertiary extensional shear zone in the southern Menderes Massif, western Turkey. *Bull.Soc.Géol.Fr.*, **168**(1): 3-14.

Bröcker, M.; Kreuzer, H.; Matthews, A. and

Okrusch, M. (1993) $^{40}Ar/^{39}Ar$ and oxygen isotope studies of polymetamorphism from Tinos Island, Cycladic Blueschist Belt, Greece. *J.Meta.Geol.*, **11**: 223-240.

Brouwer, F. (1994) Map of Livadi south area, Unpublished 4th year mapping report, housed in the University of Utrecht.

Brunn, J. H. (1956) Contribution à l'étude géologique su Pinde septentrional et d'une parti de la Macédoine Occidental. *Ann.géol.Pays.hell.*, 7: 1-358.

Burg, J. P.; Ivanov, Z.; Ricou, L. E.; Dimor, D. and Klain, L. (1990) Implications of sense of shear criteria for the tectonic evolution of Central Rhodope Massif, southern Bulgaria. *Geology*, **18**: 451-454.

Burg, J.-P.; Ricou, L.-E.; Ivanov, Z.; Godfriaux, I.; Dimov, D. and Klain, L. (1996) Syn-metamorphic nappe complex in the Rhodope Massif, structure and kinematics. *Terra Nova*, **8**: 6-15.

Calvo, J.; Stamatakis, M. G. and Maggana, A. (1985) Clastic humitite in upper Neogene formations in the Kozani Basin, Macedonia, Northern Greece. *J.Sed.Res.*, **A65**(4): 627-632.

Caputo, R. (1990) Geological and structural study of the recent and active brittle deformation of the Neogene-Quaternary Basins of Thessaly (Central Greece). Unpublished PhD. thesis, Aristotle University.

Caputo, R. and Pavlides, S. (1993) Late Cainozoic geodynamic evolution of Thessaly and surroundings (Central-Northern Greece). *Tectonophysics*, **223**: 339-362.

Caputo, R.; Bravard, J.-P. and Helly, B. (1994) The Pliocene-Quaternary tectono-sedimentary evolution of the Larissa Plain (Eastern Thessaly, Greece). *Geodinamica Acta*, 7(4): 219-231.

Celet P. and Ferrière, J. (1978) Les Hellénides internes: Le Pélagonien. *Eclog.Geol.Helv.*, **71**(3): 467-495.

Channell, J.E.T.; D'Argenio, B.; Horvath,T. (1979) Adria, the African promontory in Mesozoic Mediterranean Paleogeography. *Earth.Sci.Rev.*, **15**: 213-292

Closs, H., Roeder, D. and Schmidt, K. (1978) Alps, Apennines, Hellenides: Geodynamic Investigations along geotraverses by an International Group of Geoscientists. E. Schweizerbart'sche Verlagsbuchhandlung, Stuttgart.

Cohen, H. A.; Dart, C. J.; Akyüz, H. S. and Barka, A. (1995) Syn-rift sedimentation and structural graben development of the Gediz and Büyük Menderes Graben, western Turkey. *J.Geol.Soc., London*, **152**: 629-638.

Dalmayrac, B. and Molnar, P. (1981) Parallel thrust and normal faulting in Peru and constraints on the state of stress. *Earth Planet.Sci.Lett.*, **55**: 473-481.

Davis, G. H. and Reynolds, S. J. (1984) Structural Geology of rocks and regions. *2nd edition. John Wiley and Sons.* p 776

Deer, W. A.; Howie, R. A. and Zussman J. (1992) The rock forming minerals. *2nd Edition. John Wiley and Sons*, New York, p.696

de Jonge, M. R.; Spakman, W. and Wortel, M. J. R. (1994) Forward and inverse modelling of mantle structure in the Alpine-Mediterranean region. *Ann.Geophys.Res.*, **99**(B6): 12091-12108.

de Keyser, M. (1993) Map of Gonni area, Unpublished 4th year mapping report, housed in the University of Utrecht.

Delaloye, M.; De Souza, H.; Wagner, J. J. and Hadley, I. (1979) Isotopic ages on ophiolites from the eastern Mediterranean. In: *International Ophiolite Symposium* (edited by Panayioutou, A.), Cyprus: 292-298.

Dercourt, J. (1964) *Ann.Géol.Pays Hellén.*, **18**: 1-300

Dercourt, J.; Zonenshain, L. P.; Ricou, L.-E.; Kazmin, V. G.; Le Pichon, X.; Knipper, A. L.; Grandjacquet, C.; Sbortshikov, I. M.; Geyssant, J.; Lepvrier, C.; Pechersky, D. H.; Boulin, J.; Sibuet, J-C.; Savostin, L. A.; Sorokhtin, O.; Westphal, M.; Bazhenov, M. L.; Lauer, J. P. and Biju-Duval, B. (1986) Geological evolution of the Tethys belt from the Atlantic to the Pamirs since the Lias. *Tectonophysics*, **123**: 241-315.

de Wet, A. P.; Miller, J. A.; Bickle, M. J. and Chapman, H. J. (1989) Geology and geochronology of the Arnea, Sithonian and Ouranopolis intrusions, Chalkidiki peninsula, northern Greece. *Tectonophysics*, **161**: 65-79.

Dewey, J. F. (1980) Episodicity, sequence and style at convergent plate boundaries. In: *The continental crust and its mineral deposits*, edited by Strangway, D. W. *Spec.Pub.Geol.Soc. Canada*, **20**: 553-573.

Dewey, J. F. (1988) Extensional collapse of Orogens. *Tectonics*, 7: 1123-1139.

Dewey, J. F. and Sengör, A. M. C. (1979) Aegean and surrounding regions: complex multi-plate and continuum tectonics in a convergent zone. *Bull.Geol.Soc.Am.*, **90**: 82-91.

Dewey, J. F.; Helman, M. L.; Turco, E.; Hutton, E.; Hutton, D. H. W. and Knott, S. D. (1989) Kinematics of the western Mediterranean. In: *Alpine Tectonics. Geol.Soc.London Spec.Pub.*, **45**: 265-283.

Dewey, J. F.; Hempoton, M. R.; Kidd, W. S. F.; Saroglu, F. and Sengör, A. M. C. (1986) Shortening of continental lithosphere: the neotectonics of Eastern Anatolia - a young collion zone. In: *Collision Tectonics* (Eds Coward, M. P. and Reis, A. C.). *Geol.Soc.Spec.Pub.*, **19**: 3-36.

Dinter, D. A.; McFarlane, A.; Hames, W.; Isachsen, C.; Bowring, S. and Royden, L. (1995) U-Pb and $^{40}Ar/^{39}Ar$ geochronology of the Symvolon Granodiorite: implications for the thermal and structural evolution of the Rhodope metamorphic core complex, northeastern Greece. *Tectonics,* **14**(4): 886-908.

Dinter, D. A. and Royden, L. (1993) Late Cenozoic extension in NE Greece: Strymon Valley detachment and Rhodope Core Complex. *Geology,* **21**: 45-48.

Doutsos, T. (1984) Structural Analysis of Central Hellenic Nappes. *N.Jb.Geol.Paläont.Abh.,* **168**(1): 1-22.

Doutsos, T.; Pe-Piper, G.; Boronkay, K. and Koukouvelas, I. (1993) Kinematics of the Central Hellenides. *Tectonics,* **12**(4): 936-953.

Duermeijer, C.; Krijgsman, W.; Langereis, C. and Ten Veen, J. H. (1998) Post early Messinian counter-clockwise rotation on Crete; implications for the Late Miocene to Recent kinematics of the southern Hellenic Arc. *Tectonophysics, in press.*

Dürr, S. H. (1985) Geological map of Amorgos and Donoussa: No. 340. Institute of Geology and Mineral Exploration, Greece. 1:50,000

Dürr, S. H.; Altherr, R.; Keller, J.; Okrusch, M. and Seidel, E. (1978) The Median Aegean Crystalline Belt: stratigraphy, structure, metamorphism and magmatism. In: *Alps, Appenines, Hellenides* (edited by Closs, H., Roeder, D. H. and Schmidt, K.). Schweizerburt, Stuttgart, Germany, 455-477.

England, P. C. and Houseman, G. A. (1988) The Mechanics of the Tibetan Plateau. *Geoph.Res.Lett.* **326**(A): 301-320.

Ernst, W. G. (1975) *Metamorphism and plate tectonic regimes.* Dowden, Hutchinson and Ross, New York.

Evans, B. W. 1990. Phase relations of epidote blueschists. *Lithos,* **25**: 3-23.

Falalakis, G.; Kilias, A. and Mounstrakis, D. (1995) Late Alpine ductile deformation and related metamorphism in the Serbo-macedonian metamorphic rocks (Macedonia, N. Greece), XV Carpathian Congress,17-20 September: Athens, Geological Society of Greece.

Fassoulas, C.; Kilias, A. and Mounstrakis, D. (1994) Postnappe stacking extension and exhumation of high-pressure/low-temperature rocks in the island of Crete. *Tectonics,* **13**(1): 127-138.

Faugères, C. (1977) Naissance et dévelopment du relief de l'Olympe (Grèce): une manifestation éclatante de la téctonique récente. *Rev.Géogr.Phys.Géol.Dyn.,* **XIX**(1): 7-26.

Faupl, P.; Pavlopoulos, A.; Wagreich, M. and Migiros, G. (1996) Pre-Tertiary blueschist terrains in the Hellenides: evidence from detrital minerals of flysch successions. *Terra Nova,* **8**: 180-190.

Faure, M. and Bonneau, M. (1988) Données nouvelles sur l'éxtension néogene de l'Egee: la deformation ductile du granite miocene de Mykonos (Cyclades, Grece). *C.R.Acad.Sci.Paris,* **307**: 1553-1559.

Faure, M.; Bonneau, M. and Pons, J. (1991) Ductile deformation and syntectonic granite emplacement during late Miocene extension of the Aegean. *Bull.Soc.géol.Fr.,* **162**: 3-12.

Ferrière, J. (1976a) Étude préliminaire d'un secteur massifs cristallins interne (zone pélagonnienne): la région de Volos, Grèce continentale-orientale. *Soc.géol.Fr.Bull.,* **18**(2): 265-273.

Ferrière, J. (1976b) Étude préliminaire des terrains métamorphiques de la presqu'ile du Pélion, anterieures aux niveaus conglomeratiques presum Cretace Superieur. *C.R.Acad.Sci.(Paris),* **282**(26 avril): 1485-1488.

Ferrière, J. (1977) Le massif du Chalkodonio et sa bordure méridonale (Grèce continentale orientale): aperçus stratigraphique et tectonique. *C.R.Acad.Sci.(Paris),* **284**: 2323-2326.

Ferrière, J. (1982) Paléogeographies et tectoniques superposee dans les Hellénides internes: les massifs de l'Othrys et du Pélion (Grèce Continentale). *Soc.Géol. Nord,* 7: p 970.

Ferrière, J. (1985) Nature et Developpement des Ophiolites Helleniques du Secteur Othrys-Pelion. *Ofioliti,* **10**(2/3): 255-278.

Fry, N. (1984) The field description of Rocks. *Geological Society of London, handbook.* Series ed. K. Cox. John Wiley and Sons, London: p.110.

Fytikas, M.; Innocenti, F.; Manetti, P.; Mazzouli, R.; Peccerillo, A. and Villari, L. (1984) Tertiary to Quaternary evolution of volcanism in the Aegean Region. In: *The Geological Evolution of the Eastern Mediterranean* (edited by Dixon, J. E. and Robertson, A. H. F.). *Geol.Soc.Spec.Pubs,* **17**: Blackwell Scientific Publications, Edinburgh.

Gautier, P. (1995) *Géométrie crustale et cinématique de l'extension tardi-orgénique dans le domaine centre-égéen.* Université de Rennes, Rennes: 420p.

Gautier, P. and Brun, J-P. (1993) Structure and kinematics of upper Cenozoic extensional detachment on Naxos and Paros (Cyclade Islands, Greece). *Tectonics,* **12**(5): 1180-1194.

Gautier, P. and Brun, J-P. (1994) Ductile crust exhumation and extensional detachments in the Central Aegean (Cyclades, Evvia Islands). *Geodin.Acta,* **7**(2): 57-85.

Gautier, P.; Brun, J.-P.; Jolivet, L.; Godfriaux, I. and Bonneau, M. (1993) Ductile and brittle deformation due to post-thickening extension in the Aegean Domain (Cyclades, Euboea). In: *Late Orogenic Extension in Mountain Belts.* (edited by Seranne, M. and Malavielle, **219**: BRGM, Montpelier.

Gautier, P.; Brun, J.-P.; Moriceau, R.; Van den Dreissche, J.; Sokoutis, D.; Martinod, J. and Jolivet, L. (1996) Gravity spreading of the Aegean lithosphere during the Neogene: geological constraints and physical models. Conference Proceedings of The Mediterranean Basins: Cèrgy-Pontoise, Paris, Institute du Petrole.

Godfriaux, I. (1968) Étude géologique de la region de l'Olympe. *Annls.géol.Pays Hell.*, **19**: 1-271.

Godfriaux, I. and Pichon, J. F. (1980) Sur l'importance des évenements téctonique et métamorphiques d'age tertiare en Thessalie septentrionale (l'Olympe, Ossa, et Flamburon). *Annls.géol.Soc.Nord.*, **99**: 367-376.

Godfriaux, I. and Ricou, L. E. (1991) Direction et sens de transport associes au charriage synmetamorphe sur l'Olympe. *Bull.geol.Soc.Gr.*, **25**(1): 207-229.

Hatzfeld, D.; Kassara, I.; Panagiotopoulos, D.; Amorese, D.; Makropoulos, K.; Karakaisis, G. and Coutant, O. (1995) Microseismicity and strain patter in Northwestern Greece. *Tectonics*, **14**(4): 773-785.

Hetzel, R. and Reischmann, T. (1996) Intrusion age of Pan-African augen gneisses in the southern Menderes massif and the age of cooling after Alpine ductile extensional deformation. *Geol.Mag.*, **133**: 565-572.

Hetzel R.; Passchier, C. W.; Ring, U. and Dora, O. O. (1995) Bivergent extension in orogenic belts: The Menderes massif (southwestern Turkey). *Geology*, **23**(5): 455-458.

Hetzel, R.; Ring, U.; Akal , C. and Troesch, M. (1995) Miocene NNE-directed extension unroofing in the Menderes massif, southwestern Turkey. *J.Geol.Soc. London*, **152**: 639-654.

Jackson, J. (1994) Active tectonics of the Aegean Region. *Ann.Rev.Earth Planet. Sci.*, **22**: 239-271.

Jackson, J. and McKenzie, D. (1983) Geometrical evolution of normal fault systems. *J.Struct.Geol.*, **5**: 471-482.

Jackson, J. and McKenzie, D. (1988a) The relationship between plate motions and seismic tensors and rates of active deformation in the Mediterranean and the Middle East. *Geophys.J.Int.*, **93**: 45-73.

Jackson, J. and McKenzie, D. (1988b) Rates of active deformation in the Aegean Sea and surrounding regions. *Basin Research*, **1**: 121-128.

Jacobshagen, V. (1986) *Geologie von Griechenland.* Gebrüder Borntraeger, Berlin-Stuttgart.

Jacobshagen, V.; Risch, H. and Roeder, D. (1976) Die eohellenische Phase, Definition und Interpretation. *Z.Dtsch.geol.Ges.*, **127**: 133-145.

Jacobshagen, V.; Dürr, S.; Kockel, F.; Kopp, K. O.; Kowalczyk, G.; Berckenhemer, H. and Büttner, D. (1978) Structure and geodynamical evolution of the Aegean Region. In: *Alps, Appenines, Hellenides.* (edited by Closs, H., Roeder, D. and Schmidt, K.). *IUCG Scientific Report* **38**, Stuttgart, Germany: 537-564.

Jacobshagen, V. and Wallbrecher, E. (1984) Pre-Neogene nappe structure and metamorphism of the North Sporades and the southern Pelin Peninsula. In: *The Geological Evolution of the Eastern Mediterranean* (edited by Dixon, J. E. and Robertson, A. H. F.). *Geol.Soc.Spec.Pubs*, **17**: Blackwell Scientific Publications, Edinburgh: 591-602.

Jacobshagen, V. (1986) *Geologie von Griechenland.* Gebrüder Borntraeger, Berlin-Stuttgart.

Jamal, D. (1996) Map of Spilia area, Unpublished 4th year mapping report, housed in the University of Utrecht.

Jolivet, L.; Brun, J.-P.; Gautier, P.; Lallemant, S. and Patriat, M. (1994a) 3-D Kinematics of extension in the Aegean from the early Miocene to the Present, insights from the ductile crust. *Bull.Soc.géol.Fr.*, **165**(3): 195-209.

Jolivet, L.; Daniel, J. M.; Truffert, C. and Goffe, B. (1994b) Exhumation of deep crustal metamorphic rocks and crustal extension in back arc regions. *Lithos*, **33**: 3-30.

Jolivet, L.; Goffé, B., Monié, P.; Patriat, M.; Truffert-Luxey, C. and Bonneau, M. (1996) Miocene detachment in Crete and exhumation P-T-t paths of high pressure metamorphic rocks. *Tectonics*, **15**: 1129-1153.

Jones, C. E.; Tarney, J.; Baker, J. H. and Gerouki, F. (1992). Tertiary granitoids of Rhodope, northern Greece: magmatism related to extensional collapse of the Hellenic Orogen? *Tectonophysics*, **210**: 295-314.

Karfakis, I. and Doutsos, T. (1995) Late orogenic evolution of the Cirum-Rhodope Belt, Greece. *N.Jb.Geol.Paläont.Mh.*, **5**: 305-319.

Karig, D. E. (1974) Evolution of arc systems in the western Pacific. *Ann.Rev.Earth Planet Sci.*, **2**: 51-75.

Katsikatsos, G.; Mercier, J.-L. and Vergely, P. (1976) La fenêtre d'Attique-Cyclades et les fenêtres métamorphiques des Hellénides internes (Grèce). *C.R.Acad.Sci. Paris*, **283**(Série D): 1613-1615.

Katsikatos, G.; Migiros, G. and Vidakis, M. (1982) Structure géologique de la région de Thessalie orientale (Grèce). *Ann. Soc.Géol.Nord.*, **CI**(Octobre): 177-188.

Katsikatos, G. (1984a) Geological Maps of Greece, Istea Sheet, No. 187, 1/50000e, *Inst.Geol.Min.Greece.*

Katsikatos, G. (1984b) Geological Maps of Greece, Ayia-Panayia Ayias Sheet, No. 133, 1/50000e, *Inst.Geol.Min.Greece.*

Katsikatos, G. (1985) Geological Maps of Greece, Gonni Sheet, No. 112a, 1/50000e, *Inst.Geol.Min.Greece.*

Katsikatos, G. (1986) Geological Maps of Greece,

Volos Sheet, No. 148, 1/50000e, *Inst.Geol.Min.Greece.*

Katsikatos, G. (1987) Geological Maps of Greece, Zagora-Siki Sheet, No. 149, 1/50000e, *Inst.Geol.Min.Greece.*

Ketin, I. (1966) Tectonic units of Anatolia (Asia Minor). *Bull.Min.Res.Expl.Inst.Turkey*, **66**: 23-34.

Kilias, A. (1991) Transpressive Tektonik in den zentralen Helliniden Anderung der Translationspfade durch die Transpression (Nord-Zentral-Griechenland). *N.Jb.Geol.Paläont.Mh.*, **20**: 291-306.

Kilias, A.; Falalakis, G.; Nastos, G. and Mounstrakis, D. (1995) 17-20 September. Tertiary extensional exhumation of the HP/LT Makrynitsa metamorphic core complexes in Mt Pelion (Eastern Thessaly). In: *XV Carpatho-Balkan Congress.* Geological Society of Greece, Athens.

Kilias, A.; Fassoulas, H.; Priniotakis, M.; Sfeikos, A. and Frisch, W. (1991) HP/LT metamorphic conditions and deformation at the tectonic window of Kranea (W. Thessaly Northern/Central Greece). In: *5th Congress of the Geological Society of Greece. Bull.Geol.Soc.Greece,* **XXV**: 275-292.

Kilias, A. and Mounstrakis, D. (1985) Das 'Rizomata-Fenster' im nordöstlichen Pieria-Gebirge. Neue data zur geologischen Grenze der Pelagoniachen und der Axios-Zone in Griechenland. *N.Jb.Pal.Monat.*, **4**: 248-256.

Kilias, A. and Mounstrakis, D. (1989) The Pelagonian Nappe, tectonics, metamorphism and magmatism. *Bull.Geol.Soc. Gr.*, **23**(1): 29-46.

Kiriakidis, L. and Brooks, M. (1986) A geophysical study of the Vardar Zone ophiolite belt in Chalkidiki Northern Greece. *J.Geol.Soc.London*, **146**: 859-865.

Kisch, H. J. (1981) Burial diagenesis in Tertiary 'flysch' of the extenal zones of the Hellenides in central Greece and the Olympos region, and its tectonic significance. *Eclog.geol.Helv.*, **74**(3): 603-624.

Kissel, C.; Kondopoulou, D.; Laj, C. and Papadopoulos, P. (1986) New paleomagnetic data from Oligocene formations of northern Aegean. *Geoph.Res.Lett.*, **13**: 1039-1042.

Kissel, C.; Laj, C.; Sengör, A. M. C. and Poisson, A. (1987) Paleomagnetic evidence for rotation in opposite senses of adjacent blocks in northeastern Aegean and western Anatolia. *Geoph.Res.Lett.*, **14**: 907-910.

Kissel, C. and Laj, C. (1988) The Tertiary geodynamical evolution of the Aegean Arc: paleomagnetic reconstruction. *Tectonophysics*, **146**: 183-201.

Kissel, C. and Speranza, F. (1995) Paleomagnetism of external southern and central Dinarides and northern Albanides: implications for the Cenozoic activity of the Scutari-Pec Transverse zone. *J.Geoph.Res.*, **100**: 14,999-15,007.

Kober. L. (1952) Leitlinien der Tektonik Jugoslawiens. *Serb.Akad.Wiss.sonderausg.*, **189**(3).

Kondopoulou, D.; Atsemoglu, A. and Pavlides, S. (1996) Paleomagnetism as a tool for testing geodynamic models in the north Aegean: convergences, controversies and a further hypothesis. In: Paleomagnetism and tectonics of the Mediterranean region (Eds Morris, A. and Tarling, D. H.). *Geol.Soc.Spec.Pub.*, **105**: 277-288.

Kossmat, F. (1924) *Geologie der zentralen Balkanhalbinsel. Die Kreigsschauplätz 1914-1918, Geologisch Dargestellt.* Borntraeger, Berlin.

Koukouvelas, I. and Doutsos, T. (1990) Tectonic Stages along a traverse cutting the Rhodopian zone (Greece). *Geol.Rudsch.*, **79**(3): 753-776.

Kretz, R. (1983) Symbols for rock-forming minerals. *Am.Miner.*, **68**: 277-279.

Kreuzner, H.; Harre, W.; Lenz, H.; Wendt, L.; Henjes-Kunst, F. and Okrusch, M. (1978) K/Ar und Rb/Sr-Daten von Mineralen aus dem polymetamorphen Kristallin der Kykladen-Insel Ios (Griechenland). *Fortschritte der Mineralogie,* **56**(1): 69-70.

Le Pichon, X. and Angelier, J. (1979) The Hellenic Arc and trench system: a key to the neotectonic evolution of the eastern Mediterranean. *Tectonics,* **60**: 1-42.

Le Pichon, X. and Angelier, J. (1981) The Aegean Sea. *Phil.Trans.R.Soc.*, **300**: 357-372.

Le Pichon, X.; Bergerat, F. and Roulet, M.-D. (1988) Plate kinematics and tectonics leading to the Alpine belt formation, a new analysis. *Geol.Soc.Am. Spec.Paper,* **218**: 111-131.

Le Pichon, X.; Chamot-Rooke, N.; Lallement, S.; Noomen, R. and Veis, G. (1995) Geodetic determination of the kinematics of central Greece with respect to Europe: implications for eastern Mediterranean tectonics. *J.Geoph.Res.*, **100**(B7): 12675-12690.

Lee, J. and Lister, G. S. (1992) Late Miocene ductile extension and detachment faulting, Mykonos, Greece. *Geology,* **20**: 121-124.

Liati, A. and Seidel E. (1996) Metamorphic evolution and geochemistry of kyanite eclogites in central Rhodope, northern Greece. *Contrib.Min.Petrol.*, **123**: 293-307.

Lips, A. L. W.; Wijbrans, J. R. and White, S. H. (1998) Timing of metamorphic and deformation events in the Pelagonian Zone, Internal Hellenides, Greece. *Tectonophysics*, in press

Lister, G. S.; Banga, G. and Feenstra, A. (1984) Metamorphic core complexes of Cordilleran type in the Cyclades, Aegean Sea, Greece. *Geology,* **12**: 221-225.

Lister, G. S. and Raoozaios, A. (1996) The tectonic significance of a porphyroblastic blueschist facies overprint during Alpine orogenesis: Sifnos, Agean Sea, Greece. *J.Struc.Geol.*, **18**: 1417-1435.

Lister, G. S. and Snoke, A. W. (1984) S-C Mylonites. *J.Struct.Geol.*, **6**: 617-638.

Lister, G.S. and Forster, M. (1996) eds, Inside the Aegean Metamorphic Core Complexes, Australian Crustal Research Centre, Technical publications 45, p110.

Lonergan, L. and White, N. (1997) Origin of the Betic-Rif mountain belt. *Tectonics*, **16**(3): 504-522.

Makris, J. (1978a) The crust and upper mantle of the Aegean region from deep seismic sounding. *Tectonophysics*, **46**: 269-284.

Makris, J. (1978b) A geophysical study of Greece based on deep seismic sounding, gravity, and magnetics. In: *Alps, Appenines, Hellenides* (edited by Closs, H.; Roeder D. and Schmidt, K.). *IUCG Science Reports*, **38**: 392-401.

Makris, J. and Stobbe, C. (1984) Physical properties and state of the crust and upper mantle of the Eastern Mediterranean deduced from geophysical data. *Marine Geology*, **55**: 347-363.

Makris, J. and Vees, R. (1977) Crustal structure of the Central Aegean Sea and the islands of Evia and Crete, Greece, obtained by refractional seismic experiments. *J.Geoph.Res.* **42**: 329-341.

Marton, E. (1993) Paleomagnetism in the Mediterranean from Spain to the Aegean: a review of data relevant to Cenozoic movements. In: *Recent Evolution and Seismicity of the Mediterranean Region* (edited by Boschi, E.). Kluwer Academic Publishers, Amsterdam: 367-402.

McKenzie, D. (1972) Active tectonics of the Mediterranean region. *Geophys.J.R.astr.Soc.*, **30**: **KK**.

McKenzie, D. (1978a) Active tectonics of the Alpine-Himilayan Belt, the Aegean sea and surrounding regions. *Geophys. J.R.Astr.Soc.*, **55**: 217-254.

McKenzie, D. (1978b) Some remarks on the development of sedimentary basins. *Earth Plan.Sci.Lett.*, **40**: 25-32.

McKenzie, D. and Jackson, J. (1983) The relationship between strain rates, crustal thickening, paleomagnetism, finite strain and fault movements within a deforming zone. *Earth Planet Sci.Lett.*, **65**: 182-202.

Meijer, P. Th. (1995) *Dynamics of active continental margins: the Andes and the Aegean region.* Geologica Ultraiectina: Mededelingen van de Faculeit Aardwetenschappen, Universiteit Utrecht, **130**: 218.

Zuiderwijk, R. (1996) Map of Servia area, Unpublished 4th year mapping project report, housed in the University of Utrecht.

Mercier, J.-L. (1968) Etude geologique des zones internes des Hellenides en Macedoine centrale (Grece). *Annls.geol. Pays. Hell.*, **20**: 1-792.

Mercier, J.-L. (1973) Contribution à l'étude du métamorphisme et de l'évolution magmatique des zones internes des Hellénides. *Ann.géol.Pays Hell*, **20**: 599-792.

Mercier, J.-L.; Sorel, D.; Vergely, P. and Simeakis, K. (1989) Extensional tectonic regimes in the Aegean basin during the Cenezoic. *Basin Res.*, **2**: 49-71.

Mercier, J.-L.; Vergely, P. and Bebien, J. (1975) Les ophiolites helleniques "obductees" au Jurassique superieur sont-elles les vestiges d'un ocean tethysien ou d'une mer marginale peri-europeenne? *C.r. somm.Seanc.Soc.geol.Fr.*, **17**: 108-112.

Meulenkamp, J. E.; Wortel, M. J. R.; Van Wamel, W. A.; Spakman, W. and Hoogerduyn Strating, E. (1988) On the Hellenic subduction zone and the geodynamic evolution of Crete since the late middle Miocene. *Tectonophysics*, **146**: 203-215.

Miyashiro, A. (1973) Metamorphism and metamorphic belts. George Allen and Unwin Ltd. London: p.492.

Molnar, P. and Tapponier, P. (1975) Cenozoic tectonics of Asia: effect of a continental collision. *Science*, **189**: 419-425.

Morris, A. (1995) Rotational deformation during Paleogene thrusting and basin closure in eastern Central Greece: palaeomagnetic evidence from Mesozoic carbonates. *Geoph.J.Int.*, **121**: 827-847.

Morris, A. and Anderson, M. (1996) First paleomagnetic results from the Cycladic massif, Greece, and their implications for Miocene extension directions and tectonic models in the Aegean. *Ear.Plan.Sci.Lett.*, **142**: 397-408.

*Morris, A. and Tarling, D. H. (1996) In: *Paleomagnetism and Tectonics of the Mediterranean Region* (edited by Morris, A. and Tarling, D. H.). *Geological Society Special Publication*, **105**: **Ch2/p7**

Mountrakis, D. (1986) The Pelagonian Zone in Greece: A polyphase deformed fragment of the Cimmerian Continent and its role in the geotectonic evolution of the Mediterranean. *J.Geol.*, **94**: 335-347.

Mposkos, E. (1987) The chemical composition of calcic and sodic-calcic amphiboles in metabasic rocks from Pelagonian Zone (Greece) as an indicator of Pressure and Temperature. *Chem.Erde.*, **46**: 161-169.

Müller, R. D. and Roest, W. K. (1992) Fracture zones from combined Geosat and Seasat data. *J.Geophys.Res.*, **97**: 3337-3350.

Nance, D. (1981) Tectonic history of a segment of the Pelagonian zone. *Can.J.Earth Sci.*, **18**: 1111-1126.

Oberhänsli, R.; Candan, O.; Dora, O.Ö. and Dürr,

S. H. (1997) Eclogites within the Menderes massif, western Turkey *Lithos*, **41**: 135-150.

Okay, A. I. (1980) Mineralogy, petrology and phase relations or glaucophane-lawsonite zone blueschists from the Tavsanli region, northwest Turkey. *Contrib.Min.Petr.*, **72**: 243-255.

Okay, A. I. (1984) Distribution and characteristics of the north-west Turkish blueschists. In: *The Geological Evolution of the Eastern Mediterranean* (edited by Dixon, J. E. and Robertson, A. H. F.). *Geol.Soc.Spec.Pubs*, **17**: Blackwell Scientific Publications, Edinburgh.

Okay, A. I. (1986) High-pressure/low-temperature metamorphic rocks of Turkey. *Geol.Soc.Am.Mem.* **164**:333-347

Okay, A. I. (1989) Alpine-Himilayan Blueschists. *Ann.Rev.Earth Planet.Sci.*, **17**: 55-87.

Okay, A. I. (1991) Geology and tectonic evolution of the Biga Peninsula, northwest Turkey. *Bull.Tech.Univ.Istanbul*, **44**: 191-256.

Okrusch, M. and Bröcker, M. (1990) Eclogites associated with high-grade blueschists in the Cycladic Archipelago, Greece: a review. *Euro.J.Miner.*, **2**: 451-478.

Papanikolaou, D. (1978) Contribution to the geology of the Aegean Sea, the island of Andros. *Ann.Géol.Pays Hellén.* **XXIX**(2): 477-553.

Papanikolaou, D. (1980) Contribution to the geology of the Aegean Sea, the island of Paros. *Ann.Géol.Pays Hellén.* **XXX**(1): 65-96.

Papanikolaou, D. J. (1984) The three metamorphic belts of the Hellenides: a review and kinematic interpretation. In: *Geological Evolution of the Eastern Mediterranean* (edited by Dixon, J. and Robertson, A. H. F.). *Special Publications* **17**. Geological Society of London: 1-74.

Papanikolaou, D. J. and Skarpelis, N. (1986) The blueschists of the external metamorphic belt of the Hellenides: composition, strucutre and geotectonic significance of the Arna Unit. *Ann.Geol.Pays Hell.*, **32**: 47-68.

Passchier, C. W. and Trouw, R. J. J. (1996) Microtectonics. Springer-Verlag, Berlin Heidelberg: 289p.

Pe-Piper, G. and Piper, D. J. W. (1989) Spatial and temporal variation in late Cenozoic back-arc volcanic rocks, Aegean Sea region. *Tectonophysics*, **169**: 113-134.

Pickett, E. A. and Robertson, A. H. F. (1997) Formation of the Late Palaeozoic-Early Mesozoic Karakaya Complex and related ophiolites in NW Turkey by Palaeotethyan subduction-accretion. *J.Geol.Soc.*, **153**: 995-1009.

Platt, J. P. (1984) Secondary cleavages in ductile shear zones. *J.Struct.Geol.*, **6**: 439-442.

Platt, J. P. (1986) Dynamics of orogenic wedges and the uplift of high-pressure metamorphic rocks. *Geol.Soc.Am.Bull.*, **97**: 1037-1053.

Platt, J. P. (1993) Exhumation of high-pressure rocks: a review of concepts and processes. *Terra Nova*, **5**: 119-133.

Platt, J. P. and Vissers, R. L. M. (1989) Extensional collapse of thickened continental lithosphere: a working hypothesis for the Alboran Sea. *Geology*, **17**: 540-543.

Platt, J. P. and Vissers R. L. M. (1980) Extensional Structures in Anisotropic Rocks. *J. Struct. Geol.* **2**, 397-410.

Ramsay, J.G. and Graham, R.H. (1970) Strain variation in shear belts. *Can.J.Earth Sci.*, **7**: 786-813

Reilinger, R.; McClusky, S.; Oral B.; King, R.; Toksoz, M. N.; Barka, A.; Kinik, I.; Lenk, O. and Sanli, I. (1997) Global Positioning System measurements of present-day crustal movements in the Arabia-Africa-Eurasia Plate Collision Zone. *J.Geoph.Res.*

Renz., C. (1940) Die Tektonik der grieschischen Gebirge. *Pragm.Akad.Athinon*, **8**: 1-171.

Ridley, J. (1984) Listric normal faulting and the reconstruction of the synmetamorphic structural pile of the Cyclades. In: *The geological evolution of the Eastern Mediterranean* (Eds Dixon, J. E. and Robertson, A. H. F.). *Geol.Soc.Spec.Pub.*, **17**: 775-761.

Roberts, S. and Jackson, J. (1991) Active normal faulting in central Greece: an overview. In: *The geometry of normal faults. Geol.Soc.Spec.Pub.*, **56**: 125-142.

Robertson, A. H. F. and Dixon, J. E. (1984) Introduction: Aspects of the Geological Evolution of the Eastern Mediterranean. In: *Geological Evolution of the Eastern Mediterranean* (edited by Dixon, J. E. and Robertson, A. H. F.). *Special Publications*. Royal Society of London, **17**: 1-74.

Robertson, A. H. F.; Clift, P. D.; Degnan, P. J. and Jones, G. (1991) Tectonic evolution of the Mesozoic-Cenozoic Pindos Ocean: Greece. *Bull.Geol.Soc.Gr.*, **25**(1): 55-64.

Roesler, G. (1978) Relics of non-metamorphic sediments on Central Aegean islands. In: *Alps, Apennines, Hellenides*. (Eds Closs, H.; Roeder, D. and Schmidt, K.). *Inter-Union Comm.Geodyn.Sci.Rep.*, **38**: 480-482.

Schermer, E. R. (1993) Geometry and kinematics of continental basement deformation during the Alpine Orogeny, Mt. Olympos, Greece. *J.Struct.Geol.*, **15**: 3-51990.

Schermer, E. R.; Lux, D. R. and Burchfiel, B. C. (1990) Temperature-time history of subducted

continental crust, Mt. Olympos region, Greece. *Tectonics,* **9**(5): 1165-1195.

Schliestedt, M.; Altherr, R. and Matthews A. (1987) Evolution of the Cycladic crystalline complex: petrology, isotope geochemistry and geochronology. In: *Chemical transport in metasomatic processes* (edited by Helgeson, H. C.). Riedel, Dordecht, Netherlands, Boston, USA, 389-428.

Schmitt, A. (1983) Novelles contributions a l'étude géologique des Piéria de l'Olympe et d'Ossa (Grèce du Nord). These, Fac.Polytech. de Mons (Belgique): 385p.

Seidel, E.; Kreuzner, H. and Harre, W. (1982) A late Oligocene/early Miocene high-pressure belt in the External Hellenides. *Geol.Jb.,* **E23**: 165-206.

Sibson, R.H. (1977) Fault rocks and fault mechanisms. *J.Geol.Soc.London* , **133**, 191-213

Sengör, A. M. C. (1984) The Cimmeride orogenic system and the tectonics of Eurasia. *Geol.Soc.Am.Spec.Paper,* **195**: 1-82.

Sengör, A. M. C.; Yilmaz, Y. and Ketin, I. (1980) Remnants of a pre-Late Jurassic ocean in northern Turkey: fragments of Permian-Triassic Paleo-Tethys? *Geol.Soc.Am.Bull.*, **91**: 599-609.

Sengör, A. M. C.; Satir, M. and Akkök, R. (1984a) Timing of tectonic events in the Menderes massif, Western Turkey: implications for tectonic evolution and evidence for Pan-African basement in Turkey. *Tectonics*, **3**: 693-707.

Sengör, A. M. C.; Yilmaz, Y. and Sungurlu, O. (1984b) Tectonics of the Mediterranean Cimmerides: nature and evolution of the western termination of the Paleo-Tethys. In: *The Geological Evolution of the Eastern Mediterranean* (edited by Dixon, J. E. and Robertson, A. H. F.). *The Geological Society Special Publications* **17**. Blackwell Scientific Publications, Edinburgh.

Sengör, A. M. C.; Altiner, D.; Cin, A.; Ustaömer, T. and Hsü, K. J. (1988) Origin and assembly of the Tethyside orogenic collage at the expense of Gondwana Land. In: *Gondwana and Tethys* (edited by Audley-Charles, M. G. and Hallam, A.). *Geological Society of Special Publication* **37**. Oxford University Press, New York, 119-181.

Seyitoglu, G. and Scott, B. C. (1996) The cause of N-S extensional tectonics in western Turkey: tectonic escape vs back-arc spreading vs orogenic collapse. *J.Geodynamics*, **22**: 145-153.

Seyitoglu, G.; Scott, B. C. and Rundle, C. C. (1992) Timing of Cenozoic extensional tectonics in West Turkey. *J.Geol. Soc. London,* **149**: 533-38.

Sfeikos, A.; Bohringer, C.; Frisch, W.; Kilias, A. and Ratschbacher, L. (1991) Kinematics of Pelagonian nappes in Kranea area, north Thessaly, Greece. In: *Proceedings of the 5th Congress, May 1990, Bull.Geol.Soc.Gr.,* **XXV/I**: 101-105.

Smith, A. G. and Moores, E. M. (1974) The Hellenides. In: *Data for Orogenic Studies: Mesozoic-Cenozoic Orogenic Belts* (edited by Spencer, A. M.). *Geol.Soc.London Special Pub.,* **4**: 154-185.

Smith, A. G.; Hynes, A.; Menzies, M.; Nisbet , E.; Price, I.; Welland, M. and Ferriere, J. (1975) The stratigraphy of the Othris Mountains, Eastern Central Greece: a deformed Mesozoic continental margin sequence. *Ecologae geol. Helv.*, 463-481

Smith, A. G. and Spray, J. G. (1984) A half-ridge transform model for the Hellenic-Dinaric ophiolites. In: *The Geological Evolution of the Eastern Mediterranean.* (edited by Dixon, J. E. and Robertson, A. H. F.). *Geol.Soc. London, Special Pub.,* **17**: 629-644.

Smith, A. G. (1993) Tectonic significance of the Hellenic-Dinaric ophiolites. In: *Magmatic processes and plate tectonics* (edited by Pritchard, H. M.; Alabaster, T.; Harris, N. B. W. and **C.R., N.**). *Geol.Soc. London Special Pub.,* **76**: 213-243.

Sokoutis, D.; Brun J-P.; van den Driessche, J. and Pavlides, S. (1993) A major Oligo-Miocene detachment in southern Rhodope controlling north Aegean extension. *J.Geol.Soc. London,* **150**: 243-246.

Sonder, L. J. and England, P. C. (1989) Effects of a temperature-dependent rheology on large-scale continental extension. *J.Geophys.Res.*, **94**(B4): 7603-7619.

Sowa, A. (1985) Die Geologie der Insel Folegandros (Kykladen, Griechenland): *Er.geol.Abhand.*, **112**: 85-101.

Spakman, W.; Wortel, M. J. R. and Vlaar, N. J. (1988) The Hellenic subduction zone: a tomographic image and its geodynamic implications. *Geophys.Res.Lett.,* **15**: 60-63.

Speranza, F.; Islami, I.; Kissel, C. and Hyseni, A. (1995) Paleomagnetic evidence for Cenozoic clockwise rotation of the external Albanides. *Earth Planet Sci.Lett.,* **129**: 121-134.

Spray, J. G.; Bébien, J.; Rex, D. C. and Roddick, J. C. (1984) Age constraints on the igneous and metamorphic evolution of the Hellenic-Dinaric Ophiolites. In: *The Geological Evolution of the Eastern Mediterranean* (edited by Dixon, J. E. and Robertson, A. H. F.). *Geol.Soc.Spec.Pubs,* **17**: Blackwell Scientific Publications, Edinburgh.

Sylvester, A. G. (1988) Strike-Slip Faults. *Geol.Soc.Am.Bull.,* **100**: 1666-1703.

Taymaz, T.; Jackson, J. and Westaway, R. (1990) Earthquake mechanics in the Hellenic Trench near Crete. *Geophys.J.Int.,* **102**: 695-731.

Taymaz, T.; McKenzie, D. and Jackson, J. (1991) Active tectonics of the north and central Aegean area.

Geophys.J.Int., **106**: 433-490.

Tchalenko, J. S. (1968) The evolution of kinkbands and the development of compression textures in sheared clays. *Tectonophysics,* **6**: 159-174.

Ten Veen, J. and Meijer P. Th. (1998) Late Miocene to Recent tectonic evolution of Crete (Greece): geological observations and model analysis. *Tectonophysics*, in press.

Theye, T. and Seidel, E. (1991) Petrology of low-grade high-pressure metapelites from the External Hellenides (Crete, Peloponnese): a case study with sodic minerals. *Eur.J.Min.*, **3**: 343-366.

Theye, T.; Seidel, E. and Vidal, O. (1992) Carpholite, sudoite and chloritoid in low-grade high-pressure metapelites from Crete and the Peloponnese, Greece. *Eur.J.Min.*, **4**: 487-507.

Tromp, A. (1996) Map of north Servia area, Unpublished 4th year mapping report, housed in the University of Utrecht.

Tsokas, G. N. and Hansen, R. O. (1997) Study of the crustal thickness and subducting lithosphere in Greece from gravity data. *J.Geophys.Res.*, **102**(B9): 20585-20597.

Underhill, J. R. (1989) Late Cenozoic deformation of the Hellenide foreland, western Greece. *Geol.Soc.Am.Bull.*, **101**: 613-634.

Vandenberg, L. and Lister, G. S. (1996) Structural analysis of basement from the Aegean metamorphic core complex of Ios, Cyclades, Greece. *J.Struct.Geol.*, **18**(12): 1437-1454.

Verge, N. J. (1993) Oligo-Miocene orogenic collapse tectonics in western Anatolia and the extensional exhumation of the Menderes Massif metamorphic core complex. *In: Late orogenic extension of mountain belts,* (eds: Séranne M. and Malaveille J.), *Doc.B.G.R.Mm.France,* **219**: 202p.

Vergély, P. and Mercier, J. (1990) La fenêtre métamorphique de l'Olympe (Macédonie, Grèce): compression et extension cénozoiques. *Bull.Soc.géol.Fr.*, **6**: 819-829.

Wallbrecher, E. (1976) Geologie und Tectonik auf dem Südteil der Magnesischen Halbinsel (Nord Griechenland). *Z.dtsch. geol.Ges.*, **127**: 365-371.

White, S. H.; Burrows, S. E.; Carreras, J.; Shaw, N. D. and Humphreys, F. J. (1980) On mylonites in ductile shear zones. *J.Struct.Geol.*, **2**(1/2): 175-187.

White, S. H.; Bretan, P. G. and Rutter, E. H. (1986) Fault-zone reactivation: kinematics and mechanisms. *Phil.Trans.R. Soc.London,* **A317**: 81-97.

Whitechurch, H.; Juteau, T. and Montigny, R. (1984) Role of the eastern Mediterranean ophiolites (Turkey, Syria, Cyprus) in the history of the Neo-tethys. In: *The geological evolution of the eastern Mediterranean* (edited by Dixon, J. E. and Robertson, A. H. F.). *Special Publications* **17**. Geological Society of London, 301-317.

Williams, P. F. and Price, G. P. (1990) Origin of kinkbands and shear-band cleavage in shear zones: an experimental study. *J.Struct.Geol.*, **12**(2): 145-164.

Wijbrans, J. R. and McDougall, I. (1986) $^{40}Ar/^{39}Ar$ dating of white micas from an Alpine high-pressure metamorphic belt on Naxos (Greece): resetting of the argon isotopic system. *Contrib.Min.Pet.*, **93**: 187-194.

Wijbrans, J. R. and McDougall, I. (1988) Metamorphic evolution of the Attic-Cycladic metamorphic belt on Naxos (Cyclades, Greece). *J.Met.Pet.*, **6**: 571-594.

Wijbrans, J.; Lips, A. and White, S. H. (1996) High pressure metamorphism in the Cyclades and beyond: heading for Olympos. Conference Proceedings: *The Mediterranean Basins*: Cèrgy-Pontoise, Paris, Institute du Petrole.

Wilson, J. (1993) The Meso-Hellenic Trough: a model for detachment basement formation above an extensional fault.

Wilson, J. T. (1966) Did the Atlantic close and then reopen? *Nature,* **211**: 676-681.

Wortel, M.J.R. (1980) Age dependent subduction of oceanic lithosphere. Ph.D. Thesis, University Utrecht, 147p.

Wortel, M. J. R. and Spakman, W. (1992) Structure and dynamics of subducted lithosphere in the Mediterranean region. *Proc. KNAW,* **95**: 325-347.

Yardley, B. W. D. (1989) An introduction to metamorphic petrology (Eds Zussman, J. and MacKenzie, W. S.). Longman Scientific and Technical Series, John Wiley and Sons Inc., New York: 248p.

Yarwood, G. A. and Aftalion, M. (1976) Field relations and U-Pb geochronology of a granite from the Pelagonian zone of the Hellenides (High Pieria, Greece). *Bull.Soc.Geol.Fr.*, **18**: 259-265.

Yarwood, G. A. and Dixon, J. E. (1977) Lower Cretaceous and younger thrusting in the Pelagonian rocks of the High Pieria, Greece. In: *Proc.6th Colloq.Aegean Region, Athens,* 1977: 269-280.

Zuiderwijk, M. (1993) Map of Ambelakia area, Unpublished 4th year mapping report, housed in the University of Utrecht.

Appendix A: Mineral Abbrieviations

Abbrieviations used in thesis. The symbol * refers to abbreviations not found in Kretz (1983)

Act	Actinolite	Czo	Clinozoisite	Pmp	Pumpellyite
Ab	Albite	Dol	Dolomite	Prh	Prehnite
Alm	Almandine	Ep	Epidote	Qtz	Quartz
Ap	Apatite	Grt	Garnet	Ser	Sericite
Asb*	Asbestos	Gln	Glaucophane	Spn	Sphene
Aug	Augite	Hbl	Hornblende	Sps	Spessartine
Bar*	Barroisite	Jd	Jadiete	Stp	Stilpnomelane
Bt	Biotite	Kfs	K-Feldspar	Tlc	Talc
Cal	Calcite	Lws	Lawsonite	Tr	Tremolite
Chl	Chlorite	Ms	Muscovite	Whm*	White mica
Cro*	Crossite	Pl	Plagioclase	Wn*	Winchite
				Zo	Zoisite

Appendix B: Representative microprobe analyses

The mineral chemical analyses presented below were determined using energy-dispersive spectrometry (EDS) on the JOEL JXA8600 Superprobe housed at Utrecht University.

Sample	A	A,C,D	B	B	B	C	D	D	D	D	E
	Bar	**Ab**	**Grt** rim	**Grt** core	**Rt?**	**Lws**	**Di**	**Gln**	**Ep**	**Whm**	**Act**
SiO2	51.54	68.66	37.89	37.15	0.52	39.34	52.12	58.38	37.92	55.60	35.82
TiO2	0.09	0.00	0.05	0.24	74.05	0.07	0.54	0.00	0.08	0.05	0.67
Al2O3	5.39	20.08	21.68	20.55	0.35	32.22	2.04	10.56	22.27	7.75	32.22
Cr2O3	0.00	0.00	0.01	0.00	0.01	0.00	0.17	0.00	0.00	0.00	0.00
MgO	11.25	0.00	2.10	0.48	0.19	0.00	16.16	7.94	0.00	8.62	6.24
CaO	6.72	0.34	8.29	6.23	1.38	16.25	21.54	0.35	23.68	7.70	0.60
FeO	16.96	0.00	30.62	21.85	3.13	0.79	7.54	14.09	13.13	7.38	8.84
MnO	0.70	0.00	1.13	14.72	0.00	0.00	0.00	0.00	0.00	0.00	0.00
ZnO	0.00	0.00	0.00	0.00	0.00	0.00	0.36	0.00	0.00	0.00	0.43
Na2O	3.81	10.47	0.04	0.00	0.00	0.00	0.36	7.76	0.02	3.72	2.39
K2O	0.06	0.00	0.00	0.00	0.07	0.00	0.00	0.00	0.13	0.00	0.07
Cl	0.00	0.00	0.00	0.00	0.02	0.00	0.01	0.00	0.00	0.01	0.00
F	0.07	0.00	0.00	0.00	0.00	0.00	0.08	0.00	0.04	0.00	0.22
Total	96.58	99.54	101.80	101.23	79.71	88.67	100.91	99.08	97.27	90.84	87.51
Si	7.969	11.99	5.951	5.979	1.385	2.046	1.919	8.036	3.123	7.848	5.745
Ti	0.010	0.000	0.006	0.029	8.718	0.003	0.015	0.000	0.005	0.005	0.081
Al	0.982	4.130	4.013	3.898	1.291	1.975	0.089	1.713	2.161	1.289	6.091
Cr	0.000	0.000	0.001	0.001	0.000	0.000	0.007	0.000	0.000	0.000	0.000
Mg	2.592	0.000	0.493	0.116	0.674	0.000	0.887	1.629	0.000	1.814	1.493
Ca	1.114	0.063	1.394	1.075	0.222	0.906	0.850	0.052	2.089	1.164	0.103
Fe	2.194	0.000	4.022	2.940	0.930	0.035	0.232	1.581	0.904	0.871	1.186
Mn	0.091	0.000	0.150	2.006	0.019	0.000	0.000	0.000	0.000	0.000	0.000
Zn	0.000	0.000	0.000	0.000	0.000	0.000	0.010	0.000	0.000	0.000	0.052
Na	1.142	3.544	0.012	0.000	0.023	0.000	0.000	2.071	0.003	1.018	0.744
K	0.012	0.000	0.000	0.000	0.000	0.000	0.000	0.000	0.014	0.000	0.015
Cl	0.000	0.000	0.000	0.000	0.003	0.000	0.001	0.000	0.000	0.002	0.000
F	0.033	0.000	0.000	0.000	0.000	0.000	0.009	0.000	0.010	0.000	0.110

Appendix C: Table of Dates obtained in the Aegean

Table summarising geochronological data from basement of Thessaly and Macedonia. The orientation of stretching lineations from the locations that data are from maps of Schermer (1993), Kilias et al (1991). References are as follows : (A) Mercier 1963, (B) Yarwood and Aftalion 1976, (C) Yarwood and Dixon 1977 (D) Barton 1976 (E) Schermer et al 1990

Loc	Rock	Age	(Ma)				Method	Ref	*Ls trend*
NE Macedonia	QF Gneiss with Ab		140-133				K/Ar: Ms (12TC,13 TC)	A	*NNW-SSE*
	QF schist with Ab		134				K/Ar:Bt (147T)	A	*NNW-SSE*
	Bt Granite			101-98			K/Ar:Bt (37TC)	A	*NNW-SSE*
Intermediate Series	Granite	302 ±5					U/Pb:Zr	B	*E-W*
North Thessaly (Kinaros Mts)	QF gneiss	290	135 ± 2		63 ±4		Ar/Ar:Ms (P8,9)	E	*NE-SW*
	QF gneiss?	457 ±7					Ar/Ar:Hb IP(4)	E	*NE-SW*
						23±0.3	Ar/Ar:Kfs (P8)	E	*NE-SW*
	QF gneiss?			99 ±3	54 ±3		Ar/Ar:Ms (IP2-3)	E	*NE-SW*
	QF gneiss			119 ±3 116 ±5			Rb/Sr: WR	C	*NE-SW*
Lower Series			141				Rb/Sr: WR	D	*NE-SW*
NE Thessaly (Olympos)	QF gneiss		124 ±4				Rb/Sr: Iso	D	*NE-SW*
	Qtz Phyllite				39 ± 1		Rb/Sr: WR	D	*NE-SW*
	'metased' QFgneiss	297 ±4					Ar/Ar:Hb (P7)	E	*NE-SW*
	'metased' QFgneiss				62-36		Ar/Ar:Ms (P1-7)	E	*NE-SW*
	'metased' QFgneiss					28-35	Ar/Ar:Kfs (P1,P7)	E	*NE-SW*
	'metased' QFgneiss			98 ±2	56		Ar/Ar:Mu (IP1)	E	*NE-SW*
									NE-SW
Pelion Nth						37	K/Ar: WR	D	*NE-SW*
Interpreted Meta.		*Intrus.*	*Amph/ u Gns*	*Bls*		*Gns ?*			

Appendix D: EBSP details

Scanning Electron Microscopy (SEM) enable discriminatory CPO measurements to be made using Orientation Contrast Imaging (OCI) and Electron Back-Scatter Probe (EBSP) patterns. Electron back-scatter probe is a scanning electron microscopy technique which permits measurement of the full or complete orientation of grains with sizes down to 0.5 μm. In SEM, orientation contrast imaging in Back-Scattered-Electron (BSE) mode is possible by mounting a solid state back-scattered electron detector underneath the EBSP detector, i.e., in the forward scattered position. In the resulting image the contrast is related to the orientation of the (sub)grain. By combining orientation contrast images with EBSP patterns the misorientation across all the grain and subgrain boundaries can be determined.

For EBSP analysis, the SEM sections were polished on a polyurethane lap for three hours using a suspension of 0.05 μm silicon in water. The samples were analysed at 15 - 20 kV using beam currents around 0.5 nA (spot size 4 - 6). EBSP patterns were indexed using the Channel+ package (Schmidt & Olesen 1989).

Orientation measurements have been used to establish the misorientation relationship between two adjacent grains and between subgrains. The misorientation between any two grains can be described in terms of an axis of rotation and a rotation about that axis . The rotation axis is a direction which is common to both grains or subgrains about which the first must be rotated by the angle of misorientation in order to achieve the orientation of the second. A misorientation between two trigonal grains can be described in terms of 6 solutions of the axis/angle pair. Any of these 6 misorientations may be chosen as they are physically indistinguishable. Commonly, the axis/angle pair giving the smallest possible rotation is chosen as the misorientation and this is the approach adopted in this study. As the accuracy in the CPO data is at maximum 1° it is assumed that the accuracy in misorientation angle is as good..

Acknowledgements

In completing this thesis I have many people to thank. The first (big) thankyou must go to my supervisor, Stan White, who offered me the position in the first place and who with patience, thorough reviewing and attentiveness helped get me to the end. On the technical side I would primarily like to take this opportunity to mention what an excellent library service Utrecht has. Thanks to the folk in the library and in particular Jan. I would also like to thank the helpful staff in the sedimentology and thin-sectioning labs. Thank you to Martin Drury for helping me with EBSP, and Rene de Kloe, Julie Newman and Herman who all helped me with the dull task of collecting my data. Thanks to Martin Drury, Hans de Bresser and Julie Newman for those numerous calcite discussions.

Thank you to all the folk I with whom I discussed tectonics of Greece, Andrew Curtis, Tanja Zegers, Andor Lips and Paul Meijer. Paul Meijer kindly plotted the rotation path of Africa (Figure 2.01) for me.Time in the field was supported by the Panteli family, of Camping Sikia, Kala Nera, who kindly looked after my whatnots between field seasons. Thanks to my field assistants, Nigel (Max) Smith, Wouter van de Zee and in particular Dagmar Olbertz.

I would also like to thank: the NW corner folk who help make the department have such an enjoyable atmosphere, Fraukje Brouwer, Armelle Kloppenburg, Julie Newman, Arjan Dijkstra, Rene de Kloe and specially to my collaborator in caffeine imbibing and all things Greek, Andor Lips; and to Magda Maartens who holds the place together. A special thanks to my office mate for the first 3 years, Tanja Zegers who tolerated and deciphered my gibberish and mess. I think we covered most topics and I thoroughly enjoyed and appreciated having such a great office mate. Shame I can't take you with me! Thanks to all the other Utrecht folk who made my stay in Utrecht a very happy memory Jan-Kees Blom, Anthony and Colette van Dooren, and Dagmar Olbertz and Joerg Schmalzl. Particularly to Colette who offered me a room, feed me whisky and fine food during the final lengthy gasp of PhD production.

I would also like to thank my hard working proof readers that bet my thesis into a readable document: Andor Lips, Jan-Kees Blom, Tanja Zegers, and most of all the rescue crew Andrew Curtis and Tania Aslund.

A penultimate thankyou must go to Dave Craw of Otago University whose enthusiasm for science was an inspiration and who encouraged me to go forth and seek PhD pastures.

Lastly I would like to thank my dear husband, Andrew Curtis. It may be a cliche but I really don't know how I would have fared without his support, friendship, laughter, advice and in the end his boot!

CURRICULUM VITAE

Born in London, England in 1966.
1979-1983 Hutt Valley High School, Lower Hutt, New Zealand
1985-1989 B.Sc.(hons) Dept of Geology, Otago University, Dunedin, New Zealand.
1989-1990 M.Sc. Dept of Geology, Otago University, Dunedin New Zealand.
1993-1997 A.I.O. Teaching assistantship at the University of Utrecht, The Netherlands